UNDERSTANDING THE ROLE OF EPSTEIN-BARR VIRUS IN T- AND NK-CELL DISORDERS

*b*y

Lindsay Clare George

A thesis submitted to

The University of Birmingham

for the degree of

DOCTOR OF PHILOSOPHY

Institute of Cancer and Genomic Sciences

College of Medical and Dental Sciences

University of Birmingham

January 2016

ABSTRACT

Epstein-Barr virus (EBV) is associated with B- and epithelial cell malignancies. It is also associated with lymphoproliferations and malignancies of T- and natural killer (NK) cells. The global impact of these conditions is significant, and although rare, they are aggressive and are often resistant to treatment. Diagnosis is often delayed, and evidence-based treatment strategies are limited due to their rarity.

Viral gene expression in extranodal T- and NK-cell lymphoma (ENKTL), chronic active Epstein-Barr virus (CAEBV) and haemophagocytic lymphohistiocytosis (HLH) is limited. The viral latent membrane proteins LMP1, LMP2A and LMP2B have growth-transforming properties in B- and epithelial cells. Their effects on cellular gene expression in primary NK cells include pathways involved in cell cycle and stress responses. LMP1 and LMP2B expression by ENKTL and CAEBV cell lines is associated with increased survival in the absence of relevant growth factors, but also with increased susceptibility to apoptosis. This cannot be fully explained by variation in the expression of proteins involved in the intrinsic apoptotic pathway.

Finally, we describe PrimeFlow RNA, a new protocol for identification of the EBV-infected lymphocyte subset. Importantly, this technique means that we can begin to identify druggable targets on the EBV-infected cells directly from patient blood samples.

DEDICATION

To my amazing husband Sudhakar, without whom there would be no thesis. And to my children Alexander, Serafina and Benjamin, all of whom have contributed to the unusual duration of my research period.

ACKNOWLEDGMENTS

Cancer Research UK and Wellcome Trust for funding and encouragement.

The clinicians and collaborators both in the UK and abroad for their tireless pursuit of samples.

The patients – who never refuse yet another blood sample, secure in the knowledge that their sacrifice is helping patients of the future. I am humbled by their faith.

Professor Shimizu, without whom there would be no ENKTL cell lines.

My group – for support, practical help, coffee and camaraderie.

Most importantly...my supervisors, Dr Claire Shannon-Lowe and Professor Martin Rowe – for superb supervision and for believing in me.

TABLE OF CONTENTS

.

LIST OF FIGURES

LIST OF TABLES

ABBREVIATIONS

ANKL	*aggressive NK leukaemia*
ANOVA	*analysis of variance*
β2m	*beta 2 microglobulin*
BART	*BamHI-A rightward transcript*
BCR	*B-cell receptor*
BL	*Burkitt Lymphoma*
bp	*base-pair*
CAEBV	*chronic active EBV*
cDNA	*complementary deoxyribonucleic acid*
CD	*cluster differentiation (antigen)*
CDF	*chip definition file*
CTAR	*C-terminal activating region*
CTL	*cytotoxic T lymphocytes*

DAVID	*Database for Annotation, Visualization and Integrated Discovery*
DLBCL	*Diffuse large B-cell lymphoma*
DMSO	*dimethyl sulphoxide*
DNA	*deoxyribonucleic acid*
dNTPs	*deoxynucleotide triphosphates*
dsDNA	*double-stranded DNA*
EBER	*Epstein-Barr virus-encoded small RNA*
EBNA	*Epstein-Barr nuclear antigen*
EBV	*Epstein-Barr virus*
EDTA	*diaminoethanetetraacetic acid*
ENKTL	*extra-nodal NK/T lymphoma*
FACS	*fluorescence activated cell sorting*
FC	*fold change*
FCS	*fetal calf serum*
FFPE	*formalin-fixed, paraffin-embedded*
GAPDH	*glyceraldehyde-3-phosphate dehydrogenase*

GCB	*germinal centre B-cell*
GFP	*green fluorescent protein*
gp	*glycoprotein*
HA	*haemagglutinin*
HL	*Hodgkin Lymphoma*
HLA	*human leukocyte antigen*
HLH	*haemophagocytic lymphohistiocytosis*
HSCT	*haematopoietic stem-cell transplant*
Ig	*immunoglobulin*
IL	*interleukin*
IM	*infectious mononucleosis*
IFN	*interferon*
JNK	*c-Jun N-terminal kinases*
kbp	*kilobase pair*
kDa	*kilo Dalton*
LCL	*lymphoblastoid cell line*

LDH	*lactate dehydrogenase*
LMP	*latent membrane protein*
MAPK	*mitogen-activated protein kinase*
MHC	*major histocompatibility complex*
miRNA	*microRNA*
MS	*multiple sclerosis*
NFκB	*nuclear factor kappa-light-chain-enhancer of activated B-cells*
NHL	*non-Hodgkin lymphoma*
NK	*natural killer*
NPC	*nasopharyngeal carcinoma*
PBMC	*peripheral blood mononuclear cell*
PBS	*phosphate buffered saline*
PI	*propidium iodide*
PCR	*polymerase chain reaction*
PTLD	*post-transplant lymphoproliferative disease*
qPCR	*quantitative polymerase chain reaction*

REAL	*Revised European and American Lymphoma*
RNA	*ribonucleic acid*
RS	*Reed Sternberg*
RT	*reverse transcription*
SNP	*single nucleotide polymorphism*
TCR	*T-cell receptor*
TNF	*tumour necrosis factor*
TR	*terminal repeats*
Tween	*polyoxyethylenesorbitan monolaurate*
WHO	*World Health Organisation*
XLP	*X-linked lymphoproliferative disorder*

CHAPTER 1 - INTRODUCTION

1.1 Epstein Barr virus

Epstein-Barr virus (EBV), a member of the gammaherpes virus subfamily, is characterised by high prevalence (>95%) within the adult human population, lifelong asymptomatic infection, low pathogenicity in the majority of infections and oncogenicity in a minority of cases. It is associated with a wide range of conditions ranging from the relatively benign (infectious mononucleosis), to association with at least 9 human malignancies. As well as cancer, EBV can play a driving role in the inflammatory conditions haemophagocytic lymphohistiocytosis (HLH) and chronic active EBV (CAEBV), and is associated with multiple sclerosis (MS) and chronic fatigue syndrome.

The history of EBV

The story of the discovery of EBV has passed into folklore as an example of serendipity in science. Denis Burkitt, a young Irish surgeon working in Uganda, described a childhood tumour, Burkitt lymphoma (BL), predominantly affecting the jaw. In an attempt to map its distribution within the country, he surveyed medical units throughout Africa and determined that the disease was not seen at altitudes above 5000 feet. In order to further clarify the situation, he toured the hospitals at the south-eastern tail of the tumour distribution – his famous "tumour safari" - and determined that the critical environmental variable for the tumour was

temperature, rather than altitude, as the “safe” altitude diminished as they travelled further from the equator (1), as shown in figure 1-1.

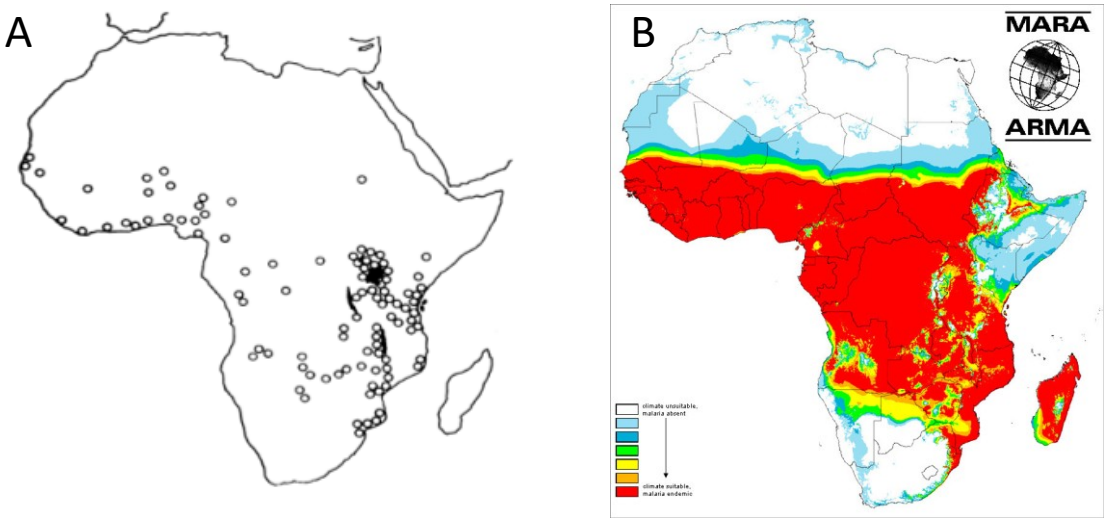

Figure 1-1 - A. Distribution of endemic Burkitt lymphoma in Africa (from (1)) B. Distribution of holoendemic malaria in Africa (2).

This raised the possibility of an arthropod-borne disease, and it is now known that endemic BL is associated with holoendemic malaria, although the precise mechanism for the association remains unclear. However, during the quest for the infectious agent, in 1961 Anthony Epstein, an enthusiastic young pathologist, listened to a lecture by Burkitt and became intrigued by the as-yet-unknown virus. He was first able to see the virus by electron microscopy in cultured cell lines derived from Burkitt lymphoma (BL) biopsies (3). The presence of a transmissible oncogenic agent was demonstrated when co-culture with irradiated Burkitt cells resulted in the immortalisation of primary lymphocytes (4). Finally, viral DNA was demonstrated in fresh tumour tissue (5), confirming its presence in the tumour *in vivo*.

Structure of the virus

EBV is a member of the herpesvirus family, which is subdivided into α, β and γ subclasses; EBV together with Kaposi Sarcoma herpesvirus (KSHV) belong to the latter group.

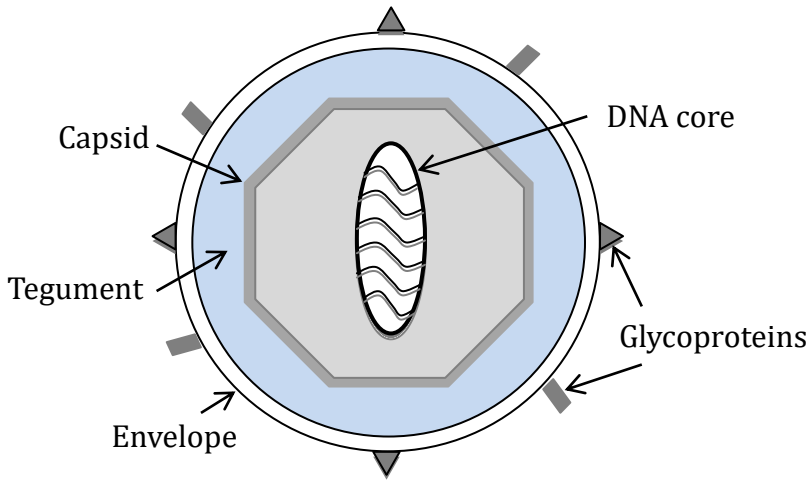

Figure 1-2 – Schematic diagram of the structure of the EBV virion. The viral genetic material is wound around a protein core; this is surrounded by a nucleocapsid, then a tegument, and the whole is contained within a virus envelope studded with glycoproteins.

The core of the virus is composed of a doughnut-shaped protein core containing the viral genetic material, linear double-stranded 184 kilobase pair (kbp) DNA (dsDNA). The DNA is contained within a nucleocapsid made of 162 capsomers surrounded by a protein tegument and all contained within the virus envelope (6). The envelope is derived from the plasma membrane of the infected cell and is embedded with the glycoproteins gp350, gp42, gH/gL and gB (7) (see figure 1-2). At each end of the linear DNA is a terminal repeat (TR) region consisting of 4-12 copies of a 500bp tandem, reiterated sequence. When the viral DNA enters the target cell

nucleus, the DNA circularises by recombination of these terminal repeats generating the characteristic episomal viral DNA with subtly different sizes of terminal repeats (see figure 1-3) (8, 9). When infected cells replicate, the episome is also faithfully replicated so that each daughter cell will contain identical episomes (10); this can be exploited to demonstrate clonality of the infected cells. This is particularly useful when considering EBV-associated malignancies, (see section 1.2).

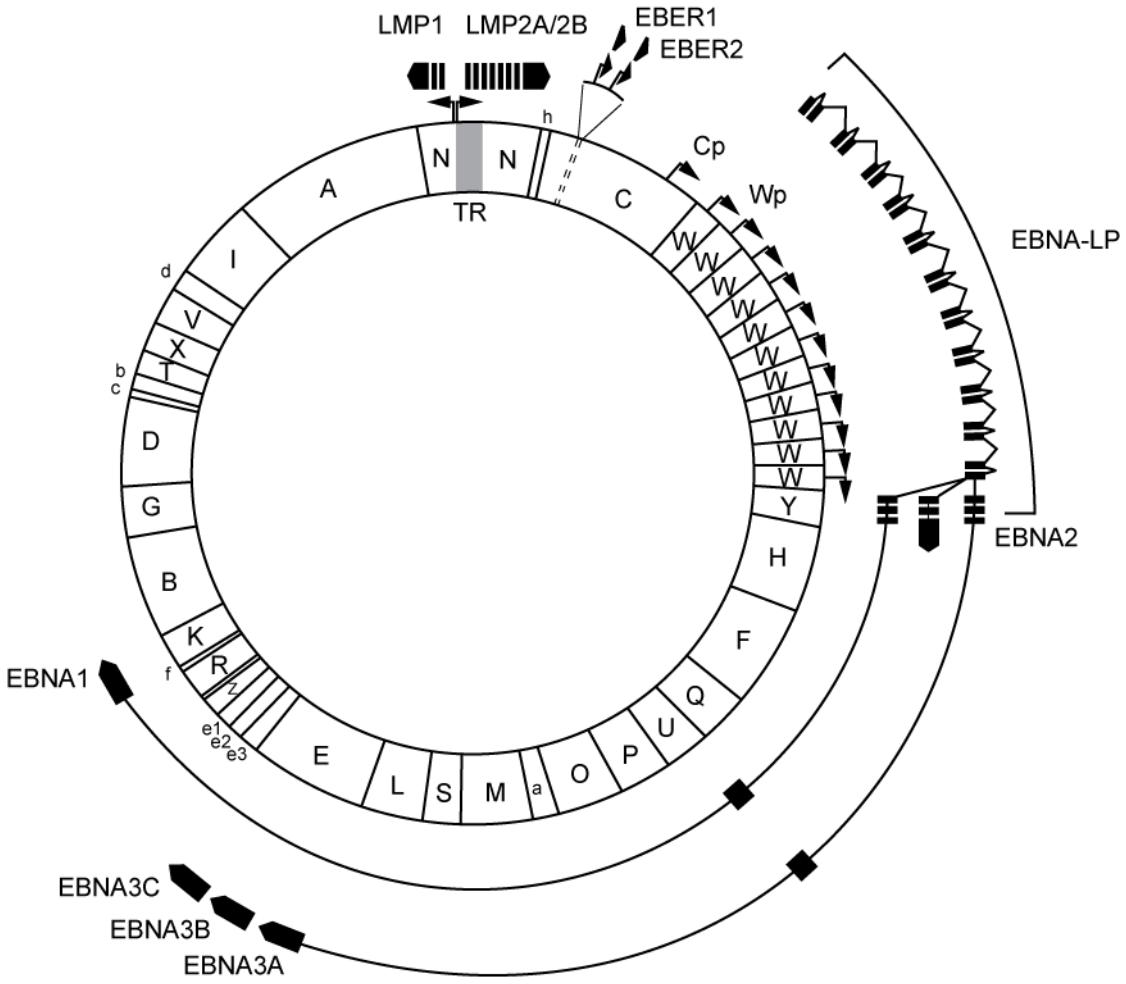

Figure 1-3 - Structure of the EBV genome. Capital letters are used to designate BamH1 fragments, small arrows represent transcription promoters, solid boxes represent latent gene coding sequences and the grey box represents the TR segment. Reproduced by permission of Prof M. Rowe.

EBV was the first herpes virus to be sequenced in its entirety. A first map of the virus was produced by analysing restriction enzyme fragments of the B95-8 strain (11). It was subsequently sequenced by sequencing EcoR1 or BamHI restricted cloned fragments (12). As a result, the virus is still organised by BamHI fragments, which are named alphabetically by size. There are 2 major strains of the virus, EBV-1 and -2 (or -A and –B). Type 1 is much more common except in equatorial Africa and Papua New Guinea, which are interestingly the areas where BL is endemic (13). The main differences between the virus strains are observed in the DNA sequences of EBNA-2 and EBNA 3A/B/C (14). The majority of the viral DNA sequence is otherwise generally well-conserved, although there are numerous polymorphisms which have revealed geographical variation of the viruses (15). In general, patients with EBV-associated cancers have the same virus strains as their healthy counterparts; no mutations have been identified which correlate with disease or cancer (16-18).

Cell entry

EBV efficiently infects B-cells following the interaction between the viral envelope glycoproteins gp350 and gp42 with the B cell specific CD21 and HLA class II, respectively. This interaction triggers recruitment of gH/gL to the binding complex and then endocytosis of the virus, whereupon the fusion protein gB interacts with an unknown receptor to trigger fusion between the viral envelope and the endosomal membrane, releasing the capsid into the cytoplasm. In epithelial cells, which lack CD21, virus is transferred from the surface of B-cells via a B lymphocyte: epithelial cell synapse which creates a very close interaction between the two cells,

thereby enabling transfer of the virus from the B cell to the epithelial cell (19). Binding to the epithelial cells occurs through the interaction of gH/gL with the integrins $\alpha v\beta 5$, $\alpha v\beta 6$ and $\alpha v\beta 8$. This triggers recruitment of gB and fusion of the viral envelope with the plasma membrane (20). In T- and NK-cells, which also lack CD21, it is not clear how infection occurs *in vivo*, and despite isolated reports to the contrary (21), it has, until recently, been considered impossible *in vitro.* A recent publication has suggested that type 2 EBV may be able to infect $CD8^+$ T-cells *in vitro* resulting in cell proliferation and aggregation, viral gene expression and dysregulated cytokine release (22). However, there are several criticisms to be made of this study. Firstly, there is no evidence that type 2 EBV infects T-cells *in vivo*; all of the cases published or studied by our group involve type 1 virus. Secondly, the methods used by the authors involved concentrating large volumes of cell culture supernatant by centrifugation; this inevitably results in contamination of the cell culture with debris and is likely to be sufficient to activate T-cells independent of any virus activity. The authors show LMP1 expression by Western blot at 24 hours; this seems implausibly early to represent true latent infection.

Occasional EBV-positive T- and NK cells are seen in the blood (23), tonsils (24, 25) and lymph nodes (26) of infectious mononucleosis patients, although the significance of this is not clear.

Life cycle

Despite 50 years of intensive research, there is still considerable uncertainty surrounding the details of the virus life cycle, primarily because initial infection by EBV is usually asymptomatic.

It is known that primary infection is often a result of ingestion of infected cells, or cell-free virus, in saliva, and as such either occurs in infancy due to sharing utensils and toys, or in adolescence due to early romantic liaisons. The virus is also found in genital secretions, but it is unlikely that direct sexual transmission occurs in the absence of salivary contact (27). Once it has entered the host little is known about how the virus infects the B-lymphocyte population and two main theories prevail: firstly, EBV may directly access B-cells in the lymphoid-rich oropharynx across gaps in the single-cell thick epithelial cells, such as in the tonsillar crypts (28). Secondly, EBV may directly infect oropharyngeal epithelial cells, replicate and infect underlying B-cells with new progeny virus (25, 29). In either case, it is thought that the infected naïve B-cells, which express the viral latency-associated proteins, enter the circulation where the majority are eliminated by the innate immune system (6). The virus establishes a life-long persistence in memory B-cells.

There are two possible pathways by which the infected B-cells establish a pool of virus in memory B-cells. The "germinal centre" model (30) suggests that the remaining infected naïve B cells, together with their uninfected counterparts, are trafficked to the germinal centres of lymph nodes and there undergo class switching and somatic hypermutation to become memory cells – the normal process of B-cell maturation. At this stage, B-cells without surface immunoglobulin (Ig) with a high-affinity for antigen would usually undergo apoptosis; the viral proteins LMP1 and LMP2 can rescue infected B-cells (31), however, and allow them to differentiate into memory cells and return to the circulation, providing a pool of virus within the blood – approximately one in $10^{5\text{-}6}$ peripheral blood B-cells. In healthy, EBV-positive patients

the virus is found almost exclusively in the memory cell compartment. No viral proteins are expressed in the majority of these cells which makes them poor targets for the immune system (6, 32). In the "direct infection" model, it is postulated that the virus infects memory B-cells, which have already undergone the germinal centre reaction, and drives their proliferation.

There are, however, problems with both of these models. EBV can be found in non-isotype switched B-cells (33), suggesting a germinal-centre-independent route of infection; this is highlighted in the case of XLP where germinal centre formation is absent and yet the virus persists in non-switched memory cells (34). This suggests that EBV may be able to make B-cells into memory cells itself without the need for the germinal centre.

In order to infect new hosts and to maintain the pool of infected B-cells, the virus must be stimulated to enter productive (lytic) replication. Viral lytic replication can occur in both B-cells and the oropharyngeal epithelial cells. In B-cells, lytic reactivation is thought to be stimulated by memory B-cell differentiation into plasma cells (35). However, in the oropharynx, EBV undergoes lytic reactivation in the differentiated epithelial cells (36), where virus is shed into the saliva and is thereby passed onto new, susceptible hosts.

Transformation of B-cells

When primary B-cells are infected with EBV, they become growth-transformed and, as lymphoblastic cell lines (LCLs), can grow indefinitely in culture. The value of this to the study of

EBV virology has been immense, and as a result it is a particularly well-documented phenomenon.

Once the virus has entered the B-cell, transcription of the viral genome is initiated by host RNA-polymerase from the Wp promoter (see figure 1-3), resulting in the expression of the viral proteins **E**pstein-**B**arr **N**uclear **A**ntigens **L**eader **P**rotein (EBNA-LP) and EBNA-2, which reach the levels seen in a mature LCL by 24-36 hours after initial infection (37). Promoter use is switched from Wp to Cp by EBNA-2 (see figure 1-3), and it has recently been shown that by 36 hours after the initial infection both the Wp and Cp promoters are active (38). From the Cp promoter the virus is able to express the 6 nuclear proteins EBNA-1, -2, -3A, -3B, -3C and –LP. EBNA-2 also acts to upregulate expression of the viral **L**atent **M**embrane **P**roteins LMP1 (39), LMP2A and LMP2B (40) – these, along with the EBNA proteins, complete the nine viral proteins expressed in the "latency III" pattern (41). By 72 hours the majority of the infected B-cells have divided. In order for transformation to take place, the viral proteins LMP1 (42, 43), EBNA-2 (44), EBNA-3A and EBNA-3C (45) are essential. Expression of the EBNA proteins from the Cp and Wp promoters is only seen in B-cells (46, 47); in other cell types the Q promoter (Qp) is responsible for latent EBNA expression, and apparently only EBNA-1 is expressed (6, 48-50).

Epstein Barr Virus Latency

The ability to sustain a latent infection in a host is an important survival feature of human herpes viruses. As the name suggests, the virus is maintained in the infected cell in a 'dormant' state; thus proliferation and de-novo virus production have ceased. What have become known as the EBV latency gene expression profiles were identified in EBV-associated malignancies and

EBV-transformed B-cell lines; in these scenarios, whilst the virus is not undergoing lytic replication, a limited number of "latent" genes are expressed consistent with the proliferative states of the malignant or transformed cells. The virus employs its different promoters to express different patterns of gene expression; these profiles can be classified as latency I, II and III (see figure 1-4). Different EBV-positive malignancies have been shown to be associated with different latency states (see table 1-1); however, this model should be considered as a framework rather than a prescriptive list. To illustrate this point, extranodal NK/T lymphoma (ENKTL) is considered a latency II tumour, yet LMP1 is not expressed in every case (51). Furthermore, even within LMP1-positive tumours, LMP1 may be expressed in only a subset of malignant cells (52). Despite this, the latency I/II/III nomenclature is widely used and has proved useful.

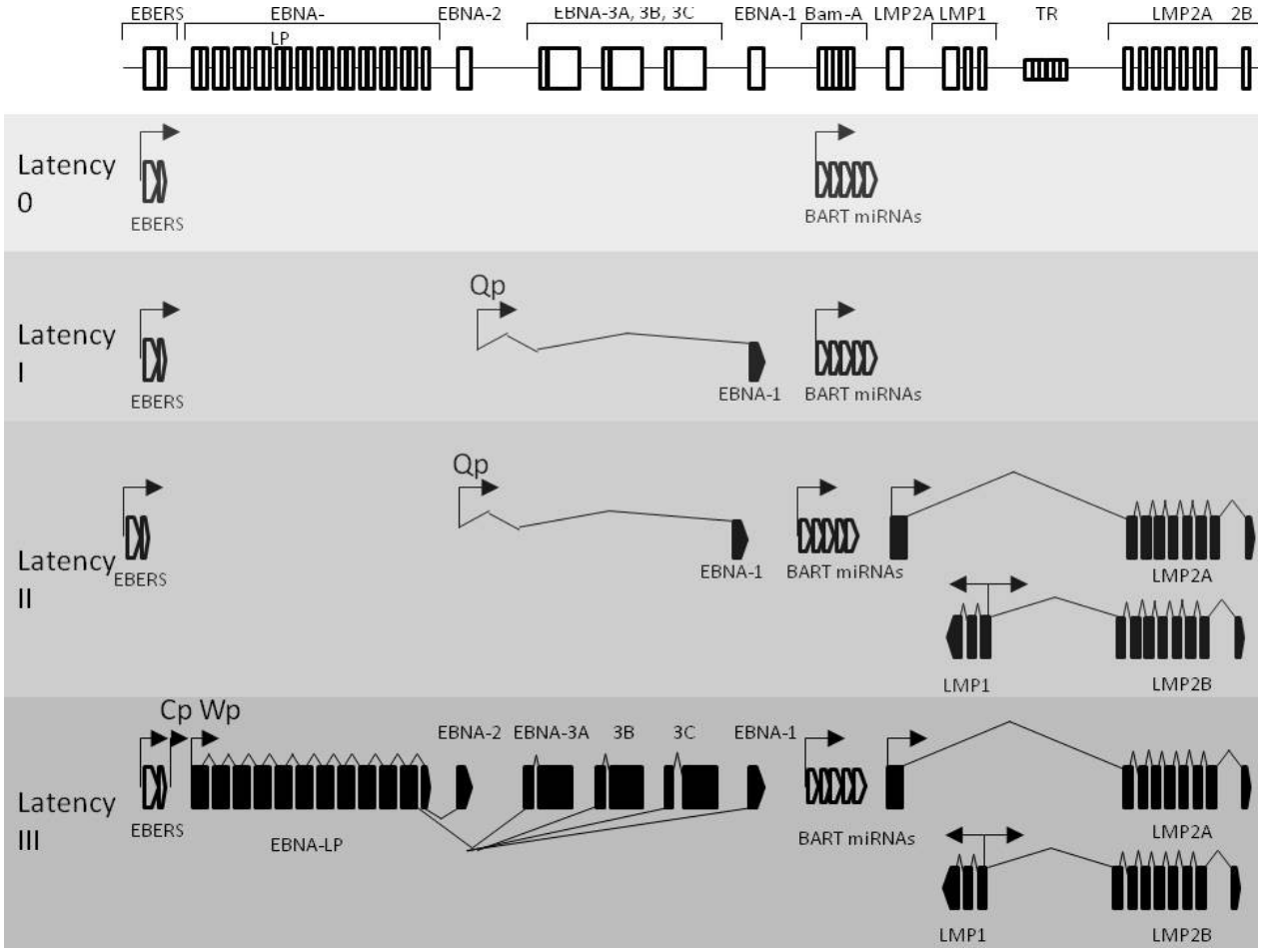

Figure 1-4 – Schematic of how different viral latency patterns arise. The EBV genome is shown in the top panel. Open boxes indicate reading frames for latent genes. Small arrows indicate viral promoters, open arrow heads show non-translated RNA, closed arrowheads show translated gene products. Redrawn from (69).

Table 1-1 - Latency patterns seen in various EBV-associated malignancies.

Latency pattern	Cell of origin	Malignancy	Viral proteins expressed
I	B cell	BL	EBNA-1
I/II	Epithelial cell	Gastric carcinoma	EBNA-1, LMP2
II	B cell	HL	EBNA-1, LMP1,2
		DLBCL of the elderly	EBNA-1, LMP1,2
	T/NK cell	ENKTL	EBNA-1, LMP2, LMP1 (+/-)
		Angioimmunoblastic T-cell lymphoma	EBNA-1, LMP2, LMP1 (in B-cells)
	NK	Aggressive NK leukaemia	EBNA-1, LMP1, LMP2
	Epithelial cell	Nasopharyngeal carcinoma	EBNA-1, LMP2, LMP1 (+/-)
III	B cell	PTLD	EBNA-1, -2, -3a, 3b, 3c, -LP; LMP1, LMP2
	B cell	DLBCL	EBNA-1, -2, -3a, 3b, 3c, -LP; LMP1, LMP2

This list is not exhaustive but demonstrates the range of viral proteins expressed. Hodgkin lymphoma (HL), diffuse large B-cell lymphoma (DLBCL), extranasal NK/T-cell lymphoma (ENKTL), EBV-encoded RNA (EBER).

The maintenance of EBV in B-cells is achieved by carefully balancing the need to limit viral gene expression in order to reduce immunogenicity of the infected cells, and the need for the virus to replicate and maintain its cellular presence. In memory B-cells *in vivo*, the virus gene expression is limited to the EBERs; no viral proteins are expressed. This is now termed latency 0 (6, 53).

In contrast, Latency III (discussed above) is not only observed in transformed B-cells (LCLs) following infection *in vitro,* but it is also observed *in vivo*, in post-transplantation lymphoproliferative disorder (PTLD) (54) and infectious mononucleosis (IM) (55). By its nature, PTLD affects immunocompromised patients, and the initial treatment is always, where possible, to reduce immunosuppression (56); this is effective as so many viral genes are expressed that the infected cells are highly immunogenic. Most EBV-associated malignancies, however, rely on

restricting their viral gene expression to slip under the radar of the host immunological response. This is possible because changes in cellular gene expression make it unnecessary for the full complement of latent genes to be expressed.

The Latency I pattern of viral gene expression is characterised by the expression of EBNA-1 from the Qp, the EBERs and miRNAs plus the silencing of the Wp, Cp and LMP promoters. Latency I is consistently observed in endemic BL. However, cell lines adapted from endemic BL are frequently observed to "drift" towards a Latency III phenotype, with expression of EBNA-2 and LMP1, suggesting that Latency III is the default viral expression pattern in B-cells in the absence of host immune control.

Latency II is an intermediate pattern of EBV gene expression and was originally identified in undifferentiated nasopharyngeal carcinoma (NPC); it is now considered to include the viral gene expression pattern observed in ENKTL, Hodgkin lymphoma (HL) and gastric carcinoma. Like latency I, latency II is characterised by the expression of EBNA-1 from the Qp promoter plus the EBERs and viral micro RNAs (miRNAs). Additionally, the latent membrane proteins LMP1, LMP2A and LMP2B are expressed. However, as stated above, there is considerable heterogeneity in expression of the LMPs, both between and within tumours of the same type (52, 57).

EBV Latency-Associated Proteins

The vast majority of our knowledge of the role of EBV proteins comes from work on either B-lymphocytes or epithelial cells – the "natural" hosts of the virus. There is some evidence that at least some of the effects of the proteins are different according to the cell background (58), and this must be borne in mind when considering the following descriptions. Transformation of B-cells, as discussed, requires the co-operative action of at least 5 latent genes, and loss of any one of these will result in substantial impairment to the transformation process. Similarly, EBV-associated malignancies generally express characteristic subsets of latent genes that may reflect either the cell of origin of the tumour, or alternatively the specific pathogenesis of this disease. Cellular mutations associated with each type of malignancy may substitute for some EBV transforming functions, thus allowing a more restricted pattern of viral gene expression in the established tumour (with the immunological advantage that this presents). For example, in BL the overexpression of the oncogene *myc* along with other cell-cycle genes is thought to be the prime proliferative driver in the established tumour, and the continued presence of EBV may only be required to provide a survival advantage, thus allowing the virus to express a more restricted number of genes and gain a useful immunological advantage.

EBNA-1

The primary function of EBNA-1, which is expressed in every EBV-associated malignancy, is to facilitate replication of the circularised EBV episome during cell division to ensure efficient transmission to progeny cells (59). It contains a glycine-alanine repeat region which inhibits its

degradation and reduces its presentation by host cell MHC class I molecules thereby reducing its immunogenicity (60, 61). Potential oncogenic actions include protection from p53-mediated apoptosis (62) and contribution to cellular genomic instability via the induction of reactive oxygen species; the resulting DNA damage may explain in part how EBV contributes to malignant transformation of cells (63).

EBNA-2, -3 and –LP

EBNA-2 and EBNA-LP are the first proteins expressed by the virus in latent infection of B-cells. EBNA-2 is vital for EBV-mediated growth transformation, and it is speculated that the differences in EBNA-2 may explain why the EBV type 2 strain is less efficient at transforming lymphocytes *in vitro* (44). EBNA-2 activates transcription of the cellular proteins CD23, CD21 and CMYC (6, 37, 39, 64-67). EBNA-LP augments the actions of EBNA-2 on the promoters of LMP1 and LMP2B, and is important for transformation (68).

There are 3 members of the EBNA-3 family, designated EBNA-3A, EBNA-3B and EBNA-3C. The EBNA-3A/B/C family of proteins is particularly interesting as it is highly immunogenic and is a potent target for cytotoxic T-lymphocytes (CTLs) (69, 70). EBNA-3A and 3C are important for B-cell transformation into LCLs (45, 71). In contrast, EBNA-3B is dispensable for transformation but seems to act as a tumour suppressor gene by attracting host T-cells to the tumour (72).

LMP1

Latent **M**embrane **P**rotein 1 (LMP1) is considered the key protein in EBV-induced cellular transformation. It is critical for EBV-induced B-cell transformation (42) and functions as a classical oncogene in rodent fibroblast models (6, 73); LMP1 expression under the control of the Ig promoter in transgenic models is associated with the development of lymphoma (74). LMP1 can inhibit cellular differentiation in epithelial cells (75) and can cause the downregulation of CD10 and upregulation of CD11a, CD23, CD40 and CD54 – similar to the changes seen in the cell surface phenotype upon EBV infection of B-cells (76-78). It acts as a constitutively active tumour necrosis factor receptor (TNFR), resembles CD40 functionally, and provides growth and differentiation signals to B-cells. It is a key modulator of cell signalling via the NFκB (79) and JNK (80) pathways and induces expression of a number of anti-apoptotic proteins, including BCL2 and A20 (TNFAIP3) (81, 82), as well as adhesion and activation proteins.

First described in 1984 (83), LMP1 is a 63 kDa protein with a short amino and long carboxy terminal spanning 6 transmembrane domains, which oligomerises in the plasma membrane independent of any ligand binding, enabling it to be constitutively active (84, 85) (see figure 1-5). The amino terminal is necessary to tether the protein in the plasma membrane (86), and the transmembrane loops are required for oligomerisation. The cytoplasmic tail is necessary for the transforming properties of the protein (87).

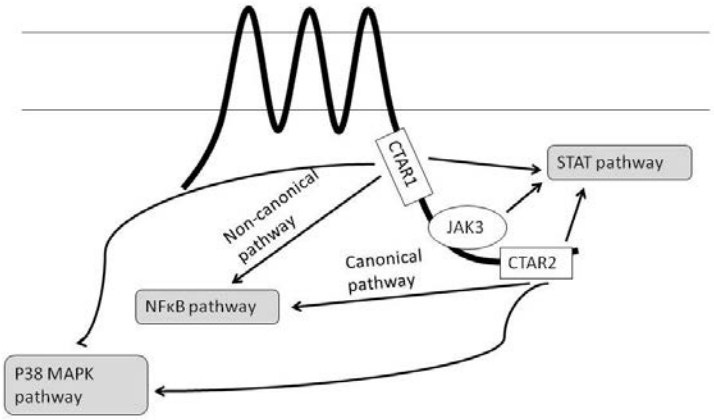

Figure 1-5 Schematic representation of the structure of LMP1. The protein has 6 transmembrane segments and a long cytoplasmic tail. The two C-terminal activating regions (CTARs) can activate downstream signalling via the NFκB, STAT and MAPK pathways. From (88).

The cytoplasmic C-terminal contains two "C-terminal activating regions" (CTAR1 and 2), which are vital for the recruitment of factors which stimulate various intracellular signalling pathways (79). Between them they can activate the canonical and non-canonical nuclear factor κ B (NFκB) pathway, which is important in multiple cellular processes including apoptosis, differentiation and proliferation, and there is evidence that blocking it may remove the ability of EBV to transform B-cells (89). In EBV-infected cells, NFκB is responsible for upregulating cytokines, antiapoptotic proteins and cell surface antigens such as CD40 (88). High-throughput RNA sequencing of the effects of CTAR1 in C33 epithelial cells showed enrichment in growth, survival, migration and proliferation pathways (90).

Other cellular signalling cascades are also activated by LMP1. The mitogen-activated protein kinase (MAPK) pathway (91) is important in mediating cellular responses to external stimuli.

The Janus kinase/Signal Transducers and Activators of Transcription (JAK/STAT) pathway is a major pathway for the transduction of signals from cytokine and growth factor receptors (92) and was thought to be activated by LMP1, although it is not clear whether this is a direct effect (93).

The **i**nterferon **r**egulatory **f**actor IRF7 pathway is also likely to be important. IRF7 is expressed in lymphoid cells (94); it is both induced by and induces LMP1 (95), is co-expressed in some EBV-positive lymphomas and acts to enhance its effect on growth transformation of fibroblasts (96). LMP1 has been shown to activate the c-**J**un **N**-terminal **k**inase (JNK) pathway, known to be important in cellular proliferation and differentiation, via the CTAR2 pathway; this is independent of the NFκB pathway (80) and has an important role in LMP1-induced lymphocyte transformation (97).

LMP2A and B

Transcripts for the Latent Membrane Proteins LMP2A and LMP2B-TR share the majority of their sequence but are generated by transcription from different viral promoters (see figure 1-4) (98). Interestingly, the transcripts span the TR section of the genome; this suggests that the virus must have assumed its circular form before transcription can take place (99). The first exon of LMP2A encodes 119 amino acids whereas the first exon of LMP2B is non-coding; they then share the remaining 8 exons after the TR (98). In structure, they are characterised by 12 membrane-spanning domains with a cytosolic C-terminal domain. Although these proteins

facilitate immortalisation (100) and lytic cycle, they are not essential for B cell transformation *in vitro*. LMP2A can act as a "surrogate" B-cell receptor to drive the proliferation and survival of B-cells (101) via constitutive activation of the Ras/PI3K/Akt pathway (102), such that its expression can rescue B-cells with crippled Ig genes from apoptosis (103). Its expression is vital for the survival and proliferation of infected B-cells in culture, and also for their early activation and proliferation (104). LMP2A can also activate the Ras/PI3K/Akt pathway in epithelial cells (105).

Multiple cell signalling pathways have been hypothesised to be influenced by expression of LMP2A and B (see (106) for review). LMP2A can modulate signalling by the B-cell receptor (BCR) by blocking its phosphorylation after cross-linking (107); amongst other things this prevents the BCR-induced switch from latent to lytic cycle (108). LMP2A and 2B co-localise in B-cells, and LMP2B antagonises the effects of LMP2A by impairing the phosphorylation of its N-terminus, and thus prevents its effect on BCR signalling (109) and facilitates the switch to lytic cycle (108). It appears that LMP2B is not important in long-term growth of EBV-infected B-cells in vitro, and has no major role in their activation, proliferation or survival in the early stages of viral infection (104).

In epithelial cells, LMP2A and 2B can increase cell spreading and motility, and in contrast to the situation in B-cells, seem to have similar roles (110, 111). They are both also involved in limiting the response of epithelial cells to interferons α and γ by increasing the turnover of their receptors (112). There are very little data available on the roles of LMP2A or LMP2B in T- or NK cells.

EBERs

EBER transcripts are double-stranded RNA molecules that are the most highly expressed viral gene products in EBV-transformed cells. This abundance has proven to be particularly useful in the detection of EBV in tissue samples, with *in situ* hybridisation providing a sensitive and specific assay in fixed and fresh tissues. They are predicted to form a double stranded structure and associate with the cellular protein La (113).

The function of EBERs in B-cells remains enigmatic. There is some evidence to suggest that EBER expression can protect cells from apoptosis and contribute to cell transformation and proliferation (114, 115). EBER1 transcripts are detected in the culture supernatant of BL and LCLs, and in the serum of patients with EBV-associated inflammatory disorders including haemophagocytic lymphohistiocytosis (HLH), chronic active EBV (CAEBV) and infectious mononucleosis (IM) patients (116). The transcript can act via the toll-like receptor 3 to induce the release of inflammatory cytokines from cell lines, as well as inducing the activation of dendritic cells in culture. This leads to a model whereby EBER1 could be responsible for the marked and often overwhelming immune response to EBV infection seen in these conditions (116). La is present in exosomes produced by epithelial cells, suggesting that EBER1 may be actively secreted in combination with the protein (117). EBER2 is seen at much lower levels but is probably transcribed at similar rates at least in cell lines; it has a much shorter half-life, which may explain the lower levels (118).

miRNA

MicroRNA (miRNA) describes a non-coding RNA which acts to regulate translation of messenger RNA by binding it and either preventing translation or accelerating its degradation (119). There are at least 700 human miRNAs described to date, of which many have been implicated in oncogenesis (120). EBV itself encodes at least 44 miRNAs from 25 precursors (120), with potential targets including cell cycle control, apoptosis and transcription (121). EBV miRs are clustered within 2 areas of the viral genome, the BART (BamH1-Associated Rightward Transcripts) and the BHRF1 cluster (see figure 1-4). In general, the BHRF1 cluster miRs are only expressed during latency III or lytic cycle, and thus are not seen in either HLH or ENKTL, whereas BARTs are expressed at low levels in all forms of lytic and latent infection (6). The expression and function of the BART miRNAs in nasopharyngeal carcinoma, another EBV-associated malignancy with a 'latency II' pattern of EBV gene products, have been more comprehensively studied and are implicated in apoptosis protection (122) (123) and immune evasion; they also inhibit the expression of LMP1 (124, 125) and act to maintain viral latency by inhibiting EBNA-2 (126) (see (127) for review).

BHRF1 and BALF1

BHRF1 and BALF1 are viral homologues of BCL2, an anti-apoptotic protein (discussed in detail below). BHRF1 (128) protects B-cells from apoptosis; BALF1 has a more ambiguous role. In

some cells lines it has been suggested that it may provide apoptosis protection, or it may act by regulating the activity of BHRF1 (129, 130). They are highly expressed in lytic cycle and are thought to prevent apoptosis in response to viral infection, allowing time for more virus to be produced (131). The fact that two BCL2 homologues are expressed suggests the importance of this pathway in the EBV life cycle.

It has recently been shown, however, that BHRF1 is present in latent infection as well – at low levels in LCLs and at very high levels in the context of Wp-restricted Burkitt lymphoma – a subset of the disease where the virus has a mutation resulting in the loss of EBNA-2. Furthermore, the EBNA-2 deletion results in the constitutive expression of the BHRF1 from the Wp promoter, thereby providing the high levels observed. In this latter case BHRF1 is responsible for the marked apoptosis-resistance of these cells in culture (132).

1.2 EBV-associated diseases.

B-cell disorders

Infectious mononucleosis

When primary EBV infection occurs during adolescence there is a risk of between 25 and 70% of developing clinical IM (133-136), an immune-driven, self-limiting illness characterized by lymphadenopathy, sore throat and fever as well as profound fatigue. Large, activated $CD8^+$ lymphocytes can be seen on blood film examination, and are thought to drive the clinical manifestations of the disease as well as giving it its name. Although other primary infections,

notably cytomegalovirus and toxoplasmosis, may cause a similar clinical picture, 90% will be attributable to primary EBV infection.

The association of EBV with (IM) was uncovered when a technician in an EBV research group contracted the condition. She had previously donated cells and serum for laboratory experiments, but it was noted that when she returned to work with IM symptoms she had evidence of EBV infection (137). The link between EBV and IM was then confirmed on various further populations, including army cadets at West Point (138). Of particular charm in this latter study, the peak incidence of IM amongst the young soldiers was in February, 6 weeks after their return from their first Christmas break. Presumably their new haircuts and developing physiques were appreciated by the young women of their home towns.

However, primary infection during adolescence can also be asymptomatic, and it is not clear what determines whether or not IM will develop. One theory is that the size of the viral inoculum may be significant, using for evidence the increased risk of IM in sexually active students, and postulating that deep kissing at the time of intercourse is likely to be the mode of transmission as although the virus is present in genital secretions, the levels are much lower than that seen in saliva (27, 134, 135). HLA type is also important, with polymorphisms at the HLA class I site associated with an increased risk of IM (133), and this, combined with the evidence that prior IM is also associated with the development of Hodgkin lymphoma (139) and multiple sclerosis (140) suggests that the development of IM may reflect a poorer ability by the individual to control the virus (141). This is corroborated by the fact that HLA class I polymorphisms are associated with both IM (133) and EBV-positive Hodgkin lymphoma (142).

X-linked lymphoproliferative disorder (XLP)

The X-linked lymphoproliferative disorders are characterised by excessive and often fatal inflammatory responses to infectious triggers (see (143) for review). XLP1 results from a mutation in the SAP gene, which is expressed in NK, NKT, $CD4^+$ and $CD8^+$ cells. Amongst its other functions, SAP is necessary for NK- and $CD8^+$ T-cell cytotoxicity of EBV-infected B-cells. It is likely that this results in prolonged activation of the cytotoxic cells, and hyperinflammation. When affected boys are infected with EBV they are unable to control the infection and it may prove fatal; if they survive they may progress to lymphoma or dysgammaglobulinaemia. XLP2 is caused by a defect in the XIAP/BIRC4 gene.

Burkitt lymphoma

As discussed earlier, the association of BL with EBV was made early on in the course of its investigation. However, as it became clear that EBV-infection was nearly universal, the temperature-sensitive, presumably arthropod-borne cofactor was sought. Although by then cases had been reported from all over the world, Burkitt and his team focused on Papua New Guinea, the only area outside Africa where the disease was commonly seen, and suggested that common factors between these two locations should be sought (144). Holoendemic malaria (i.e. infection occurring throughout the year) had been postulated for some time to be a common feature in the BL areas, and in 1970 it was accepted that the co-operation between

EBV and high malarial parasite loads was necessary for endemic BL(145). It had initially been observed in 1964 that the distribution of BL mirrored that of holoendemic malaria (146) and as EBV showed no evidence of being vector-borne, mosquito-borne malaria infection was seriously considered as the vector-borne co-factor for BL pathogenesis (147). The evidence for the association is still primarily epidemiological, but it has been shown that there is a positive correlation between BL incidence and malarial transmission intensity (148), that the distribution of endemic BL distribution mimics that of holoendemic malaria, and that reducing malarial burden reduces the incidence of BL in endemic areas (149)

As mentioned above, cases of BL are seen, albeit at much lower frequencies, all over the world. These sporadic BL cases are less strongly associated with EBV (only about 15% are EBV positive (150, 151) compared to close to 100% in endemic BL (152)).

A defining characteristic of BL, regardless of its origin or EBV status, is the presence of a genetic translocation moving the c-myc gene from chromosome 8 into the influence of an immunoglobulin promoter region, either on chromosome 14 (Ig heavy chain), 2 (κ) or 22 (λ) (153). The resulting overexpression of c-myc is necessary for the development of BL, and is sufficient to transform an LCL culture into an EBNA-2-independent, Burkitt-like cell line (154, 155).

EBV-positive BL classically has a “latency I” pattern of infection, with only EBNA-1, EBERs and BARTS transcribed. Transcription of EBNA-1 is initiated from the Qp promoter. However, a subset of BL samples (15%) was shown to carry both the wild-type and an EBNA-2-deleted virus

and exhibited an unusually high resistance to apoptosis (156, 157). These cells do not express EBNA-1 from the Q-promoter, but alternatively use the Wp promoter and express the EBNA-1, EBNA-3A, -B, -C and -LP proteins and the BCL2 homologue BHRF1 (132). This pattern of latency is termed "Wp" restricted BL. Interestingly, in these cases EBNA-2 is deleted, presumably due to its antagonistic effect on c-myc (156), and consequently the latent membrane proteins are not expressed either.

EBV is likely to be important in BL pathogenesis. This is evidenced by its ubiquitous association with endemic cases, frequent association with sporadic cases and stereotyped pattern of viral gene expression. Loss of the viral genome from cultured BL lines results in the loss of transferrable tumorigenicity and increased sensitivity to apoptosis (158); restoring the virus reversed these changes (159). These, along with other studies, suggest that the virus is playing an important role in lymphomagenesis. However, it is still not at all clear exactly how the virus, with its limited viral expression, can contribute to the disease pathogenesis.

Hodgkin Lymphoma (HL)

Hodgkin lymphoma (HL) is a lymphoma of B-cells, characterised by the presence of large, malignant Hodgkin-Reed-Sternberg (HRS) cells in a reactive infiltrate of inflammatory cells (160). It has a bimodal age distribution, with peaks occurring in the twenties and fifties in the West, although the early peak is somewhat earlier in less economically developed countries. It has a slight male preponderance (161). Modern classification defines two subtypes, classical HL and

nodular lymphocyte-predominant HL (162); the latter is likely to present earlier, has a more favourable clinical course and is much rarer than the former (163). Although it has generally been considered to have no association with EBV, this dogma has recently been challenged (164).

EBV was first demonstrated in HL samples in 1987 (165). It is seen in about 40% of HL cases, with an increased prevalence in tumours from children from lower income countries and in males; there are also high incidences in tumours from patients of Asian and Hispanic origin (166). There is a significant association of HL with IM in young adult cases, particularly in EBV positive disease (OR 2.94) , and it is suggested that a late first exposure to EBV (i.e. in teens or early adulthood) may increase the risk of developing EBV+ HL in higher-income countries (167); this is mirrored by a peak in the disease in childhood in lower-income countries, where initial EBV infection is earlier (168). EBV-positive disease in older adults might reflect virus reactivation. However, interestingly IM is also associated with EBV-negative disease, suggesting a shared lifestyle factor between IM and a possible aetiological agent in EBV-negative disease.

Virus is demonstrable in the HRS cells and shows a latency II pattern (6). The virus, specifically LMP2A, is thought to “rescue” cells with crippling immunoglobulin gene receptor rearrangements allowing their progression into Hodgkin Reed-Sternberg (HRS) cells (31, 169).

PTLD

Post-transplant lymphoproliferative disorder (PTLD) encompasses a range of conditions affecting immunosuppressed patients who have undergone either a solid organ or haematopoietic stem cell transplant (HSCT). The phenomenon was first described in 1969 (170) and 90% are associated with EBV, with the majority showing a latency III pattern of infection (171). The current model for the disease is that primary infection or viral reactivation is able to proliferate uncontrolled due to the incompetent T-cell response resulting from iatrogenic immunosuppression. In allogeneic HSCT recipients the incidence is highest between 1 and 5 months after transplantation and falls rapidly after a year; this coincides with the period of maximal T-cell impairment and B-cell regeneration. These epidemiological data, however, precedes the use of Alemtuzamab in conditioning regimens, and may no longer be accurate (172). Overall incidence of PTLD in HSCT recipients is about 1% but if T-cell depletion or anti-T-cell immunotherapy is used this can rise significantly (173), reflecting the vital importance of T-cells in controlling the virus. After solid organ transplant the risk of PTLD varies with which organ was transplanted, but the incidence is highest in the first year regardless, and is increased if the recipient was EBV seronegative at the time of transplantation (171).

The World Health Organisation (WHO) divides PTLD into 4 pathological categories; early lesions, polymorphic PTLD, monomorphic and classical HL-type PTLD (174). Monitoring of EBV viral loads may detect viral reactivation before PTLD develops; the reduction of immunosuppression (where possible) with anti-B-cell antibodies such as Rituximab to target the virus-containing B-cells is routinely used in these situations and has been shown to reduce the risk of developing

PTLD (175). In established disease, conventional chemotherapy is used and, if available, in HSCT recipients donor T-cell infusions may be useful (176).

The malignant cells, particularly in early and polymorphic PTLD, often show a latency III pattern of gene expression, which makes them a very attractive target for infused EBV-specific T-cells, as they express the immunogenic EBNA-3s. There is also evidence that lytic replication may be significant in PTLD, which suggests the possibility of using the immunogenic lytic antigens, particularly BZLF1, as immunotherapeutical targets (177). This is a very promising future direction, and may eventually replace conventional chemotherapy, particularly in bone marrow transplant recipients; however, in monomorphic lesions the expression of viral proteins is often more restricted (178) and immunotherapy is therefore less likely to be successful (179).

Non-B-cell disorders

CAEBV

CAEBV is characterised by recurrent or chronic IM-like symptoms, with high virus loads and unusual serological responses with no previous immunological deficit (180). It was first described in 1978 (181). Early reports of a chronic symptomatic EBV infection (182) relied upon clinical symptoms for more than a year and unusual serological responses with no anti-EBNA, in the background of a previously normal immune system. About 40% of patients have an initial IM-like illness (180).

Intriguingly, in CAEBV cases in Japan, EBV is most commonly found in $CD4^+$ T and NK cells (23, 183-185), whereas in the USA the virus is more usually found in B-cells (186). This is especially interesting when we consider that ENKTL, another EBV-associated NK-cell disorder, is also more prevalent in Asia than the West, which suggests a genetic or environmental predisposition for non-B-cell infection. The mean age of onset is 19 years in the USA but is younger for T-cell disease (7 years) than B-cell (23 years) when they are considered separately (186). In Japan the median age of onset is 14 years, and B-cell disease is very rare (187). Symptoms include fever, lymphadenopathy, splenomegaly, thrombocytopenia and hypersensitivity to mosquito bites; less commonly uveitis, hepatomegaly, pancytopenia, haemophagocytosis, skin rash, oral ulcers, coronary artery aneurysm, interstitial pneumonitis and lymphoma occur (180, 188). The disease is predominantly clonal (187). T-cell CAEBV seems to carry a worse prognosis than NK-cell disease, and is characterised by more prominent fever, lymphadenopathy and anaemia, whereas NK disease has more large granular lymphocytosis and high IgE levels (187-189).

Treatment is difficult in both B- and non-B-cell disease – initial responses to steroids, immunosuppression, chemotherapy and cytotoxic T-cell therapy are not durable and haematopoietic stem cell transplant seems to offer the only chance of cure (186). The prognosis is worse if older than 8 years, if thrombocytopenia is present at presentation and in T-cell disease (187).

Haemophagocytic lymphohistiocytosis

Haemophagocytic lymphohistiocytosis (HLH) describes a clinical syndrome of macrophage activation, cytokine release and haemophagocytosis. It was first described as "histiocytic medullary reticulosis" in 1939 (190). The authors described a syndrome of "asthenia, emaciation and a profound general intoxication" as well as hepatomegaly, splenomegaly, lymphadenopathy, cytopenia and erythrophagocytosis seen on histological examination. Until the first formal international guidelines were published in 1991 (see table 1-2) (191) this remained the only framework for diagnosing the condition. The diagnostic guidelines were revised in 2004 to include hyperferritinaemia, elevated sCD25 and reduced NK cell activity (192). HLH is often insidious and atypical, and clinical features may fluctuate during the course of the illness (193), further complicating the process of diagnosis. It is also useful to think of HLH as the "extreme end of the spectrum of inflammatory reactions " (194) as the published diagnostic criteria are not specific to HLH and will be seen, to some extent, in all patients undergoing a systemic inflammatory response.

Table 1-2. HLH-2004 diagnostic guidelines (193).

5 of the following 8 diagnostic criteria	
Fever*	
Splenomegaly*	
Cytopenias affecting ≥2 of 3 lineages in the peripheral blood*	Hb <9.0 g/dL (10.0 g/dL in infants less than 4 weeks old) Platelets < 100 x 10^9/L Neutrophils < 1.0 x 10^9/L
Hypertriglyceridaemia *	(fasting triglycerides ≥ 3mmol/L) and/or hypofibrinogenaemia (fibrinogen ≤ 1.5 g/L)*
Low or absent NK activity	
Haemophagocytosis in BM, spleen, lymph nodes or liver	
Ferritin ≥ 500mg/L	
Soluble CD25 ≥ 2400 U/ml	
Other supporting evidence	Spinal fluid pleocytosis &/or raised spinal fluid protein Chronic persistent hepatitis on liver histology Cerebromeningeal symptoms, lymphadenopathy, jaundice, oedema, rash, deranged liver enzymes, hypoproteinaemia, hyponatraemia, raised VLDL, low HDL

Primary, or familial, HLH is classically associated with X-linked lymphoproliferative disorder (XLP) as well as with other congenital immunodeficiencies such as Chediak-Higashi syndrome. The genetic mutations associated with HLH to date all involve perforin-mediated cytotoxicity (see table 1-3). Cytotoxic T-cells, NK and NKT cells are able to induce apoptosis in virus-infected or malignant cells by forming an immunological synapse and releasing the contents of their secretory granules into the cytoplasm of the target cell; mutations in this pathway are associated with familial HLH including perforin (195), Munc13-4 which is necessary for required for cytolytic granule exocytosis (196), syntaxin 11 (197) and Munc18-2(198) which are needed for vesicle trafficking.

Table 1-3 - Genetic mutations associated with familial HLH.

Syndrome	Gene	Encoded protein	Chromosomal location	Reference
FHL-1	Unknown	Unknown	9q21.3-q22	Ohadi *et al* (199)
FHL-2	PFR1	Perforin	10q21-q22	Stepp *et al* (195)
FHL-3	UNC13D	Munc13-4 (required for cytolytic granule exocytosis)	17q25	Feldmann *et al* (196)
FHL-4	STX11	Syntaxin11 (vesicle trafficking)	6q24	zur Stadt *et al* (197)
FHL-5	STXBP2/UNC18B	Munc18-2 (co localises with syntaxin 11 and may be necessary for its function)	19p13.2-3	zur Stadt *et al* (198)
Chediak-Higashi	CHS/LYST	Lyst	1q42.1-q42.2	Barbosa *et al* (200), Nagle *et al* (201)
Griscelli	RAB27a	Rab27a	15q21	Menasche *et al* (202)
XLP1	SH2D1A	SAP	xq25	Filipovich *et al* (143)
XLP2	BIRC4	XIAP	xq25	Filipovich *et al* (143)

The most comprehensive international study of HLH to date, the HLH-94 trial, showed a median age of onset of 8 months, and a slight male preponderance, which is postulated to represent undiagnosed X-linked immunodeficiencies (203). The geographical distribution of HLH is similar to that of ENKTL. It predominantly affects young children, with mortality rates around 30%. Immunosuppressive treatment may lead to a complete response and relapse is rare in the West, although possibly more common in Asian countries (204).

The syndrome of HLH can be seen in response to many diverse insults and is seen in both immunodeficient and immunocompetent patients. The triggers include infection, malignancy

and autoimmune diseases (see (205) for review). Infectious associations include leishmaniasis, influenza, parvovirus and hepatitis A (206-208), as well as EBV.

The first coherent suggestion of HLH as a consequence of herpes viral infection was in 1979 (209), when an increase in EBV-specific IgM, consistent with primary infection, was demonstrated in 2 cases of HLH. EBV-associated HLH, which accounts for up to 60% of cases, is now defined as the association of EBV-positivity with the diagnostic criteria above (210), but there is no consensus on how this should be defined which limits its usefulness in the clinical setting. Molecular detection of EBV-DNA in peripheral blood by PCR is commonly used to determine viral load, but variation between laboratories, tests and limits of detection means that there is no consensus on the lower limit of viral DNA necessary to diagnose EBV-HLH. The wide range of reported viral loads in the literature is somewhat concerning, as a low level of detectable EBV-DNA may reflect a "high-normal" virus load, or low-level reactivation as a result of HLH-induced immune dysregulation. In these cases the virus is unlikely to be driving the disease and other explanations should be sought.

Unlike classical EBV infection, where the virus shows complete tropism for B-cells, T-cell infections, particularly $CD8^+$ and NK cell infections, are seen in HLH. T-cell infection was first reported in 1993 (211), and has been confirmed in small studies (23) and case reports in various geographical populations since (see (212) for review). NK cell infection in the context of HLH was first reported in 1995 (213) and has since been confirmed in an adult series in the UK (214), however, it seems to be less common than in T-cells. These observations may provide a useful tool for defining EBV-HLH, whereby non-B-cell infection could become a diagnostic requirement.

As with some EBV-associated cancers, it is not clear how the virus is contributing to the pathogenesis of HLH. EBV infection of T-cells experimentally has been shown to result in the secretion of tumour necrosis factor α (TNFα); culture supernatant from these cells resulted in the activation of a macrophage cell line (215). However, the same group reports that these effects can be attributed to LMP1 (216, 217), and there is evidence that EBERs are the only EBV genes significantly expressed in EBV-associated HLH, at least in adults (218).

HLH in adults is rare, but probably under-reported due to the combination of non-specific symptoms, low diagnostic suspicion and often rapid fatality. This makes the true incidence difficult to estimate, but a recent study in Los Angeles estimated that 0.9 cases per million per year were diagnosed in the region (219).

A humanised mouse model of EBV-driven HLH has recently been developed, and offers exciting possibilities to study this condition in more depth (220). However, EBV is not seen in T- or NK-cells in these mice and so does not exactly mirror the situation in humans, although HLH with the EBV in the B-cell population has been described in XLP patients (221).

Extra-nodal NK/T lymphoma

Extranodal NK/T-cell lymphoma (ENKTL) is a rare malignancy usually affecting the upper aerodigestive tract and consistently associated with the presence of EBV in the malignant cells. Early descriptions of destructive nasal tumours, suggestive of ENKTL, date back over 100 years (222-224), and have been defined variously as “lethal midline granuloma”, “rhinitis gangrenosa

progressive", "polymorphic reticulosis" or "malignant midline reticulosis". The 1994 Revised European and American Lymphoma (REAL) classification suggested the term "angiocentric lymphoma" (225), but it was not until the World Health Organisation (WHO) publication of 1999 that the disease reached its modern name and description (174). The malignant cells were shown to react to anti-T-cell sera in 1982 (226); subsequently, the development of antibodies against the CD56 antigen questioned the T-cell phenotype of the malignant cells (227-229) and it is now considered likely that polyclonal anti-CD3 antibodies in the T-cell sera reacted to the cytoplasmic ε-chain of the CD3 molecule in formalin-fixed, paraffin-embedded (FFPE) material in the original study (230). The discovery that the malignant cells had germline T-cell receptor (TCR) gene configurations supported the idea that, at least in the majority of cases, the cell of origin was a natural killer (NK) cell, rather than a T-cell (229, 231).

The characteristic phenotype of ENKTL, as defined by the WHO, consists of $CD2^+$, $CD56^+$, surface $CD3^-$ (as demonstrated on fresh/frozen tissue), cytoplasmic CD3ε (as demonstrated on FFPE tissues), together with expression of EBERs. A recent review by the International T cell project of 136 ENKTL cases confirmed an NK phenotype and genotype in the majority of cases but also showed a cytotoxic $CD8^+$ phenotype in 14% of the tumours (232).

Epidemiology and clinical features of ENKTL

An aggressive malignancy, ENKTL is very rare in the West, comprising approximately 0.5% of all non-Hodgkin lymphoma (NHL), or 4% of all NK and T-cell lymphomas (233). It is, however, much

more common in East Asia and Central and South America (233, 234). In East Asia in particular it accounts for 4-6% of all NHL and about one third of mature T and NK cell cancers (235, 236). It is not clear why there is such a marked disparity between continents, although, as will be seen, it is similar to that seen in other EBV-associated T- and NK-cell disorders. EBV infection is, however, nearly ubiquitous in the adult population worldwide, so it seems likely that genetic or environmental factors may be implicated.

Within East Asia, where the relative frequency of the disorder allows for more accurate characterisation of patient series, the median age at presentation is 45-50 with a male: female ratio of 2-3:1 (233). Although there are reports of cases in immunosuppressed patients (237-239), the majority are immunocompetent.

ENKTL usually affects the upper aero-digestive tract, characteristically the nasal cavity, and presents with localised symptoms such as a mass, pain or bleeding (240). Extranasal disease may account for up to a quarter of all cases, including adrenal glands (241), uterus (242), skin (243, 244), heart (245) and brain (246), although it is important to bear in mind that there may be co-existing occult nasal disease, and naso-endoscopy and biopsy are recommended even in the absence of macroscopic pathology (233). Primary lymph node involvement is rare in the absence of extranodal disease, but has been described (247). Staging investigations should involve bone marrow examination, although involvement is probably rare (248).

Current treatment

The rarity of ENKTL, even in high-risk populations, means that large-scale studies on treatment options are scarce. Disease is often localised at presentation, leading to an initial vogue for involved-field radiotherapy as a single treatment modality; however, despite initially promising responses, the majority of patients relapse with either local or systemic disease (249). The tumour cells are thought to be inherently chemoresistant due to frequent expression of the P-glycoprotein efflux pump (250, 251), which actively extrudes chemotherapy drugs from the cell (252), and success rates with conventional chemotherapy regimens such as CHOP (cyclophosphamide, doxorubicin, vincristine and prednisolone) are poor (253). However, it has been suggested that the P-glycoprotein expressed by NK cells may differ from the conventional form, and possibly P-glycoprotein expression should not be taken as a reason to abandon anthracycline chemotherapy (254).

With localized disease, impressive results have been reported with upfront radiotherapy combined with concurrent cisplatin as a radiosensitiser, followed by chemotherapy with ifosfamide and methotrexate which are unaffected by the P-glycoprotein pump (255). This group reported an 86% 3 year overall survival, which represents a great improvement on that reported previously.

With disseminated disease at presentation, treatment is much more difficult and response rates are significantly poorer. L-asparaginase, which acts by depleting the milieu of available asparagine, has shown early promise in trials, but outcomes still remain poor (256-258).

Prognosis

A variety of factors have been shown to have prognostic relevance in ENKTL, including serum β2-microglobin (β2m) levels (259), bone marrow involvement (248, 260), low lymphocyte count (261), ki67 overexpression (262) and p53 gene mutation status (263). The Korean International Prognostic Index was developed as a means of determining prognosis in ENKTL, and relies upon stage, performance status, extranodal involvement and non-nasal origin (264). A Japanese group has a similar scoring system that includes "B" symptoms, stage, lactate dehydrogenase (LDH) level and lymph node involvement (265). Most interestingly, a recent study shows that circulating EBV levels act as a marker for tumour mass at diagnosis, and also their fluctuation during the course of treatment is the most significant prognostic factor in patients treated with modern chemotherapy regimens (266).

Pathogenesis and role of EBV in ENKTL

Cellular genetic lesions

Macroscopically, ENKTL lesions are often destructive and ulcerated and, as a result, biopsy specimens tend to be necrotic. Repeated biopsies are often required for diagnosis (267) and, accordingly, availability of unfixed tissue for molecular genetic studies has historically been limited. To date, no disease-defining translocation events have been confirmed although genetic complexity is common (268-270). Deletions of the long arm of chromosome 6 are seen both with conventional karyotyping and with comparative genomic hybridisation (271),

implicating tumour suppressor genes within these regions in the pathogenesis of ENKTL (269, 272).

Comparative genomic hybridization of NK cell lines and primary tumours showed three candidate genes within the common region of deletion in chromosome 6q21 - PRDM1, ATG5 and AIM1 - and identified PRDM1 as an important target gene by functional studies in cell lines (273). However, another study showed heterogeneity in PRDM1 and suggested alternative candidate genes such as HACE1, a tumour suppressor gene (272). The limitations of poor-quality and scarce biopsy material, with a reliance on cell lines for molecular studies, means that much more work is needed in this area before these results can be extrapolated to the clinical situation. The JAK/STAT pathway is another promising target as it is constitutively activated in some ENKTL cell lines, and in tumour samples, and is associated with proliferation and migration; the expansion in small molecule inhibitors may make this a promising clinical target (274-276). Interestingly, a single nucleotide polymorphism (SNP) in the gene encoding perforin has recently been described in a series of Caucasian ENKTL patients (277) – as will be discussed later. Perforin mutations are associated with X-linked lymphoproliferative disorder (XLP) which is characterised by overwhelming and often fatal EBV infection.

The role of EBV in T- and NK- lymphomagenesis

The first serious evidence that EBV could be implicated in the development of T and NK lymphomas arose from the observation of 3 patients who went on to develop T-cell lymphoma

after a diagnosis of chronic active EBV (CAEBV)(183). On closer examination, their tumour cells were found to contain clonal copies of the virus, as determined by analysis of the terminal repeat sequence. This suggested that EBV infection of the cell had occurred before its clonal expansion. Subsequently, EBV genomes and/or EBV-encoded RNAs (EBERs) were demonstrated within the tumour cells of both nasal and extra-nasal T and NK lymphomas arising in children and adults (185, 231, 278). The most robust association with EBV was seen in extra-nodal lymphomas and those arising in the nasopharynx (279).

There is compelling evidence that EBV infection of the NK or T-cell is an early event in lymphomagenesis. Firstly, the virus is seen in virtually all cases regardless of patient ethnicity (233, 280), such that the absence of EBV from tumour cells is highly suggestive of an alternative diagnosis (174). Secondly, the virus within the tumour is clonal and EBV genomes are seen in every tumour cell within the lesion (281, 282). Interestingly, a case of ENKTL was recently reported to have lost the viral episome – this coincided with its dissemination to the skin, which might suggest that EBV-loss clones have a metastatic advantage(283). Thirdly, the virus within the tumour cells is expressing transcripts and proteins such as LMP1 and EBNA-1 (52, 282, 284) that have been shown to be important in the growth-transformation of B-cells in vitro and in vivo(285).

Typically there are no more than 20 EBV genome copies per cell. As will be discussed later, this relatively low number suggests latent episomal infection, although higher loads are seen on occasion and may have prognostic relevance (286). Evidence of active lytic cycle within tumour

tissue is relatively rare and limited to only occasional cells (52). It has been proposed that quantification or monitoring of EBV genome copy numbers in serum or whole blood may predict treatment outcome in both advanced and limited stage ENKTL (256, 287-290). However, this is limited by the fact that most qPCR assays will detect both encapsidated virions and cell-free EBV DNA, so high EBV loads in the circulation may simply reflect tumour bulk and necrosis rather than virus replication – although as a surrogate marker for tumour bulk it may have some significance. EBV-containing T- or NK cells are sometimes seen (291), although this has not been systematically examined. In particular, the frequency and significance of EBV-harbouring NK and/or T cells in the peripheral blood at diagnosis and follow-up has not been adequately studied.

What is not at all clear at present is how such a relatively small number of EBV genes can be responsible for the phenotype of ENKTL. Even LMP1, a well-characterised oncogene, has functions that are obscure in T and NK cells. Interestingly, a recent retrospective study examined EBV-gene expression in a cohort of ENKTL patients and found LMP1 expression in only 22 out of the 30 cases studied; the authors also suggest that in these patients, clinical outcomes were superior (51). This has, as yet, not been confirmed in a prospective series, but it may be that the ability to proliferate independent of LMP1 reflects a more damaged cellular genome. There is evidence that LMP1 renders cells more susceptible to DNA damage in response to radiation and chemotherapy, which might confer an improved prognosis (292). It may also be possible that this reflects the known ability of LMP1 to render cells more immunogenic by

upregulating HLA class I (76, 293) as these authors report a cytotoxic infiltrate in one of the LMP1-positive biopsies.

Despite this, however, it is not clear how LMP1 is contributing to the pathogenesis of T- and NK-cell disorders. Interestingly, immunohistochemical studies suggest that LMP1 is only expressed by a subpopulation of ENKTL cells within the tumour (52), and that the proportion of cells expressing the protein can vary between tumours (57). Of course, this could represent fluctuations in expression over time, as seen in LCLs (294), but there is as yet no evidence for this. It is also clear that environmental factors are important since IL-2 deprivation of ENKTL lines results in a fall in LMP1 expression, and IL10, IL15 and IFNγ can all increase it (295, 296). Interestingly, IL-2 is a potent activator of the JAK/STAT pathway in NK cells (297). In contrast to B-cells where LMP1 expression is regulated by EBNA-2s, in the latency II state in ENKTL where EBNA-2 is not expressed, LMP1 transcription initiates from an alternate promoter in the terminal repeat region that is not regulated by EBNA-2 (298, 299). Both the classical EBNA-2-responsive LMP1 promoter, ED1, and the alternate TP1 promoter are responsive to the activation of the JAK/STAT pathway via STAT-binding motifs present in each promoter (300). As discussed above, the JAK/STAT pathway is likely to be an important target in ENKTL, and more work is needed to uncover the connection between LMP1 and STAT *in* vivo (276). In T-cells LMP1 has been shown to upregulate tumour necrosis factor α (TNFα) (216). LMP1 also acts, in B-cells, to inhibit apoptosis by increasing BCL2 levels as well as other anti-apoptotic genes such as BFL1 (301), A20 (302) and Mcl-1 (303). Expression of LMP1 in Jurkat, an EBV-negative T-cell leukaemia cell line, resulted in the induction of BCL3 (304) and downregulation of c-myc (305).

However, in EBV-positive NK lymphoma cell lines, reducing LMP1 expression did not seem to have the same negative effect on proliferation, BCL2 levels and survival that it did in B-cells, and more work is needed to try to unravel the different functions in different cells (58).

LMP2A, and a novel LMP2B-TR transcript, have been shown to be expressed in ENKTL (306). However there is little information available on their function in T- and NK-cells. It is also extremely difficult to reliably demonstrate LMP2 protein expression in ENKTL. Although LMP2A can be detected in paraffin sections using antibodies to the N-terminus, there are no reliable antibodies for LMP2B. Conventional, non-quantitative PCR studies suggested low or absent levels of both LMP2A and 2B in primary tissue (52, 284). Notwithstanding this, adoptive T-cell preparations containing LMP2-specificities were shown to induce meaningful clinical responses in ENKTL patients (307), and LMP2-specific cytotoxic T-lymphocytes (CTLs) can recognise and kill ENKTL cell lines. These findings led to the discovery of a novel LMP2 transcript (306), which lacks the first coding and non-coding exons respectively, of the classical LMP2A and LMP2B transcripts. This alternative transcript is therefore not detected by commonly-used PCR primers designed to selectively detect LMP2A or LMP2B, but is predicted to encode a protein identical to LMP2B. Expression in primary tissue is variable but can be high, suggesting a role in the initiation or potentiation of T/NK lymphomagenesis.

When we come to consider other EBV genes that are expressed in ENKTL, the literature is particularly scanty. With regard to expression, BZLF1 is seen in a small proportion of ENKTL cells (51). There is no significant expression of BHRF1 miRNAs, but BART miRNAs, particularly miR-BART9, are increased (308). The functions of these in the ENKTL setting are not clear. The only

evidence to date of EBNA-1's role in NK cells comes from a report in which partial silencing in an EBV-positive NK cell line reduced proliferation (309). Yang *et al,* with an ingenious selectable recombinant EBV, managed to infect a few cells of a human T-cell line *in vitro* and showed that EBERs were responsible for inducing IL9 (310), which is postulated to act as an autocrine growth factor for ENKTL (311). The BART miRNAs seem to influence LMP1 expression and cell growth, suggesting that they may be significant in lymphomagenesis (308).

In summary, there is very little solid evidence about the role of EBV in ENKT lymphomagenesis, due in part to the relative rarity of the disease, but also to the difficulty in experimentally infecting T and NK cells *in vitro*. The ubiquitous presence of the virus within the tumour, the fact that infection occurs early in lymphomagenesis, and the known oncogenic potential of the virus make it seem inevitable that it has an important part to play.

Aggressive NK-cell Leukaemia (ANKL)

Defined by the WHO as "a systemic proliferation of NK-cells almost always associated with EBV and an aggressive clinical course" (174), aggressive NK-cell leukaemia (ANKL) is a rare but extraordinarily dangerous disorder. Its scarcity means that epidemiological data are based of necessity on a small series, but it appears that the median age of onset is 42 years, and that the male: female incidence is roughly equal (312). As with the other EBV-associated T- and NK-cell disorders, it is more common in Asia than in the West (313). Occasionally it is preceded by a chronic NK-cell lymphoproliferation. There are no characteristic chromosomal abnormalities (312).

The commonest presenting symptoms are fever, B-symptoms, disseminated intravascular coagulation and haemophagocytosis (313, 314). Extramedullary infiltration is common, particularly involving liver, spleen, lymph nodes and skin (312, 313). Central nervous system and gut involvement are also seen (313). EBV genomes are seen within the cells in the vast majority of cases and are clonal, again suggesting EBV infection as an early event in leukaemogenesis (174, 185). There is very little published literature investigating EBV gene expression, although one study suggests the cells are LMP1-negative (315).

Median survival is 58 days from diagnosis (312). There is no consensus on treatment although L-asparaginase seems to have an effect on overall survival (316). Allogeneic bone marrow transplantation is also likely to represent the only current possibility for long-term remission (316).

1.3 Apoptosis

Apoptosis, or programmed cell death, is a vital biological process. Its name, from the Greek word for the process of shedding leaves from a tree, reflects its non-inflammatory, controlled nature, which allows the division of the embryonic fingers, the deletion of autoreactive T-cells, and the removal of damaged cells before they can make a cancer, as well as countless other processes. Although its presence was suspected as a counter-balance to the readily-demonstrable mitosis seen within tissues, it was first named and described microscopically in 1972 in Aberdeen (317). It is characterised microscopically by rounding of the cells followed by blebbing of the cell membrane with the formation of apoptotic bodies, and condensation and

fragmentation of the nucleus. Widespread proteolytic cleavage takes place as a result of activation of the caspase cascade, and the result *in vivo* is removal of the cell by phagocytes.

Apoptosis is particularly interesting in regard to cancers – which can be regarded, at some level, as a failure of apoptosis leading to uncontrolled proliferation of damaged and malignant cells. The process by which cancerous cells are able to escape normal apoptotic triggers, as well as how chemotherapy and radiotherapy affect apoptotic pathways, is currently the subject of intense scrutiny.

It is useful to consider the situations in which apoptosis should normally take place. Firstly, it is a vital process in embryogenesis, which I will not discuss in this thesis. Secondly, it must be able to be induced by immune cells in response to intracellular infection. Thirdly, cells must be able to trigger their own apoptosis in response to stresses such as DNA damage and cytokine or hormone withdrawal. As will be discussed, the various external and internal apoptotic stimuli converge upon an evolutionarily-conserved pathway which results in the conversion of a live cell into a dead one, which can be taken up and degraded by phagocytic cells (318).

Apoptosis pathways

Although described here separately, the three main apoptosis pathways are closely entwined and show substantial areas of overlap (see figure 1-6). They all converge on the final execution pathway.

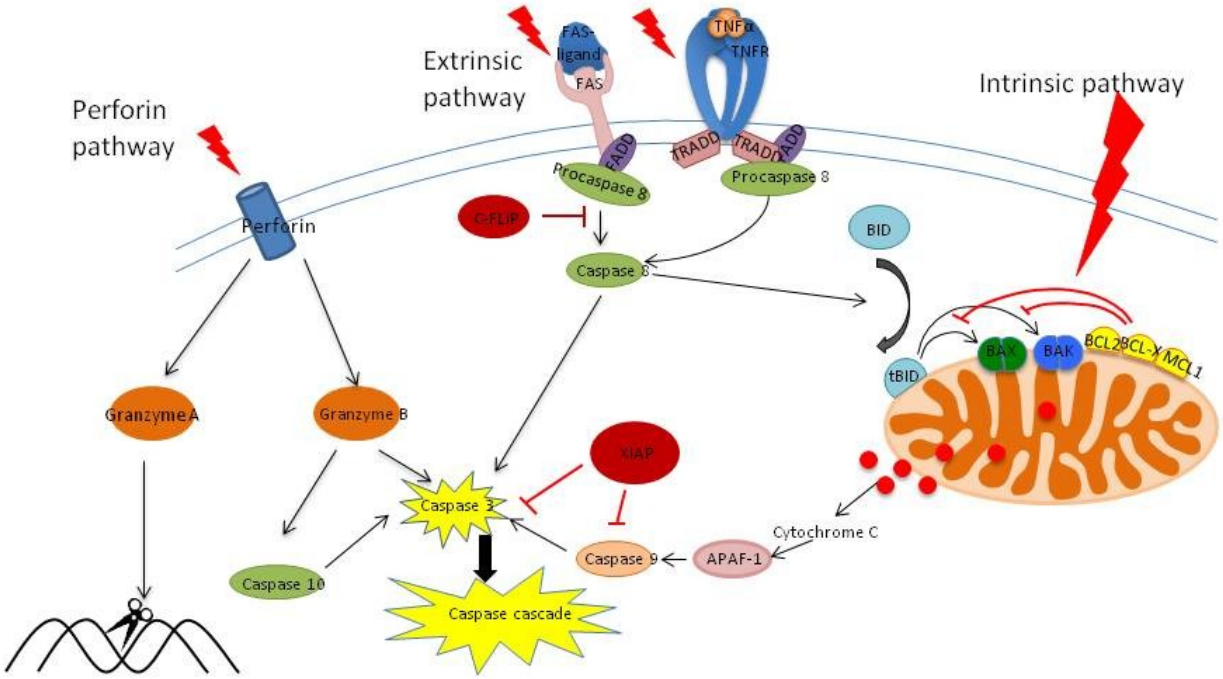

Figure 1-6 - The interaction between apoptosis pathways. There are 3 main apoptosis pathways, which converge upon the activation of the cellular caspase cascade. The perforin pathway is initiated in response to cytotoxic T- and NK-cells; the resultant activation of granzymes A and B results in caspase activation and DNA cleavage. The extrinsic pathway is ligation of cell surface death receptors. Caspase 8 is activated, which in turn activates both caspase 3 and stimulates the conversion of BID to its active form, allowing the activation of the mitochondrial pathway. Intrinsic pathway activation is a result of intrinsic stimuli and results in activation of the mitochondrial pathway. Although a simplification, this figure highlights some of the important proteins in cellular apoptosis.

Execution pathway

Caspases are a family of **c**ysteine-dependent **asp**artate-specific prote**ases** which are the central regulators of apoptosis. This family includes the initiator caspases (including caspase 2, 8, 9, 10, 11 and 12) which are closely coupled to and activated by proapoptotic signals such as DNA

damage, ligation of FAS and withdrawal of growth factors. Once activated, these initiator caspases cleave and activate the downstream effector or "executioner" caspases 3, 6 and 7. These caspases trigger apoptosis by cleaving cellular proteins (319).

The different initiator caspases are coupled to specific pro-apoptotic signals (see figure 1-6). Activation of FAS by FAS-ligand or TNFR by TNF activates caspases 8 and 10. Alternatively, DNA damage induces the expression of PIDD, which binds RAIDD and caspase 2, resulting in the activation of caspase 2. Cytochrome c released from the mitochondria activates caspase 9; pro-inflammatory cytokines activate caspase 11; ER stress activates caspase 12 and 7.

Regardless of the initial trigger, all apoptotic pathways described to date converge on a common execution pathway characterised by the activation of caspases-3, -6 and -7. These exist in healthy cells as zymogen precursors, and their cleavage sets in motion the process which will usually end with the death of the cell. In total, caspases have several hundred known substrates in human cells alone, and this number is continually increasing (320). The cleavage of cytoskeletal proteins results in the rounding of the cell and membrane blebbing (321). The nuclear membrane is also attacked, resulting in fragmentation (322), and the destruction of cell-matrix interaction sites allows the dying cell to withdraw from its surroundings. Cellular organelles are fragmented and DNAse enzymes are activated to degrade nuclear material (323).

Mitochondrial fragmentation is a result of the action of the effector BCL2 family members – BAX and BAK. These permeabilise the mitochondrial outer membrane and permit the release of

mitochondrial intermembrane contents, such as cytochrome c, into the cytoplasm (324). This will be discussed later.

Perforin/Granzyme pathway

Although cytotoxic T-cells can act via the Fas pathway, they can also induce apoptosis by the perforin/granzyme pathway. Here, granules containing perforin and granzyme proteases are released by exocytosis into a tight immunological synapse (325); the perforin, as its name suggests, can polymerise in the cell membrane of the target cell and produce a pore through which the granzymes, as well as water and salts from the extracellular environment, can enter the cell (326). These locate to the nucleus and result in the activation of the apoptotic caspase cascade by the initial cleavage of BID (327). Caspase inhibition will prevent perforin-mediated apoptosis, highlighting the importance of the caspases as final pathways (328).

The importance of the perforin pathway is shown very elegantly by the case of familial HLH, as discussed above. Here, mutations in the pathway proteins result in disease and death within the first few years of life.

Intrinsic pathway

The mitochondrial or intrinsic pathway of apoptosis is initiated by numerous cytotoxic stimuli and pro-apoptotic signal-transducing molecules which act in concert to induce **m**itochondrial **o**uter **m**embrane **p**ermeabilisation (MOMP). This is the common response to a variety of stimuli which can be either negative (for example the withdrawal of a hormone) or positive, including

DNA damage. The increased permeability of the mitochondrial membrane allows the release of pro-apoptotic proteins such as cytochrome c, SMAC/DIABLO and endonuclease G from the mitochondrial intermembrane space into the cytoplasm (329, 330). These proteins then trigger the caspase execution pathway or act as caspase-independent death-effectors.

The BCL2 proteins

The intrinsic apoptosis pathway is mediated to a great extent by a group of structurally related proteins. Named BCL2 proteins after the founding member of the family, they can be divided into 3 groups: the pro-apoptotic BH3-only group, the multidomain anti-apoptotic BCL2 group, and the multidomain pro-apoptotic effector proteins (see figure 1-7).

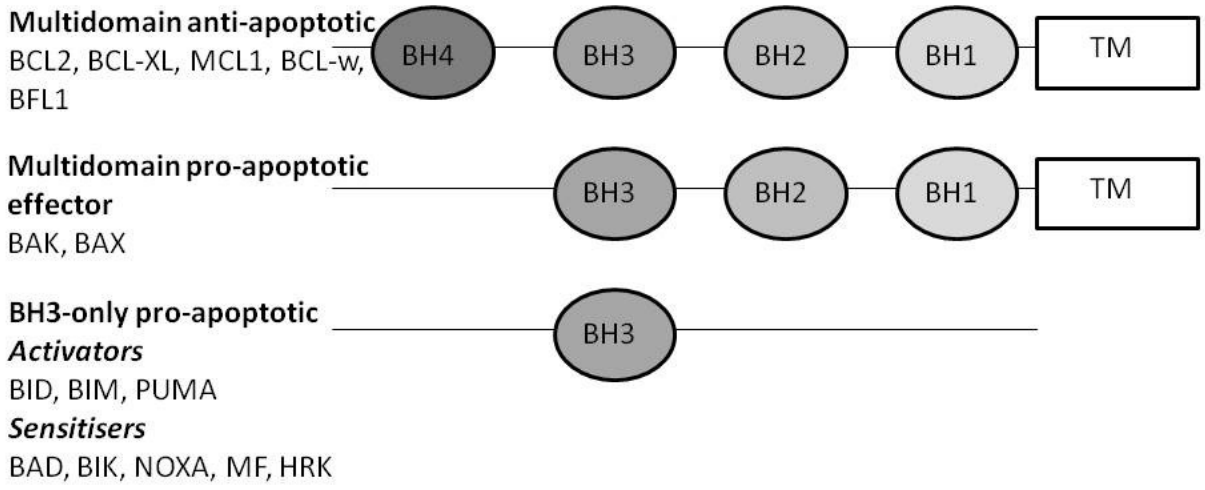

Figure 1-7. The BCL2 family proteins. These can be divided by function and by structure. The multidomain anti-apoptotic group members each contain 4 α-helical BH domains (BH1-4) and a transmembrane (TM) domain. The multidomain pro-apoptotic group have a similar structure but without the fourth BH domain. The BH3-only group, as implied by their name, consist of the BH3 domain only – they can be further subdivided by their function into activators or sensitisers.

BCL2, the founding member of the BCL2 family, was first discovered in 1985. A translocation between chromosomes 14 and 18, which is strongly associated with follicular lymphoma, was shown to put the gene encoding BCL2 into the region of influence of the Ig heavy chain promoter, resulting in its overexpression (331). Introduction into cell lines showed that it promoted cell survival, and could thus contribute to oncogenesis (332).

The structure of the BCL2 family members is highly conserved. The BCL2 and effector protein groups all share four **BCL2 h**omology (BH) domains (BH1-3) whereas the BH3 group have only BH3. BH1, 2 and 3 form a globular structure with a hydrophobic groove which interacts with the BH3 domain of the BH3-only group. This interaction occurs predominantly on the mitochondrial outer membrane (333). Whether a cell lives or dies depends upon the relative balance between the pro- and anti-apoptotic proteins present, and so disruption of this, either by pathology or pharmacology, is important in both the development and treatment of cancer.

The effector proteins

Both the pro- and anti-apoptotic groups exert their effects predominantly through the pro-apoptotic effector groups, which are essential for apoptosis to take place (334). The effector proteins are kept inactive in cells by association with the anti-apoptotic BCL2 family members. The pro-survival actions of the BCL2 proteins are reliant on their ability to bind and neutralise the effector proteins BAX and BAK. When levels of BH3-only pro-apoptotic proteins rise, the

BCL2 proteins are displaced from BAX and BAK, and apoptosis can take place. When activated, BAK and BAX oligomerise and can form pores in the mitochondrial outer membrane (335) – causing MOMP.

The pro-apoptotic BH3 group

BH3 proteins act by activating the effector proteins and by binding and neutralising the anti-apoptotic group members. Synthetic peptides corresponding to the BH3 domains have been shown to mimic the function of the naturally-occurring proteins (334, 336). There is a degree of heterogeneity in their function, with some able to bind BAK and BAX directly (for example, BID and BIM – the activator proteins), and some acting purely through their effects on the BCL2 group members (derepressor or sensitiser proteins) to release sequestered BAK and BAX (324). Similarly, some are selective for which BCL2 protein they bind whereas others are more promiscuous (see figure 1-8) (335). However, it is necessary for one of the direct activator proteins (i.e. BID or BIM) to be present for apoptosis to take place – the derepressor and sensitisers, which act by inhibiting the anti-apoptotic effects of the BCL2 family, will not suffice on their own (334, 337).

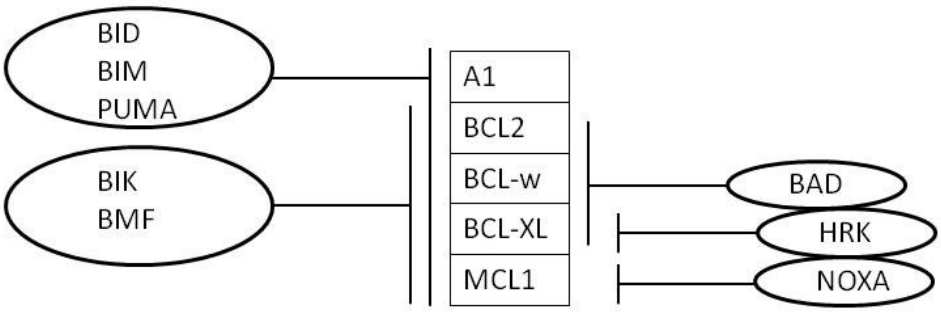

Figure 1-8. Binding profiles for the BH3 proteins and BCL2 family. As can be seen, some are selective for one target whereas others can bind more than one BCL2 family member. Redrawn from (260)

There are two current models for how BH3 proteins are able to contribute to apoptosis, although the situation *in vivo* is likely to represent a combination of these (338). The "direct activation" model assigns them two roles – as sensitisers and as direct activators. The sensitiser proteins (BAD, BMF, NOXA, HRK, BIK) interact only with the anti-apoptotic group and neutralise them, allowing the activation of the effector proteins. The direct activator group (BIM, PUMA, BID) can not only neutralise the anti-apoptotic proteins but can also directly activate BAX and BAK (324). In contrast, the "indirect activation" model suggests that BAX and BAK are spontaneously activated, and the role of the pro-apoptotic proteins is simply to release them from the control of the BCL2 family (339).

BID is inactive in its full length form as the BH3 domain is hidden; its activation requires cleavage by caspase-8, caspase-2 or granzyme B (340, 341); it is also enhanced by N-myristoylation (342).

The active t-BID moves to the mitochondrion and mediates mitochondrial outer membrane permeabilisation.

Sensitiser proteins act by binding to anti-apoptotic proteins and preventing them inhibiting the direct activators in response to stress. For example, cellular stress may induce the expression of BIM. If BCL2 is expressed the BIM will be sequestered, but if PUMA is also present then the BCL2 is neutralised and the BIM can activate the effector proteins. In de-repression, the antiapoptotic protein which is binding and neutralising an effector protein is displaced from that interaction and so apoptosis can take place (335).

The pro-apoptotic BH3 family members are also important in cellular response to chemotherapy. For example, PUMA, NOXA and BIM expression are required for maximal lymphoma toxicity by DNA damaging agents (343), and PUMA and BIM are important in mediating cell death in response to glucocorticoids or radiation (344) (see figure 1-9).

The anti-apoptotic proteins

BCL2, after its early identification as an important protein in lymphomagenesis (see above), was shown to protect cells from apoptosis induced by cellular stress and, in combination with CMYC, to contribute to lymphomagenesis (332). It, and the other family members, sequester the activator proteins and prevent them initiating apoptosis. Overexpression of BCL2 is seen not only in follicular lymphoma but also in chronic lymphocytic leukaemia (CLL), where it corresponds to poorer prognosis (345), myeloma (346) and other B- and T-cell malignancies

(reviewed in (347)). BCL2 overexpression can contribute to a failure of the cell to undergo apoptosis in response to stress (348). Malignant cells are described as being addicted to anti-apoptotic proteins, meaning they are reliant upon them to survive – it follows that by targeting these proteins we would expect to be able to induce apoptosis in these cells, a new and important direction for cancer chemotherapy.

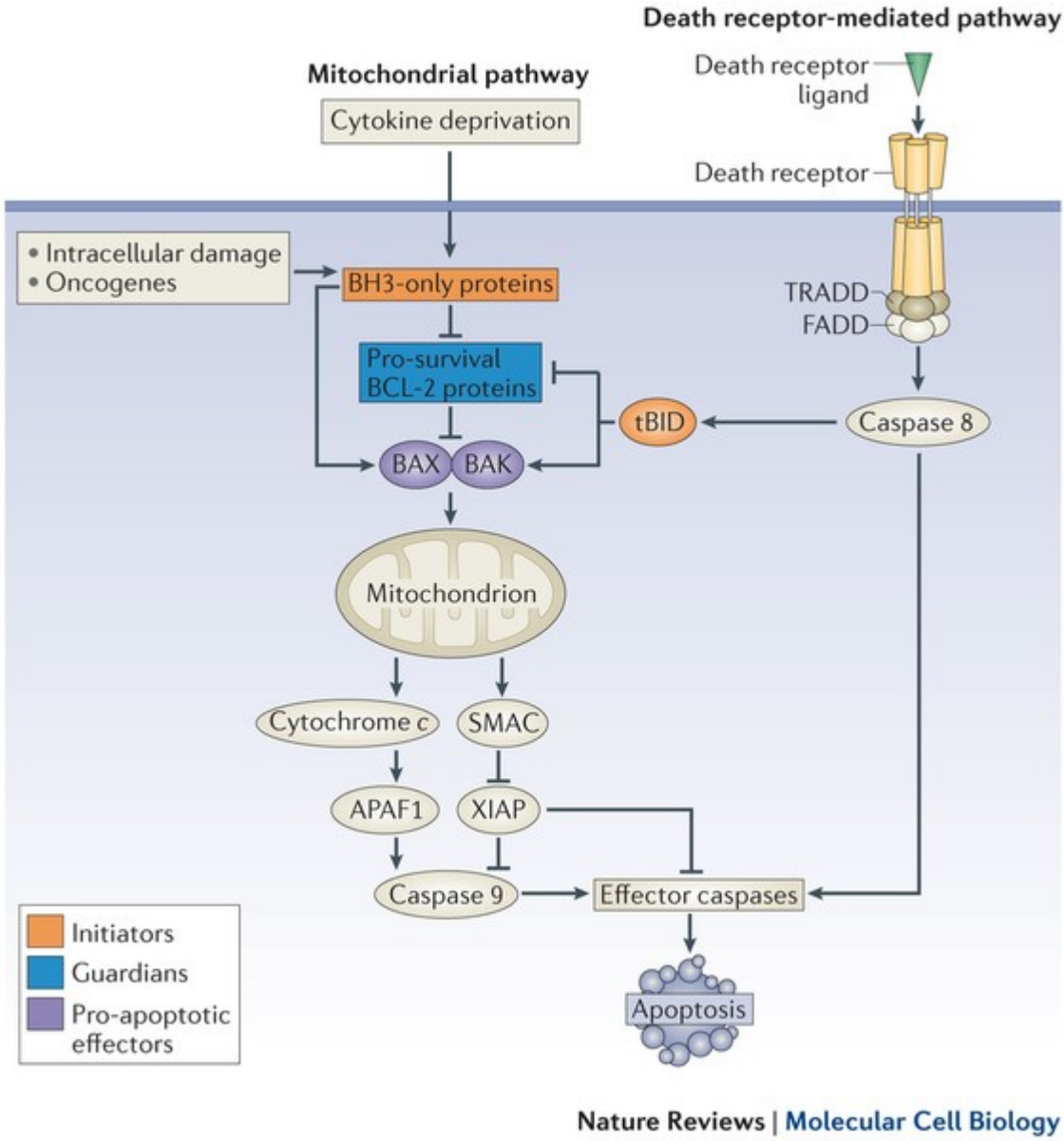

Figure 1-9 - The interaction between the BCL2 family members in the control of cellular apoptosis (from (333)). Usually the effector proteins BAX and BAK are kept neutralised by the anti-apoptotic BCL2 proteins. A pro-apoptotic stimulus, either from the intrinsic or extrinsic pathway, results in the activation of the BH3-only proteins with resulting inhibition of the anti-apoptotic BCL2 family members and activation of BAX and BAK effector proteins. These associate in the mitochondrial outer membrane and result in MOMP.

BH3 mimetics

In the quest to exploit the intrinsic apoptosis pathway for therapeutic ends, highly-specific small molecules have been designed to bind into the hydrophobic groove of the BCL2 family proteins

to inhibit the interactions between the proteins. These molecules are known as BH3 mimetics, and are currently under close scrutiny to assess their effectiveness in treating malignancies. The first to show effectiveness, ABT-737, inhibits BCL2, BCL-X_L and BCL-w, and was shown to cause cell death in lymphoma particularly CLL and small-cell lung cancer cells, and to enhance sensitivity to chemotherapeutic agents and radiation in other tumours (349). It binds to BCL2 with a higher affinity than to BCL-X_L or BCL-w in cells (350).

Unfortunately a side effect of ABT-737 mediated BCL-X_L inhibition is dose-limiting thrombocytopenia, therefore ABT-199 was engineered to be a specific BCL2 inhibitor. It can induce apoptosis in cell lines dependent on BCL2, and has activity *in vivo* (351). Clinical trials are still underway but it has shown impressive activity against CLL in particular, even in the presence of adverse prognostic features (see (347) for review and preliminary data). Although obatoclax (GX15-070) was initially thought to be a specific inhibitor of MCL1 (352), it has recently be shown to cause cell death in a manner independent of BAX, BAK and caspase 9, suggesting that its cytotoxicity is not related to the intrinsic apoptotic pathway.

AIMS OF THE THESIS

1. The T- and NK-cell EBV-associated malignancies express the viral proteins LMP1, LMP2A and LMP2B, the functions of which are poorly defined. Therefore, our first aim is to investigate their modulation of cellular genes in primary NK cells, and compare this to the effects previously observed in other cell backgrounds.

2. ENKTL and CAEBV are highly resistant to conventional chemotherapies. However, the role of the virus in this resistance is currently unknown. Our second aim, therefore, is to investigate the role of the viral proteins, particularly LMP1, on the growth, proliferation and survival of CAEBV and ENKTL cell lines.

3. EBV-associated non-B-cell disorders are rare and diagnosis is often difficult. Our third aim is, therefore, to develop an assay which can quickly and reliably determine the identity of the infected lymphocyte subsets directly on peripheral blood samples.

CHAPTER 2 - MATERIALS AND METHODS

2.1 Donors and Patients

Ethical approval for this work was provided from the West Midlands Research Ethics Committee (REC: 07/H1208/62). Patients were recruited from clinical centres with probable or confirmed diagnoses of T- or NK-cell EBV infection; after giving informed consent, blood or bone marrow samples were taken. Samples received from non-study centres were sent for diagnostic purposes, with anonymised clinical data provided subsequently. Healthy donors were recruited from departmental staff; blood samples were taken after informed consent and according to local protocols.

2.2 Cell culture methods

Maintenance of cell lines

T and NK cell lines

All cells were grown at 37°C in 5% CO_2. T and NK cell lines were grown in NK medium - CellGro° SCGM (stem cell growth medium - CellGenix™) supplemented with 10% v/v heat-inactivated, sterile-filtered human serum (Sigma), 50 U/ml penicillin/streptomycin, 6 mM L-glutamine (Invitrogen), 1 mM sodium pyruvate (Sigma), 0.13 mg/ml oxalacetic acid (Sigma) and 700 U/ml IL-2 (Novartis). Human serum was heat-inactivated by heating to 56°C for 30 minutes, cooling to 4°C then centrifuging at 3000 rpm in a Heraeus™ Megafuge™ 40 centrifuge for 30 minutes.

The serum was finally filtered through a 0.2 μm syringe filter. It was then either used immediately or frozen at -20°C. Of note, the ability of the serum to support NK growth was batch-sensitive.

The T and NK cell lines (table 2.1) were obtained from Professor Shimizu (Tokyo Medical and Dental University, Japan). MEC04 (276), SNK1, 6 and 10, and SNT8 and 16 were cultured in 25cm^2 flasks (Corning, Sigma-Aldrich, Germany) in NK medium. SNT13 and 15 were cultured in 12 well plates (Iwaki). Cells were split approximately twice a week, aiming for a cell density of approximately 1x10^6 cells/ml. In practice this usually resulted from splitting 1:3.

Table 2-1 - T- and NK-cell lines used in this study.

Name	Lineage	Underlying disease	Reference
SNK1	NK	ENKTL with CAEBV	(353)
SNK6	NK	ENKTL	(354)
SNT8	γδT	ENKTL	(354)
SNK10	NK	CAEBV	(353)
SNT13	γδT	ENKTL	(355)
SNT15	γδT	ENKTL	(355)
SNT16	αβT	CAEBV	(353)
MEC04	NK	ENKTL	(276)

Primary NK cells

Primary NK cells were cultured in 24 well plates in NK medium, as described above. Following entry into exponential growth phase, usually about a week after isolation, the cells were split to maintain a density of approximately 1x10^{6}cells/ml; in practice this resulted in splitting 1:2 every 4 days.

B-cells

Primary B-cells and B-cell lines were grown in cell culture medium consisting of RPMI 1640 (Sigma) supplemented with 10% v/v fetal calf serum (Gibco), 50 U/ml penicillin/streptomycin and 6 mM L-glutamine (Invitrogen). Primary B-cells, after infection with EBV, were cultured in 12 well plates, B-cell lines in 25 cm^2 flasks.

Epithelial cells

293FT (Invitrogen) cells were grown in 10 cm plates (Corning) in cell culture medium consisting of RPMI 1640 (Sigma) supplemented with 10% v/v heat-inactivated bovine calf serum, 50 U/ml penicillin/streptomycin, 6 mM L-glutamine (Invitrogen) plus 500 µg/ml G418 (Life Technologies). The serum was inactivated by heating to 56°C for one hour. Cells were split 1:4 when they were approximately 90% confluent using 1 ml 10% trypsin solution (Sigma) per 10 cm plate to detach them. The trypsin was inactivated in growth medium and then the cells were passaged onto fresh plates. For lentiviral production, 293-FT cells were used up to passage 15 before being discarded.

Cell cryopreservation

Up to $1x10^7$ viable primary lymphocytes and up to $5x10^5$ cells from cultured lines were cryopreserved as follows: cell lines were initially centrifuged at 1200 rpm in a Heraeus™

Megafuge™ 40 centrifuge for 5 minutes then resuspended in 1 ml of the cell-specific culture medium supplemented with 10% v/v of DMSO and a further 10% v/v of serum. Primary lymphocytes isolated from the blood were resuspended in 1 ml heat-inactivated human serum supplemented with 10% v/v DMSO. After initial slow freezing at -80° in a "Mr Frosty" isopropanol-filled container for at least 4 hours they were transferred to the vapour phase of a liquid nitrogen freezer for long-term storage at -180°C.

Recovery of cells from liquid nitrogen

Cell recovery was undertaken by quickly defrosting the vial of cells in a 37°C water bath then immediately adding the contents to 40 ml prewarmed culture medium in order to dilute the DMSO. The cells were centrifuged at 1200 rpm in a Heraeus™ Megafuge™ 40 centrifuge then resuspended in appropriate cell-specific medium.

Isolating PBMCs from whole blood or aphaeresis cones

Peripheral blood mononuclear cells (PBMCs) were obtained either from healthy volunteers working within the School of Cancer Sciences, or from aphaeresis leukocyte-depletion "cones" obtained from the National Blood Service.

UK-based patients with ENKTL, CAEBV or HLH were recruited as part of our ongoing study "EBV associated NK/T cell malignancies" (UKCRN ID: 5098). Samples of blood or bone marrow were received.

Samples were diluted 1:2 (fresh blood) or 1:5 (aphaeresis cone) with phosphate buffered saline (PBS) and layered onto LymphoPrep (Axis Shield, Oslo, Norway) in 50 ml polypropylene tubes. LymphoPrep has a density of 1.077 +/- 0.001 g/ml whereas PBMCs are generally less dense. When centrifuged at 1800 rpm in a Heraeus™ Megafuge™ 40 centrifuge for 30 minutes with no brake the PBMC compartment forms a visible layer at the interface between the plasma and the LymphoPrep. This layer was removed with a transfer pipette. Sequential centrifugation in a Heraeus™ Megafuge™ 40 centrifuge at decreasing velocities was performed to remove residual LymphoPrep and platelets; these centrifugation steps were typically 1600 rpm for 10 minutes, followed by 1200 and 1000 rpm for 5 minutes each. All washes were performed in 50 ml PBS.

Isolating primary NK cells

Primary NK cells were isolated from the PBMC suspension using the Dynabeads° Untouched™ Human NK Cells kit (Life Technologies, UK). Briefly, the PBMCs were resuspended in PBS with 2% fetal calf serum and 1 mM EDTA. They were then incubated at 4°C with a cocktail containing biotinylated monoclonal antibodies against CD3, CD14, CD36, HLA Class II, CD123 and CD235a, with heat-inactivated FCS to block non-specific binding. After washing, pre-washed streptavidin-conjugated Dynabeads, which bind to the biotinylated-antibody-coated cells, were added to the cells and incubated at room temperature with agitation for 15 minutes. The suspension was placed inside a magnetic isolator (DynaMag-15, Life Sciences) causing the bead-bound non-NK cells to be removed from suspension thereby allowing the recovery of the untouched NK-cells. The cells were washed and placed in the isolator for a second time to

recover the maximum number of non-NK cells. The isolated 95% pure NK cells were then spun down and resuspended in NK medium for culture. Primary NK cells were grown in 24 well plates at approximately $1x10^6$ cells per well. Once proliferating, cells were split approximately 1:2 twice a week.

Isolating primary B-cells

Primary B-cells were positively isolated from a PBMC suspension as prepared above. PBMCs were incubated with CD19-conjugated magnetic DynaBeads™ (Invitrogen) at a ratio of 4 beads per cell for 30 minutes at 4°C with continual agitation. The bead-coated B-cells were then removed from the non-B-cells by exposure to a magnet followed by five sequential washes and magnet exposure to purify the B-cells. The magnetic beads were then removed from the B-cells by incubation with CD19 DetachaBead™ (Invitrogen) for 45 minutes at room temperature followed by magnet exposure. The resulting B cell preparation was at least 98% pure.

B-cell infection with EBV and generation of lymphoblastoid cell lines

Primary B-cells were pelleted by centrifugation at 12000 rpm for 5 minutes in an Heraeus™ Megafuge™ 40 centrifuge and were resuspended in titrated viral supernatant at a sufficient volume to give a multiplicity of infection (MOI) of at least 10 virus particles per cell. After 2 hours incubation at 37°C the viral supernatant was removed by centrifugation and resuspension of the cells in B-cell medium in 24-well plates at $2x10^6$ cells/ml. The cells were inspected daily

and fed with fresh medium as required. As cell numbers increased the cultures were transferred to larger wells or flasks for ongoing culture.

Growth assays

Cells were counted and plated in triplicate into 24 well plates with 0.5 x 10^6 cells per well in 2 ml appropriate medium. On each day the cells were resuspended and thoroughly mixed and 10 µl of the cell suspension was combined with an equal volume of 0.4% Trypan Blue (Sigma). A 10 µl sample of this suspension was inserted into one well of a cell counter slide and the cells were counted on the BioRad TC20 automated cell counter. Total and live cells were counted and an average of the three wells was taken. Every day, half of the medium in the remaining wells was removed and replaced with fresh medium. Cells were split 1:2 when they reached 80% confluence.

Apoptosis assays

Cells were seeded into 96-well, flat-bottomed plates at 5x10^4 cells per well in 100 µl of the appropriate medium supplemented with the apoptosis-inducing drugs etoposide, ionomycin, camptothecin, ABT199 and ABT737 (described in detail in chapter 3). The cells were treated for 48 hours then harvested, washed and stained for Annexin V and PE using the eBiosciences Annexin V PE kit. This involved suspending the cells at 1x10^6cells/ml in the Binding Buffer supplied and staining at room temperature with fluorochrome-conjugated Annexin V, which

binds to phosphatidylserine (PS). Usually located on the inner leaflet of the plasma membrane, in apoptotic cells it is translocated to the outer membrane and so can be bound by Annexin V. Propidium iodide, which is actively excluded from live and early apoptotic cells, was then added (to an end concentration of 1%) immediately before analysis. Live cells were analysed by flow cytometry on the Becton Dickinson Accuri flow cytometer.

2.3 Molecular Biology Techniques

In order to minimise sample degradation or contamination, DNAse and RNAse-free water and plasticware were used for all molecular biology procedures.

RNA extraction from less than $1x10^6$ cells

In order to preserve the cellular RNA, cells were sorted by fluorescence-activated cell sorting (FACS) into DEPC-treated phosphate buffered saline (Ambion) in RNAse-free Eppendorf tubes, and were kept on ice. RNA extraction from < $1x10^6$ cells for use in the Microarray studies was performed using the RNeasy Micro centrifuge-column kit (Qiagen, Germany) according to the manufacturer's instructions. ExpressArt NucleoGuard (Amsbio, Spain), a universal nuclease inhibitor, was added to the cell lysis buffer. An additional on-column DNAse digestion was undertaken to minimise DNA contamination. The resultant RNA was frozen immediately at -80°C. Analysis of RNA quality and quantity was undertaken using the Eukaryote Total RNA Pico

Series II Bioanalyser chip (Agilent) for microarray purposes, or using the NanoDrop Fluorospectrometer (Thermo Scientific).

RNA extraction from more than $1x10^6$ cells

For RNA extraction from more than $1x10^6$ cells the NucleoSpin° RNA kit (Macherey-Nagel) was used as per the manufacturer's protocol. Briefly, the cells were lysed in a lysis buffer with added β-mercaptoethanol. The lysate was filtered then ethanol was added before the RNA was bound to a column. This was washed, then after an on-column DNAse digestion step, eluted into DEPC-treated water. The resulting RNA was quantified using the NanoDrop Fluorospectrometer (Thermo Scientific).

DNAse digestion of RNA

To minimise contamination of RNA with cellular DNA, a further DNAse digestion step was performed upon the extracted RNA using the DNA-*free* kit (Ambion). Briefly, 1 µg of RNA was treated with 1 µl of rDNase for 30 minutes at 37°C, then inactivated during a 2 minute incubation with 5 µl DNAse Inactivation Reagent. Following a brief centrifugation, the purified RNA was removed to a fresh tube and used to generate cDNA.

Generation of cDNA from RNA using reverse transcriptase

cDNA was made from the extracted RNA using QScript cDNA Supermix (Quanta Biosciences, USA) as per the manufacturer's protocol. Briefly, 400 ng of RNA was incubated with 4 µl of QScript cDNA Supermix (containing reverse transcriptase and random primers) in a total reaction volume of 20 µl for 5 minutes at 25°C, 30 minutes at 42°C and 5 minutes at 85°C. In order to control for the presence of genomic DNA contamination of the RNA, controls lacking the reverse transcriptase enzyme were prepared in exactly the same way.

DNA extraction from cells

DNA was extracted from cells using the DNEasy Blood & Tissue Kit (Qiagen) according to the manufacturer's instructions.

Conventional reverse-transcriptase PCR (RT-PCR)

In order to amplify specific cDNA sequences for subsequent cloning, primers were designed to correspond to the beginning and end of the gene of interest. PCRs were performed in a 50 µl reaction volume containing 100 ng of cDNA, 1x Expand High Fidelity buffer, 5 µl of dNTPs (2 mM), 5 µl of the forward and reverse primers (10 µM) and 1 µl of Expand High Fidelity Taq Enzyme (Invitrogen). The enzyme was added after an initial denaturation at 90°C for 1 minute. The PCR reaction consisted of denaturation at 94˚C for 5 minutes followed by 35 cycles of 94˚C

denaturation for 1 minute, 55˚C annealing for 1 minute and 72˚C extension for 2 minutes in an Eppendorf Thermocycler. Products were separated by agarose gel electrophoresis.

Agarose gel electrophoresis

The DNA PCR product was mixed 6:1 v/v with gel sample loading buffer (0.25% xylene cyanol, 0.25% bromophenol blue, 30% glycerol) and loaded onto a 0.6% agarose TAE gel (40 mM Tris-acetate, 1 mM EDTA) (Eurogentec) in 1 x TAE buffer containing 5 µg/ml ethidium bromide. A "1 kb DNA ladder" (Promega) was loaded into one lane to determine PCR product size. DNA bands were visualised using UV transillumination; the correct-sized PCR amplicon was excised and extracted from the gel using the QIAquick Gel Extraction Kit (Qiagen, Germany) and resuspended in a total volume of 50 µl, according to the manufacturer's instructions.

Phenol-chloroform purification and ethanol precipitation

The gel-extracted PCR amplicon was purified by phenol-chloroform purification and ethanol precipitation as follows. An equal volume (50 µl) of phenol-chloroform was added to the gel-extracted PCR amplicon and mixed thoroughly. This was then centrifuged at 13000 rpm in a Hereaus™ Pico™ microfuge for 5 minutes, the supernatant (aqueous layer) removed and mixed with 2.5 (v/v) x 100% ethanol and 0.1 (v/v) x 3 M sodium acetate then incubated at -20˚C for 30-60 minutes to precipitate the DNA. This was then centrifuged at 13000 rpm in a Hereaus™ Pico™ microfuge at 4°C for 30 minutes to pellet the DNA. The supernatant was discarded; the

pellet was washed in 200 µl 70% ethanol then air-dried and resuspended in 50 µl DEPC-treated water.

Digestion of DNA with restriction endonucleases

In order to insert DNA sequences specifically into plasmid vectors and to verify insertion it is possible to exploit the specificity of different restriction endonucleases for specific DNA sequences. One microgram of plasmid DNA (for cloning) or up to 500 ng plasmid DNA (for verification purposes) was digested by addition of 1 µl of the selected enzyme in a 50 µl reaction in the appropriate buffer. The digests were generally incubated at 37°C for at least an hour, and the products separated by agarose gel electrophoresis as described above.

2.4 Bacteriology

DH5α and Stbl3 competent *E.coli* bacteria were purchased from Life Technologies and grown in either sterile Lennox Broth (LB) medium or on LB agar plates. Ampicillin was added to both at a final concentration of 100 µg/ml to prevent non-specific growth.

DNA ligation reactions

The gene of interest was ligated into the appropriate plasmids by incubation of the relevant segment of DNA (either from a PCR reaction or from restriction digestion of plasmid DNA) with a

plasmid which had been pre-digested with the appropriate restriction endonuclease. After digestion, plasmids were treated with 0.5µl of calf alkaline phosphatase (CAP) per 10 µl of reaction volume to remove the phosphate thereby preventing religation of the plasmid DNA to itself at 37˚C; after 30 minutes a further 0.5 µl CAP per 10 µl reaction volume was added and incubated for a further 30 minutes at 37˚C. The CAP was then inactivated by heating to 80˚C for 5 minutes. Approximately 50 ng of phenol chloroform-purified LMP2A or LMP2B-TR gene sequence was incubated with a 1:1, 2:1 or 3:1 molar ratio of the plasmid vector and 1 µl (400 units) T_4 DNA ligase in 1 x T_4 buffer in a 20 µl reaction volume for 18 hours at 4°C. The entire ligation reaction was then transformed into competent *E.coli* by heat-shock, as described below.

Transformation of competent bacteria

Plasmid DNA or ligation reactions were transformed into competent *E. coli* cells as follows. Twenty ng of plasmid DNA or entire ligation reactions were initially incubated with 100 µl of DH5α or Stbl3 on ice for 20 minutes. The bacteria were heat shocked at 42˚C for 90 seconds then incubated at 37˚C for 1 hour in 1 ml of LB broth with agitation. The bacteria were then centrifuged at 3000 rpm in a Hereaus™ Pico™ microfuge for 2 minutes, the majority of the supernatant discarded and the cells resuspended in the remainder. This was spread on pre-warmed ampicillin-containing (100 µg/ml) LB agar plates. Colonies were picked after incubation at 37°C for 18 hours.

Preparation of plasmid DNA

A 4 ml culture of LB broth containing 100 µg/ml ampicillin inoculated with a single bacterial colony from an agar plate was incubated for 18 hours in a 37˚C shaking incubator. The bacterial DNA was then extracted using the QIAprep Spin Miniprep Kit (Qiagen, Germany). The correct insert was verified by restriction enzyme digestion and sequencing. In order to amplify the correct plasmid, 200 ml of ampicillin-containing LB broth was inoculated with a 4 ml day culture of the correct bacterial clone and incubated at 37°C overnight in a shaking incubator. The plasmid DNA was isolated using the QIAprep Spin Maxiprep Kit (Qiagen, Germany), according to the manufacturer's instructions. The resulting DNA pellet was air-dried and resuspended in DEPC-treated water at 1 µg/µl and stored at -20°C in small aliquots.

2.5 Lentiviral vectors

The lentiviral expression system

The lentiviral vector system used here was designed by Dr Marco Herold (356) and was kindly donated by him. It constitutively expresses GFP from a ubiquitin promoter, allowing identification of successfully transduced cells, but has the gene of interest under tetracycline repression. Introduction of doxycycline, a stable tetracycline analogue, allows the repressor to dissociate from the promoter sequence and thus gene expression can take place (see figure 2-1).

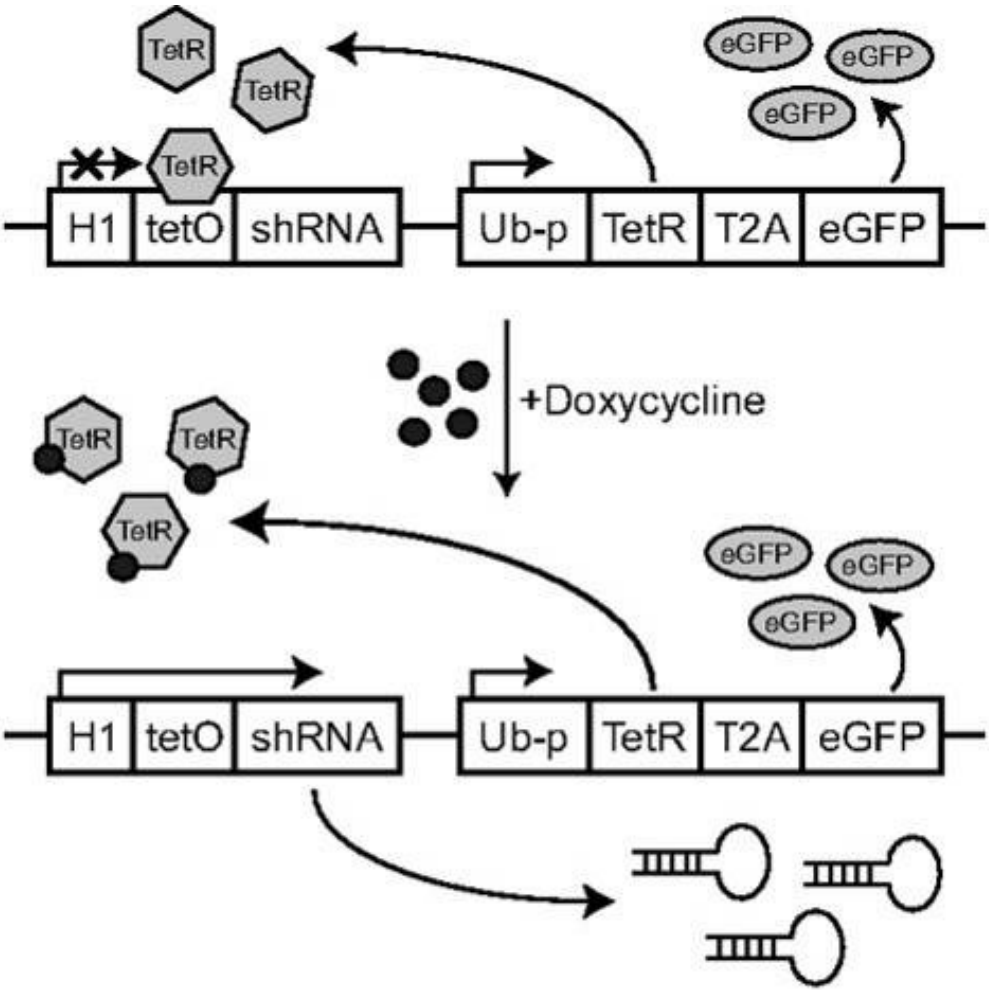

Figure 2-1 - The FH1T inducible vector showing doxycycline-induced dissociation of the Tet repressor from the genome.From Herold et al (356). In the absence of the antibiotic, the tetracycline repressor protein (TetR) is associated with the gene promoter at the tetO sequence and the gene is silenced. When doxycycline is added, the repressor protein is dissociated from the promoter and gene expression, a shRNA in this example, can take place. Green-fluorescent protein (eGFP) is expressed regardless of the presence of doxycycline which allows identification of successfully transduced cells.

PCR amplification of the relevant EBV gene

ENKTL, although rare, is proportionally much more common in Asia and South America (233, 234). EBV strains also show some geographical variation, the significance of which is not always clear (16, 17), For this reason SNK6, a Japanese ENKTL line (354), was used as the source of the

viral sequence for the LMP1 and LMP2B-TR. As LMP2A, however, is not expressed in any ENKTL line, the B95.8 sequence was used for this. There is, as yet, no reliable antibody to detect LMP2B. The LMP2B was therefore cloned with a carboxyl-haemagglutinin (HA) tag to enable detection by anti-HA antibodies for Western blot analysis.

RNA was extracted from B95.8 and SNK6 cells, which have high expression of LMP2A or LMP2B-TR as described in chapter 1. cDNA was generated from 1 μg of total cellular RNA by reverse transcription using the Qscript cDNA Supermix (Quanta Biosciences, USA) as per the manufacturer's protocol. LMP2A and LMP2B were amplified from the cDNA by Polymerase chain reaction (PCR). Primers corresponding to the beginning and end of the gene were designed using Primer Express software v2.0, and were manufactured by Alta Biosciences UK (see table 2-2). The forward primer incorporated a Kozak sequence (ACCATG) to maximise expression. The reverse primers incorporated a BglII (LMP2A) or BamH1 (LMP2B) restriction site to facilitate cloning into plasmids. The Expand High Fidelity PCR system (Roche, Switzerland), incorporating a proofreading DNA polymerase enzyme, was used to minimise PCR-induced sequence error.

Table 2-2 - Primers used in the initial PCR reaction

	Forward	**Reverse**
LMP 2A	5'-GCGCAGATCTACCATGGGGTCCCTAGAAATGGT-3'	5' -GCGCGGATCCTACAGTGTTGCGATATGGGGTCGGTGGGCG -3'
LMP 2B	5'-GCGCGGATCCAACCATGAATCCAGTATGCCTGCCTGTAATTGTTGCGCCCTACCT-3'	5' -GCGCAGATCTTACAGTGTTGCGATATGGGGTCGGTGGGCG - 3'

Cloning into pGEM°-T Easy Vector system

The cloning strategies are summarised in figures 2-2 and 2-3. The PCR product was initially cloned into the pGEM°-T Easy Vector (Promega, USA). Briefly, 1 µl purified LMP2A or LMP2B PCR amplicon was incubated with 1 µl pGEM-T vector and 1 µl T_4 ligase in 1 x T_4 buffer in a 20 µl reaction volume for 18 hours at 4°C. The ligase reaction was then transformed into competent DH5α *E. coli* cells as described. The transformed cells were plated onto ampicillin-containing agar plates pre-treated with X-galactose and Isopropyl β-D-1-thiogalactopyranoside (IPTG). The agarose plates were incubated overnight at 37˚C and white colonies, indicating that the incorporated fragment has inactivated β-galactosidase, were picked. The correct insert was confirmed by restriction enzyme digestion and sequencing.

Generating the FTGW-HA plasmid

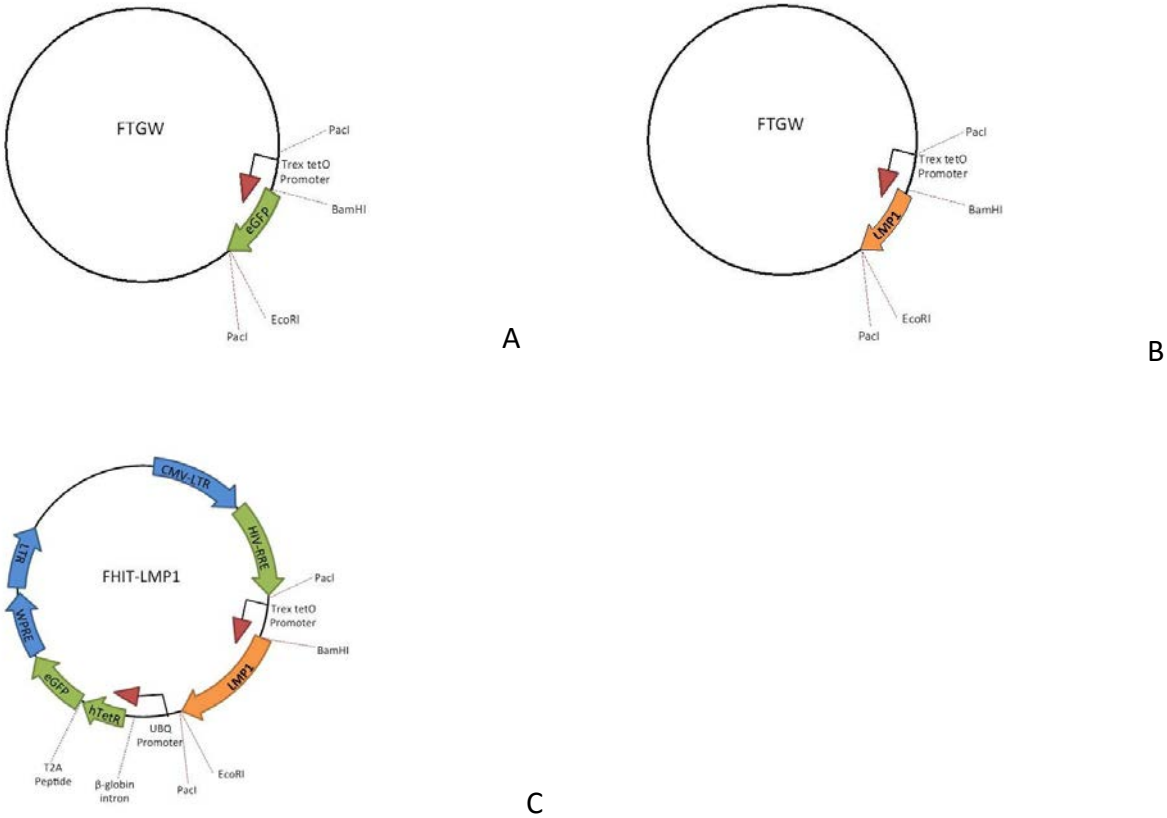

Figure 2-2. LMP1 cloning schematic. The LMP1 sequence was inserted into the FTGW plasmid (panel A) using BAMH1 and EcoR1 (panel B), then excised, with the promoter, and inserted into the FH1T vector using PacI (panel C).

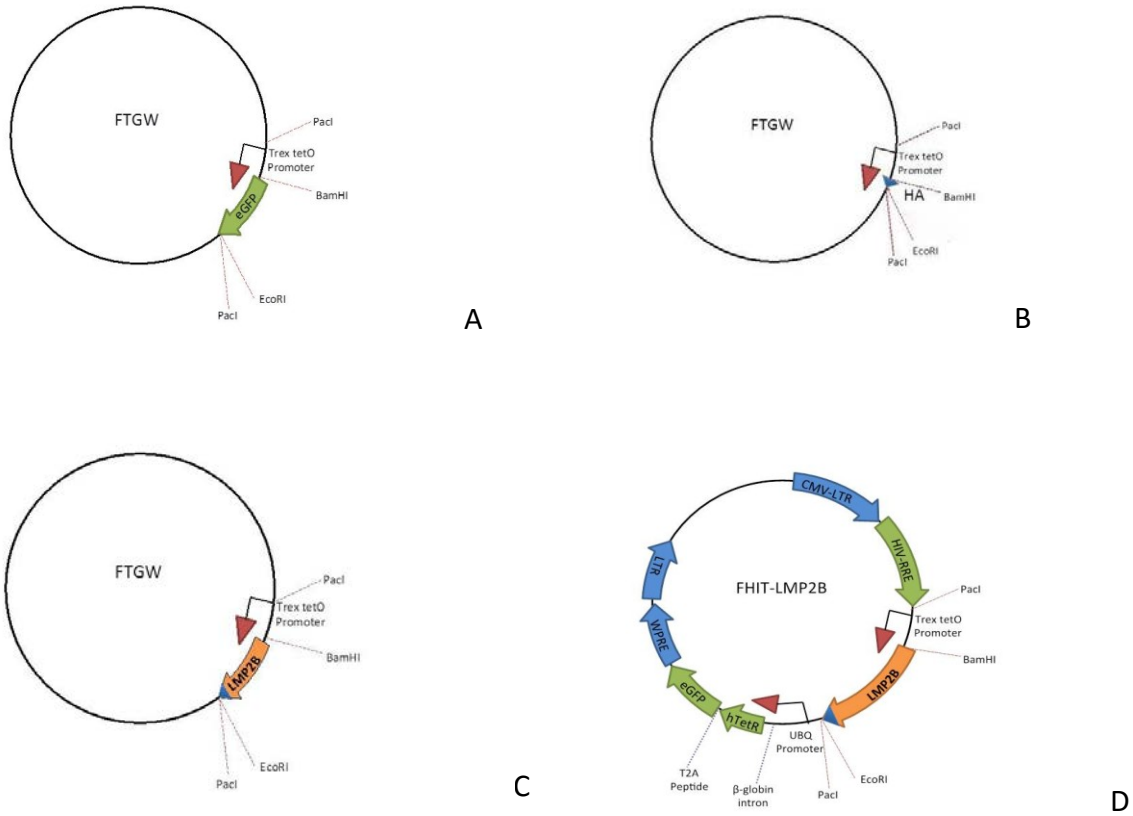

Figure 2-3 - LMP2 cloning schematic.The HA linker sequence was inserted into the FTGW intermediate plasmid (panels A & B). The LMP2 sequence, isolated from the SNK6 cell line, was inserted into the same FTGW plasmid (panel C); the protein:HA sequence, with the promoter, was then cut out using PacI and inserted into the final vector (panel D).

In order to generate an LMP2A and LMP2B protein with an HA tag, a linker sequence small scale oligonucleotide was synthesized by Alta Biosystems. The sequences were generated using MacVector software to incorporate the HA tag sequence (TACCCATACGATGTTCCAGATTACGCT), with a Bam HI restriction site at the 5' end, and a stop codon, a Pac1 site then an Eco R1 site at the 3' end (figure 2-3). The linker sequences are shown in table 2-3.

Table 2-3 - Sequences of the HA tag linkers.

HA tag linker forward	5' - GATCCTACCCATACGATGTTCCAGATTACGCTTAATTAATTAAG - 3'
HA tag linker reverse	5' - AATTCTTAATTAATTAAGCGTAATCTGGAACATCGTATGGGTAG - 3'

Two µl of each of the forward and reverse linker sequences (100 µg/ml) were incubated with 46 µl of Roche restriction buffer B at 90°C for 3 minutes, and then left to anneal at 24°C for 2 hours. 2 µg of FTGW plasmid DNA was digested with 2 µl of BamH1 and 2 µl of Eco R1, in a total volume of 100 µl in 1 x Buffer B. This was incubated at 37°C for 3 hours. The annealed HA linkers were ligated into the digested FTGW plasmid in a 20 µl total reaction volume, with a 200:1 molar ratio of insert to vector. Thus, 60 ng of digested FTGW vector and 50 ng of annealed HA linkers were incubated at 4°C overnight with 1 µl of T_4 DNA ligase in 1 x T_4 DNA ligation buffer. The HA DNA was replaced by water for a negative control. 5 µl of the ligation reaction was transformed into 50 µl competent Stbl3 cells by heat-shock; the resulting colonies were picked and screened by restriction digest to select clones containing the HA tag.

Cloning LMP2A and LMP2B into the FTGW-HA plasmid

The LMP2A- and LMP2B-pGEM-T vectors and the FTGW-HA vector were all digested with BamH1 (LMP2B), or BamH1 and Bgl-II (LMP2A) in order to clone the LMP2A/B into the FTGW-HA. Briefly, 2 µg of DNA was digested with 2 µl of the appropriate restriction enzyme(s) in the relevant buffer. The digested DNA was separated by electrophoresis on a 0.8% agarose gel. The correct size fragment was excised, gel-purified and phenol-purified as described previously. The

viral genes were ligated into FTGW-HA at a 3:1 insert:vector ratio using T_4 DNA ligase at 4˚C for 18 hours. As previously described, the ligation mix was transformed into 100 µl of competent Stbl3 cells. The Stbl3 cells were grown on ampicillin LB agar plates overnight, DNA was extracted and the correct clones identified by restriction digestion. Plasmid DNA was then extracted from 200 ml bulk preparations.

Cloning into FH1T.

The correct LMP2-HA fragment was excised from the FTGW vector by Pac1 digestion, excised from a 0.8% agarose gel, gel purified and phenol purified as previously described. Similarly, the FH1T plasmid was also digested with Pac1 then directly dephosphorylated by incubation with calf alkaline phosphatase (CAP). The LMP2-HA fragment was then ligated into the Pac1-digested FH1T with T_4 DNA ligase, transformed into Stbl3 cells and the resultant clones analysed for the presence of the correct insert. A correct clone was picked and a 400 ml bulk culture made for large scale plasmid preparation for use in making lentiviruses. Figures 2-2 and 2-3 show the cloning strategy used.

Lentivirus packaging and synthesis

Transfection of the 293FT cells to induce production of lentivirus particles required a 70% confluent monolayer; this was achieved by splitting a 90% confluent plate 1:2 the preceding day. On the day of transfection, the culture medium was changed for 10 ml fresh, pre-warmed

293FT medium without G418 for 2 hours before transfection. Care was taken not to disrupt the semi-adherent cell layer. For each 10 cm plate to be transfected, 36 µl of Lipofectamine 2000 (Life Technologies) was added to 1.5 ml OptiMEM (Life Technologies). In a separate tube, a further 1.5 ml of Optimem was incubated with 4 µg of the plasmid containing the gene of interest, 6 µg of packaging plasmid PAX-2 and 2 µg of VSV-G envelope protein-containing plasmid (kindly provided by Dr Marco Herold). These were incubated at room temperature for 5 minutes before they were combined and incubated for a further 20 minutes at room temperature. The 3 ml transfection mix was then added to the 10 ml of medium in each plate and the cells incubated overnight at 37°C. After 16 hours the medium was carefully replaced with fresh 293FT medium without G418. The virus-containing supernatant was harvested after a further 3 days, spun at 1400 rpm in a Heraeus™ Megafuge™ 40 centrifuge to pellet cells, filtered through a 4.5 µm filter and either used immediately or frozen at -80°C.

Transduction of primary NK cells with lentivirus

Primary NK cells were isolated as described above and cultured for 7 days to ensure that the cells had entered exponential growth phase. 60 ml of lentivirus was concentrated by ultracentrifugation (Beckman Ultracentrifuge) at 19,500rpm for 2 hours in 14 ml ultracentrifuge tubes (Beckman) using the SW40Ti rotor. The tissue culture supernatant was removed and discarded and the resulting fragile pellet was resuspended in 250 µl NK medium and added to $1x10^6$ cells in one well of a 24 well plate. The cells were incubated with the concentrated virus

for 18 hours, then 1 ml fresh NK medium was added. The cells were sorted after 48 hours by GFP expression by fluorescence-activated cell sorting (see below).

Transduction of SNK10 and SNT16 cell lines with lentivirus

SNK10 and SNT16 cells were transduced with concentrated lentivirus as described above. However, in order to obtain a stable population with high expression of the viral gene we performed 4 serial transductions, each a week apart, before sorting the highest GFP-expressing population.

2.6 Fluorescence-activated cell sorting

Fluorescence-activated cell sorting (FACS) was used to isolate either cells expressing green fluorescent protein (GFP) or to sort cells which had been prestained with fluorophore-conjugated primary antibodies. The FACS was performed using the MoFlo cell sorter (Beckman Coulter), and was provided as a service by the Institute for Biomedical Research at the University of Birmingham.

The PBMC were resuspended at $20x10^6$ cells per ml in cold MACS buffer (PBS with 2 mM EDTA and 0.5% v/v bovine serum albumin) then incubated with the appropriate isotype controls, single antibodies and combination of antibodies for 30 minutes at 4°C. The stained cells were then washed in 10 ml sterile MACS buffer by centrifugation in a Hereaus™ Megafuge™ at 1200 rpm, and resuspended in 1 ml sterile MACS buffer then filtered through a CellTrics° 50 µm filter

(Partec, Germany). Isotype controls and single colour stains were performed on $0.5x10^6$ cells in 25 μl MACS buffer. Antibodies used are shown in table 2-4.

Table 2-4 - Antibodies used for FACS cell sorting

Target antigen	Fluorophore	Manufacturer	Concentration used
CD4	APC	AbD (MCA1267APC)	1:20
CD8	FITC	AbD (MCA1226FT)	1:20
CD19	PE-Cy5	AbD (MCA1235C)	1:20
CD56	RPE	Invitrogen (MHCD5604)	1:20

Cells were sorted into 1 ml sterile PBS (for immediate harvest) or 1 ml sterile medium with added gentamicin at 50 mg/L to inhibit the growth of bacterial contaminants (for culture).

2.7 Real-time quantitative PCR

Real time qPCR is a method whereby quantification of a specific gene's expression can take place during PCR amplification. This relies on a fluorescent probe which hybridises to the DNA sequence of the gene of interest; by measuring the change in fluorescence as the reaction proceeds it is possible to determine the number of transcripts present at any particular PCR

cycle over 40 cycles. To calculate the number of DNA/transcripts, a threshold is set at mid-exponential phase of PCR amplification when the primers, probes and dNTPs are non-limiting to ensure the qPCR is truly quantitative.

A total of 25 ng of cDNA was subjected to each multiplexed PCR reaction in a 25 μl reaction volume, comprising the gene of interest plus a house-keeping gene for normalisation, usually GAPDH. Each PCR reaction comprised of 1 x TaqMan™ MasterMix (Invitrogen); 25 pmol gene-specific forward and reverse PCR primers; 5 pmol gene-specific FAM-labelled PCR probe; 25 pmol GAPDH-specific primers; 5 pmol VIC-labelled probe and DEPC-treated water. The PCR was performed in a 7500 Real-Time PCR System (Applied Biosystems) machine, where the samples were heated to 95°C for 10 minutes to activate the polymerase enzyme, followed by 40 cycles of denaturation at 95°C for 15 seconds and primer annealing and extension at 60°C for 60 seconds. The resulting data were analysed using the 7500 system software.

Absolute quantitation using the AQ-plasmid

A plasmid was commercially synthesized to encode EBV DNA sequences corresponding to qPCR amplicons of 45 latent and lytic EBV genes, and 3 cellular "housekeeping" genes (B2M, GAPDH and PGK). Details of the AQ-plasmid have been published (38). The sequence was inserted into the pUC57 plasmid vector (GenScript). The plasmid was quantified as plasmid copies per μl, then a 10-fold serial dilution series was set up from $1x10^5$ copies/μl to 1 copy/μl and was subsequently used to generate standard curves for absolute qPCR of EBV mRNA transcripts and

B2M, GAPDH and PGK. Prior to the development of the AQ plasmid, cDNA from well-characterised cell lines was used as a standard.

Fluidigm specific target amplification and 48:48 Dynamic Array integrated fluidic circuit (IFC) analysis

Amplification of the specific mRNA transcripts of interest from the cDNA was achieved by specific target amplification (STA) using the new Fluidigm technology as described in (38). Each STA reaction comprised of 25 ng of cDNA or AQ plasmid, 2.5 µl of 2x TaqMan PreAmp Master Mix (Life Technologies) and 1.25 µl of 20x TaqMan assays. The reactions were incubated at 95°C for 10 minutes, followed by 12 cycles of 95°C for 15 seconds and 60°C for 4 minutes. The pre-amplified samples were then diluted 1:5 with DNA Suspension Buffer.

The 48:48 Dynamic Array IFC was prepared and run in a Biomark HD instrument as per the manufacturer's instructions; the data were analyzed using Biomark Real-Time PCR Analysis Software Version 2.0 (Fluidigm).

2.8 Western Blotting

Sample preparation

Each cell sample was initially washed in PBS, then resuspended at $1x10^6$ cells per 100 µl urea buffer (9 M urea, 50 mM Tris, pH 7.5). The disrupted cells were then sonicated for 20 seconds using an ultrasonic cell disrupter (Misonix) to reduce viscosity before protein determination

using the Bio-Rad DC assay kit according to manufacturer's instructions. The quantified samples were diluted to 1-2 mg/ml in urea gel sample buffer (4% SDS (sodium docecyl sulphate), 62.5 mM Tris pH 6.8, 5% β-mercaptoethanol, 5 M urea, 10% glycerol, 0.01% bromophenol blue) then heated to 100°C for 5 minutes to denature the proteins.

Protein electrophoresis

A 20 µg aliquot of each protein sample was loaded into each well of a Criterion™ TGX™ Precast gel. SeeBlue° Plus2 prestained ladder (Invitrogen) was pre-diluted (10 µl SeeBlue plus 15 µl gel sample buffer) and run alongside the samples to estimate the molecular weight of the proteins of interest. The gels were run in Tris-Glycine running buffer at 120 V for 60 minutes, or until visual examination showed completion of protein separation.

Blotting

Transfer of the proteins from the gel to PVDF membranes was achieved using the TurboBlot system (BioRad), using a preset 7 minute protocol at 25 V, 2.5 A. Trans-Blot transfer packs, which include 2 presoaked ion reservoir stacks with a prewetted PVDF membrane were used. Examination of the transfer of the SeeBlue size markers from the gel to the membrane confirmed complete transfer of protein to the membrane.

Immunostaining

The PVDF membranes were blocked in 5% skimmed milk powder in PBST (phosphate-buffered saline with 0.1% V/V Tween 20) at room temperature for 1 hour to prevent non-specific antibody binding. The membranes were then incubated with appropriately-diluted primary antibodies in 5% milk-PBST (see table 2-5). The membranes were washed 4 times for 5 minutes with PBST then incubated for 1 hour at room temperature with the appropriate secondary antibodies conjugated to horseradish peroxidise (Sigma). The blots were then washed 6 times with PBST over a minimum of 1 hour. The proteins were visualised by Amersham ECL Western Blotting Detection Reagent (GE Healthcare) with the ChemiDoc documentation system (BioRad).

Table 2-5 - Antibodies used in Western blotting.

Antigen	Antibody	Stock concentration	Dilution used	Incubation conditions	Secondary antibody	Secondary antibody concentration
LMP1	CS1-4 (357)	1 mg/ml	1:1000	Overnight at 4°C	Mouse	1:1,000
LMP2a	14B7 (Abcam)	1 mg/ml	1:1000	Overnight at 4°C	Rat	1:1,000
Haemagglutinin (HA)	3F10 (Sigma)	50 µg/ml	1:1000	Overnight at 4°C	Rat	1:1,000
EBNA-1	"AM" sera	1:1	1:200	Overnight at 4°C	Human	1:1,000
EBNA-2	PE2 (Abcam)	1 mg/ml	1:25	Overnight at 4°C	Mouse	1:1,000
Calregulin	H-170 (Santa Cruz)	200 µg/ml	1:1000	1 hour at 18°C	Rabbit	1:5,000
BAD	D24A9 (Cell Signaling)	Not provided	1:1000	Overnight at 4°C	Rabbit	1:1,000
BAX	D2E11 (Cell Signaling	Not provided	1:1000	Overnight at 4°C	Rabbit	1:1,000
BID	#2002 (Cell Signaling	Not provided	1:1000	Overnight at 4°C	Rabbit	1:1,000
BIM	#2993 (Cell Signaling	Not provided	1:1000	Overnight at 4°C	Rabbit	1:1,000
BCL2	50E3 (Cell Signaling	Not provided	1:1000	Overnight at 4°C	Rabbit	1:1,000
BCL-XL	54H6 (Cell Signaling	Not provided	1:1000	Overnight at 4°C	Rabbit	1:1,000
MCL1	5453 (Cell Signaling	Not provided	1:1000	Overnight at 4°C	Rabbit	1:1,000

2.9 EBER-ISH in solution

Freshly isolated PBMCs or control cell lines were washed in MACS buffer prior to staining for 30 minutes at 4°C with the antibodies described in table 2.6. The cells were then washed a further two times in PBS before fixation for 20 minutes at room temperature in 4% Paraformaldehyde in DEPC H_2O. They were then permeabilised in permeabilisation solution (250 µl Tween 20 in 50 ml PBS) for 10 minutes at room temperature. Formamide buffer was made by adding 75 µl of 100% formamide and 25 µl hybridisation buffer (100 mM NaCl, 50 mM Na_2EDTA, 500 mM Tris-HCl pH 7.5) to 100 µl DEPC H_2O; this was added to the sample then immediately centrifuged off. The cells were resuspended in EBER PNA probe (Dako) and incubated for 60 minutes at 56°C before adding permeabilisation solution and incubating for 10 minutes at 56°C. The cells were centrifuged, the supernatant discarded and the pellet resuspended in permeabilisation solution and incubated for 10 minutes at 56°C. They were then centrifuged, the supernatant discarded and the cells resuspended in permeabilisation solution before analysis by flow cytometry. If amplification of the EBER signal was required, the cells were then incubated at 4˚C for 30 minutes with an anti-FITC antibody; this was then washed off before analysis.

2.10 Human PrimeFlow™ RNA Assay

The Human PrimeFlow™ RNA Assay (eBioscences) is a technique whereby in situ hybridisation to an mRNA sequence is performed in conjunction with conventional cell surface or intracellular

staining and analysed by flow cytometry, summarised in figure 2-4. Briefly, a dual-probe set is hybridised to the mRNA of interest; the probe set is subjected to pre-amplification, amplification then labelling with up to 400 molecules of fluorophore. Only when both probes of the probe set are bound will signal amplification occur, giving the assay its specificity. The large number of fluorescent molecules loaded onto each probe makes the assay highly sensitive. Each mRNA will have at least 10 probe sets, thereby increasing sensitivity of mRNA detection. Together, the assay is able to identify one copy of mRNA in a specific cell type identifiable by flow cytometry.

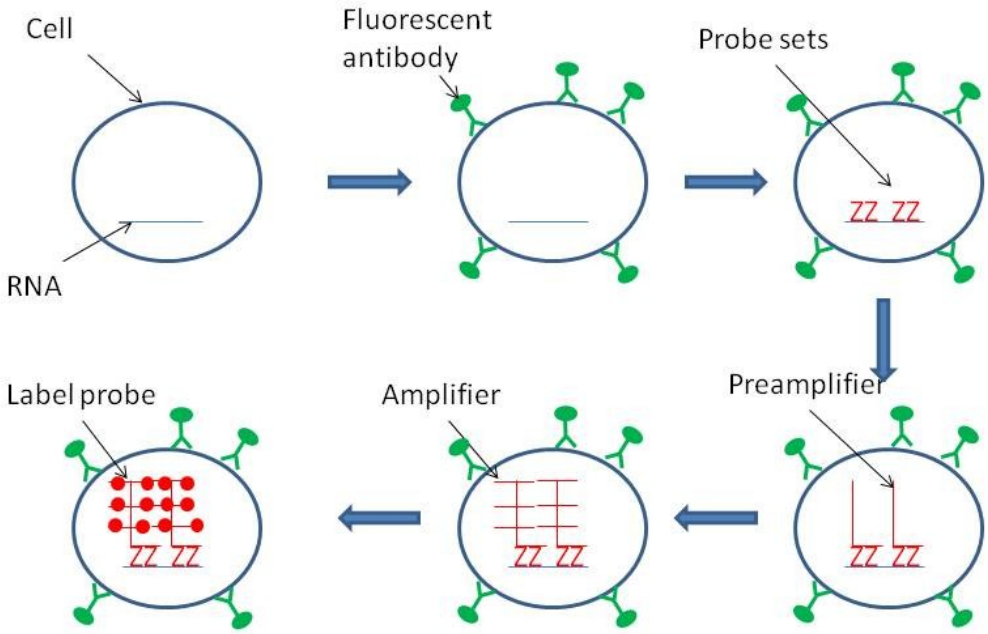

Figure 2-4 - Schematic of the PrimeFlow workflow. Firstly, cell surface staining is carried out. Next, specific probesets are hybridised to RNA. Firstly a preamplifier, then an amplifier are hybridised to the probesets, then multiple copies of a fluorescent label probe are attached to the amplifier molecules. The resulting cells can be examined by flow cytometry and gene expression within different cells can be examined.

Two probe-sets were designed to the EBER non-translated EBV RNA and to cellular β2-microglobin mRNA as a positive control. All hybridisation steps were carried out at exactly 40°C in a temperature-calibrated hybridisation oven. The cells were initially stained for cell surface markers using the antibodies shown in table 2-6. Staining was performed in MACS Buffer for 30 minutes at 4°C; the cells were then washed in the same buffer.

Table 2-6 - Antibodies used for cell surface staining in the Human PrimeFlow™ RNA assay.

Cell surface marker	**Fluorophore**	**Clone name**	**Manufacturer**	**Concentration**
CD3	AF700	OKT3	eBiosciences	1:20
CD4	ECD	SFCI12T4D11	Beckman Coulter	1:50
CD8	AF488	SK1	Biolegend	1:20
CD14	Pacific Blue	HCD14	Biolegend	1:20
CD19	PeCy7	HIB19	eBiosciences	1:20
CD56	PE	MEM-188	Invitrogen	1:20

The cells were then fixed in Fixation Buffer 1 for 30 minutes at 4°C, permeabilised by washing twice in Permeabilization Buffer and fixed with Fixation Buffer 2 for 60 minutes at 14°C. The cells were again washed twice in Wash Buffer.

The Target Probes were diluted 1:20 in pre-warmed Target Probe Diluent, then the cells were incubated in 100 µl of the diluted target probes in a 1.5 ml tube at 40°C for 2 hours. The cells

were then washed twice in Wash Buffer and stored overnight suspended in Wash Buffer containing RNAse inhibitor.

Signal amplification was achieved by incubating the cells with pre-warmed PreAmp Mix for 90 minutes at 40°C, washing 3 times with Wash Buffer, incubating with pre-warmed Amp Mix for 90 minutes at 40°C, then washing twice with Wash Buffer. Finally, the cells were incubated with the Label Probes diluted 1:100 in pre-warmed Label Probe Diluent for 1 hour at 40°C, before washing twice with Wash Buffer and once with storage buffer. The samples were then analysed using the BD™ LSRII Flow Cytometer.

CHAPTER 3 – MICROARRAY ANALYSIS OF THE EFFECTS OF LMP1 ON NK CELLS

3.1 Introduction

ENKTL is almost universally EBV-positive, with expression of a latency 2 pattern of gene expression – EBNA-1, LMP1, LMP2, EBERs and miRNAs (see chapter 1). Clonality of EBV episomes indicates that viral infection occurs early in the process of malignant transformation. This strongly suggests that the virus plays an important role in lymphomagenesis, and yet the role of these EBV gene products is still obscure.

The roles of LMP1 and LMP2 are well-characterised in B- and epithelial cell malignancies. LMP1 acts as an oncogene in rodent fibroblast models and is critical for human B-cell transformation by the virus (6). It induces the expression of anti-apoptotic proteins (81, 82). In ENKTL, however, the role is much less clear and in two NK lymphoma cell lines, reducing LMP1 levels does not seem to impact on cell proliferation to the same extent as in B-cells (58).

LMP2A is relatively well characterised in B-cells as it acts as a surrogate B-cell receptor (103). However, LMP2A expression in ENKTL is low to absent (52, 284) and it is only recently that LMP2B-TR, whose function is much more obscure even in B-cells, was shown to be expressed at significant levels in ENKTL (306).

There is very little published work to date using primary NK cells that is relevant to the role of EBV in ENTKL.

As a first step to investigating the role of EBV in the pathogenesis of ENKTL, we sought to identify the transcriptional effects of LMP1 and LMP2 in primary NK cells. Our experimental approach was to establish cultures of normal NK cells then transduce them with lentiviral vectors expressing LMP1, LMP2B or LMP2A, and then perform microarray analysis to examine changes in gene expression profile as a result of the expression of the viral protein.

3.2 Methods

The design and cloning strategy of the lentiviruses is described in detail in chapter 2. In brief, the relevant gene was amplified from the transcriptome of an EBV-positive cell line for insertion into the lentiviral plasmid. ENKTL, although rare, is proportionally much more common in Asia and South America (233, 234, 236). EBV strains also show geographical variation, the significance of which is not always clear (6); for this reason SNK6, a Japanese ENKTL line (354), was used as the source of the viral sequence for the LMP1 and LMP2B-TR. As the majority of previous LMP2A functional studies have been performed with the prototypic B95.8 sequence, and LMP2A is poorly expressed if at all in ENKTL lines, we cloned the B95.8 LMP2A sequence for comparison with the SNK6 LMP2B-TR sequence in these array experiments. As there is no reliable antibody to LMP2B, a haemagglutinin (HA) sequence was included in the LMP2B-TR and 2A vectors to enable detection of the protein with an anti-HA antibody.

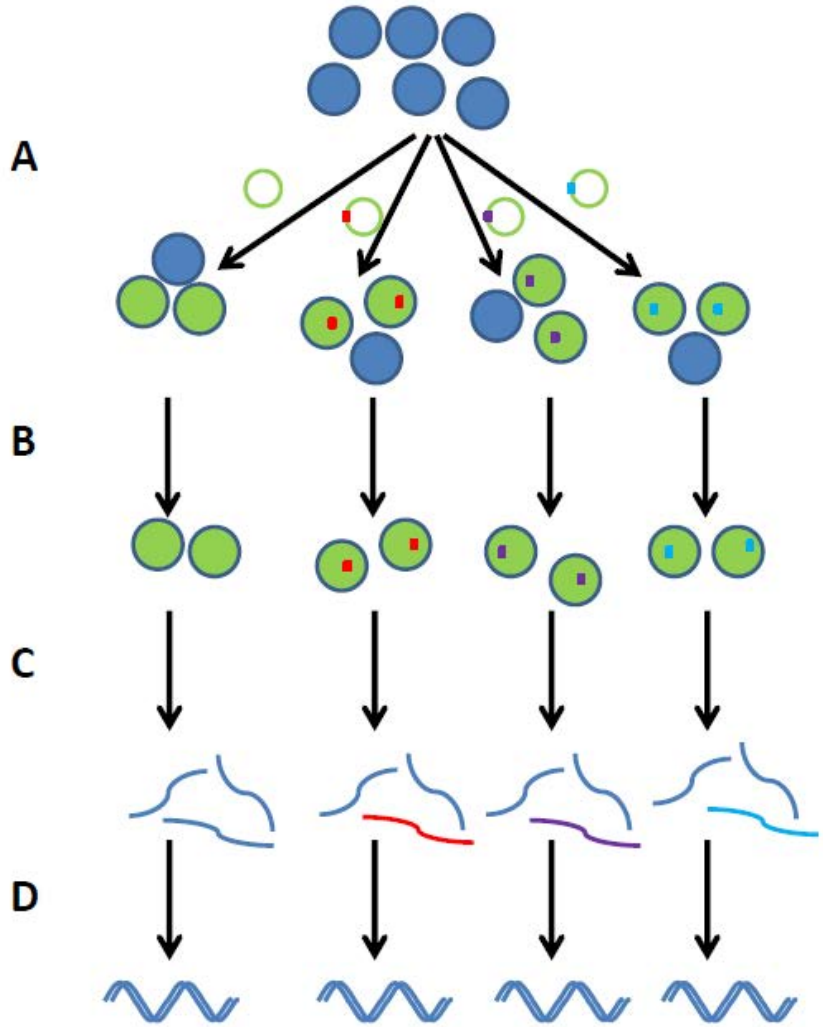

Figure 3-1 - Schematic of microarray sample preparation. A: Primary NK cells were transduced with the "empty" lentivirus or one expressing LMP1, LMP2B-TR or LMP2A. B: Cells were sorted for GFP positivity. C: RNA was extracted from sorted cells. D: cDNA was generated from the RNA.

Figure 3-1 summarises the workflow for generation of the samples for the microarray. NK cells were isolated from three different laboratory donors using the Miltenyi Human NK Cell Isolation Kit, as described in chapter 2. After one week in culture they were transduced with concentrated lentivirus - either LMP1, LMP2A or LMP2B. Samples of primary NK cells harvested with no lentiviral transduction and those transduced with an “empty” lentiviral construct with

no EBV gene expression (although GFP was constitutively expressed) were also included. Matched samples transduced with each of the lentiviruses permitted pair wise analysis using the "empty" lentivirus-transduced population as a control sample, thus minimizing detection of non-specific genetic changes as a result of in vitro culture or as a result of lentiviral transduction. More importantly, pairwise analysis gets around biological variation in NK cells from different donors.

In cell lines it is possible to generate stable cultures with lasting expression of the viral protein. However, ex vivo NK cells have a finite lifespan in culture so it is more appropriate to experiment on fresh, actively-replicating NK cells before they begin to senesce. In view of this we exploited the burst of unregulated viral protein expression seen on first transducing the cells to examine the effects of the viral protein in untransformed NK cells, harvesting at 72 hours. This has the advantage that the cells are freshly isolated and can be presumed to more closely resemble their in vivo counterparts. Figures 3-2 – 3-4 show the expression of the viral proteins in primary NK cells by qPCR and Western blot analysis. The limitations of the sample size meant that we were unable to perform protein analysis on the same samples sent for microarray analysis; we could, however, using a tiny amount of RNA perform RT-Q-PCR using the Fluidigm system (38).

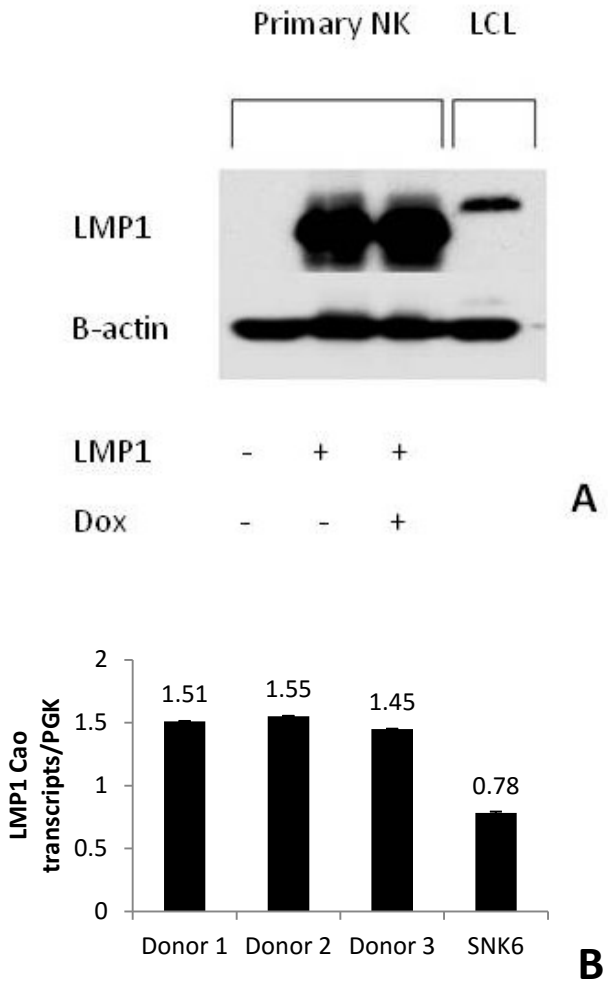

Figure 3-2 - Expression of LMP1 in primary NK cells, compared to an LCL (Western blot, panel A) and SNK6 (qPCR, figure B). As can be seen, early on following transduction the lentivirus is promiscuously expressed at a high level and is not inducible by doxycycline as the vector has not fully integrated. We took advantage of this early burst of gene expression in order to examine the effects of viral proteins on freshly-isolated NK cells. The molecular weight of the SNK6 sequence transduced into the NK cells is less than that of the B95.8 from which the LCL was derived.

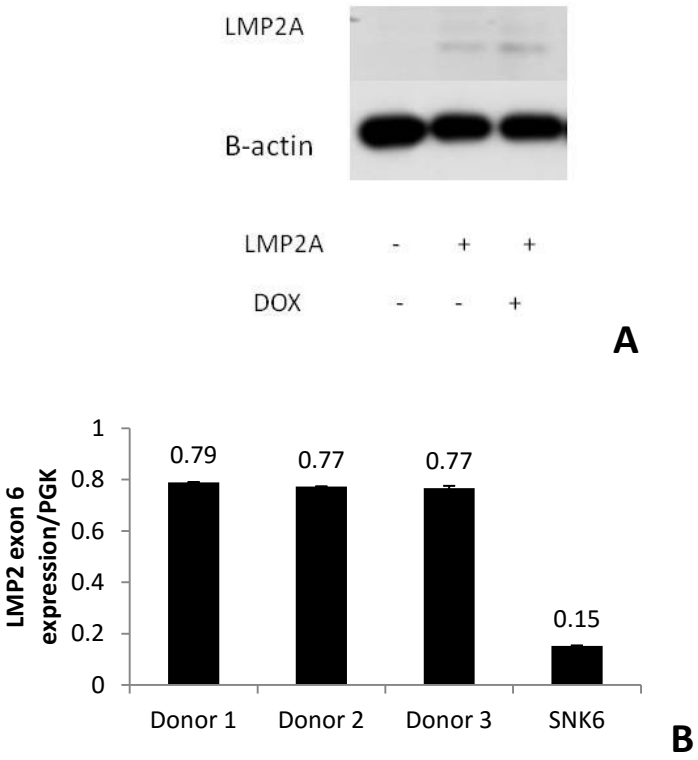

Figure 3-3 - Expression of LMP2A in primary NK cells Again showing non-inducible early expression, by Western blot (panel A) and by qPCR (panel B) in relation to SNK6.

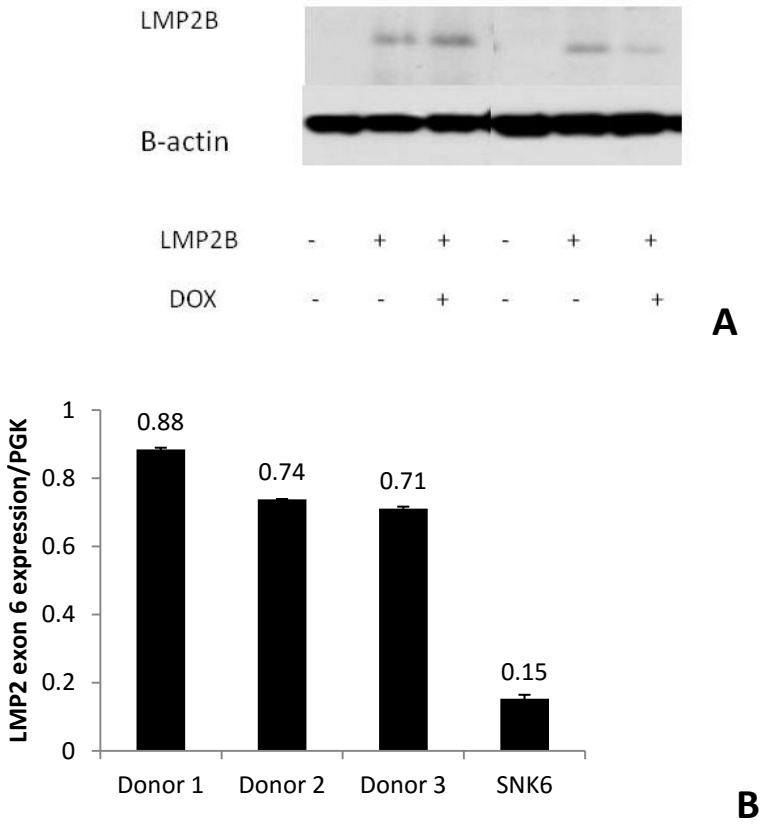

Figure 3-4 - LMP2B in primary NK cells.LMP2B in primary NK cells from 3 different donors. As there is no reliable antibody to LMP2B, the Western blot (panel A) uses an antibody to the HA tag engineered into the plasmid, and so a control with endogenous levels of expression cannot be shown. However, in the qPCR figure (panel B) it can be seen that levels of expression are significantly higher than in SNK6. Again, the expression is not inducible at this early stage after transduction.

The lentivirus constitutively expresses green fluorescent protein (GFP), enabling successfully transduced cells to be sorted after 3 days by FACS and then harvested immediately. RNA was extracted using the RNAEasy kit (Qiagen, UK) as per the manufacturer's protocol, and stored at -80°C until needed. Analysis of RNA quality and quantity was undertaken using the Eukaryote Total RNA Pico Series II Bioanalyser chip (Agilent).

The Affymetrix U133 Plus 2 array was performed at the University of Manchester as a Cancer Research UK service. Briefly, cDNA was generated from the sample RNA by reverse transcription, and then a second strand was produced. Fluorescently-labelled cRNA was then made from the double-stranded cDNA, fragmented and hybridised to the array chip. By analysing which array probe hybridises to a fluorescent RNA fragment it is possible to quantify gene expression by the cells studied.

3.3 Data analysis

Initially, the probesets were matched to their corresponding genes using the Affymetrix chip definition file. Array chips are designed with multiple probe sets running forwards and backwards across the genome. These are not limited to known genes as this would mean that as new genes are identified the chips would become obsolete. However, the existing situation means that any probe set not, as yet, associated with a known gene is impossible to interpret in the context of a gene expression array. Thus, Affymetrix-defined probe sets that have not yet been matched to a corresponding gene were discarded in this analysis. This left 42450 probe sets matching to 21014 gene symbols.

A LIMMA pair wise analysis was then performed on the resulting data by Dr Wenbin Wei. The expression of each probe set was compared between the control sample and the sample of interest. This allowed detection of any significant change of expression between the two populations. Due to biological variability, small changes in gene expression are inevitable, and

difficulties may arise when trying to determine when these approach biological significance. In order to minimise the possibility of a type I error, rigorous statistical methods are used. We set a significance limit of P<0.01 – i.e., there is a probability of less than 1% that the observed change in gene expression is due to chance rather than to a biological effect of the newly expressed gene. We also defined a significant fold-change (FC) as >1.5 for upregulated and <-1.5 for downregulated genes. The selected genes can then be categorised depending on whether they are up- or down-regulated, and lists compiled accordingly.

3.4 Results

Firstly, gene expression was compared between cells expressing the latent membrane proteins and those expressing the empty lentivirus. This gives us a core set of genes which, by this analysis, are significantly up- or down-regulated by the expression of the gene of interest (Table 3-1).

Table 3-1 - Genes differentially regulated by viral proteins in primary NK cells (FC>1.5 or <-1.5, P<0.01)

	LMP1	LMP2B	LMP2A
Number of genes upregulated	109	84	115
Number of genes downregulated	146	154	189

DAVID analysis

The **D**atabase for **A**nnotation, **V**isualization and **I**ntegrated **D**iscovery (DAVID) provides a means by which lists of differentially altered genes can be compared to those involved in known cellular pathways. This allows the identification of areas of enrichment within an expression profile (358, 359). The lists of differentially regulated probesets, as defined by the above LIMMA analysis, were entered into the database (DAVID 6.7) (360). Pathways significantly overrepresented (modified Fisher's exact test, $P<0.05$) are summarised in Table 3-2.

Table 3-2 – Pathways significantly overrepresented by expression of LMP1, LMP2B-TR and LMP2A in primary NK cells

	Pathway	**Fold enrichment**	**P value**
LMP1	Transcription (GO:0006351)	2.4	0.00000041
	Mitochondrion organisation (GO:0007005)	6.2	0.008
	Response to nutrient levels (GO:0031667)	4.4	0.011
	Cellular response to stress (GO:0033554)	2.7	0.016
	Regulation of cell death (GO:0010941)	2.3	0.017
	Response to extracellular-stimulus (GO:0009991)	4.0	0.017
	Negative regulation of cell death (GO0060548)	3.3	0.018
	Cell proliferation (GO:0008283)	2.7	0.029
	Cell cycle arrest (GO:0007050)	5.6	0.033
	Cellular amino acid biosynthetic process (GO:0008652)	10.1	0.035
	Negative regulation of gene-specific transcription (GO:0045892)	9.1	0.042
	ncRNA metabolic process (GO:0034660)	3.7	0.044
	Anion transport (GO:0006820)	4.8	0.05

	Pathway	Fold enrichment	P value
LMP2B	Transcription (GO:0006351)	1.7	0.002
	Transcription initiation from RNA polymerase II promoter (GO:0006367)	8.6	0.0026
	Amine catabolic processes (GO:0009310)	12.0	0.0029
	Cellular macromolecule catabolic process (GO:0044265)	2.4	0.0031
	Mitochondrion organisation (GO:0007005)	5.1	0.0062
	Cellular macromolecule localisation (GO:0070727)	2.6	0.024
	Protein localisation in mitochondrion (GO:0070585)	10.4	0.033
	Nitrogen compound biosynthetic process (GO:0044271)	3.6	0.048
	Histidine metabolic process (GO:0006547)	38.9	0.049
	G-protein signalling coupled to cAMP second messenger (GO:0007188)	8.2	0.05
LMP2A	Organelle localisation (GO:0051640)	6.8	0.0021
	Endoplasmic reticulum calcium ion homeostasis (GO:0032469)	38.9	0.005
	Interphase (GO:0031525)	5.3	0.015
	Positive regulation of cell differentiation (GO:0045597)	3.4	0.016
	Negative regulation of cell activation (GO:0050866)	7.3	0.017
	Regulation of cellular protein metabolic process (GO:0032268)	2.4	0.025
	Positive regulation of developmental process (GO:0051094)	2.8	0.037
	RNA splicing (GO:0008380)	2.8	0.041

As can be seen, the 255 genes differentially regulated by LMP1 are significantly enriched for pathways involved in cell cycle and cellular responses to stress. This is consistent with the previously reported effects of LMP1 in other cell types, and suggests that LMP1 may have an oncogenic effect in the NK cell. However, the 255 genes with significantly altered expression by LMP1 in NK cells is fewer than the number of genes changed in most studies where LMP1 was expressed in other cell types, e.g. 1926 genes in germinal centre B-cells (361). The reason for this difference is not clear.

It is possible that this reflects a technical issue with the microarray itself. However if that is the case the DAVID analysis suggests that, whilst there may be a reduced sensitivity in detecting significant changes, qualitatively the range of altered genes represents changes consistent with known LMP1 functions. It is also possible that the difference between the two arrays reflects the fact that we used a lentiviral expression vector whereas in the B cell array, electroporation of the plasmid was used. This may affect the way in which the cell responds to the foreign molecules. Despite the fact that adequate controls were used in both cases, it is theoretically possible that the two different strategies might result in different thresholds for detecting LMP1-specific effects.

It is also important to note here that the number of genes significantly altered is affected by the starting transcriptome as well as the final transcriptome. Consider the situation with B-cells – GC B-cells and naive B-cells are transcriptionally very different but LCLs generated from either

background are identical. As the data are analysed in a pairwise fashion, this will affect the number of genes identified as significantly altered by the expression of the protein of interest; I will show later that data from the Murray group (361) indicate that expression of LMP1 in naive B-cells results in a much smaller number of changes than that resulting from its expression in GCB-cells.

The case with LMP2A is less clear-cut. We do not know how LMP2A functions in NK cells as its most well-characterised functions depend on the ITAM signalling motifs that modulate the B cell receptor signalling pathways - these may not be operational in NK cells. However, apoptotic pathways seem to be significantly affected, which is in keeping with what we know about the function of the protein in B-cells. It is important to remember, however, that there is little evidence that LMP2A is expressed in ENKTL and so the significance of these effects is unclear. LMP2B, in contrast, is known to be expressed in ENKTL samples and cell lines, but the cellular pathways enriched do not include those classically associated with oncogenesis, further highlighting how little is understood about the function of this protein. Yet another important consideration is that relatively few genes are significantly altered using our stringent statistical limits – this inevitably results in fewer pathways being identified. However we know that LMP2B-TR is expressed in ENKTL, and the LMP2B molecule lacks the ITAM signalling sequences, suggesting that the LMP2A and LMP2B may have similar effects in an NK cell background. As can be seen in figure 3-5 and Table 3-3, there is a significant overlap in the genes up- and downregulated by LMP2B and LMP2A.

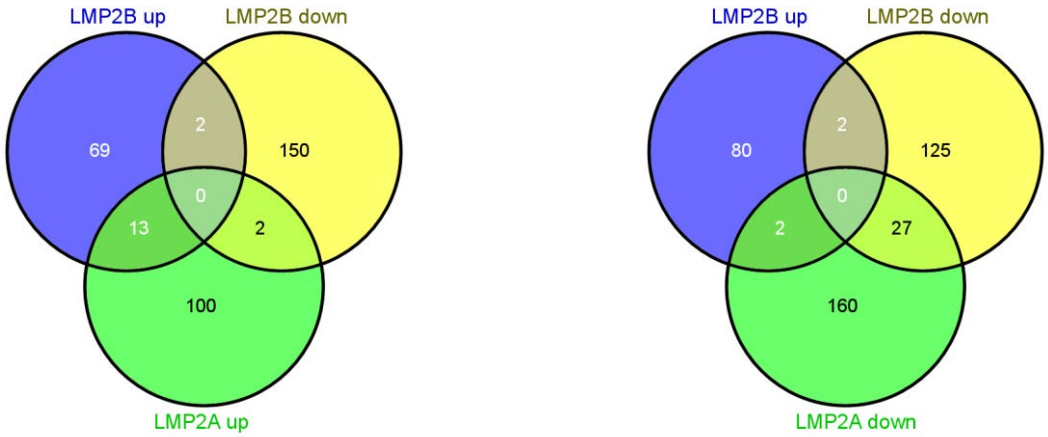

Figure 3-5 - Venn diagram showing overlap between differentially regulated genes by LMP2B-TR-TR and LMP2A in primary NK cells.

Table 3-3 - Comparison of genes differentially expressed by LMP2B-TR or LMP2A in NK cells (FC>1.5 or <-1.5, P<0.01).

Denominator: 21,014					
NK LMP2B	**NK LMP2A**	**Overlap**	**OR**	**Chi sq**	**P**
Up (84)	**Up (115)**	13	37.36	342.10	**<0.0001**
	Down (189)	2	2.71	2.05	0.15
Down (154)	**Down (189)**	27	27.12	473.71	**<0.0001**
	Up (115)	2	2.41	1.59	0.21

Comparing to other arrays

We have access to data from similar arrays performed by past and present colleagues in our department, and we used the same array platform. This allowed us to examine and compare the effects of LMP1 and LMP2 in different cell backgrounds. The most comprehensive set of

array data is for LMP1 in different B cell and epithelial cell backgrounds. As both LMP1 and LMP2A arrays have been performed on germinal centre (GC) B-cells, in the first instance, we compared our data on these two EBV genes in NK cells with corresponding array results in GC-B-cells ((361), M. Vockerodt, unpublished data). Raw data were obtained from the authors and analysed exactly in the same way as our own data; this means that the final dataset we used is slightly different to that published by the authors, but means that our comparisons are fairer. When the affected genes in this array were compared with those in one using a GC B-cell background, there was a significant overlap in the genes both up- and down-regulated by LMP1 (Table 3-4, figure 3-6). Reassuringly, there was no significant overlap in genes upregulated by LMP1 in one background and downregulated in the other.

Table 3-4– Comparison of genes differentially expressed by LMP1 in NK or germinal centre B (GCB) cells (FC>1.5 or <-1.5, P<0.01).

Denominator: 21,014					
NK LMP1	**GCB LMP1**	**Overlap**	**OR**	**Chi sq**	**P**
Up (109)	**Up (952)**	19	4.51	40.04	**<0.0001**
	Down (1732)	6	0.65	0.99	0.609
Down (146)	**Down (1732)**	22	1.98	8.25	**0.0162**
	Up (952)	10	1.55	1.733	0.424

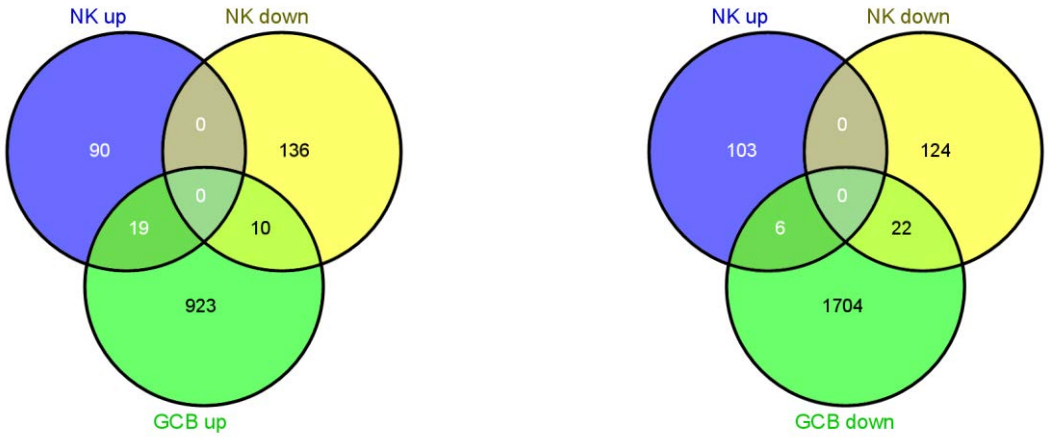

Figure 3-6 – Venn diagram of genes altered by LMP1 in NK and germinal centre B (GCB) cells. (362)

This is very reassuring as it suggests that the actions of LMP1 in NK cells are similar to those in a related lymphocyte background.

Next we compared the effects of LMP2A on NK and GCB-cells (Table 3-5).

Table 3-5 - Comparison of genes differentially expressed by LMP2A in NK or germinal centre B (GCB) cells (FC>1.5 or <-1.5, P<0.01).

Denominator: 21,014					
NK LMP2A	**GCB LMP2A**	**Overlap**	**OR**	**Chi sq**	**P**
Up (115)	**Up (79)**	1	2.34	0.75	0.69
	Down (112)	2	3.34	3.14	0.208
Down (188)	**Down (112)**	4	4.15	8.89	**0.0117**
	Up (79)	2	2.88	2.34	0.31

Interestingly there was very little overlap between the genes differentially regulated by LMP2A in the GCB and NK cells. The only sub-group where this became significant was in genes downregulated by LMP2A, and it must be emphasised that the number of genes involved is very small, so this result should be interpreted cautiously.

In B-cells, LMP2A is known to act as a surrogate B-cell receptor (BCR), and is capable of "rescuing" germinal centre B-cells with crippling mutations of their BCRs from apoptosis (103), and to modulate BCR-mediated signalling in B-cells with a functional BCR (see (106) for review). NK cells do not express a BCR, and so it is difficult to predict with any confidence firstly how the expression of LMP2A will affect the cell, and secondly whether there is any physiological relevance to the changes that are seen. This may explain why the degree of overlap between the differentially regulated genes in the two cell backgrounds is so small compared to that seen with LMP1.

There are no data available on the effects of LMP2B in other cell backgrounds, and so we are unable to compare the effects in NK cells with, for example, B-cells.

What genes are altered?

Next we focused our attention on single genes identified by the microarray findings. Beginning with LMP1, we examined the 10 genes upregulated (or downregulated) with the smallest P values. We excluded genes with no published function, and genes with very low levels of expression. When microarray data are analysed at the single gene level, care must be taken not to rely on fold-change alone as a marker of significance, as when expression of a gene is very

low a small absolute change can lead to a large fold change which seems less likely to be biologically significant. Results are shown in Table 3-6 and 3-7.

Table 3-6 – Ten genes increased by LMP1 (FC>1.5, P<0.01)

Gene name	Proposed function
MEF2C (myocyte enhancer factor 2C)	Seen in B- but not T-cells, thought to regulate differentiation and function. (363)
BCAT1 (branched chain amino-acid transaminase 1)	Overexpressed in NPC probably by *c-Myc* and thought to be involved in cell proliferation, migration and invasion (364, 365)
SNCA (synuclein, alpha (non A4 component of amyloid precursor))	Highly expressed in the brain; involved in the pathogenesis of Parkinson disease. (366)
SCD (stearoyl-CoA desaturase (delta-9-desaturase))	Enzyme involved in the synthesis of fatty acids; upregulated in many cancers and a possible target for novel chemotherapeutic agents (367)
PHGDH (phosphoglycerate dehydrogenase)	Enzyme involved in the synthesis of L-serine; contributes to oncogenesis in some cancers (368)
ARID1B (AT rich interactive domain 1B)	Subunit of the human ATP-dependent SWItch/sucrose nonfermentable (SWI/SNF) complex; important in ontogeny and possibly functions as a tumour suppressor gene in pancreatic cancer (369)
ORAI2 (calcium release-activated calcium modulator 2)	Calcium channel important in mast cell mediator release (370)
KLHL23 (kelch-like family member 23)	Novel gene, may be some association with cancer (371)
MAGI3 (membrane associated guanylate kinase, WW and PDZ domain containing 3)	Ubiquitously expressed in all tissues; involved in intracellular signalling (372)
NFRKB (nuclear factor related to kappa-B-binding protein)	Involved in DNA replication and repair, chromatin remodelling and transcription regulation (373).

Table 3-7- Ten genes downregulated by LMP1 (FC <-1.5, P<0.01)

AKAP13 (A kinase (PRKA) anchor protein 13)	Binds to protein kinase A (PKA) and localises it within the cell; may be increased in some cancers (374)
CUL3 (cullin 3)	Involved in ubiquitination and degradation of proteins, may be significant in bladder cancer invasiveness (375).
TNFSF4 (tumour necrosis factor (ligand) superfamily, member 4)	Cytokine belonging to the tumour necrosis factor (TNF) family; involved in T-cell:antigen-presenting cell interactions. This protein and its receptor are reported to directly mediate adhesion of activated T cells to vascular endothelial cells. [provided by RefSeq, Jul 2008]
CDK19 (cyclin-dependent kinase 19)	Member of the mediator complex involved in regulation of transcription (376)
ZFP28 (zinc finger protein 28)	Zinc finger protein thought to have some association with melanoma (377)
ITGA1 (integrin, alpha-1, CD49a)	Upregulated in T- and NK-cells in response to viral infection leading to T-cell inflammatory cytokine production(378)
CLNK (cytokine-dependent hematopoietic cell linker)	Expressed in cytokine-stimulated haematopoietic cells and involved in immunoreceptor signalling (379)
CCND3 (Cyclin D3)	Necessary for cell division
MPZL2 (myelin protein zero-like 2)	A member of the immunoglobulin superfamily, expressed in thymus epithelium , important in T-cell maturation (380)
LHX9 (Lim-homobox 9)	Transcription factor important in neural cell differentiation; reduced expression in paediatric gliomas associated with migration and invasiveness (381)

With the intriguing exception of genes associated with neural tissue, the others identified here fit well with the pathways demonstrated by the DAVID analysis; most interestingly, they are biologically plausible for the predicted role of LMP1 in ENKTL.

3.5 Validating the array

Conventionally, gene expression arrays are validated using qPCR. Assays are made (either by the user or by a commercial company) by designing primers and probesets predicted to react

specifically with the major transcripts(s) of the gene of interest. By simultaneously including an assay for a ubiquitously expressed "housekeeping" gene we can control for variability in the RNA.

Whilst qPCR assays are reliable, one of the limitations of this technique is that realistically only a few genes can be validated at a time. To improve our validation, therefore, we utilised a new high-throughput chip system. This has been designed for use on small amounts of RNA (382). The Fluidigm Dynamic Array™ integrated fluidic circuit uses a chip containing a system of channels, valves and chambers to enable automatic assembly of multiple simultaneous qPCR reactions. The advantage in our case is that the amount of cDNA required is small and so a portion of the identical sample used for the microarray could be used rather than simply a biological replicate. Briefly, qPCR assays containing forward and reverse primers and a labelled probe, are made or purchased (TaqMan® Gene Expression Assays, Applied Biosystems, USA) for each gene of interest. These are pooled, combined with cDNA from the sample and subjected to a pre-amplification stage to selectively amplify the cDNA of transcripts of interest. The amplified cDNA is loaded on to the chip with the single assays and the chip is subjected to qPCR analysis. The combination of each sample with each qPCR assay is automated and takes place in a chamber within the chip.

When choosing which genes to validate, several factors must be borne in mind. Firstly, in order to maximise the biological relevance, genes with a statistically significant change in expression should be used. Secondly, the absolute level of expression must be sufficiently high to be detected by qPCR. Finally, to minimise the problem of genomic DNA contamination, a qPCR

assay spanning more than one exon must be available. Of course it is also relevant and important to validate the expression patterns seen in unchanged genes, or indeed in non-expressed genes, and the nature of the Fluidigm process, where every sample is tested with every assay, allowed us to use genes that were not altered by one protein as controls in this way. Bearing these factors in mind, we chose 25 genes for analysis by Fluidigm (see table 3-8).

We were surprised to find that only about half of our chosen genes seemed to show similar changes with Fluidigm qPCR analysis as were seen in the original microarray. Similar results were obtained for all 3 EBV genes studied. There are little available data in the literature on array validation. It is often difficult to tell from published work exactly how validation was undertaken and what were the results; commonly, validation data are only shown for individual "interesting" genes. However, the proportion of genes that validated in our NK cell arrays was consistent with the experience of colleagues in this department who have used the Affymetrix U133 Plus 2 array platform extensively (personal communications).

Possible reasons for the discrepancies between the array results and the qPCR validations that were experienced by ourselves and others include: 1) selective amplification of some transcripts in the Fluidigm Specific Target Amplification (STA) step, 2) low gene expression initially leading to potentially large fold change variation with small absolute changes or 3) detection by array and qPCR of different subsets of alternative transcripts for a particular gene. However, a recurring theme in the literature concerned the complexity and reliability of annotation of the Affymetrix array probesets, which we explored further.

On average, every gene in the Affymetrix Human Genome U133 Plus 2.0 array is represented by 2.8 probesets, so called “sibling probesets” (383). However, we noticed that where several probesets map to a single gene, not all of them are necessarily altered in the same way by the expression of the viral protein. For example, BHLHB9 has 3 probesets in the array of which one was significantly upregulated by the expression of LMP1 in the NK cells and the other 2 were downregulated, although this change did not reach statistical significance.

The Affymetrix probe sets were generated with the intention of covering the entire genome, rather than just targeting known genes. This concept was intended to allow the array chips, and indeed array data, to be interrogated for the presence of novel gene transcripts as they were defined, and thus prolong the useful life of the technology. Affymetrix provides updated annotations to try and deal with this but does not address the situation where a subset of probes within the probeset maps to another gene, either instead of, or as well as, the one to which it is attributed. It therefore appears that some probes have been misattributed to the relevant gene, with incorrect directions of reading of the genome and sequences. As a result, relying on the Affymetrix annotation system alone may produce erroneous conclusions. For example, ISG20L2 has 3 probesets attributed to it by the Affymetrix chip definition file (CDF). Of these, one was significantly upregulated by LMP2A; on further analysis, this probeset is for the non-coding direction (see Figure 3-7).

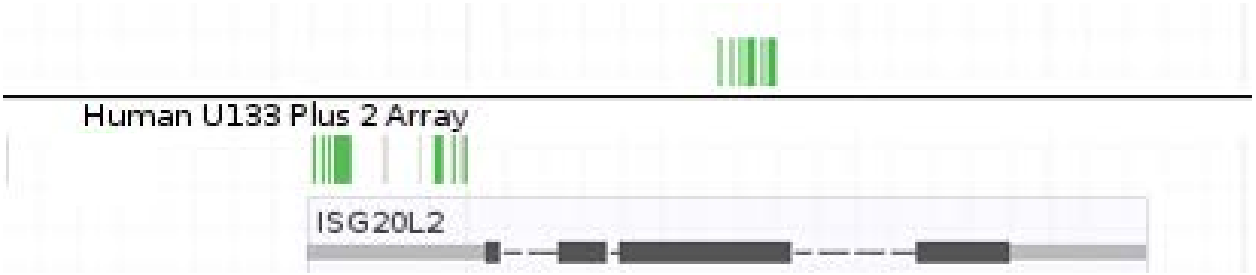

Figure 3-7- Location of the probesets attributed to ISG20L2. Black bars indicate coding exons, grey bars non-coding exons, dashed lines introns and green lines Affymetrix probes. Genes and probesets above the solid line are read left-to-right; below the line right-to-left. Note that of the 3 probesets shown, only 2 are in the same direction as the gene coding. From the Annmap Genome Browser (384, 385)

When this is compared to MYC, which has only 2 probesets attributed to it, we can see that they are both directed to the correct strand (Figure 3-8).

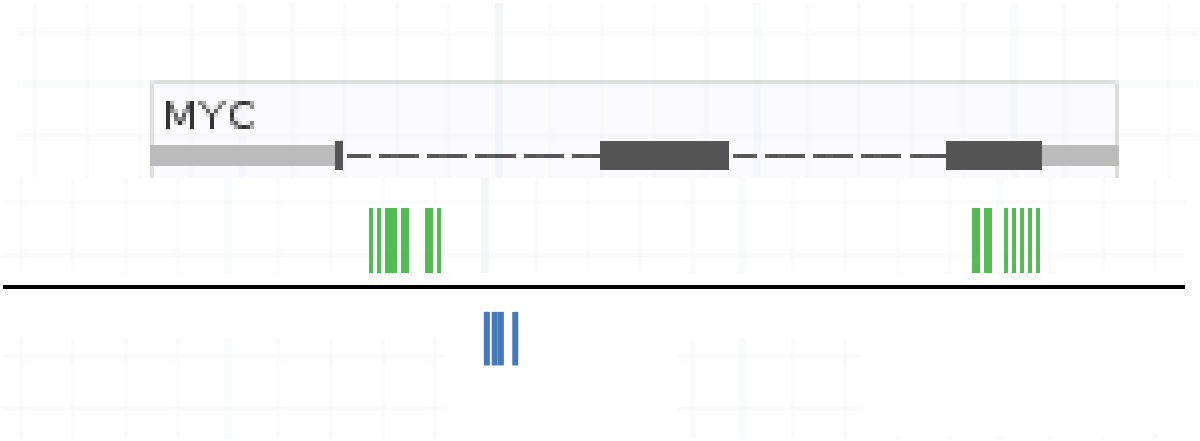

Figure 3-8 - Location of the probesets attributed to MYC. Black bars indicate coding exons, grey bars non-coding exons and dashed lines introns. Genes and probesets above the solid line are read left-to-right; below the line right-to-left. The green lines represent probesets attributed to MYC; the blue lines represent probesets not attributed to MYC. Note that both MYC probesets are in the same transcriptional direction as the gene. From the Annmap Genome Browser (384, 385)

Bearing this in mind, we returned to our Fluidigm validation and this time compared the results with those of every probeset annotated with the name of the relevant gene (Table 3-8).

Table 3-8 – Fold change of selected genes by microarray and by Fluidigm validation. Note that where there is more than one probeset labelled for a gene, the results for each probeset are shown individually. DNA indicates that the PCR reaction did not amplify. Green shades indicate upregulation and red shades downregulation.

	LMP1 Fold Change						LMP2B-TR Fold Change					
Gene	Array					Fluidigm	Array					Fluidigm
MEF2C	3.09	1.95	1.81			-1.18	1.48	1.36	1.14			1.05
SNCA	2.46	1.54	1.29	1.24	1.00	1.63	-1.20	1.15	1.05	1.05	1.02	1.26
PHGDH	2.35					2.05	1.36					-1.16
ITGA1	-2.29	-2.21				-2.00	1.12	1.27				1.38
RSAD2	-1.59	-1.50				1.07	-2.01	-1.49				1.12
HOXA5	1.14					1.70	2.12					-1.68
RAP1GAP2	1.18					1.00	1.18					4.19
DIAPH2	1.51	1.60	-1.06			-1.33	-1.24	1.99	-1.12			-1.84
HBEGF	1.19	1.08	1.08	1.08		2.35	1.19	-2.49	-1.62	-1.00		-1.00
PDE8B	-1.49	1.26	-1.05			DNA	1.31	-2.44	1.15			DNA
HLA-A	1.08	1.02				-1.28	1.17	1.07				-1.30
BIRC5	1.33	1.23	1.25			1.69	-1.09	1.08	1.04			2.01
CD74	1.21	1.15	1.23			-1.51	1.03	1.13	-1.00			-1.78
DUSP6	1.21	1.36	1.01			1.19	-1.03	-1.41	-1.07			-1.32
MYC	1.66	1.12				1.31	-1.10	-1.05				-1.47
SOCS1	1.43	1.34	1.22	1.17		-1.57	-1.21	-1.15	-1.14	-1.09		-2.56
ZEB2	-1.50	1.23	-1.34	-1.46		-1.57	-1.20	-1.26	-1.20	1.12	1.11	-1.54
BCL2	-1.29	-1.09	1.07	1.04		-1.19	-1.12	-1.20	1.29	-1.18	1.00	-1.28
CXCR3	1.59	-1.11				-1.06	1.55	-1.14				-1.49
EGR1	-1.12	1.13	1.01			-1.05	-1.07	-1.04	-1.03			-2.13
TBX21	-1.00					-1.05	-1.18					-1.20
CIITA	-1.70	-1.17	-1.05			-1.85	-1.36	-1.12	-1.18			-1.47
PMAIP1	1.04	-1.02				1.12	-1.56	-1.47				-1.56
DICER	1.42	1.25	-1.07	-1.10	-1.02	1.12	-1.47	-1.38	1.38	-1.12	-1.06	-1.15
GLT8D2	2.71	1.53				DNA	-1.12	1.12				DNA
IFT74	1.97	1.18				-1.74	1.64	-1.09				-2.78
PHGDH	2.35					1.77						-1.69
SCD	2.39	2.00	1.91	1.39	1.43	1.28	1.42	1.40	1.23	1.07	1.03	-1.57
C17orf66	-2.14					-1.28						2.64
FCHO2	-2.07	1.03				DNA	1.22	1.17				-2.71
MRC2	-2.20	1.04				-2.56	-1.30	1.18				-1.87
TGFB1T1	-2.08					-2.26	-1.55					-2.48
TNFSF4	-2.68					-2.51	-1.16					-2.32
ZNF383	-2.16					-2.13	-1.08					-1.74

ZNF527	-2.63	1.21				-2.95	-1.64	1.15				-3.12
ZNF565	-2.04					-3.76	-2.01					-4.26
RAD9B	2.24	1.11				-3.30	2.62	1.29				DNA
GSTM4	1.48	1.00				-1.41	2.13	1.54				-2.08
KCNMB4	1.31	1.39				-1.32	1.91	1.37				-1.06
SYNGR3	1.24					1.03	1.85					1.35
ARG1	-1.29	-1.29	1.01	-1.00		DNA	1.78	1.39	1.17	-1.05		DNA
ALDOC	1.30					-1.32	1.73					-1.32
HCN3	-1.74					-1.15	-2.20					1.14
SRFBP1	-1.42					-1.65	-2.41					-3.15
ZNF573	-1.74	1.10				-2.95	-2.35	1.03				-4.03
NID2	-1.38					1.80	-2.28					1.32
SCG5	-1.05					-1.89	-1.72					-2.03
BEX1	1.09					DNA	1.71					DNA

As can be seen here, there are several genes where the different probesets show a lack of conformity in their response to either LMP1 or LMP2B. The situation with LMP2A was similar (data not shown).

There are two important conclusions which can be drawn at this stage. Firstly, the lack of agreement between the Fluidigm data and the original microarray can be explained at least in part by the dissimilarity between expression patterns of probesets attributed to the same gene. Secondly, and more worryingly, this suggests that relying on the Affymetrix probeset annotation for analysis of the microarray data to identify interesting genes is likely to be inaccurate.

In order to overcome this, we next performed our comparison analyses using the Affymetrix probe set identifiers rather than the gene names. Any probeset without a named gene was discarded from the analysis even if the resulting change in expression appeared significant. Results are shown in Table 3-9.

Table 3-9 - Genes differentially regulated by viral proteins in primary NK cells when analysed at the probeset level (FC>1.5 or <-1.5, P<0.01).

	LMP1	LMP2B	LMP2A
Number of probesets upregulated	113	88	122
Number of probesets downregulated	148	160	199

When compared to the analysis performed at the gene level using the Affymetrix gene labels (Table 3-1), the results are similar. This suggests that although we know that some genes have several allocated probes on the Affymetrix chip, in our analysis there do not appear to be many genes with multiple probes altered by the viral proteins. This is concerning as we know that many genes do have multiple probesets in the array; our results suggest that possibly only one of these is being altered by the EBV gene, which raises questions about the reliability of the data, as if a gene's expression is truly being altered then we would expect to see this reflected in all of the probesets attributed to that gene.

The preceding analyses comparing the effects of LMP1 in NK- and GC-B-cells were repeated at the probeset level (Table 3-10).

Table 3-10 – Analysis of LMP1 effects on NK and GCB-cells at the probeset level (FC>1.5 or <-1.5, P<0.01).

Denominator: 42,450					
NK LMP1	**GCB LMP1**	**Overlap**	**OR**	**Chi sq**	**P**
Up (113)	**Up (953)**	11	4.74	28.23	**<0.0001**
	Down (1656)	1	0.22	2.64	0.27
NK LMP1 down (148)	**Down (1656)**	6	1.04	0.0089	0.9956
	Up (113)	1	0.22	2.64	0.27

When compared to table 3-4 (analysis of the effect of LMP1 using Affymetrix gene annotation), although there was significant overlap in the probesets upregulated by LMP1 in NK and GCB-cells, those downregulated were not statistically similar. Also, the number of overlapping probes is much lower than the number of genes. This suggests that some of the overlapping genes as defined by the Affymetrix notation were, in actual fact, represented by different probe sequences, and that not all of the probesets purported to represent a given gene were altered by the same magnitude and direction by the viral protein – due to multiple mRNA isoforms cross-hybridising to different probes, probesets that target more than one gene and mislabelled probesets. These issues with Affymetrix microarray analysis are well described (383, 386), albeit usually ignored. To illustrate the scale of the problem, when the ambiguous cross-hybridising and incorrectly orientated probesets are removed, only 11,837 genes remain identified from an original number of 20,932 (Dr Wenbin Wei, personal communication).

The analysis is further complicated by the fact that genes are represented by different numbers of probesets – some as many as 20, some as few as 1; and genes with more probesets are more likely to appear in the lists of significantly altered genes purely by chance. Therefore, although the denominator for this analysis is 42,450, these are not actually 42,450 *independent* probesets. Correcting for this statistically is complex. One method is to group all the probesets by the number of probesets per gene and analyse them separately – for example, all the probesets where there is only one probeset per gene in one group, where there are 2 probesets per gene in a second group, and so on. However, not only is this particularly time-consuming, the denominators of some of the groups become so small as to be unreliable. Furthermore, even this doesn't resolve the problem where multiple probesets against the same gene do not change in the same way. This situation, in combination with the low rate of qPCR validation, caused us to consider carefully the appropriateness of the Affymetrix annotation in this case.

There have been several strategies reported in the literature to try to correct for this problem. The problems with a probeset analysis are discussed above. Choosing one probeset to represent a certain gene and discarding the others has been suggested (see (383)) but means discarding potentially useful data. Li et al (387) proposed a method whereby probesets to the same gene which behave in the same manner for a certain array (as determined by statistical analysis) are grouped together whereas other probesets to the same gene are not. The disadvantages here are that these groupings will vary from dataset to dataset, making comparison between datasets difficult, again, data are lost by the analysis. A more sophisticated approach is to combine statistical analysis of sibling probesets with sequence

analysis of the probesets as described by Schneider et al (383), but the drawbacks of this method are similar.

The other reported solution to the problem is the use of custom chip definition files (CDFs) as discussed by Dai et al (386). A CDF can be considered as a "key" to the microarray chip; it is a file which matches probe sequences to that of known genes. Affymetrix provide a CDF as a matter of course, but the problems with this have been discussed above. Custom CDFs generate an entirely new set of probe labels matching stringent criteria. For example, Dai et al demanded that firstly the probe sequence should match the gene sequence exactly. Secondly, each probe in a probe set should have only one perfect match within the genomic sequence. Thirdly, the probe should match a genomic region corresponding to a transcribed mRNA, not just an expressed sequence tag (EST), as these have high rates of error. Fourthly, the probe must not match another gene. Fifthly, the probes within a set should all match to the same genomic sequence. Finally, each probe set must contain at least 3 probes (386). The authors suggest that with their custom CDF there can be as much as a 40% difference in the final list of differentially regulated genes when compared to conventional analysis. Drawbacks include the need to reanalyse the raw data with the custom CDF file (which may be problematic in comparing to historical arrays if only processed data are available), and, again, the discarding of some potentially accurate data due to the stringent entry criteria. Finally, the CDF file must be constantly updated as new sequence information becomes available, and care must be taken to use the most recent version in analysis (see (388) for file downloads). This last point also applies to the Affymetrix CDF, although it is updated less frequently and, apparently, with less rigour.

We therefore repeated our analysis using the Entrez custom CDF file (388), with interesting results (Table 3-11).

Table 3-11 - Comparison of genes differentially expressed by LMP1 in NK or germinal centre B (GCB) cells using the Entrez CDF gene labels (FC>1.5 or <-1.5, P<0.01).

Denominator: 18,718					
NK LMP1	**GCB LMP1**	**Overlap**	**OR**	**Chi sq**	**P**
Up (44)	**Up (492)**	3	2.72	2.94	0.0864
	Down (753)	2	0.23	0.030	0.863
Down (78)	**Down (753)**	5	1.64	1.11	0.292
	Up (496)	2	0.97	0.00217	0.962

Unlike the previous analyses (Table 3-3 and Table 3-9), the overlap between genes upregulated by LMP1 in the two cell backgrounds (NK cells vs. GC B-cells) is no longer significant. When, using the custom CDF file, the effect of LMP1 in NK- and naive B-cells (M. Vockerodt, unpublished data) is compared the results are even more striking (Table 3-12)

Table 3-12 - Comparison of genes differentially expressed by LMP1 in NK or naive B-cells using the Entrez CDF gene labels (FC>1.5 or <-1.5, P<0.01).

Denominator: 18,718					
NK LMP1	**Naive B**	**Overlap**	**OR**	**Chi sq**	**P**
Up (44)	**Up (27)**	0	0	0.063	0.969
	Down (54)	0	0	0.13	0.9371
Down (78)	**Down (54)**	0	0	0.23	0.89
	Up (27)	0	0	0.11	0.95

As discussed above, the usual host cells for EBV are B-lymphocytes and epithelial cells; it could be expected that the virus would have evolved to have a stereotyped and coherent strategy for infection of these cells whereas that in NK cells may be less well developed. With this in mind, we then compared the effects of LMP1 in NK cells with AdAH (an epithelial hybrid nasopharyngeal cell line (389)) and SCC12F (a squamous epithelial cell line (75, 390)) (Table 3-13 and Table 3-14). As can be seen there is no significant overlap between genes upregulated or downregulated by LMP1 in these cell backgrounds. The significant result for LMP1 upregulated genes in NK cells and downregulated in AdAH cells highlights the fact that, in these very different cell backgrounds, LMP1 appears to be having very different effects.

Table 3-13 - Comparison of genes differentially expressed by LMP1 in NK or AdAH nasopharyngeal carcinoma cells using the Entrez CDF gene labels (FC>1.5 or <-1.5, P<0.01).

Denominator: 18,718					
NK LMP1	**AdAH LMP1**	**Overlap**	**OR**	**Chi sq**	**P**
Up (44)	**Up (461)**	1	0.92	0.00646	0.94
	Down (494)	4	3.71	6.94	**0.008**
Down (78)	**Down (494)**	3	1.48	0.43	0.512
	Up (461)	1	0.513	0.44	0.507

Table 3-14 - Comparison of genes differentially expressed by LMP1 in NK or SCC12F squamous epithelial cells using the Entrez CDF gene labels (FC>1.5 or <-1.5, P<0.01).

Denominator: 18,718					
NK LMP1	**SCC12F LMP1**	**Overlap**	**OR**	**Chi sq**	**P**
Up (44)	**Up (45)**	0	0	0.106	0.74
	Down (40)	0	0	0.094	0.76
Down (78)	**Down (40)**	0	0	0.167	0.68
	Up (45)	0	0	0.188	0.66

We next compared the effects of LMP1 in naive and germinal centre B-cells (Table 3-15). As expected, there was a significant degree of overlap between genes upregulated and downregulated by LMP1 in these very similar cellular backgrounds.

Table 3-15 - Comparison of genes differentially expressed by LMP1 in GCB or naive B-cells using the Entrez CDF gene labels (FC>1.5 or <-1.5, P<0.01).

Denominator: 18,718					
GCB	**Naive B**	**Overlap**	**OR**	**Chi sq**	**P**
Up (492)	**Up (27)**	5	8.49	25.94	**<0.0001**
	Down (54)	2	1.42	0.238	0.626
Down (753)	**Down (54)**	10	5.48	28.21	**<0.0001**
	Up (27)	2	1.91	0.77	0.38

We next compared the effects of LMP1 on the two epithelial cell lines (Table 3-16). Again, there is a marked and significant degree of overlap between differentially regulated genes within these cells.

Table 3-16 - Comparison of genes differentially expressed by LMP1 in AdAH nasopharyngeal carcinoma cells or SCC12F squamous epithelial cells using the Entrez CDF gene labels (FC>1.5 or <-1.5, P<0.01).

Denominator: 18,718					
AdAH LMP1	**SCC12F LMP1**	**Overlap**	**OR**	**Chi sq**	**P**
Up (461)	**Up (45)**	6	6.15	21.59	**<0.0001**
	Down (40)	1	1.02	0.00022	0.99
Down (494)	**Down (40)**	15	22.78	184.19	**<0.0001**
	Up (45)	9	9.37	51.39	**<0.0001**

Finally, we compared the effects of LMP1 on epithelial cells and B-cells (table 3-17), and showed that there was no significant overlap in gene expression. This corroborates our findings when epithelial cells were compared with NK cells, and suggests that the pattern of gene expression imposed by the viral gene may be different in different cell backgrounds.

Table 3-17 - Comparison of genes differentially expressed by LMP1 in AdAH nasopharyngeal carcinoma cells or naive B-cells using the Entrez CDF gene labels (FC>1.5 or <-1.5, P<0.01).

Denominator: 18,718					
AdAH LMP1	**Naive B LMP1**	**Overlap**	**OR**	**Chi sq**	**P**
Up (461)	**Up (27)**	0	0	0.66	0.42
	Down (54)	0	0	1.33	0.25
Down (494)	**Down (54)**	2	1.42	0.23	0.63
	Up (27)	1	1.42	0.12	0.73

In conclusion, we can see that LMP1, whose function is well-characterised in B- and epithelial cells, also causes differential expression of several cellular genes in an NK cell background, although not necessarily the same ones.

There are no published microarrays looking at LMP1 in NK cells with which to compare our data, but we do have access to data from a series of ENKTL samples (391). We analysed these by comparison to uninfected NK cells rather than to those transduced with the empty lentivirus. The repeat analysis was necessary as the published array data did not include relevant controls that would have allowed direct comparison with our array. When this was compared with the effects of LMP1 and 2B on primary NK cells (table 3-18 and Table 3-19) we can see that the genes differentially regulated by LMP1 are significantly similar to those seen when the gene

expression profile of the ENKTL is compared to that of our uninfected primary NK cells. LMP2A shows an overlap with downregulated but not upregulated genes (data not shown). However, LMP2B shows no significant overlap with ENKTL samples (table 3-19).

Table 3-18 - Comparison of genes differentially expressed by LMP1 in NK cells with those expressed in ENKTL biopsies compared to uninfected NK cells using the Entrez CDF gene labels

Denominator: 18,718					
NK LMP1	**ENKTL**	**Overlap**	**OR**	**Chi sq**	**P**
Up (44)	**Up (2869)**	14	2.58	7.81	**0.0052**
	Down (2769)	2	0.27	3.12	0.0773
Down (78)	**Down (2769)**	21	2.12	7.76	**0.0053**
	Up (2869)	11	0.91	0.076	0.7828

Table 3-19 - Comparison of genes differentially expressed by LMP2B in NK cells with those expressed in ENKTL biopsies compared to uninfected NK cells using the Entrez CDF gene labels

Denominator: 18,718					
NK LMP2B	**ENKTL**	**Overlap**	**OR**	**Chi sq**	**P**
Up (42)	**Up (2869)**	6	0.92	0.0297	0.8632
	Down (2769)	2	0.29	2.86	0.0908
Down (54)	**Down (2769)**	12	1.65	2.01	0.1563
	Up (2869)	7	0.822	0.197	0.6572

3.6 Discussion

There are two main conclusions to be drawn from these results. Firstly, the data are consistent with LMP1 exerting a significant oncogenic effect on the primary NK cells – this is perhaps unsurprising given its known function as an oncogene in other cell backgrounds, but given the lack of any significant overlap with the gene expression in B- and epithelial cells suggests that it may have a different mechanism of action in NK tumours. Secondly, there is no significant overlap in genes differentially expressed in ENKTL and as a result of LMP2B-TR expression, suggesting that LMP1 makes a greater contribution to the transcription profile of ENKTL than LMP2B does.

With this in mind, it is perhaps surprising that LMP2B does not show more overlap with the ENKTL data set. There are several possible explanations for this. Firstly, it must be considered that the number of differentially regulated genes in the primary NK arrays is relatively small. This is, to some extent, a reflection of our stringent statistical criteria. It is possible that longer term expression of the viral protein might have led to more striking changes in gene expression, but in view of the short lifespan of primary NK cells *in vitro*, this is likely to introduce significant inaccuracies. The existence of the stereotyped latency patterns of EBV gene expression suggests that the EBV proteins may act co-operatively to produce a phenotype; if this is the case then LMP2B may be unable to exert a significant effect without LMP1 co-expression. Finally, when considering ENKTL primary tissue, it is necessary to bear in mind that the tumours are characteristically necrotic, with the resultant changes in gene expression as well as infiltration

by inflammatory cells. For this reason, gene expression profiling of biopsy material in this case is inevitably somewhat inaccurate when trying to obtain a picture of the cancer cells *per se*, and is one of the reasons why so many of such studies rely upon established cell lines.

In summary, we expressed the EBV proteins LMP1, LMP2A and LMP2B in primary NK cells using a lentiviral vector, and examined the resultant changes in gene expression profiling using an Affymetrix U133 Human Genome microarray. Differentially regulated genes included those involved in cell cycle and apoptosis. Using a custom CDF to avoid inaccuracies due to probeset misannotation we compared our results with those seen with the same proteins in B and epithelial cells, and showed that although there was limited overlap between those seen in NK cells, the results seen when compared to ENKTL were strikingly similar. LMP1 in particular shows a marked overlap with the ENKTL samples, and the role of this protein in NK cells needs further elucidation.

Further work which could be performed in this area includes a thorough analysis of the genes either up- or down-regulated by both LMP1 and in the ENKTL samples. This was limited by lack of time (the issues with the interpretation of the microarray results arose late in the course of this study), but also by an understandable reluctance on the part of the researchers to commit further time and money to this somewhat flawed data set. Although we are fortunate to have access to the ENKTL data, there are various issues with it: firstly, the controls used (fresh and IL-2-stimulated NK cells, in culture for a maximum of 24 hours (297)) seem inadequate as we know that NK cells are dependent upon IL-2 to grow *in vitro* and the cytokine-induced changes to the cells will not be complete at 24 hours. Secondly, the ENKTL data included a subgroup of γδ T

cell malignancies and EBV-negative tumours (391), and despite appeals to the authors we have been unable to determine which these are in order to remove them from the analysis. In summary, we feel that the above results, although intriguing, should be followed up in a different manner.

RNA sequencing involves sequencing the entire RNA transcriptome, or just a selected section of it (for example, coding mRNA, miRNA, etc). RNA is isolated and reverse transcribed into cDNA. The transcriptome is then constructed either by *de novo* assembly or by comparison to a reference genome. This technique allows analysis of gene expression without any of the probe issues discussed above, and has the advantage of providing the actual RNA sequence, so permitting the detection of mutations or polymorphisms. Excitingly, it can also be used to simultaneously analyse viral RNA if required (392). The technology is relatively new, and not without problems (393), but it would seem that the next logical step in this situation is to repeat the experiment using RNA sequencing, including well-characterised tumour samples with appropriate controls.

CHAPTER 4 - CHARACTERISING THE APOPTOSIS RESISTANCE PHENOTYPE IN ENKTL

4.1 Introduction

Many investigations have been performed over the last 50 years to try to elucidate how EBV contributes to lymphomagenesis. The majority of these studies have been performed on B cell derived lymphomas; to date the role played by EBV in T cell and NK cell lymphomas has been largely neglected primarily due to the rarity of these diseases and the access to lymphoma tissue before treatment. The contribution of the virus is better understood in Burkitt lymphoma (BL), where it is thought that it can contribute to tumour maintenance via anti-apoptotic effects as well as a likely role in tumour initiation (reviewed in (394)). Recent studies have shown that EBV provides BL with an apoptosis-resistance phenotype, which is significantly enhanced if the cells exhibit the Wp-restricted viral gene expression profile (132, 395). We therefore sought to determine if EBV contributes towards the apoptosis-resistance phenotype commonly observed in ENKTL compared to the non-malignant and apoptosis-sensitive CAEBV.

Apoptosis is vital not only for the maintenance of normal tissues but also provides a means whereby the body can protect itself from cancer. Upon detecting potentially oncogenic damage, for example double-stranded DNA breaks, the cell can initiate an apoptotic cascade and effectively commit suicide before it can divide and form a tumour. Many of the currently-used chemotherapy agents exploit these apoptotic pathways, either by causing sufficient damage to the cell that it initiates apoptosis itself, or, increasingly, by directly feeding in to the

cascades. ENKTL in particular is resistant to many conventional chemotherapeutic agents, which may suggest that the tumours have an apoptosis-resistance phenotype similar to that seen in BL.

The rarity and clinical behaviour of ENKTL and other EBV-positive T- and NK-cell disorders means that we rely heavily upon cell lines in order to examine cell behaviour. The cell lines we used in this study are summarised in table 2-1. These have been created by careful and methodical culture of patient samples, and represent both the malignant ENKTL and non-malignant CAEBV.

We first examined the EBV gene expression by both the levels of EBV mRNA transcripts and protein and compared these between a panel of 'malignant' cell lines with 'non-malignant' cell lines.

4.2 - Characterising the EBV gene expression profile of ENKTL and CAEBV cell lines.

Analysis of the EBV gene expression profile has only previously been performed on a very limited subset of the ENKTL cell lines. We have since collected further ENKTL cell lines and analysed the EBV gene expression profile using an extensive panel of viral qPCR assays using the Fluidigm Specific Target Amplification system for viral mRNA expression. The EBV qPCR assays used were developed and validated by Dr A Bell, and have all been published (38, 50, 396).

Representative results from these experiments are shown in figures 4-1 to 4-5. Sequence variations in EBV strains have been noted particularly in LMP1; the LMP1 Cao assay has been designed specifically to detect the sequence variant prevalent in SE Asia and Japan, and therefore seen in the ENKTL cell lines, whereas the B95.8 assay detects the gene first sequenced

from a Caucasian IM patient and prevalent outside SE Asia including African BL samples. The TR assays for LMP1 and LMP2 detect transcripts initiated from the terminal repeat region of the genome; LMP2 exon 6 assay was developed to detect both LMP2A and LMP2B via their common region. For each individual assay, the viral gene expression was normalised to the input of cDNA to control for any differences in the amount of cDNA added to each assay.

Surprisingly we noted that the levels of EBV gene expression not only varied between the ENKTL and the CAEBV cell lines, but also varied significantly between the ENKTL cell lines. LMP1 transcription can be initiated from either the EBNA-2-regulated promoter which is usually active in B-cells, or else from one located in the terminal repeat region (TR). Figure 4-1 shows that in the ENKTL and CAEBV lines, the vast majority of the transcripts are from the B-cell promoter, and there is significant variation in levels between the cell lines, with SNK6, SNT8 and SNT13 showing higher expression (note the different scales used to demonstrate expression of the less abundant transcripts). LMP1 expression is variable both between and within ENKTL samples, and so this variability is plausible and intriguing (52, 57).

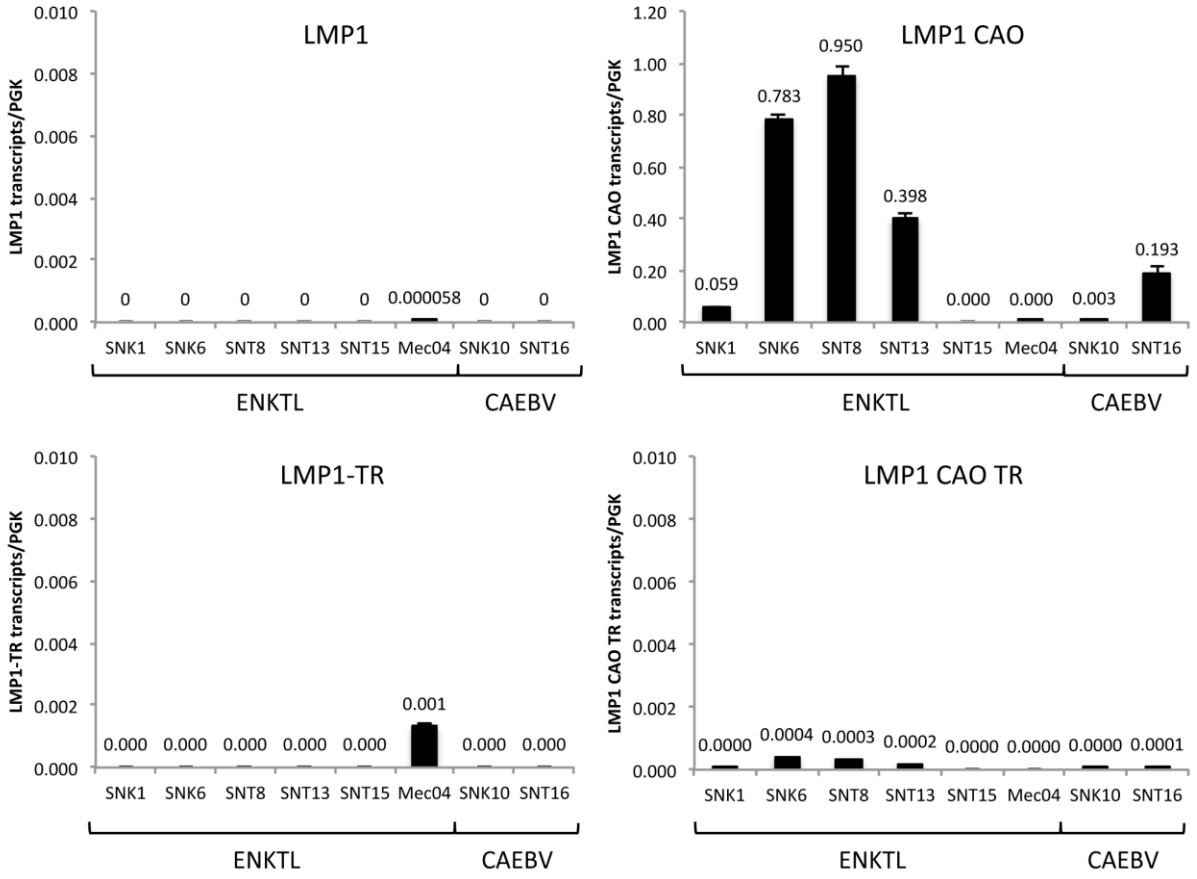

Figure 4-1 – LMP1 expression in ENKTL and CAEBV cell lines analysed by Fluidigm Specific Target Amplification. Four sets of primers were used to detect the conventional (EBNA-2 regulated promoter) and terminal repeat promoter (TR) alternative transcripts, and the B95.8 and Cao sequences. Conventional LMP1 with the Cao sequence is the only transcript significantly expressed in the lines studied, and its expression is significantly higher in SNK6, SNT8 and SNT13

Figure 4-2 shows LMP2 expression. The exon 6 assay was designed to detect all LMP2 transcripts; however, even when LMP2A, 2B and 2B-TR are accounted for there is still an excess of exon 6 detected in most of the cell lines. It is possible that this represents a sequence variation, or may be the result of transcription from an as-yet unknown promoter. Of note, both LMP1 and LMP2A levels are comparable to that seen in an LCL (approximately 1 and 0.1 copies per PGK respectively (38).

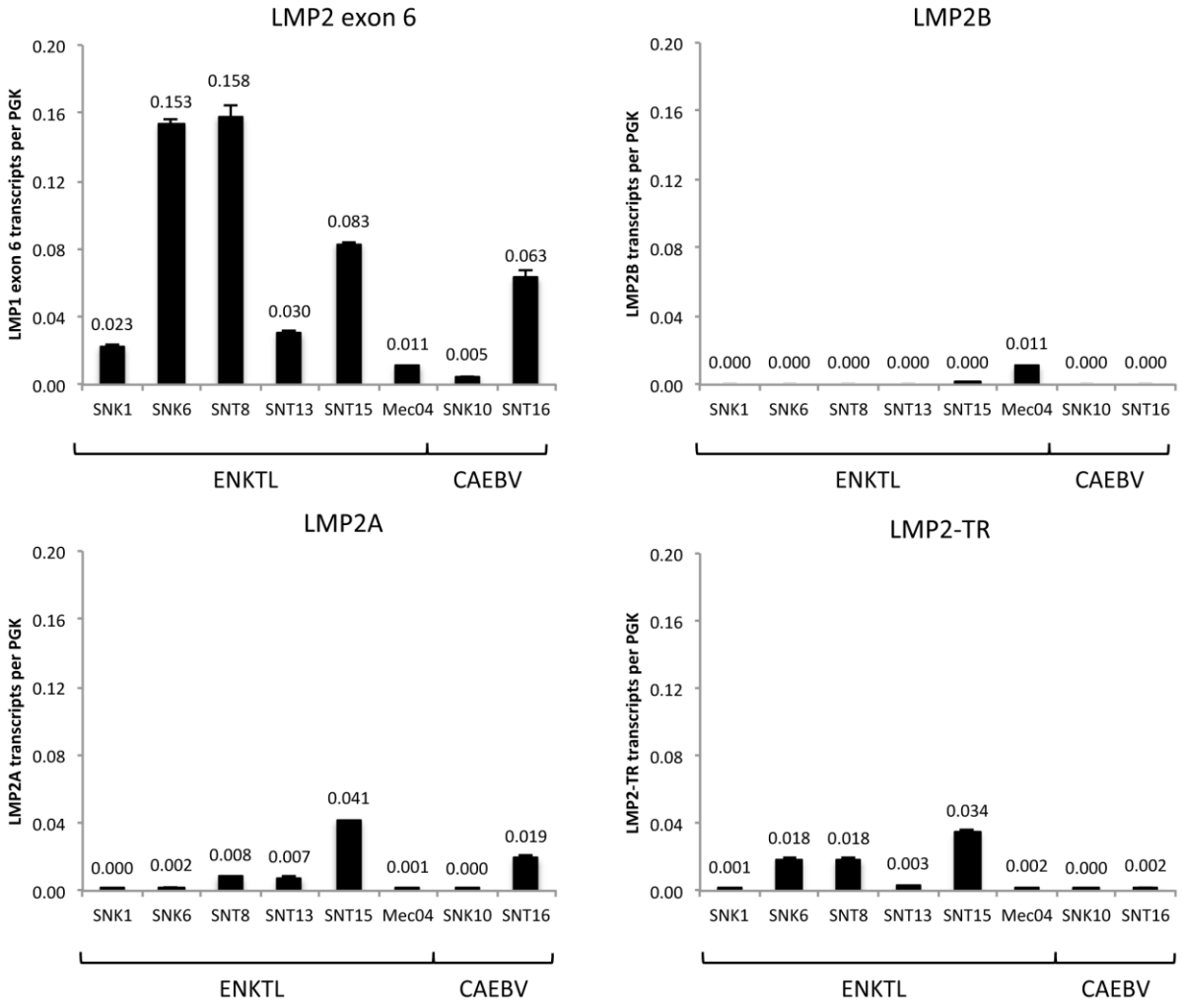

Figure 4-2 – LMP2 expression in ENKTL and CAEBV cell lines by Fluidigm Specific Target Amplification. Four sets of primers were used. The LMP2 exon 6 primers will detect both LMP2A and LMP2B. Absolute expression of LMP2 transcripts is much lower than that of LMP1 (figure 4-1), and the predominant form is the LMP2-TR transcript. The differences in expression between the ENKTL cell lines is not as apparent as the levels of transcripts observed for LMP1.

Figure 4-3 shows EBNA-1 expression. This about ten times lower than that seen in an LCL (38) and is more consistent across the class than the latent membrane proteins.

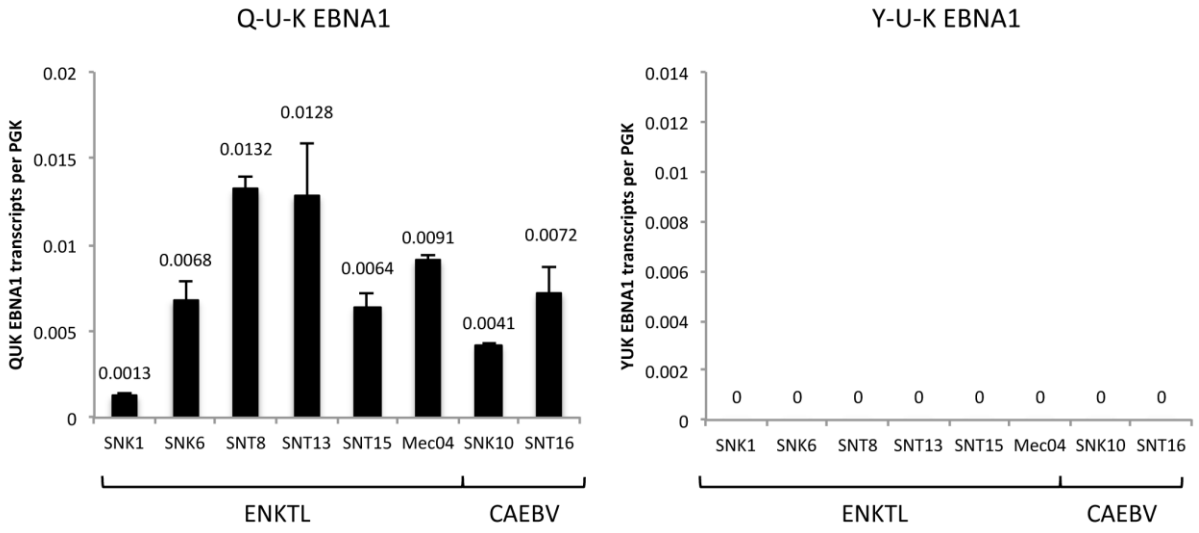

Figure 4-3 - EBNA-1 expression in T and NK cell lines by Fluidigm Specific Target Amplification. The Q-U-K probe set detects EBNA-1 initiated from the Q promoter. Expression is low however it is much less varied across the cell lines. Expression from the C and W promoters was absent, as shown by the lack of expression by the Y-U-K probe set.

Figure 4-4 shows EBER expression – again, EBER1 and EBER2 are shown on different scales to demonstrate the variability between cell lines. SNK13 and SNT15 show greatly elevated levels compared to the other cell lines; for comparison, EBER1 expression in LCLs is approximately 2-8 copies per PGK (38).

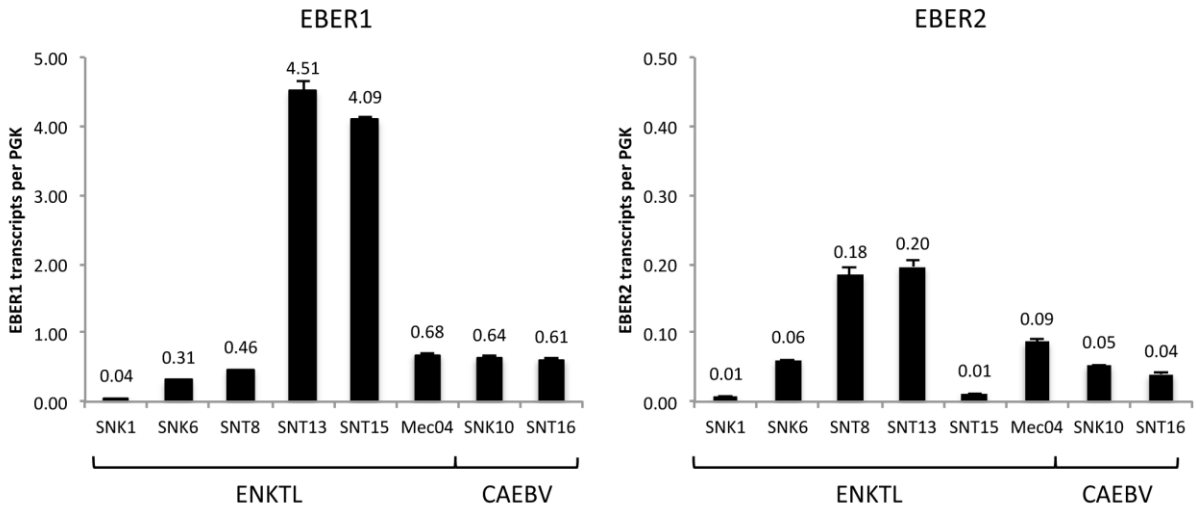

Figure 4-4 - EBER expression in T- and NK-cell lines by Fluidigm Specific Target Amplification. EBER1 expression is generally higher than EBER2 expression across all the cell lines. However, EBER1 expression is remarkably high in both SNT13 and SNT15. The significance of this is not clear.

Figure 4-5 shows that levels of BZLF1 are low across the cell lines, suggesting that little lytic replication is taking place. For comparison, in lytic cycle in an Akata cell the levels of BZLF1 peak at around 35 copies per PGK (38). EBNA-2 levels are low, as expected.

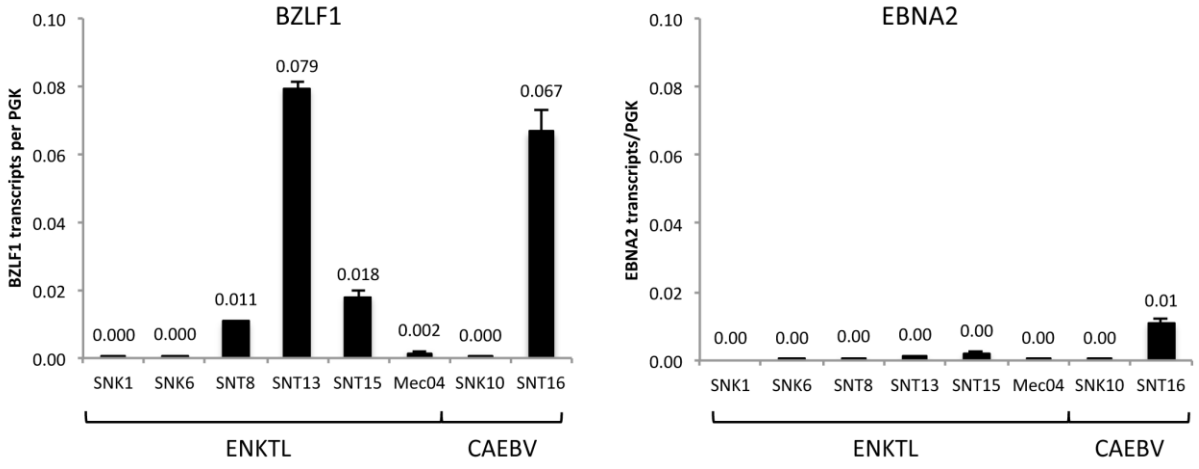

Figure 4-5 - Expression of EBNA-2 and BZLF1 in ENTKL and CAEBV lines by Fluidigm Specific Target Amplification. Expression of EBNA-2 is extremely low as would be expected in these cell lines given the usage of the Wp and Cp promoters are B cell specific. The very small levels of EBNA-2 can probably be accounted for by the low levels of lytic cycle observed and represented here by BZLF1.

Characterising protein expression in ENKTL and CAEBV cell lines.

Quantitative PCR to examine the relative levels of viral mRNA transcripts is a convenient tool to examine which viral genes are being expressed. However, gene expression does not always correlate with translation of the message or indeed the final levels of protein. We therefore also characterised the viral gene expression at the protein level by Western blot for all the cell lines used. Western blots were performed for the proteins reported to be expressed in T/NK cell lymphomas including EBNA-1, LMP1 and LMP2A, shown in figure 4-6. As an EBV-negative control we used Jurkat and as an EBV-positive control we used an LCL which expresses high levels of LMP2A. EBNA-1 was expressed in every cell line albeit at lower levels than those observed in an LCL, consistent with the RT-Q-PCR findings. However, the LMP1 levels observed in SNK1, SNK6 and SNT8 were significantly higher than that observed in an LCL. The protein expression for SNK1 is in contrast with the relatively low mRNA levels detected by Q-RT-PCR, suggesting a polymorphism in the LMP1 primer/probe sequence. As previously observed, we could not detect LMP2A in either the ENKTL or the CAEBV cell lines. Unfortunately an antibody does not exist for LMP2B meaning we could not verify the Q-RT-PCR results for the LMP2B and LMP2B-TR transcripts.

Neither BZLF1 or EBNA-2 were detected by Western blot, consistent with the very low levels of mRNA transcripts.

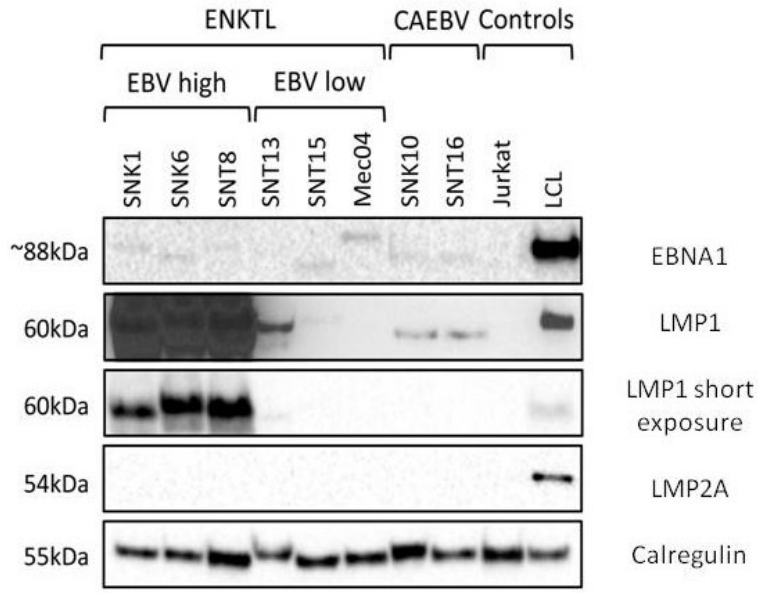

Figure 4-6. Viral proteins expressed in the ENKTL and CAEBV cell lines. Western blots confirming EBNA-1 and LMP1 protein expression in the ENKTL and CAEBV cell lines. The Western blots for LMP1 were exposed for 3 minutes (short exposure) or 10 minutes to confirm the low level of expression of LMP1 in the ENKTL cell lines SNT13, 15 and Mec04, and the CAEBV cell lines SNK10 and SNT16.

4.3 Examination of the impact of high level EBV gene expression on the growth of ENKTL.

The significant differences in EBV gene expression, particularly LMP1 and LMP2, between the ENKTL cell lines prompted us to question the role of these proteins in T/NK lymphomagenesis. Previous work examining the role of LMP1 in the absence of EBNA-2 expression (397-399) showed that LMP1 expression may be cytokine dependent. LMP1 levels fall following IL-2 removal, and this is quickly followed by apoptosis of the cells. However, given the individual cell lines express both high levels or extremely low levels of LMP1, we wanted to examine if, in very low levels of LMP1, the ENKTL cell lines responded to IL-2 withdrawal in the same manner as the cells expressing high levels of LMP1. All the ENKTL cells and CAEBV cells are IL-2 dependent for proliferation. We therefore first reproduced the loss of LMP1 following IL-2 withdrawal by Q-

RT-PCR for the cell lines expressing high levels of LMP1 (figure 4-7). We performed all experiments on the cells expressing high levels of LMP1 by Western blot and Q-RT-PCR, SNK1, SNK6 and SNT8, plus SNT13 as the higher intermediate level of LMP1. The cells were removed from their culture medium, washed three times in medium without IL-2 and re-plated in medium without IL-2 for 1 hour. To ensure the IL-2 was completely washed off, the cells were once more re-plated in fresh medium without IL-2. The Q-PCR results indicate LMP1 mRNA was significantly reduced over the first 24 hours following IL-2 withdrawal and was maintained at a similar low or reducing level over the following 4 days (figure 4-7).

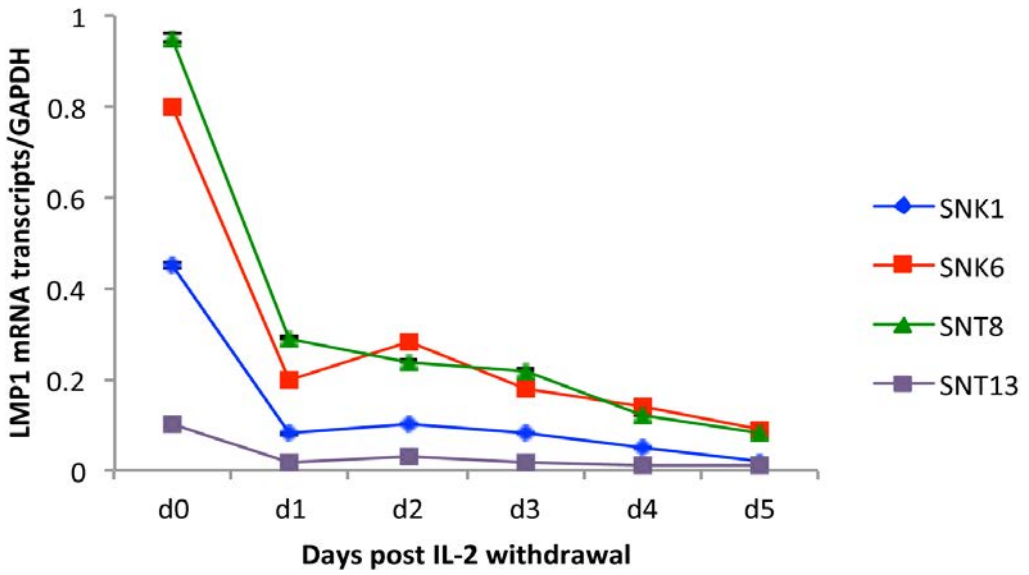

Figure 4-7 Analysis of LMP1 mRNA transcripts following IL-2 withdrawal. Although the initial level of LMP1 expression is variable between cell lines, it invariably falls after 24 hours of IL-2 withdrawal and remains low for the duration of the cytokine deprivation.

Given the levels of LMP1 significantly reduced within 24 hours following IL-2 withdrawal, we wanted to determine what effect the IL-2 withdrawal would have upon the survival of the cells

which originally expressed LMP1 at high levels, compared to intermediate levels and low/negative LMP1 expression. We therefore performed viability assays on the ENKTL cell lines expressing high levels of LMP1 and compared them to ENKTL expressing intermediate levels of LMP1 and no LMP1. We also wanted to determine if cell lineage (T cell or NK cell) or ENKTL or CAEBV diagnosis induced a differential sensitivity to IL-2 withdrawal.

As above, the cells were washed three times to remove IL-2 and re-plated in fresh medium without the cytokine at a density of $1x10^5$cells/ml. The cells were then harvested every day, stained with propidium iodide, analysed by flow cytometry and the total number of live cells recorded. All assays were performed three times, each in triplicate. The results are represented as % of cells alive after IL-2 withdrawal and are shown in figures 4-8 and 4-9. Statistical analysis was performed using a one-way analysis of variance (ANOVA) analysis.

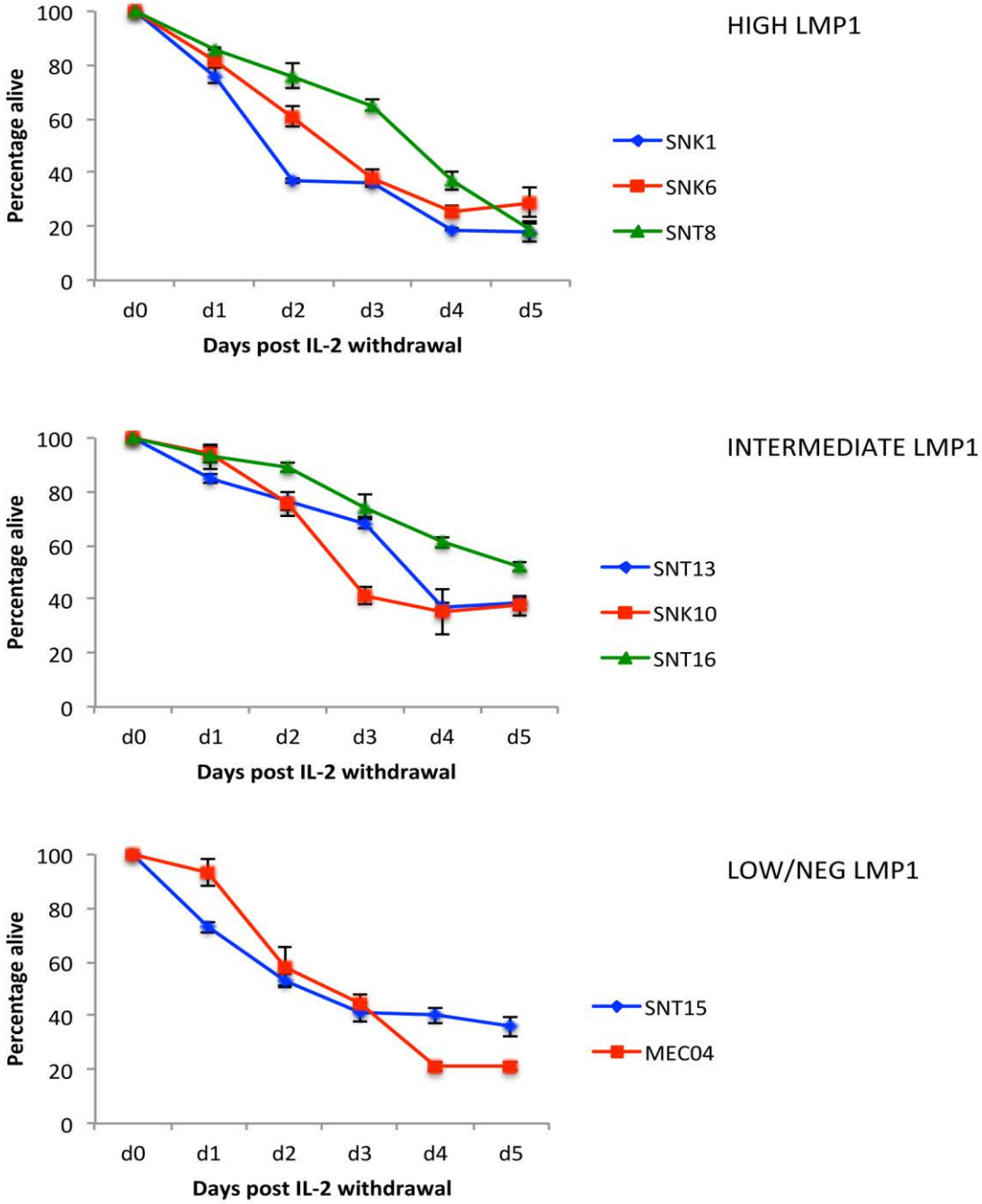

Figure 4-8 - The effect of IL-2 withdrawal in the LMP1 high, intermediate and low/negative cell lines. IL-2 withdrawal caused a significant decline in cell survival over the subsequent 5 days. Each assay was performed three times in triplicate.

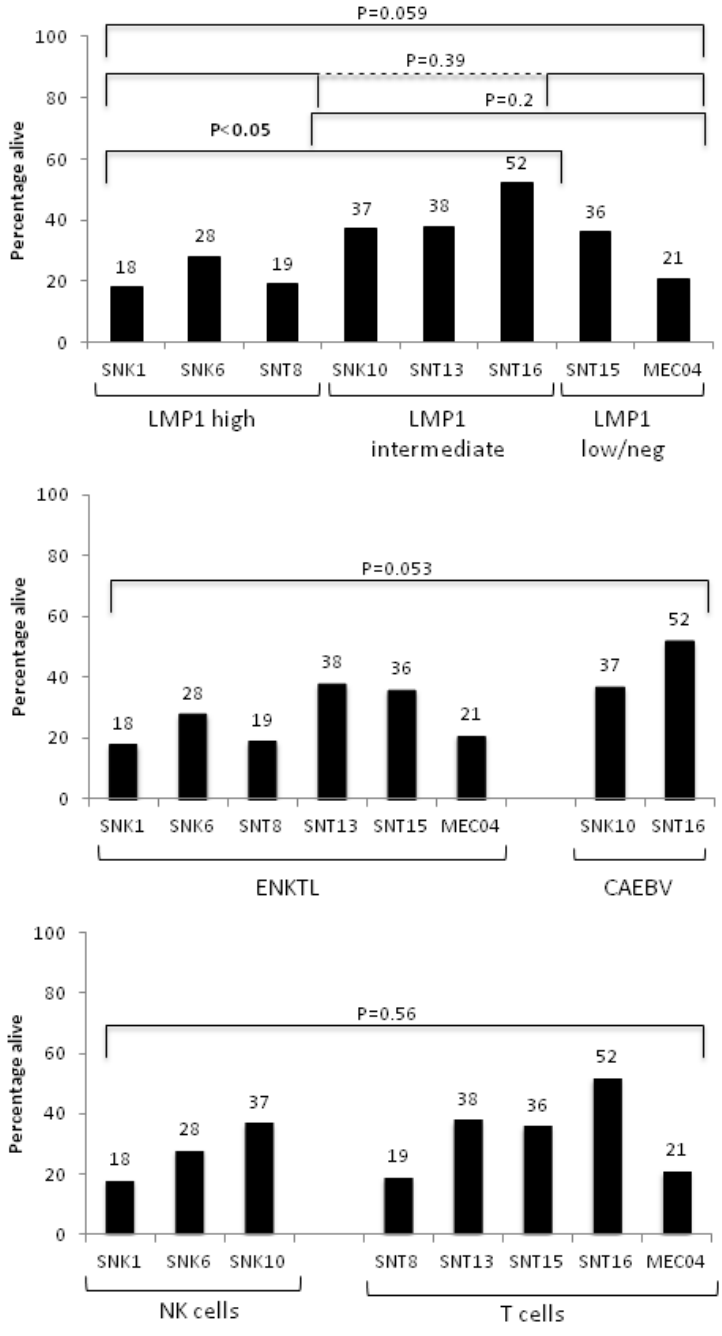

Figure 4-9 - Analysis of cell survival at day 5 following IL-2 withdrawal according to LMP1 expression, disease and cell type. Further analysis was performed on the ENKTL and CAEBV cell lines to determine if cell survival following IL-2 withdrawal could be accounted for by LMP1 expression, disease or cell lineage.

The cells expressing the highest initial levels of LMP1 (SNK1, SNK6 and SNT8) appeared to show the poorest survival following IL-2 withdrawal, with the average survival by day 5 of between only 18 and 28% (figure 4-9, top panel). This suggests that the coincident loss of LMP1 in these cells following removal of IL-2 may be responsible for the loss of survival. The cells expressing the intermediate level of LMP1 (SNT13, SNK10 and SNT16) appeared to show better survival following IL-2 withdrawal, with survival rates between 37 and 52% (figure 4-9, top panel). The difference between these two groups was statistically significant (p=0.02) by ANOVA analysis. Interestingly the MEC04 cells not expressing LMP1 showed a poor survival of 20% and the SNT15 expressing a very low level of LMP1 showed 35% survival (figure 4-9, top panel). When all three groups were compared (p=0.059), or when the high LMP1 group was compared to the combined intermediate and low group (p=0.07) there was a trend towards different survival although this did not reach statistical significance.

When ENKTL-derived lines were compared to CAEBV, there was a trend towards cells of CAEBV origin surviving better than ENKTL following IL-2 withdrawal (figure 4-9, middle panel); but this did not reach statistical significance (p=0.053). There was no difference between cells of T- and NK-origin (figure 4-9, bottom panel, p=0.56).

Both the ENKTL and CAEBV cell lines are dependent upon growth factors such as IL-2 for their survival. This dependence is variable between cell lines, and infected cell type, and may show some association with LMP1 expression.

In order to further investigate apoptosis susceptibility in these cells we next examined the cells for differences in expression of the pro- and anti-apoptotic members of the intrinsic apoptosis pathway (figures 4-10, 4-11 and 4-12). As a control, the IL-2 independent T cell leukaemia line Jurkat (400) was treated with camptothecin at 5 mM concentration for 18 hours to induce the expression of the pro-apoptotic proteins. NKL, an NK line derived from NK leukaemia (401) and Mutu, a BL line (402), were included as controls.

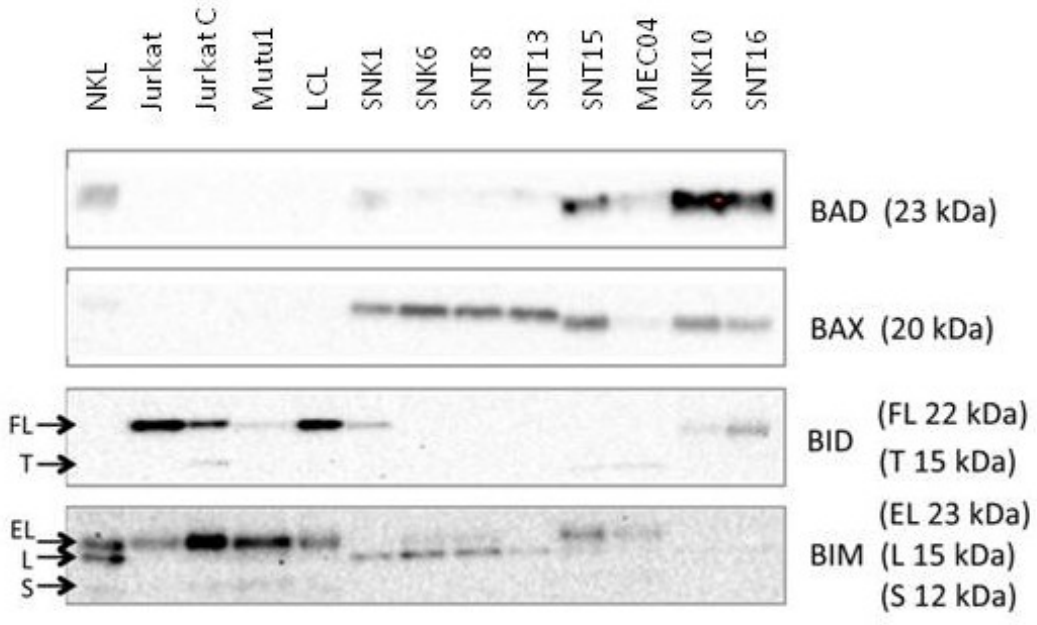

Figure 4-10 - Expression of proapoptotic BCL2 family members in the ENKTL and CAEBV cell lines. BAD is seen at high levels in the CAEBV lines only. BAX is interestingly expressed at very similar levels across the cell lines with the exception of MEC04. Two BID isoforms, full-length (FL) and truncated (T) are seen although expression is only significantly detected in SNK1 and the CAEBV lines. 3 BIM isoforms – extra long (EL), long (L) and short (S) – are generated by alternative splicing of the transcript. There is only very weak BIM expression in the CAEBV lines.

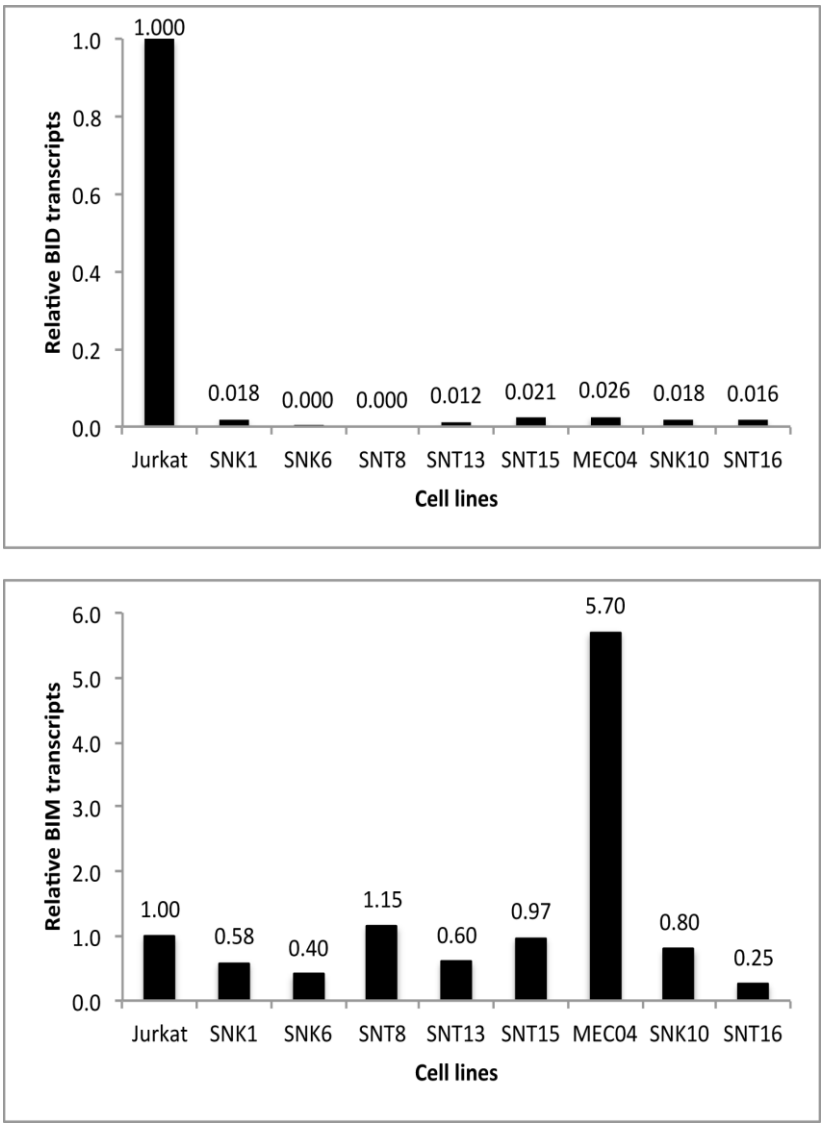

Figure 4-11 - Analysis of BID and BIM mRNA transcripts in the ENKTL and CAEBV cell lines. The mRNA transcripts of the ENKTL and CAEBV cell lines were compared to mRNA transcripts detected in the control Jurkat cell line. The Jurkat transcripts were given an arbitrary value of 1, so the mRNA transcripts of BID (upper panel) and BIM (lower panel) could be compared to the control Jurkat cell line.

The expression of the pro-apoptotic proteins in the ENKTL and CAEBV lines (figure 4-10) was significantly different to that in the control cell lines, which included an EBV-negative NK lymphoma (NKL), an EBV-negative T cell lymphoma (Jurkat), an EBV-positive Burkitt lymphoma

and a lymphoblastoid cell line. Of particular note, the expression levels of the pro-apoptotic BID were significantly decreased in ENKTL and CAEBV compared to relevant controls. Furthermore, the two cell lines SNK6 and SNT8 which express the highest levels of LMP1 were completely negative for BID, both when assayed for protein by Western blot (figure 4-10) and for mRNA by RT-Q-PCR (figure 4-11). This could potentially have significant impact on susceptibility to mitochondrial apoptosis and interestingly could have an impact on extrinsic apoptosis given BID is one intersect between both pathways.

BIM can be present in three isoforms formed by alternative splicing; BIM_{EL}, BIM_{L} and BIM_{S}, with BIM_{S} being recognised as the most potent pro-apoptotic isoform (403, 404). Surprisingly the majority of ENKTL cells express the BIM_{L} isoform, which again is unusual as most untreated cells will express the BIM_{EL} isoform, as demonstrated by the controls assayed in parallel which included NK-cells (NKL), T-cells (Jurkat) and B-cells (Mutu1 and LCL). By Q-RT-PCR we demonstrated that the levels of BIM transcripts were similar in all the cell lines, with the exception of MEC04, which had at least 6-fold higher levels of transcripts than the Jurkat control cell line. This does not correspond to a higher level of protein by Western blot, but BIM is subject to post-transcriptional regulation (reviewed in (405)). Also, our BIM assay did not differentiate between the different isoforms, so could not confirm or refute the finding that BIM_{EL} is expressed in these cell lines.

Furthermore, the proapoptotic BAD protein is expressed at higher levels in the CAEBV lines compared to the ENKTL cell lines or controls. BAX protein expression is also significantly higher

in all the ENKTL and CAEBV cell lines compared to the control cells, with the exception again of MEC04, which was significantly lower (figure 4-10).

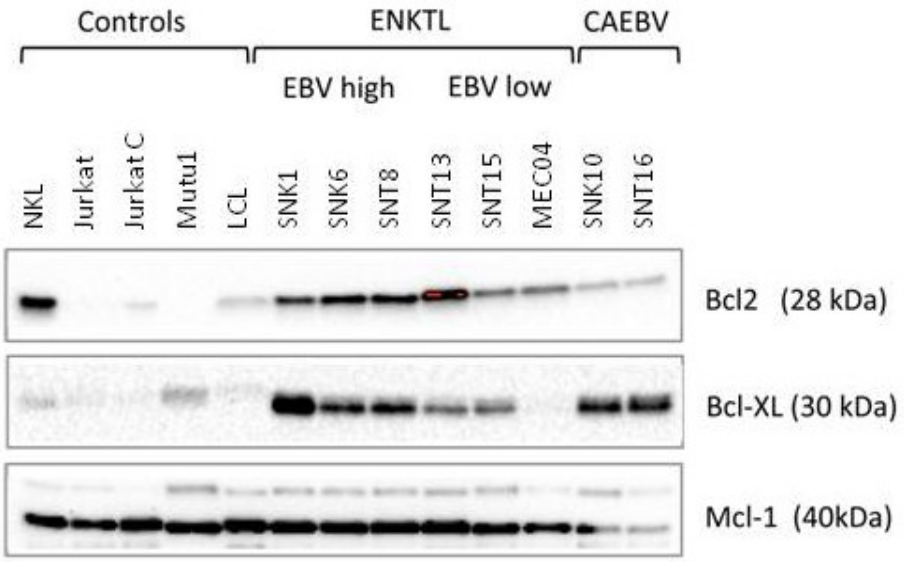

Figure 4-12 - Expression of protein levels of antiapoptotic BCL2 family members in the ENKTL and CAEBV cell lines by Western blot. In general, the expression of BCL2 and BCL-XL is increased in these cells compared to controls, and the level of MCL1 was low in the CAEBV lines. MEC04 has no expression of BCL-XL.

The expression level of anti-apoptotic BCL2 family members is shown in figure 4-12. Expression of BCL2 was increased in SNK1, SNK6, SNT8 and SNT13 compared to controls (except NKL); interestingly, these cell lines also show the highest levels of LMP1 expression (figure 4-6). However, the SNT15, MEC04, SNK10 and SNT16 also appear to have increased levels of BCL2 which cannot be accounted for by LMP1 , particularly in SNT15 and MEC04 which have very little or no LMP1 expression. BCL-XL was increased in all the ENKTL and CAEBV lines compared

to relevant controls, with the notable exception again of MEC04, which shows no BCL-XL expression. Little difference can be observed in expression of MCL1 between the cell lines.

4.4 Examination of the impact of BCL2 family and EBV gene expression on apoptosis

ENKTL is a remarkably chemo-resistant tumour, resulting in poor outcomes with conventional treatment. We wished to examine the sensitivity of the cell lines to apoptosis in order to see if there was an association between EBV or BCL2 family gene expression and cell death in response to apoptotic agents, which could have important therapeutic implications. The expression data above were taken from proliferating cell lines with no IL-2 depletion.

We treated them with a variety of apoptosis-inducing agents. Etoposide acts by forming a complex with DNA and the topoisomerase II enzyme, which is necessary for the cleavage and religation of both DNA strands during transcription and replication (406). In contrast, camptothecin affects DNA topoisomerase I (407). Both drugs prevent DNA religation; the resulting double-stranded DNA breaks trigger apoptosis. Ionomycin acts as a calcium ionophore. In lung cancer cells it triggers apoptosis by activating calpains, and results in activation of the intrinsic pathway of apoptosis (408).

The apoptosis assays were carried out as described in chapter 2. Cells were stained for Annexin V and propidium iodide (PI), and analysed by flow cytometry. Live cells were gated as PI and

Annexin V negative, apoptotic as Annexin V positive, and necrotic as PI positive (see figure 4-13); the latter two gates were combined for analysis. All assays were performed three times, each in triplicate. Standard deviations for all assays are shown.

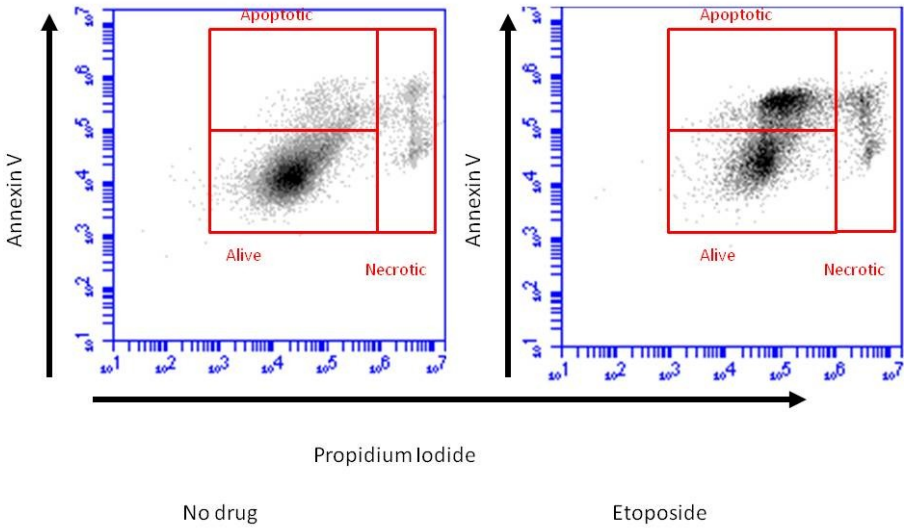

Figure 4-13 - Flow cytometric analysis of apoptosis assay showing SNT16 either with no drug or treated with etoposide. The flow cytometry dot plots are shown to highlight the gating strategy for the apoptosis assays.

Initially we titrated the chemotherapy agents on EBV-negative control Jurkat and MOLT4 (T lymphoblast (409) cells), measuring response at 24 hours. The results are shown in figure 4-14. For ease of comparison to similar studies, the cell death induced by the drug was calculated as follows: (total cell death - spontaneous cell death)/(100 – spontaneous cell death) (343). This is particularly important as the ENKTL cell lines in particular have a relatively high rate of spontaneous apoptosis.

Both cell lines show good dose-response apoptosis in response to ionomycin and etoposide, and time-dependent apoptosis in response to camptothecin at 5 µM concentration.

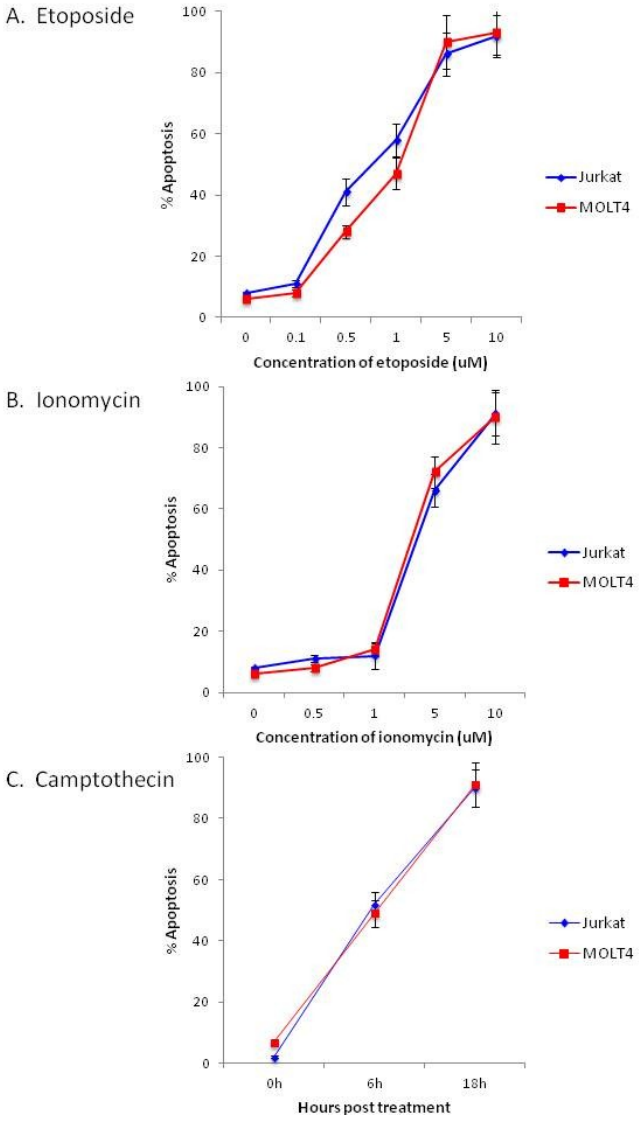

Figure 4-14 - Treatment of the control cell lines Jurkat and MOLT4 with apoptosis-inducing drugs. The cell lines were either treated with increasing concentrations of etoposide (A), Ionomycin (B), or with 5µM Camptothecin over 18 hours (C). The % apoptosis was determined with Annexin V and PI staining and the results plotted against drug concentration.

As can be seen in figure 4-14, the Jurkat and MOLT4 cell lines are equally susceptible to induction of apoptosis by the drugs etoposide (A), ionomycin (B) and camptothecin (C), making these cell lines good controls for the efficacy of the apoptosis-inducing drugs.

The ENKTL and CAEBV cells were treated in parallel with the apoptosis-inducing drugs (figures 4-15 – 4-18). Statistical analysis was performed on results from a representative drug concentration. ANOVA analysis was used to compare the cell lines (grouped by LMP1 expression) to the control cell lines.

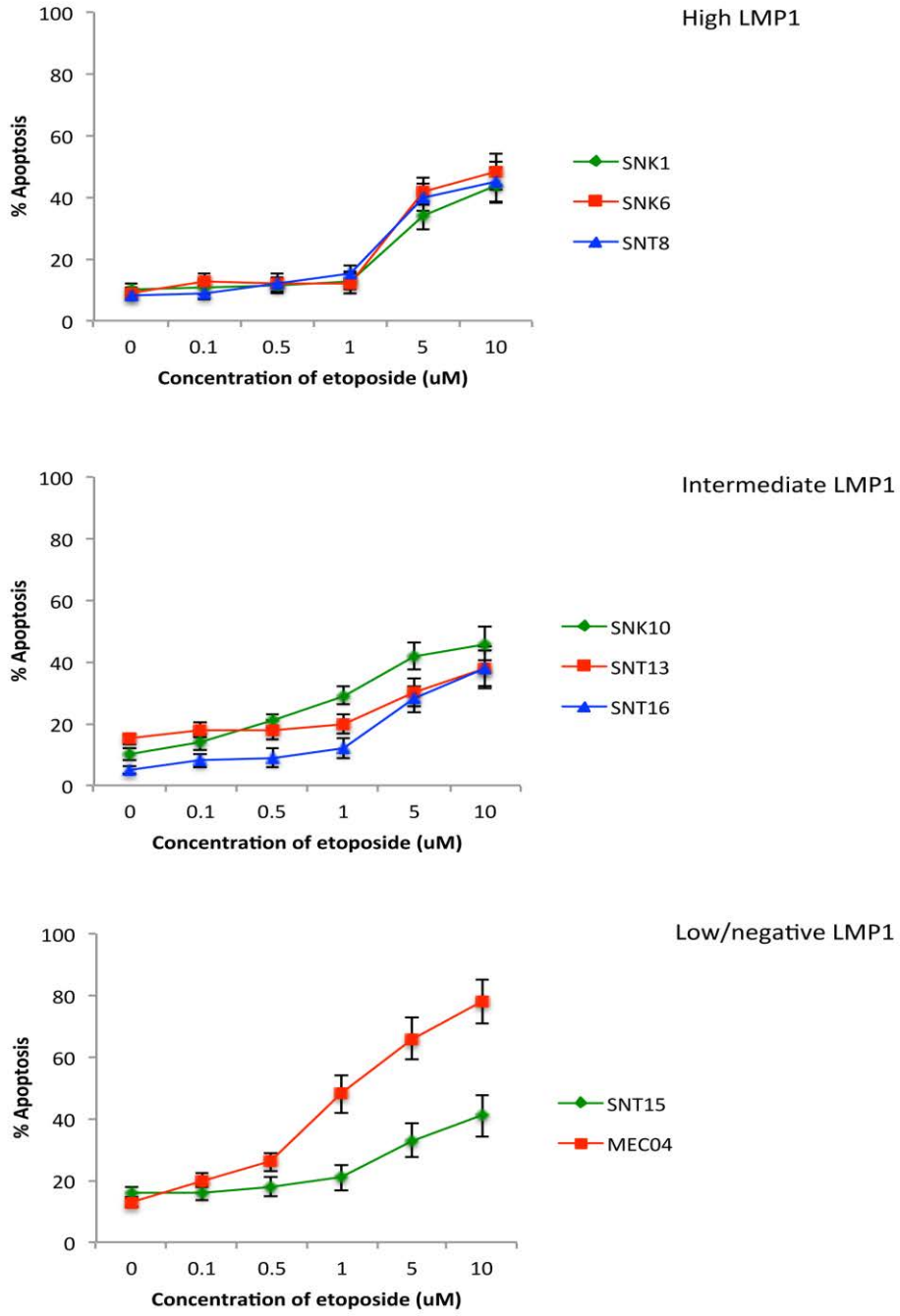

Figure 4-15 - Analysis of apoptosis induced by increasing concentrations of etoposide on ENKTL and CAEBV cell lines. The cell lines were treated with increasing concentrations of etoposide for 48 hours. The % apoptosis was determined with Annexin V and PI staining and the results plotted against drug concentration. Assays were performed three times in triplicate.

Figure 4-15 shows apoptosis in response to etoposide. There is a significant difference between the control cells (figure 4-14) and the LMP1 high group ($p=0.0007$) in their sensitivity to the drug at 5μM concentration. This is also the case when the controls are compared to the LMP1 intermediate group ($p=0.003$). However, when the control and LMP1 low groups were compared there was no significant difference ($p=0.14$). This suggests that LMP1 expression may be associated with resistance to apoptosis associated with etoposide.

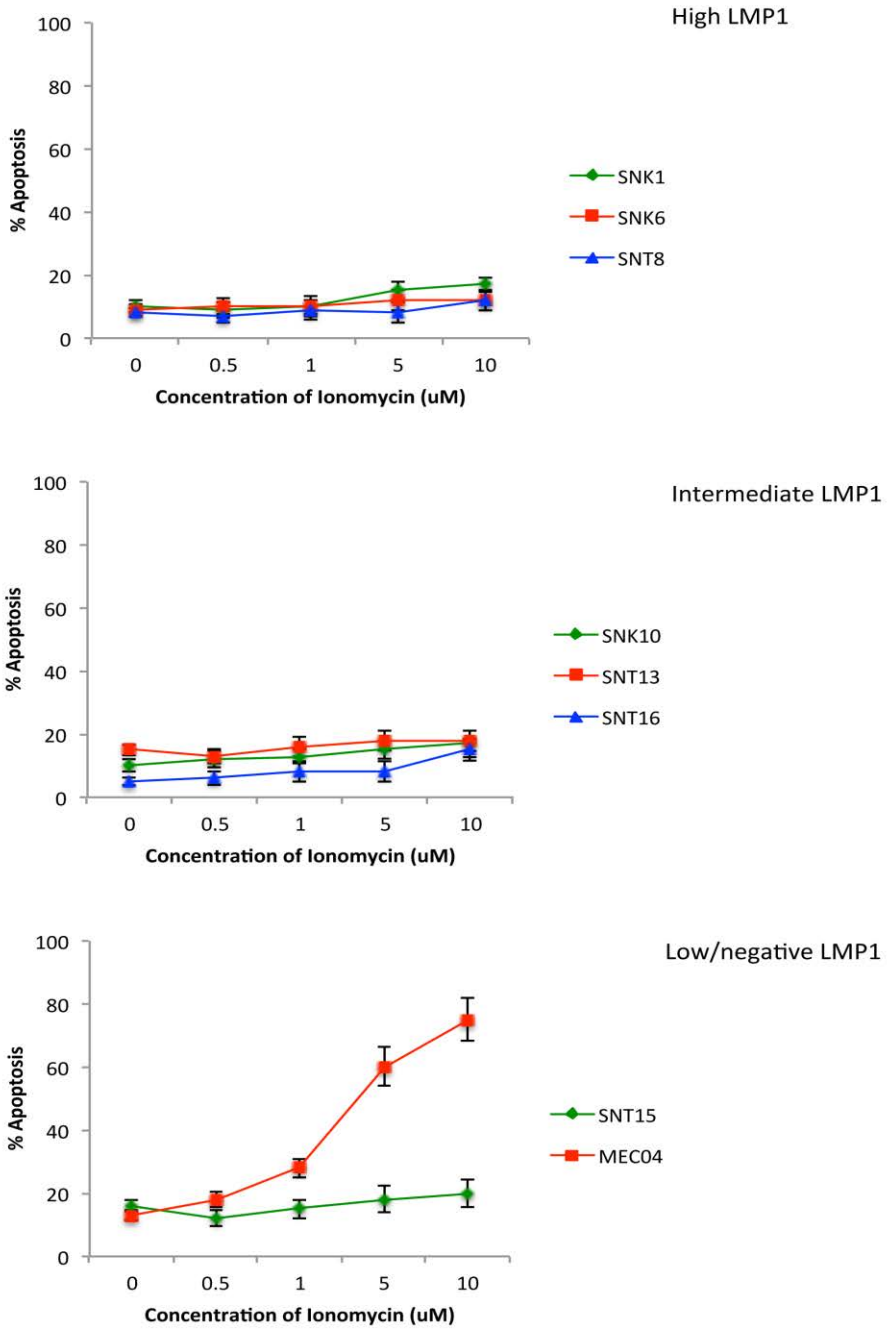

Figure 4-16 - Analysis of the apoptosis induced by increasing concentrations of ionomycin in the ENKTL and CAEBV cell lines.

The cell lines were treated with increasing concentrations of Ionomycin for 48 hours. The % apoptosis was determined with Annexin V and PI staining and the results plotted against drug concentration. Assays were performed three times in triplicate.

Responses to ionomycin showed a similar pattern to etoposide, with the LMP1 high group ($p=0.0005$) and the LMP1 intermediate group ($p=0.0003$) showing significantly less apoptosis than the control cells at 5µM, but the LMP1 low group showing no significant difference ($p=0.31$). Again, this suggests that LMP1 may contribute to the ENKTL resistance to ionomycin.

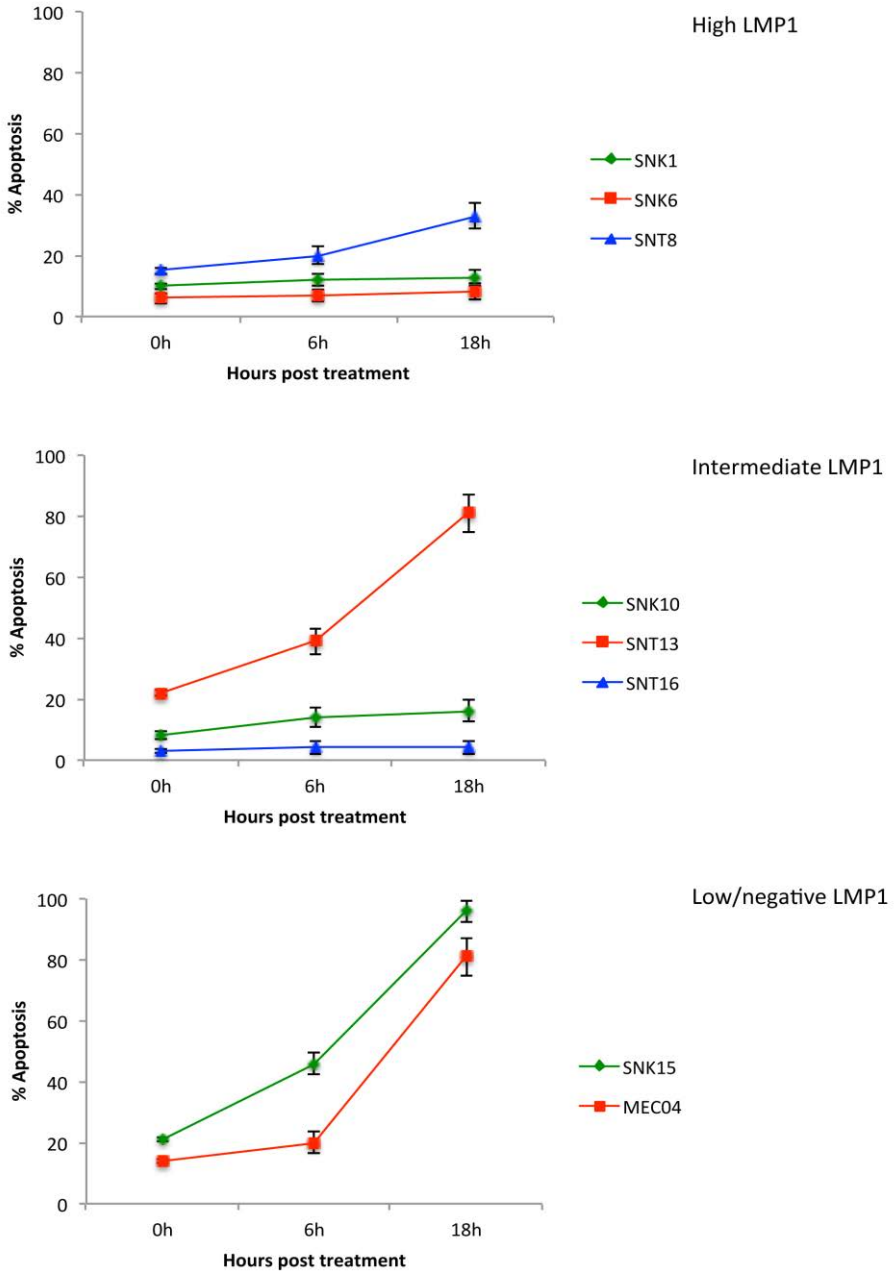

Figure 4-17 - Analysis of the induction of apoptosis over 18 hours by camptothecin. The cell lines were treated with 5µM camptothecin over 18 hours. The % apoptosis was determined with Annexin V and PI staining and the results plotted against drug concentration. Assays were performed three times in triplicate.

Again, camptothecin sensitivity was reduced in the LMP1 high group by 18 hours (p=0.005), although the intermediate (p=0.16) and low (0.81) were not different.

These data are interesting as they show that LMP1 expression may be associated with some degree of protection from apoptosis induced by chemotherapeutic agents, and suggests that high levels of the protein may confer chemoresistance. Given that LMP1 is expressed in ENKTL, and that the tumours are particularly difficult to treat with conventional agents, this is a plausible and important finding.

Whilst the MEC04 line both lacks LMP1 and is the most sensitive to etoposide-induced apoptosis, this line is noticeably different from all the other ENKTL and CAEBV lines with respect to its pattern of expression of the BCL2 family of proteins. When taking into account the lack of expression of BAX and BCL-XL and the low levels of BAD in MEC04, the picture is more complicated than can be explained simply through LMP1 expression.

4.5 The effect of BH3 mimetics in inducing apoptosis in ENKTL and CAEBV lines

Small molecules engineered to interact with the BH3 pathway, the BH3 mimetics, are currently in clinical trials in the treatment of lymphoid malignancies including CLL, lymphoma and myeloma (reviewed in (347)). ABT-737, a "BAD-like" BH3 mimetic, binds to and inhibits BCL2, BCL-X_L and BCL-w in cells (350). ABT-199 is a specific BCL2 inhibitor (351). Given the apparent inherent chemo-resistance of ENKTL and CAEBV, plus the *in vitro* resistance demonstrated

herein, we decided to examine the sensitivity of the ENKTL and CAEBV cell lines to the currently available members of this class. We titrated the BH3 mimetics alone onto the cell lines and examined the induction of apoptosis following 48 hours incubation. Similar to the assays above, we performed apoptosis assays on the treated cells and plotted the percentage apoptosis over the increasing concentrations of drugs (figure 4-18).

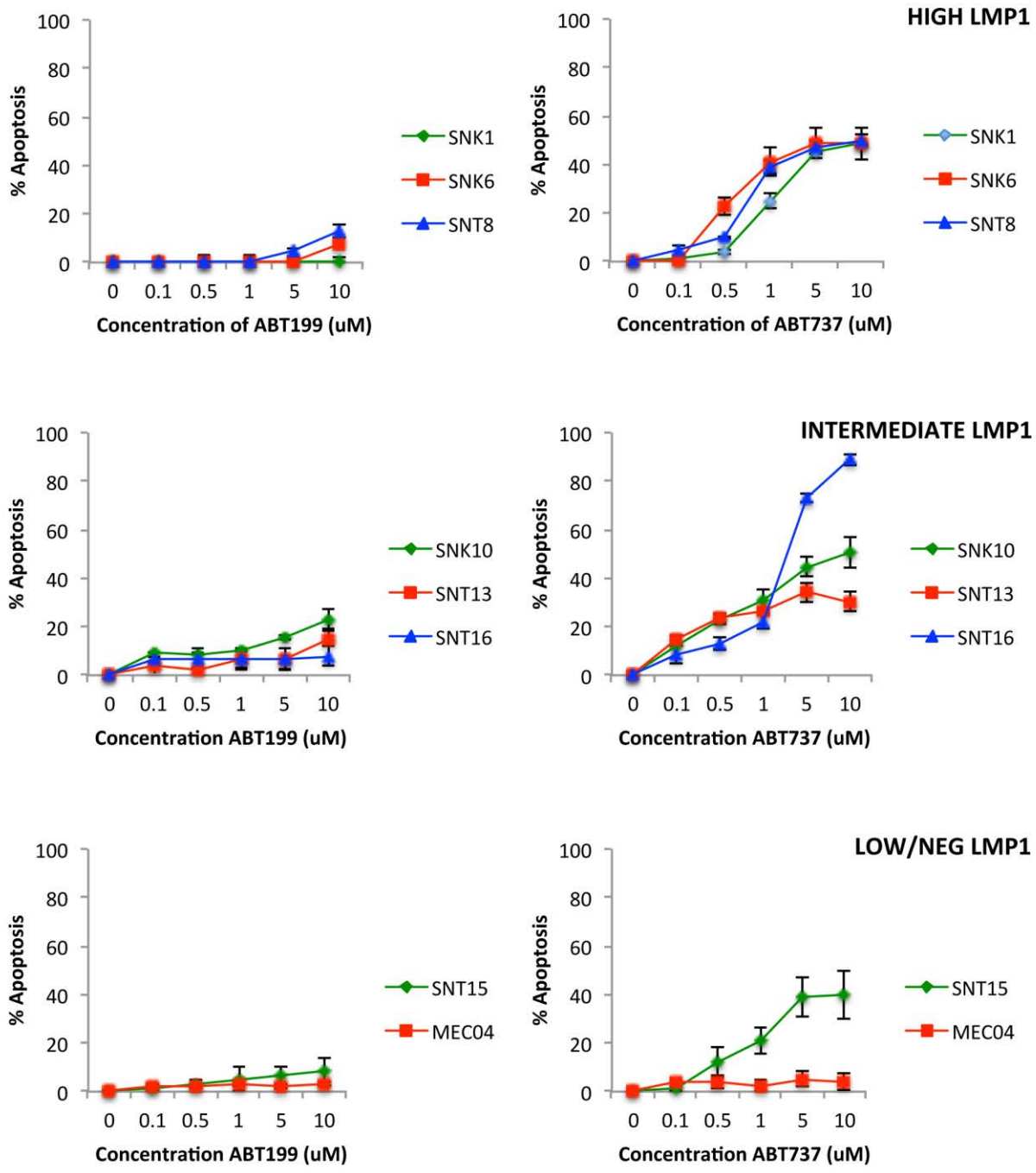

Figure 4-18 - Analysis of BH3 mimetic mediated apoptosis. The ENKTL and CAEBV cells were treated with increasing concentrations of the BH3 mimetics ABT199 (left hand graphs) or ABT737 (right hand graphs) for 48 hours. The percentage cell death was plotted against drug concentration. Each assay was performed 3 times in triplicate.

Every cell line treated showed remarkable resistance to ABT199 – this is surprising as BCL2 was expressed in each cell line, and raises issues about the efficacy of the drug in our system. In contrast, every cell line, except for MEC04, was similarly sensitive to ABT737 (figure 4-18). MEC04 is completely resistant to the tested doses of ABT737; it may be pertinent that this line does not express BCL-X_L, and it may be that this is the major way in which ABT737 is acting upon the other cell lines (figure 4-19).

In summary, despite their similar backgrounds, the ENKTL cell lines show a remarkable heterogeneity in their expression of intrinsic pathway proteins and their sensitivity to chemotherapeutic agents. This is likely to be reflected in their parent clinical diseases, and makes a strong case for considering profiling of individual tumours when planning treatment. BH3 profiling (reviewed in (410)) involves subjecting cells to different BH3 mimetics and measuring mitochondrial outer membrane permeabilisation; this is quickly becoming the gold standard for pre-treatment analysis where BH3 mimetic use is being considered.

4.6 The role of LMP1 and LMP2 in protection from apoptosis.

The expression of EBV genes has been shown to protect B-cells from apoptosis (411). BHRF1 (128) and BALF1 (129) are viral homologues of the anti-apoptotic cellular protein BCL2. LMP1 also has a well-defined anti-apoptotic role – its effects in B-cells are complex but include upregulation of the anti-apoptotic BCL2 (81, 412), although it is important to note that this may not be the case in non-B-cells. There is little currently known about the role of LMP2B in

apoptosis, but LMP2A expression results in constitutive activation of the Ras/PI3K/Akt pathway which in turn induces the expression of BCL2 and BCL-XL (102).

With this in mind, we repeated the earlier apoptosis assays using cell lines stably transduced with an LMP1 or LMP2B lentivirus. The creation of the lentiviral vector and cell transduction strategies are described in chapter 2.

We first wanted to ensure the transduced cell lines expressed the LMP1 and LMP2B from the integrated lentiviruses. We transduced 293 cells as a positive control as they produce good levels of protein from lentivirus transductions. We also transduced SNK10 as it has low levels of endogenous LMP1 expression. Following transduction, the cells were sorted for GFP expression to ensure every cell was capable of making LMP1 or LMP2B. We titrated doxycycline onto the cells to ascertain the optimal lowest concentration to induce expression of the viral proteins. Expression was compared to an average LCL. Figure 4-19 shows the induction of LMP1 in the SNK10 cells. Expression was induced maximally at 100 ng/ml doxycycline and levels of LMP1 expression in the SNK10 cells were significantly higher than that of the LCL.

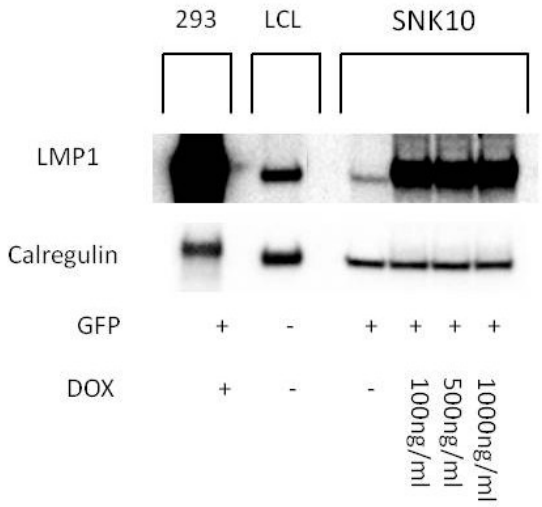

Figure 4-19 - Induction of LMP1 expression in transduced 293 cells and SNK10 cells by Western blot. LMP1 expression was induced by increasing concentrations of doxycycline (DOX). Maximal expression was achieved with 100 ng/ml. Expression in the transduced cells was significantly higher than in the LCL control; LMP1 expression in the transduced 293 cell shows supranormal levels.

We then sought to quantitate the mRNA transcripts of LMP1 following doxycycline induction of the 293 cells and SNK10 cells compared to the LCL. As controls, empty lentiviruses were employed and subjected to the same doxycycline-induction. The mRNA transcripts were normalised against PGK and shown in figure 4-20.

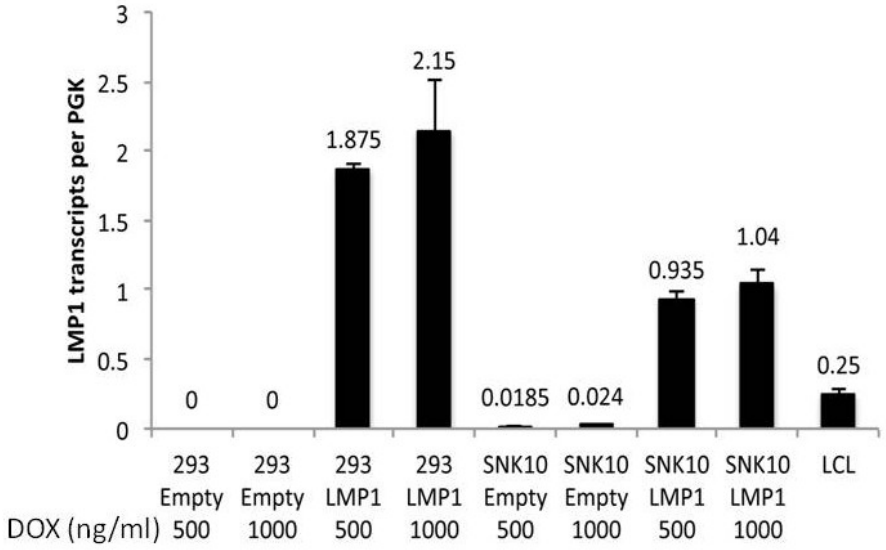

Figure 4-20 - Analysis of LMP1 mRNA transcripts by Q-RT-PCR in 293 cells and SNK10 cells transduced with LMP-1 expressing lentivirus. 293 cells and SNK10 cells were transduced with either empty lentiviruses or LMP1 lentiviruses then expression of LMP1 was induced with either 500ng/µl or 1µg/µl of doxycycline. The mRNA was analysed by Q-RT-PCR for levels of LMP1 mRNA transcripts. All experiments were performed in triplicate. An LCL is shown as a control.

The results represented in figure 4-20 confirm the Western blot data shown in figure 4-19 Induction of LMP1 expression was performed at 500 ng/ml for all future experiments.

The same set of experiments was performed following LMP2B lentivirus transduction into 293 cells and SNK10 cells. Unfortunately no antibody to LMP2B is available, so natural levels of LMP2B in control cells such as SNK6 or SNT8 could not be performed by Western Blot. However, the LMP2B lentiviruses were constructed with an HA-tag to enable analysis of expression (figure 4-21). Similarly to the LMP1 experiments above, LMP2B protein in transduced 293 cells was expressed at a higher level than in transduced SNK10 cells. However, this is not entirely surprising given that LMP2B transcript levels in SNK6 and SNT8 are naturally significantly lower than those of LMP1.

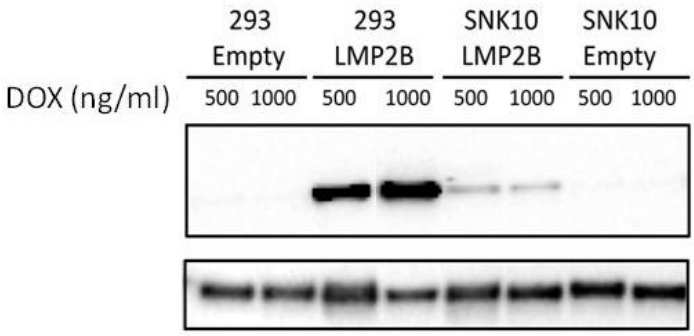

Figure 4-21 - Analysis of induction of LMP2B expression in transduced 293 cells and SNK10 cells by Western blot. Top panel: LMP2B-TR expression was induced by 500ng/μl or 1μg/μl of doxycycline and expression was detected by anti-HA antibody. Bottom panel shows the calregulin loading control of the proteins examined.

Similar to the LMP1 lentivirus, we also examined the levels of LMP2B-TR transcripts in the transduced cells by qPCR and compared them to a positive control, shown in figure 4-22. Transcript levels in the transduced SNK10 cells are detected at higher levels than the naturally expressed transcripts in SNK6 cells.

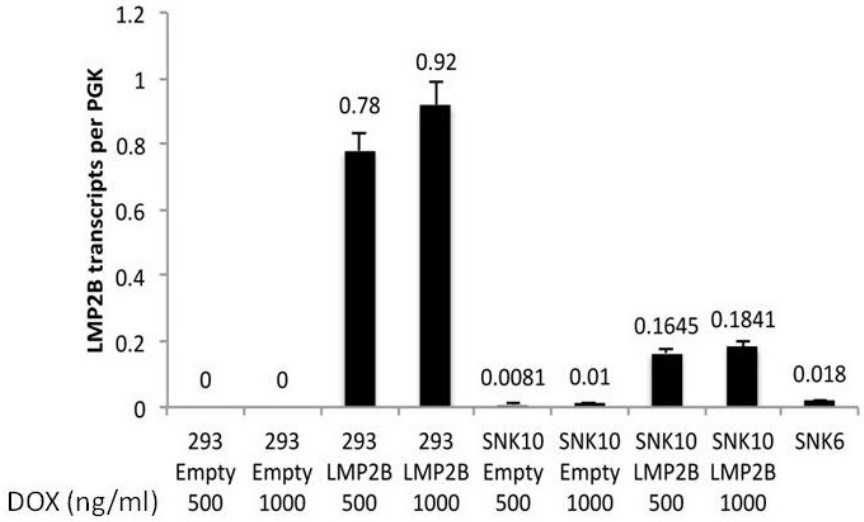

Figure 4-22 - Analysis of LMP2B expression in transduced 293 and SNK10 cells by qPCR. 293 cells and SNK10 cells were transduced with either empty lentiviruses or LMP2B lentiviruses. Expression of LMP2B was induced with either 500ng/µl or 1µg/µl of doxycycline. The mRNA was analysed by qPCR for levels of LMP1 mRNA transcripts. SNK6 is shown as a control. All experiments were performed in triplicate.

Given our findings on the apparent LMP1-mediated reliance upon the growth factor IL-2, we performed IL-2 withdrawal assays on SNK10 and SNT16 cell lines transduced with the LMP1 and LMP2B lentiviruses. After doxycycline induction we subjected the cells to 5 days of IL-2 deprivation in culture to see if the viral protein could protect them from the apoptotic stimulus of cytokine withdrawal (figure 4-23). These assays were performed three times in triplicate and statistical analysis was performed on the results at day 5 using a Student *t* test.

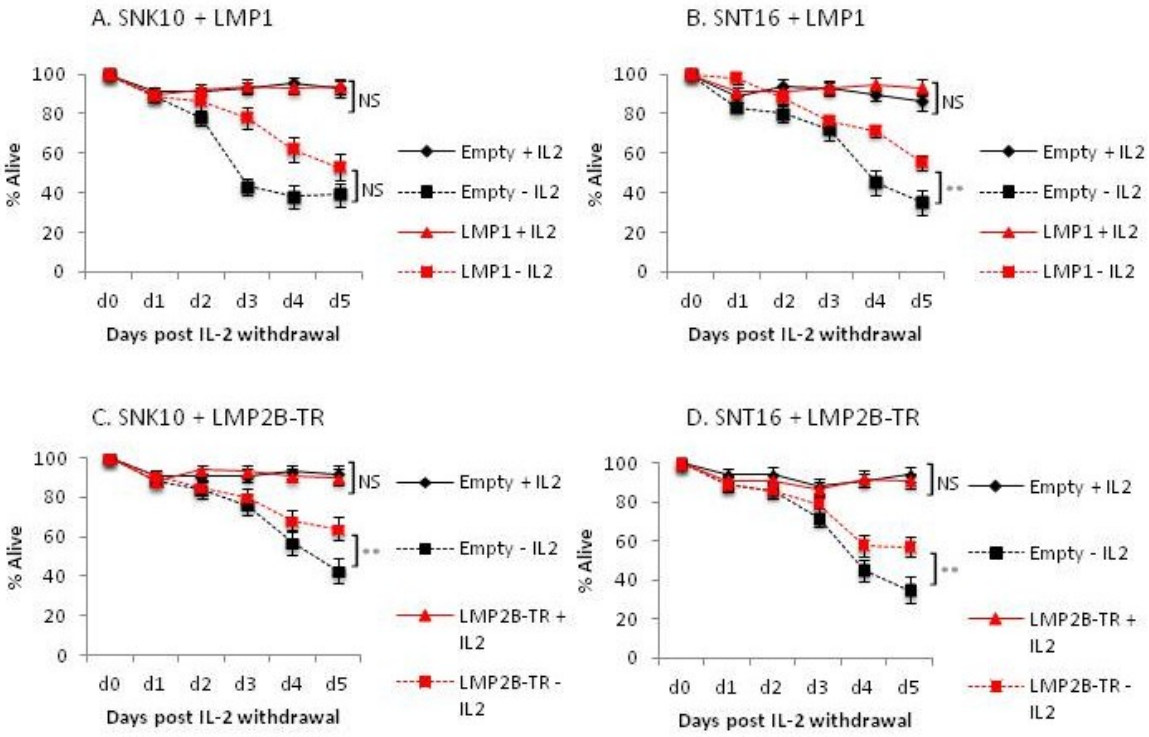

Figure 4-23 - Analysis of IL-2 withdrawal on cells expressing high levels of LMP1 and LMP2B. The CAEBV cell lines were transduced with lentiviruses encoding LMP1 and LMP2B. Expression was induced and IL-2 was withdrawn from the culture medium. The cells were stained with PI and the % alive cells plotted against days post IL-2 withdrawal. Statistical analysis by paired *t*-test showed significant differences between the empty and viral protein-expressing cells in the absence of IL2. **indicates p<0.05

Overexpression of LMP1 compared to cells transduced with empty lentivirus resulted in a small increase in survival following IL-2 withdrawal in SNT16 cells (p=0.09 for SNK10, p=0.003 for SNT16). This confirmed our early experiments when we stratified the cells according to the level of expression of LMP1. However, following over-expression of the LMP2B in the SNK10 and SNT16 cell lines, the LMP2B also appeared to provide a small but reproducible survival advantage (p= 0.009 for SNK10, p=0.009 for SNT16). In the presence of IL-2, the proteins had no

effect on survival (SNK10 p=0.67 for LMP1, 0.07 for LMP2B; SNT16 p=0.06 for LMP1, 0.09 for LMP2B).

LMP1 has previously been shown to have anti-apoptotic activity in B-cells, for example, by inducing the expression of BCL2 (81); it also increases the expression of BCL3 in Jurkat cells (304). Following stratification of our cell lines into high-, intermediate- and low/negative LMP1 protein expression (figure 4-6), we saw a significant protection from drug-induced apoptosis in cells expressing high endogenous levels.

We therefore decided to repeat the apoptosis assays using stably transduced cells which can be induced to express LMP1 and LMP2B. We used Jurkat lines transduced with the same lentiviruses as a control (figure 4-24), and showed that LMP1 increased susceptibility to ionomycin-induced apoptosis.

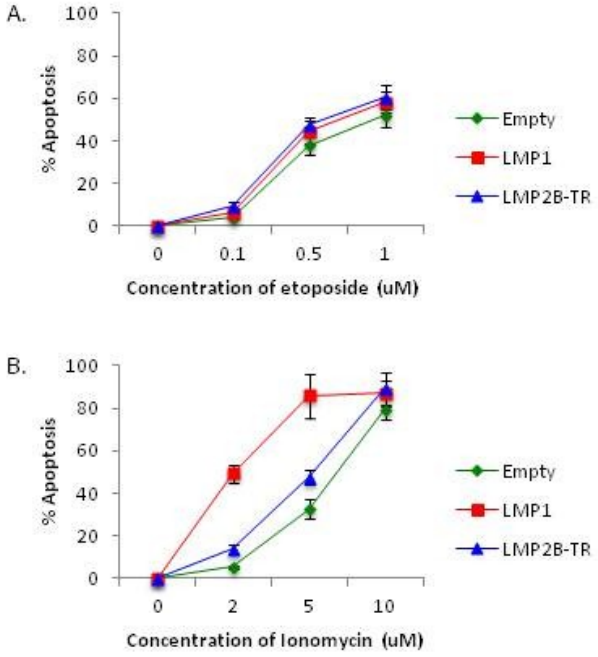

Figure 4-24 - Analysis of apoptosis-inducing drug titrations on Jurkat cells expressing LMP1 or LMP2B-TR. Jurkat cells were transduced with either empty, LMP1- or LMP2B-TR expressing lentiviruses. The gene expression was induced and the cells were then treated with increasing concentrations of (A) Etoposide or (B) Ionomycin. The % apoptosis was determined by annexin V and PI staining. The % apoptosis was plotted against drug concentration.

We then repeated the experiments using stably transduced SNK10 and SNT16 cells (figure 4-25).

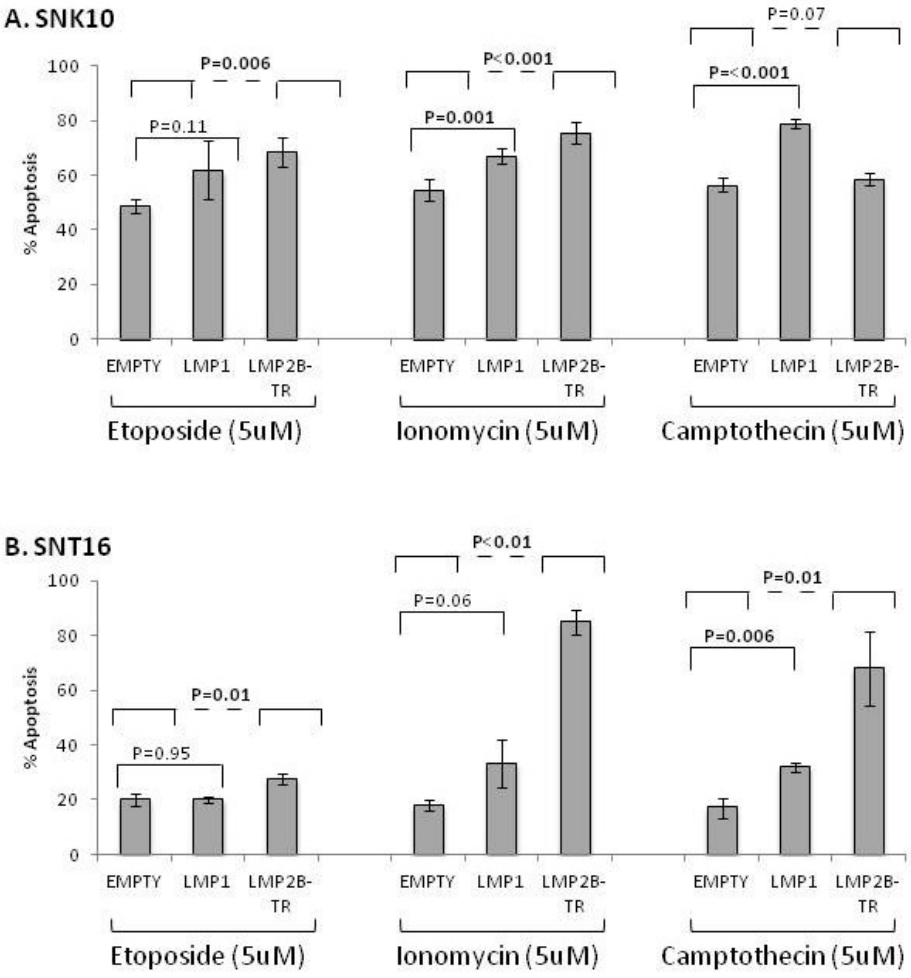

Figure 4-25 - Analysis of apoptosis in response to etoposide, ionomycin and camptothecin in SNK10 and SNT16 cells expressing either LMP1 or LMP2-TR. Apoptosis was measured with Annexin V and PI, and apoptosis plotted against the top drug concentration previously used. The assays were performed three times in triplicate.

Interestingly, LMP1 significantly increased the susceptibility of SNK10 cells to ionomycin and to camptothecin, and the SNT16 cells to camptothecin. Also, LMP2B led to an increased susceptibility of SNK10 to etoposide and ionomycin, and of the SNK16 cells to all 3 agents.

These assays were performed three times in triplicate, therefore the results are robust. However these assays were performed on just the two cell lines so before any firm conclusions can be drawn, the assays need to be repeated on a greater range of cells including both T cell lines and NK cell lines. Also, both viral proteins are usually expressed at low levels in both of these cell lines (see figures 4-1 and 4-2) and our lentiviral system resulted in expression levels that were probably supraphysiological (see figures 4-19 – 4-22). However in the cells transduced by the LMP1 and the LMP2B lentiviruses, the transcripts were significantly higher than the SNK6 cell line, which exhibited one of the highest levels of these proteins. Although these results are intriguing, it is necessary to address these issues with further investigation before any kind of extrapolation to an *in vivo* situation can be considered.

We then sought to determine if we saw the same picture by inducing apoptosis with the BH3 mimetics as previously performed in the ENKTL and CAEBV cell lines. The SNK10 and SNT16 cell lines transduced with the empty, LMP1 or LMP2B were treated with 10 μM of the BH3 mimetic ABT199 and 1 μM of ABT737, stained for Annexin V and PI after 48 hours and analysed for induction of apoptosis. The results are represented in figure 4-26. Statistical analysis was performed using the Student *t*-test.

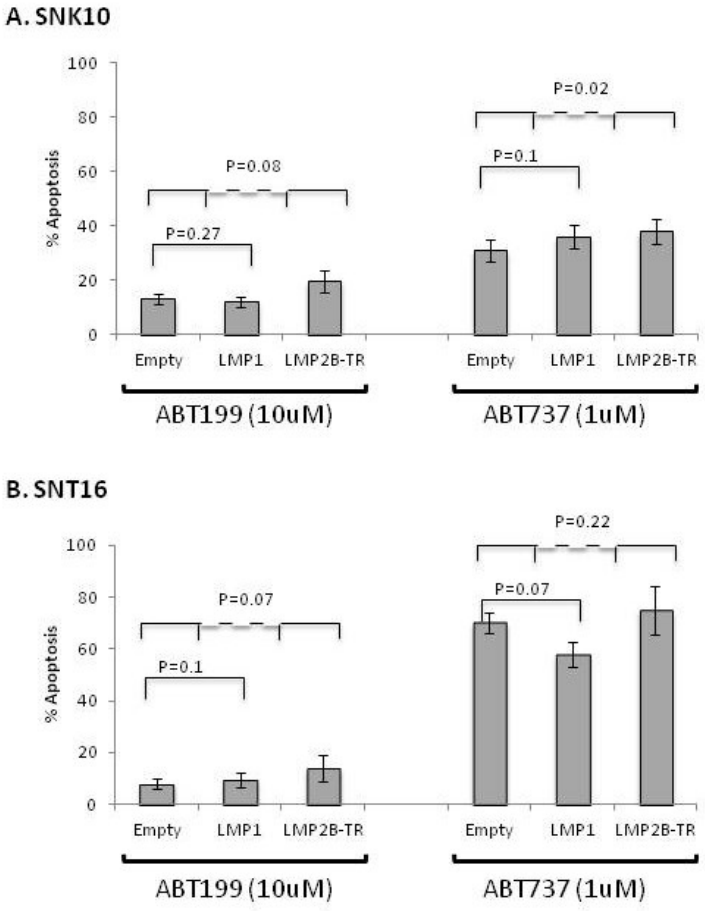

Figure 4-26 - Analysis of apoptosis in response to the BH3 mimetics ABT199 and ABT737 in SNK10 and SNT16 cells expressing either LMP1 or LMP2-TR. Apoptosis was measured with Annexin V and PI, and apoptosis plotted in response to the drugs. The assays were performed three times in triplicate. The results were compared by Student *t*-test.

Aside from LMP2B, which resulted in increased susceptibility to apoptosis induced by ABT737 in SNK10 cells, there were no significant effects of the viral proteins in the cell lines in their response to BH3 mimetics. However, there were trends towards an increased susceptibility to apoptosis from ABT199 in both cell lines expressing LMP2B, although given the extraordinary resistance shown, this may not be biologically significant.

4.7 Discussion

Most EBV-positive T- and NK-cell lines are derived from either ENKTL or CAEBV, and vary in their expression of viral proteins. They are all dependent upon IL-2 for proliferation and survival (276, 353-355), but neither this dependence nor their sensitivity to apoptosis seems to correlate with viral expression. However, they also vary in their expression of the BCL2 family members, and it is likely that this can explain, at least to some extent, the patterns of drug sensitivity seen.

In our hands, IL-2 withdrawal resulted in a fall in LMP1 expression, in keeping with the literature (397, 398). It has been demonstrated that EBV-positive cell lines require less IL-2 to proliferate than EBV-negative lines (398); given that LMP1 is an oncogene, we would expect cells with a high endogenous level of LMP1 to show a particular sensitivity to IL-2, and thus LMP1, withdrawal – and this is the case. However, cells with low levels of LMP1 were similarly affected, suggesting that the effects of IL-2 withdrawal are not purely mediated by a fall in LMP1. Most intriguingly, cells with an intermediate level of LMP1 expression were significantly less susceptible to IL-2 deprivation.

The role of LMP1 in non-B-cell infections is not straightforward. Its expression in ENKTL samples and cell lines is variable (52, 57), but may correlate with an improved prognosis (51) – this may correspond to the high sensitivity of the LMP1-high group of cell lines to cytokine withdrawal in our results. However, reducing LMP1 expression in ENKTL lines does not have the dramatic effects on proliferation that are seen in B-cells (58).

It seems likely that the JAK/STAT pathway is involved in the interaction between IL-2 and LMP1 effects in NK cells. IL-2 can act via the JAK/STAT pathway in NK cells (297) and STAT-binding elements are seen in both of the LMP1 promoters (300). STAT has also been shown to be constitutively activated in at least one ENKTL cell line (276). Interestingly, LMP1 has also been shown to induce CD95 expression in B-cells thus rendering them more vulnerable to T-cell (or CD95-ligand) killing; this effect is mediated by NFκB and STAT pathways (413).

It is important to bear in mind that these are malignant, transformed cells with complex cytogenetic changes, and although it is tempting to conclude that LMP1 must be a factor, there are many possible overlaps in what is a very small sample. This having been said, there is an interesting overlap in the pathways by which LMP1 and cytokines can signal within a cell. IL-10 exposure results in an increase in LMP1, CD25 and CD54 in EBV-positive but not EBV-negative NK cell lines (397, 398); this suggests that the virus may in some way mediate the effects of cytokines upon the cells, maybe amplifying the cytokine signal to maximise the proliferative advantage of the infected cells. Overexpression of LMP1 using a lentiviral vector shows protection from the effects of IL-2 withdrawal in SNT16, a CAEBV line, but increased the susceptibility of the cells to apoptosis induced by ionomycin and camptothecin. In SNK10 cells it did not show a protective effect from cytokine withdrawal, but also increased susceptibility to ionomycin and camptothecin. It is plausible that the CAEBV lines are more sensitive to the effects of the EBV proteins as they lack the other oncogenic mutations accumulated by the cancer lines, but the effects of artificial overexpression of a protein may not mirror those seen with endogenous expression.

LMP2B, interestingly, also showed a protective effect on apoptosis associated with cytokine withdrawal in both SNK10 and SNK16; it also increased the susceptibility of both cell lines to ionomycin, etoposide and camptothecin. Expression is very low in untransduced SNK10 cells although slightly higher in SNT16; the significance of these findings is not yet clear, particularly as very little is known about LMP2 in T- and NK-cell backgrounds.

The role of EBV proteins in the expression of members of the BH3 families is also unclear, but interesting. LMP1 can increase levels of BCL2, BFL1 (301), A20 (302) and MCL1 (303) in B-cells, and in a T-cell line was able to induce BCL3 expression (304), although reducing LMP1 levels in ENKTL cells did not reduce BCL2 expression (58), suggesting a more complex interaction. Interestingly, BCL2 levels are particularly high in the "LMP1-high" group (SNK1, SNK6 and SNT8) which were particularly susceptible to IL-2 withdrawal – this may suggest a mechanism whereby these cells rely upon a high level of BCL2 for their survival, and IL-2 withdrawal and the resulting fall in LMP1 removes this prop.

Proapoptotic BH3 family members also vary between the cell lines. BID levels are low and are absent from SNK6 and SNT8. BAD expression is higher in the CAEBV cell lines and BAX is high in all of the cell lines compared to the controls. There is evidence that, contrary to the accepted model, BID may be primarily responsible for BAK activation and BIM for BAX (414). Based upon our observation, this would suggest that the ENKTL and CAEBV cells are more reliant upon the BIM-BAX pathway. In keeping with this, BIM is associated with cell death in response to growth factor withdrawal (415) and BID is implicated in cell death in response to topoisomerase

inhibitors (416). A lack of BID could explain some of the resistance seen to etoposide and camptothecin.

Another possible factor to take into account is the viral homologues of the BH3 family. BHRF1 and BALF1 act in the same way as BCL2 to protect cells from apoptosis (128, 129) and BHRF1 is expressed in ENKTL, albeit at low levels (417). It would be interesting to examine expression of these proteins in the cell lines and see if they provide some of the answers to the questions posed above.

ENKTL in particular is notoriously difficult to treat with conventional chemotherapy, and novel strategies are badly needed. BH3 profiling is a technique whereby the expression of the BCL2 family proteins can be examined and suitable chemotherapeutic agents trialled within a short space of time – our results here would support this strategy in clinical practice. Newer BH3 mimetics are under investigation – MCL1 and BCL-$_{XL}$ in particular are favoured targets – and it will be interesting to see how they affect this varied panel of cells (418).

CHAPTER 5 - THE CLINICAL IMPACT OF EBV-INFECTION OF NON-B-CELLS

5.1 Introduction

EBV-associated T- and NK-cell disorders are rare in the UK, and, particularly in the case of HLH, often diagnosed late in the condition or even after death. This means that data regarding the incidence, clinical course and biological characteristics of the diseases are limited, and we are often reduced to extrapolating from case series from Asia, where these conditions are more common. The extent of the resemblance between Western and Asian pathology remains unknown and it is important to systematically examine cases in the UK in order to determine whether it is appropriate to consider them as similar entities. As a result, our group has set up a network of 17 UK sites, with ethical approval to obtain blood, biopsy and bone marrow samples from cases of ENKTL, HLH, CAEBV and ANKL.

Despite the wide range of our network, recruitment to the study is predictably slow due to the reasons stated above. However, we have recruited some interesting patients over the lifetime of the study, and some of the recent recruits with a variety of pathologies will be shown here.

5.2 Materials and methods

Ethical approval for this work was provided from the West Midlands Research Ethics Committee (REC: 07/H1208/62).

Patients thought to have non-B-cell EBV-associated disorders were recruited by local clinicians. Upon obtaining informed consent, samples of 60 ml of peripheral blood were obtained in lithium heparin-containing Vacutainer® tubes (BD, USA). Samples were sent to us by courier, arriving within 24 hours.

PBMCs were obtained from the blood samples as described in chapter 2. Briefly, after dilution with sterile PBS the sample was layered onto LymphoPrep (Axis Shield, Oslo, Norway) and centrifuged; PBMCs form a layer at the interface between the LymphoPrep and the plasma and can be retrieved using a transfer pipette.

The mononuclear cells were sorted into lymphocyte subsets (T cells, B-cells and NK cells) by fluorescence-activated cell sorting following staining for the cell surface expression of anti-CD4 (APC) and -CD8 (FITC), anti-CD19 (PE-Cy7) and anti-CD56 (PE). Once sorted, the DNA was extracted from each subset using the DNeasy Blood & Tissue Kit (Qiagen) and analysed for viral load per cell by qPCR. The Burkitt cell line Namalwa was used as a standard – it is known that each Namalwa cell harbours 2 integrated copies of the EBV genome(419). Quantitative PCR for the single copy EBV DNA polymerase gene BALF5 (Pol) was performed and normalised to β-2-microglobin to give copies of virus per cell (see table 5-1 for primers and probe sequences).

Table 5-1 - Sequences of EBV pol primers and probe used for DNA quantification by qPCR

EBV pol forward primer	5'-AGTCCTTCTTGGCTAGTCTGTTGAC-3'
EBV pol reverse primer	5'-CTTTGGCGCGGATCCTC-3'
EBV pol probe	5'(FAM)CATCAAGAAGCTGCTGGCGGCCT(TAMRA)-3'

Using this technique we were able to demonstrate which lymphocyte population was infected with EBV and what the mean virus load was in each lymphocyte subset in a range of EBV-positive disorders. To determine the range of virus loads in the B-cells of healthy virus carriers, we first performed the analysis on six healthy laboratory donors. Figure 5-1 shows the lymphocyte distribution and EBV load of six healthy laboratory donors. In general the virus load in PBMC of healthy virus carriers is low at less than 3,000 copies per million cells. One donor had a load of nearly 9000 - this is a surprisingly high load, but the range of virus loads seen in healthy carriers (0-3,000 copies per million cells) and of IM (5,000 – 50,000 copies per million cells) is very wide(420, 421). EBV infection was confined to the CD19-positive B-cells, with none of the other lymphoid subsets showing any evidence of EBV infection.

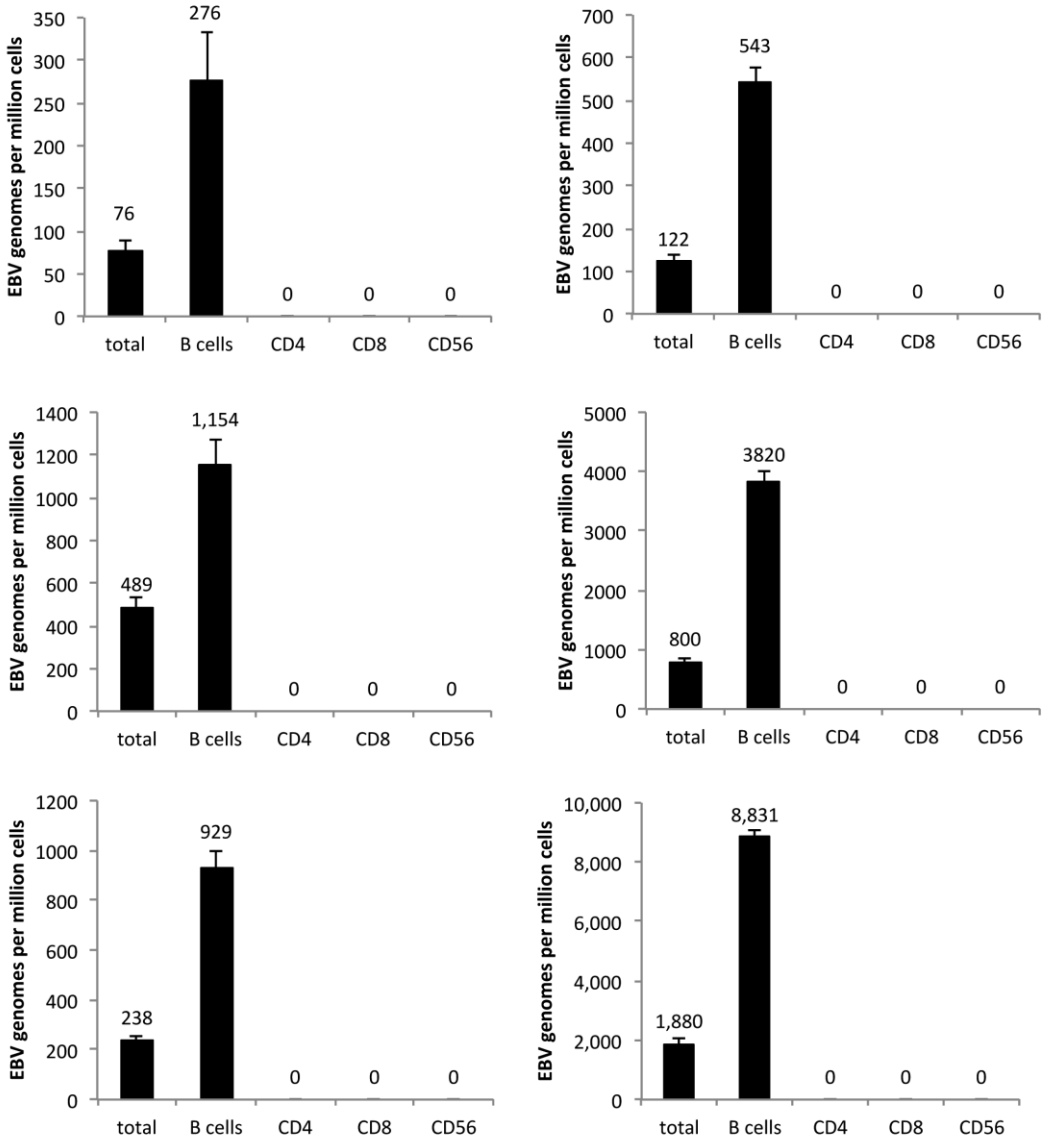

Figure 5-1 - Distribution of EBV in the PBMCs of healthy laboratory donors. In all cases the virus was only seen in B-cells. Viral loads vary somewhat but are all within the normal range for latent infection.

5.3 Patient Samples

We then performed the same set of experiments on a small number of patients with different EBV-associated T/NK cell lymphoproliferations or malignancies. Patient 1 was a young male patient who had been treated for nasal ENKTL in 2007 with combined chemo-radiotherapy. He had relapsed locally after one year and was treated with further radiotherapy and palliative chemotherapy, then developed skin and bladder lesions in 2010, when we received our sample. As above, we isolated the lymphocyte subsets by FACS, extracted the DNA and performed Q-PCR for mean EBV load (figure 5-2). In contrast to the healthy EBV carriers, we observed two clear differences: (i) the virus load was significantly higher in the B cell subset, at 81427 genomes per million B-cells, (ii) the virus was not restricted to the B lymphocytes, but was instead also observed in the CD56 NK cells and the CD8 T cells. The virus load observed in the CD8 cells was within the range of the EBV load in healthy carrier B-cells, but the load in the CD56 cells was considerably higher at 47883 genome copies per million cells. The cell populations were reported as 99% pure after sorting, which would suggest that neither of the virus loads present in the T- or NK cells could be explained by any B cell contamination during the FACS procedure. Unfortunately, the follow-up sample contained insufficient PBMC for this analysis; the patient subsequently underwent a sibling allograft and died during conditioning.

These results are interesting for a number of reasons. EBV infection of NK cells, as discussed in the introduction, is likely to be a rare and possibly dangerous event, thus it is reasonable to suggest that the EBV-positive, CD56-positive cells seen here represented the malignancy

entering a leukaemic phase, although without demonstrating clonality this can't be confirmed. Pre-treatment serum EBV levels have been shown to be an independent prognostic marker in ENKTL, although the cell in which the virus exists in these cases has not been systematically studied. The high viral titres in the B-cells are also interesting – this may represent EBV reactivation as a result of treatment- or disease-induced immunosuppression. Finally, the CD8 results are intriguing – this is unlikely to represent contamination as the purity of the sorted populations was excellent. It is possible that, in the conditions of high EBV, occasional CD8 cells have become infected as is speculated to occur in IM.

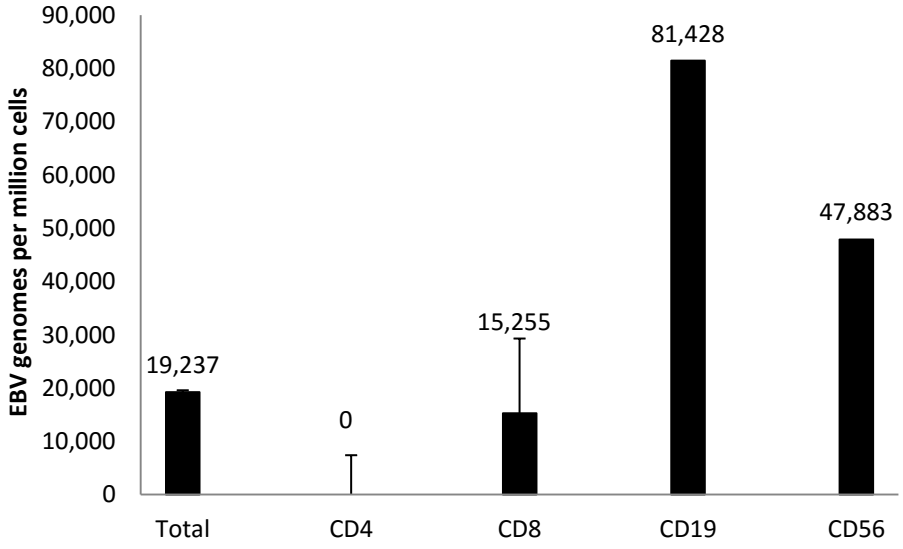

Figure 5-2 - Distribution of EBV load in the lymphocyte subsets of a patient 1 with nasal ENKTL. The majority of the viral copies were observed in CD19-positive B-cells. However a significant virus load was observed in the CD56-high NK cells and a smaller amount in CD8-positive T-cells.

Patient 2 was a young female who had had a combined heart-lung transplant in childhood for primary pulmonary hypertension. She developed clinical manifestations of HLH with a high EBV

load in her peripheral blood 6 months after transplant. Lymphocyte subsets were sorted by FACS and qPCR performed as described above (see figure 5-3).

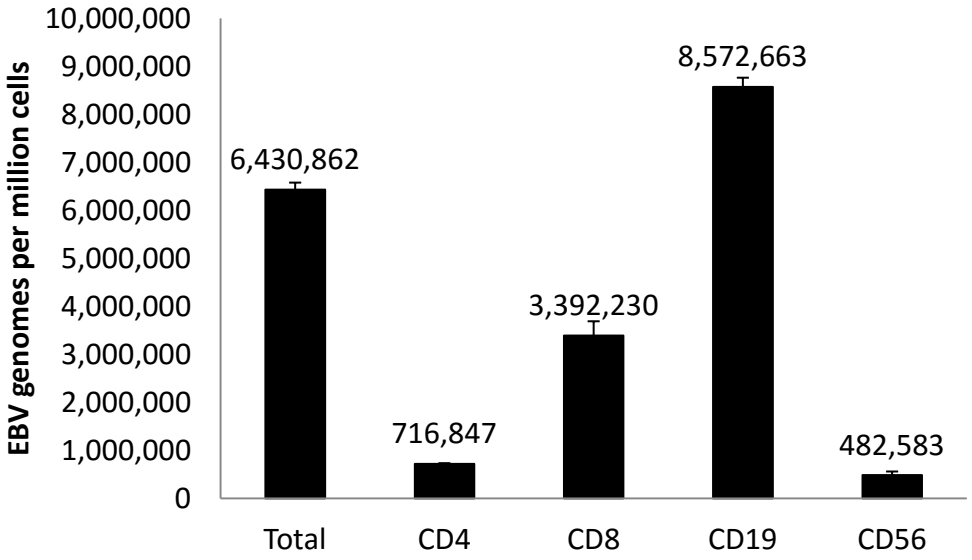

Figure 5-3 – Distribution of EBV load in the lymphocyte subsets from patient 2 with HLH and PTLD. There is a very high overall viral load, and the majority of this represents CD19-positive B-cells, but there is also a very high level of infection in $CD8^+$ T-cells.

In contrast to what has previously been published on EBV-associated HLH, we unexpectedly demonstrated an extremely high viral load in the CD19-positive B-cells at 8,572,663 EBV genomes per million B-cells (figure 5-3). Additionally we also found high viral loads in all the $CD4^+$ T cells (716,847), the $CD8^+$ T cells (3,392,236) and the CD56 cells (482,582). Again, these virus loads cannot be explained by a possible contamination of the sorted subsets. The B-cell population was found to be clonal by immunoglobulin gene rearrangement studies (performed at her clinical centre), suggesting a B-cell malignancy. A subsequent diagnosis of EBV-driven

PTLD suggested that this malignancy was probably contributing to the concurrent HLH. She was initially treated with IVIg, methylprednisolone and etoposide as per the HLH 2004 guidelines; rituximab was added upon the diagnosis of PTLD and she obtained a rapid reduction in EBV loads. A significant population of EBV-positive T-cells remained after her initial treatment (figure 5-4) and she continued with HLH 2004 chemotherapy; at this stage she had no detectable B-cell population as a result of the Rituximab treatment. EBV became undetectable in her peripheral blood by six months after treatment and she has continued to make good clinical progress.

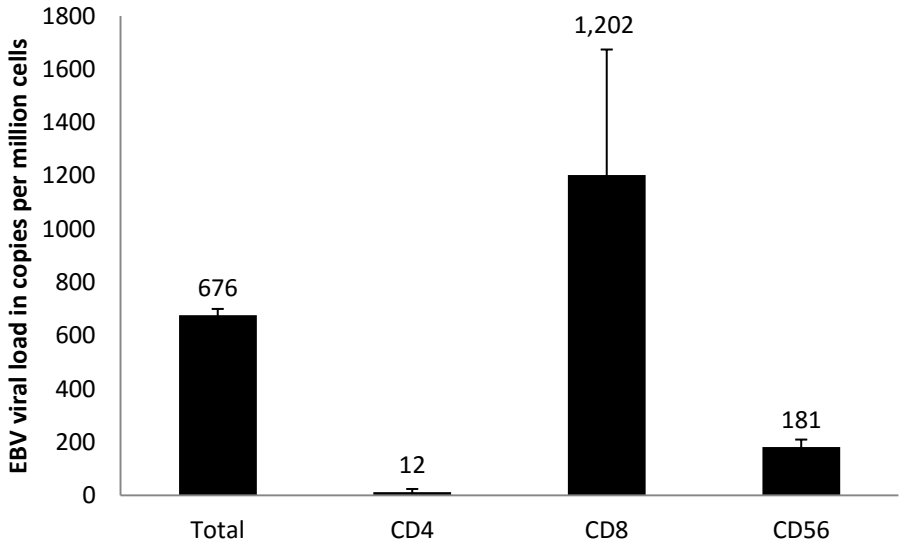

Figure 5-4 – Distribution of the EBV load in lymphocyte subsets from patient 2 with HLH following treatment with chemotherapy including rituximab. As can be seen, the viral load fell dramatically. No CD19 cells were sorted due to rituximab-induced cell clearance. There is still a significant viral load remaining in the $CD8^+$ T-cells.

Patient 3 was a paediatric patient with XLP, who had received a matched, unrelated donor allograft for lymphocytic vasculitis 2 years previously. Although EBV reactivation at the time of transplant had been treated successfully with Rituximab, he subsequently became persistently EBV positive, with no response to further Rituximab, but with no clinical symptoms. Our investigations (Figure 5-5) showed that the virus was predominantly restricted to the CD56-high NK-cells (110,496); furthermore, EBV was also detected in the CD8 T cells at a significant level (40,082). The patient's family refused further treatment and his viral titres have remained stable.

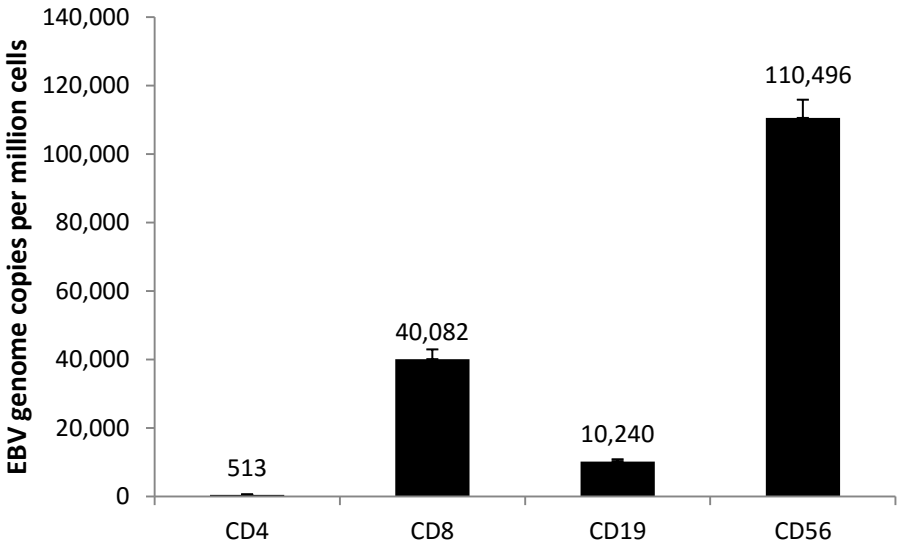

Figure 5-5 - Distribution of EBV load in lymphocyte subsets from patient 3 with persistent EBV reactivation after BMT for XLP. The majority of the virus is seen in the CD56-bright NK cells; there is also a significant viral load in the $CD8^+$ T-cells.

Patient 4 was a middle-aged male patient with HLH and moderate viral titres. Blood was obtained after induction chemotherapy with steroid and etoposide. Here, in keeping with the current UK data on HLH (218) the virus was restricted predominantly to the CD56-bright NK cells (figure 5-6) but the viral load in these was much lower (2,366 copies per million cells) than is usually seen. This may reflect the effects of the chemotherapy. The low levels seen in the $CD4^+$ and $CD8^+$ cells may represent contamination. Unfortunately the patient died before further sampling could take place.

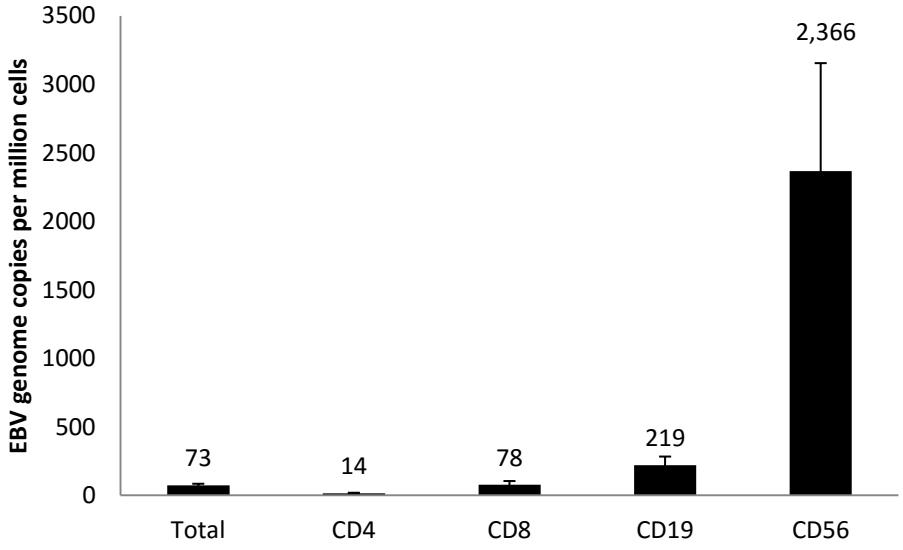

Figure 5-6 – Distribution of EBV load in lymphocyte subsets from patient 4 with HLH. The majority of the viral genomes are located in the CD56-bright NK cells.

Patient 5 was a young male patient who had undergone unrelated bone marrow transplantation for aplastic anaemia and had been found on routine monitoring to have a very high EBV load; there was a suggestion clinically that his presentation was not typical for PTLD and so his blood

was sent for us to investigate for the possibility of a non-B-cell infection. His results are shown in figure 5-7 – here the vast majority of the virus is seen within the CD19-positive B-cells. Due to the exceptionally high levels, it is likely that the values seen in the other cell populations represent minor B-cell contamination. He was treated for PTLD with rituximab and chemotherapy.

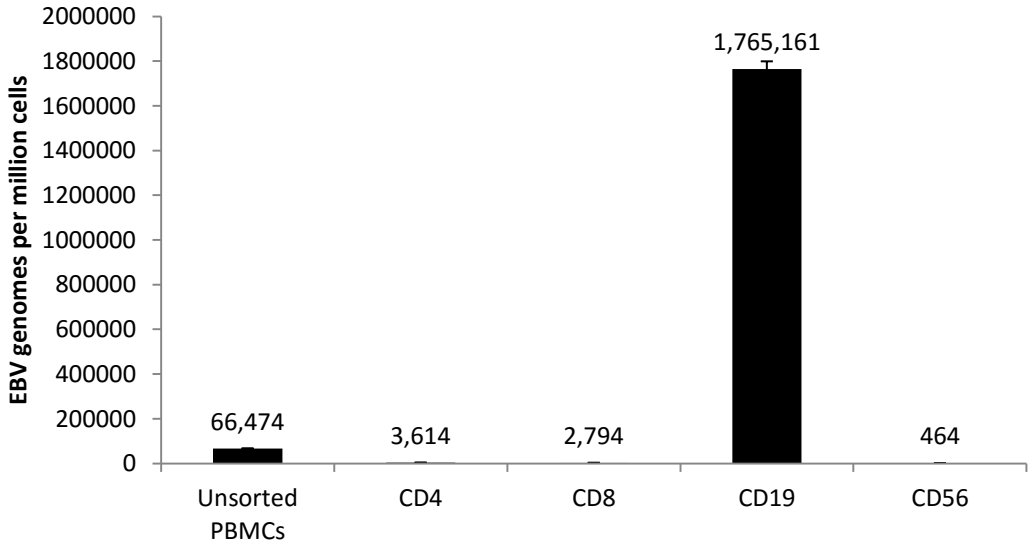

Figure 5-7 – Distribution of EBV load in the lymphocyte subsets from patient 5 with PTLD. The vast majority of EBV was restricted to the B cell subset, with what appears to be minor contamination with B-cells in the remaining subsets.

5.4 The PrimeFlow RNA system

All of the patient samples above were sorted into lymphocyte subsets by fluorescence-activated cell sorting and subsequently analysed for the EBV load by Q-PCR performed on DNA extracted from sorted cell subsets. This has several limitations. Firstly, from 60 ml of whole blood it is usual to obtain approximately $20x10^6$ PBMCs; this number of cells is only just adequate to obtain sufficient purified cells from each lymphocyte subset following FACS and to extract sufficient DNA for the qPCR analysis. Unfortunately, all the cells are used for this one parameter and it is impossible to obtain further data, for example, virus and cellular gene expression, from the sample. It is not usually possible to obtain repeat samples due to the high early mortality in these patients. Secondly, although we can determine which lymphocyte population is infected and the average amount of virus present within the total subset, we cannot determine what percentage of cells are infected within the individual subsets. Thirdly, we cannot perform these types of analyses on paediatric patients as it is not possible to obtain sufficient volumes of blood. Finally, there is little consensus as to which of the EBV genes is actually expressed in HLH – in the experience of our group, only the EBERs have been reliably seen which cannot be detected using conventional flow cytometry. The inability to detect expression of other EBV genes may be due to a lack of sensitivity of our assays. If only a small percentage of cells are actually infected, the number of viral mRNA transcripts may be below the threshold of detection by qPCR assays. We therefore need an assay which is sensitive and specific enough to identify EBV infected lymphocyte subsets from a very small amount of blood to be of use in paediatric diagnosis.

To this end, we first investigated the use of a previously published method of analysing EBV-infected cells using a combination of cell-surface staining and fluorescent in-situ hybridisation for EBER RNA (FLOW-FISH) (422) in the context of T and NK cell disorders (423). However, we encountered several problems, the most pressing of which were (i) an insufficient separation of the EBER positive and negative populations, and (ii) an insufficient separation of the lymphocyte subsets following cell surface staining. This made identification of the infected lymphocyte subset unacceptably subjective. We therefore tried to reproduce the results of the original authors to examine both the sensitivity and specificity of the FLOW-FISH technique (422). Firstly we examined the sensitivity of the technique to determine if it could identify low levels of EBER expression. We previously demonstrated that when primary resting B-cells are infected with EBV, the expression levels of the EBERs remain low until the infected cells begin to replicate at day 3 post-infection. We therefore infected primary resting B-cells at a range of multiplicities of infection (MOI) 1, 10 and 100, then examined the expression levels of the EBERs at day 3 post infection by Q-RT-PCR. As a control, we also examined EBER transcripts from the EBV-positive Burkitt lymphoma cell line Akata to highlight the low level of EBER expression in the primary B-cells.

Assays were performed on 3 independent sets of infected B-cells and Q-RT-PCR assays were performed in duplicate. The results were normalised against GAPDH and plotted in figure 5-8. The first thing of note was the number of EBER1 transcripts were significantly higher than EBER2 transcripts in the newly infected B-cells (Fig 5-8 A). However, the number of EBER transcripts in the newly infected B-cells were at least 300-fold less than those observed in the Akata cells (Fig

5-8 B). As controls for EBV infection of the B-cells, we also performed Q-RT-PCR assays and immunofluorescence for EBNA-2 to ensure that the levels of EBER1 & 2 expression reflected the expected levels of EBV infection.

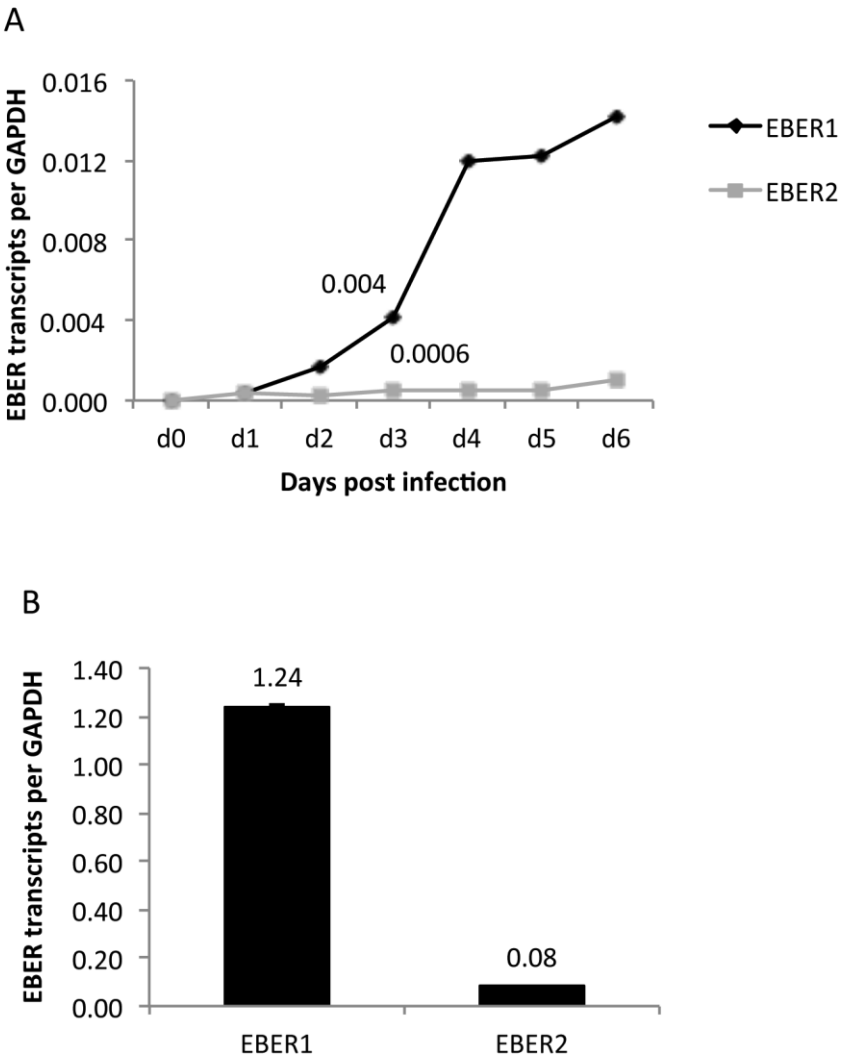

Figure 5-8 – Analysis of EBER 1 & 2 expression in newly-infected primary resting B-cells and Akata Burkitt lymphoma.EBER 1 & 2 RNA transcripts were quantitated by Q-RT-PCR and plotted against GAPDH. Panel A shows the timecourse of EBER expression during primary infection. EBER1 levels rise quickly after infection whereas EBER2 remain low; however, on day 3 both are low. Panel B shows EBER1 and 2 expression in Akata BL cell lines.

We then performed FLOW-FISH on the newly-infected B-cells at day 3 post infection. As above, we infected primary resting B-cells with EBV at an MOI of 1, 10 and 100. For this assay we limited the number of B-cells tested to $1x10^6$ for each time point. The cells were analysed by flow cytometry and plotted as histograms in figure 5-9. Although we achieved good signals for the MOI of 10 and 100, applying gates to accurately identify the positive and negative populations was still subjective.

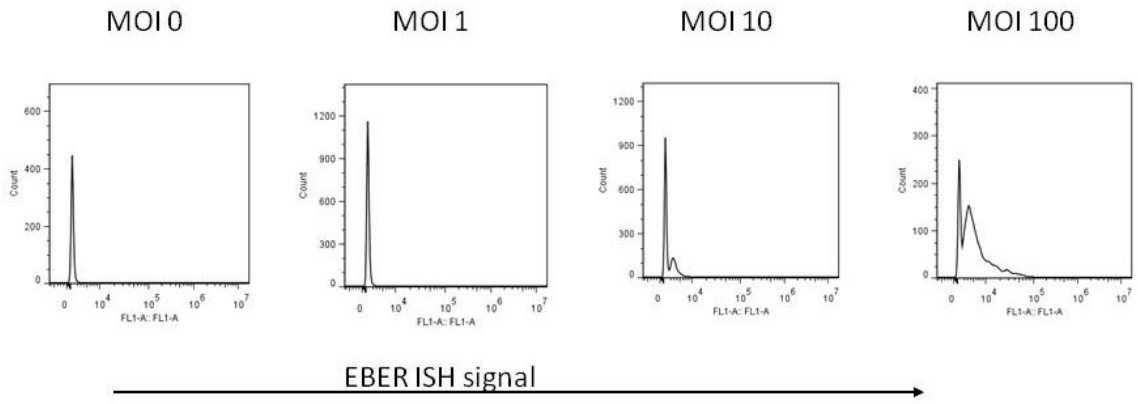

Figure 5-9 - FLOW-FISH analysis of EBER RNA transcripts in newly-infected B-cells. Primary resting B-cells were infected with EBV at increasing MOI. Cells were analysed by FLOW-FISH for EBER transcripts on day 3 post infection. The results of one such experiment is shown.

In order to improve the separation, the authors of the original publication performed an additional amplification step using an anti-FITC AF488-conjugated antibody, which bound to the FITC on the FISH probe to amplify the FITC signal. AF488 and FITC both fluoresce in FL1 on the

flow cytometer (excitation 490, emission 519), so this second antibody effectively doubled the fluorescent signal.

We therefore performed the B cell infection experiments and performed the FLOW-FISH with this additional amplification step, shown in figure 5-10. Interestingly the FLOW-FISH now picked up EBER RNA in the MOI 1 infected B-cells and, as predicted, doubled the fluorescence in the MOI 10 infected B-cells. However, the separation between the positive and negative populations would still have been subjective, even at high MOIs. This could be envisaged as a significant problem when using clinical samples as the levels of EBER expression are not predictable before starting the experiment, and the technique does not appear to be sufficiently sensitive to identify cells with low levels of EBER expression.

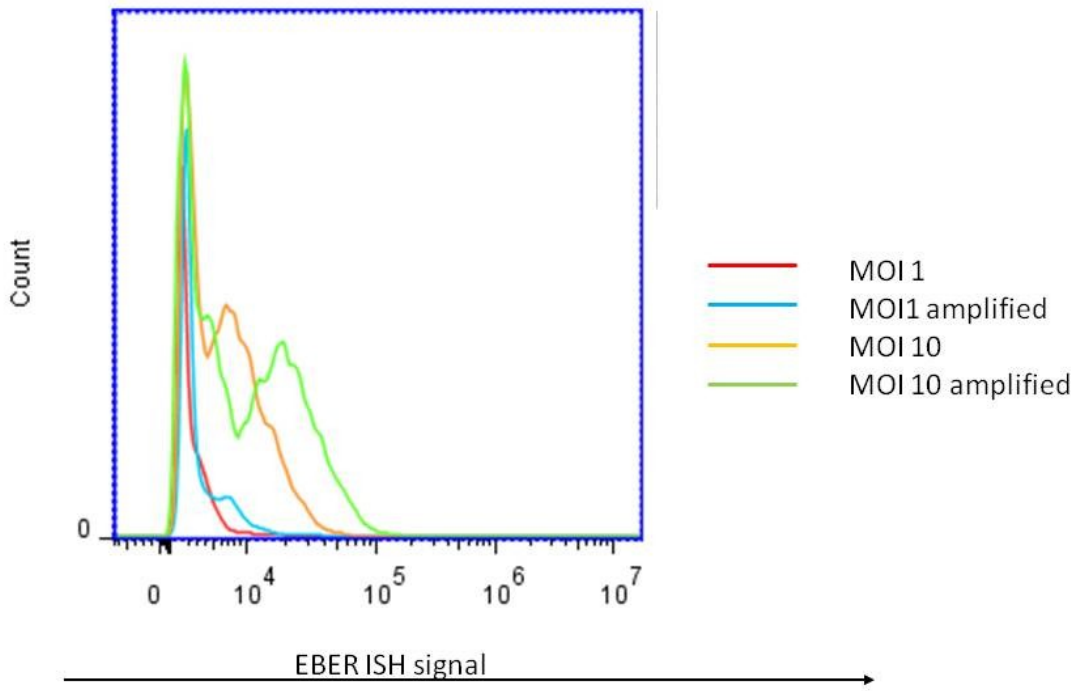

Figure 5-10 - Amplification of the EBER signal in the FLOW-FISH analysis of newly-infected primary B-cells. B-cells were infected with EBV at an MOI of 1 or 10, and were either subjected to an amplification step to improve separation between the populations or processed by the traditional method. As can be seen, amplification improved separation of the populations but where the MOI was low there is still significant overlap.

Given we had previously identified it as the only viral transcript which appeared to be present in the T- or NK cells of HLH patients, *in situ* hybridisation for EBERs appeared to be the only technique that we could use to identify the EBV-infected lymphocyte subset in small numbers of patient cells. We therefore decided to use another newly-marketed fluorescence ISH kit (eBioscience PrimeFlow RNA) to identify the EBERs with simultaneous cell surface staining. This kit is marketed as being both highly specific and highly sensitive. The specificity is achieved by using two 20-mer probes which anneal to the RNA adjacent to each other. The absence of one

probe results in the loss of the downstream amplification and no fluorescent signal. However, importantly the single biggest difference between the two techniques is the high level of signal amplification of the EBER probes in the PrimeFlow kit. The PrimeFlow RNA method is described in detail in chapter 2, but briefly involves the hybridisation of the two adjacent probes to the EBER RNA, then the attachment of a branched, amplifier molecule which captures up to 400 fluorescent molecules per probe. This results in significantly-amplified fluorescence of the hybridised probe thereby giving excellent separation between the EBV-positive and negative populations. This technique can be performed with cell surface staining to identify the lymphoid subsets and we have performed the technique on as few as $1x10^6$ cells.

In order to be useful in a clinical context, the PrimeFlow RNA technique needed to be both sensitive and specific. As shown earlier in this chapter, EBER expression is low in the first week following primary B cell infection and levels at day 3 post infection are approximately 300-fold lower than those of Akata BL. We therefore used the primary B-cells and Akata BL cells as models for testing the PrimeFlow RNA.

First we applied the PrimeFlow RNA assay to the infected B-cells at day 3 post-infection to determine the sensitivity of the assay to detect the low levels of EBER transcripts. The forward-scatter/side-scatter plots (Figure 5-11, top panel) identified that at day 3 post infection the B-cells were activated and beginning to increase in size, consistent with the growth transformation into LCLs. We gated on the live population of cells as shown and analysed the levels of EBER RNA transcripts in uninfected B-cells (figure 5-11, lower left panel), in infected B-

cells at day 3 post infection (lower middle panel) and we substituted the EBER probe for a house-keeping probe beta-2-microglobulin (B2M) (lower right panel).

We can clearly see a very small population of EBER-positive cells in the uninfected B-cells. This might indicate one of two things: either the healthy donor from which the B-cells were isolated were already infected with a natural isolate of EBV, or the EBER probe may be non-specifically labelling cells and this needed to be examined. The second observation was that EBER expression could be detected over a two-log range, indicating that the cells expressed from low levels to high levels of EBERs even at this early stage of infection. The third observation is that the housekeeping B2M probe did not appear to label all the cells. Again, this needed further examination, but suggested that we needed to rule out contaminating dead cells.

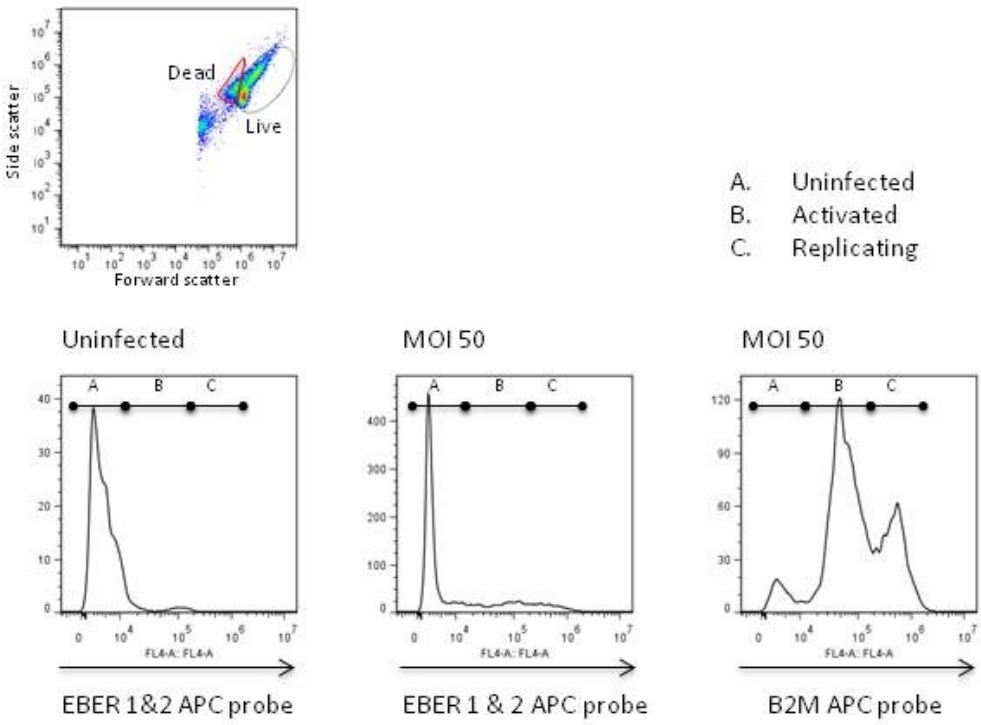

Figure 5-11 – Analysis of EBER expression following infection of primary resting B-cells by the PrimeFlow RNA technique. Gates were drawn around the live cells on the FS/SS plots (Top panel). The bottom panel left shows a very small percentage of cells expressing EBERs, suggestive of endogenous virus. Bottom middle shows a two-log spread of EBER transcripts in newly-infected B-cells. Bottom right is a positive control for the ISH using the housekeeping B2M as a control.

In order to demonstrate that the EBER signal detected in the primary infected B-cells was truly specific, we also performed immunofluorescence on the B-cells to determine the percentage of cells expressing EBNA-2 as a marker of EBV infection, using the PE2 mAb. EBNA-2 is one of the first proteins expressed following B cell infection, and every infected B cell expresses EBNA-2, making it an ideal marker for infection. The percentage of EBNA-2-expressing B-cells was measured by flow cytometry and plotted against the percentage of cells positive for EBER

transcripts measured by PrimeFlow RNA. The results are shown in figure 5-12, and highlight that both assays detect an equivalent percentage of infection of the B-cells at 3 days following infection.

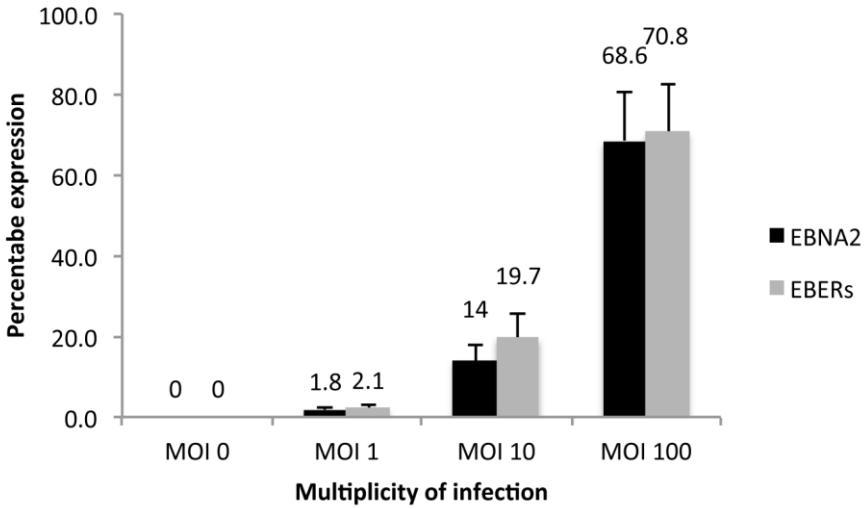

Figure 5-12 - EBNA-2 expression and PrimeFlow RNA measurement of EBER RNA. Primary resting B-cells were infected with EBV for 3 days, then either stained for EBNA-2 expression or subjected to PrimeFlow RNA for EBER analysis. Both assays were measured by flow cytometry and show equivalent percentage of infection whether determined by EBNA-2 staining or by PrimeFlow RNA for EBERs.

We then focussed on the specificity of the PrimeFlow RNA assay. Firstly, we performed the PrimeFlow RNA assay on EBV-negative Akata BL cells (158) and showed no signal with the EBER probe set (Figure 5-13). As a control for the ISH, we also performed the assay using the B2M probe set. As we saw in the primary B cell infection experiment, we found the B2M probe set

did not bind to all the cells as would be expected (approximately 10% were unstained) and again we suspected that this might be due to dead cells within the culture.

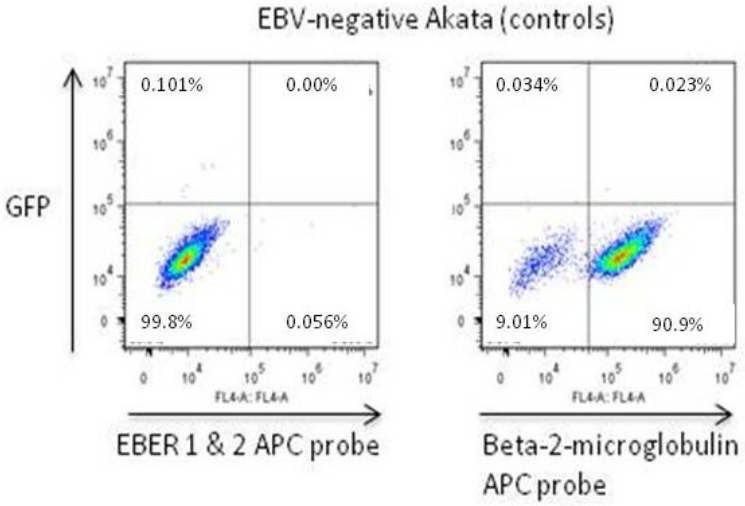

Figure 5-13 – Analysis of EBER and B2M transcripts in EBV-negative Akata BL cells using the PrimeFlow RNA assay. The PrimeFlow assay was performed on EBV negative Akata BL cells to determine how specific the EBER and B2M probe sets were for EBV infection. No signal was detected for EBERs as would be expected, and a good signal was detected for the house-keeping gene B2M. However a small number of cells did not stain with the B2M probe, suggesting the presence of dead cells.

We then made use of a fortuitous set of EBV-positive and EBV-negative Akata BL cultures, established in our laboratory as part of an unrelated project. The EBV-positive Akata BL cells contain a recombinant GFP-expressing EBV. The EBV-negative Akata BL cells are a matching EBV-loss clone and are GFP-negative. This provided an excellent internal control for the following set of experiments. We "spiked" the GFP-negative Akata BL cells with 5% and 1% of the EBV/GFP-positive Akata BL and performed the PrimeFlow RNA assay (Figure 5-14). All the EBER-positive cells were also GFP-positive and provided a double-positive population, thereby

demonstrating the specificity of the assay (upper panel). The assay was again performed with the B2M probe set as a positive control for the assay. All cells were positive for B2M.

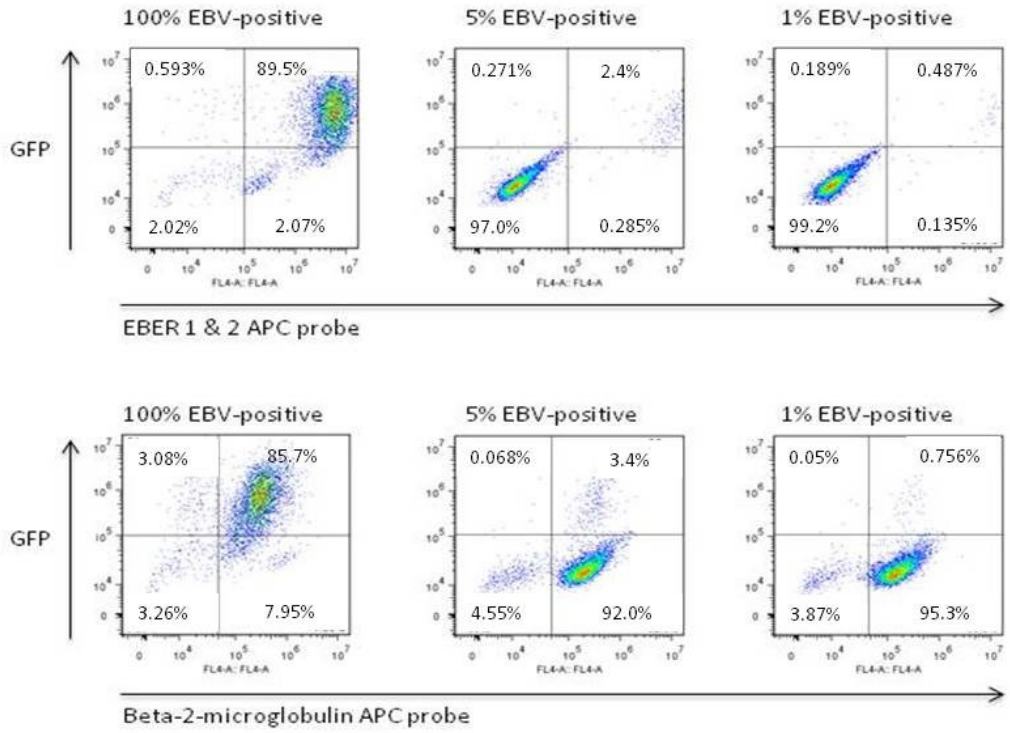

Figure 5-14 – PrimeFlow-RNA analysis of Akata cells. EBV-negative Akata cells, which are GFP-negative, were mixed with GFP-positive EBV-positive Akata cells. The top panel shows the correlation between GFP expression and detection of EBERs by PrimeFlow-RNA at different concentrations of test cells. The bottom panel shows the B2M housekeeping gene, with a small population of negative cells. In both panels the sensitivity to GFP is excellent and is not affected by the ISH signal.

5. 5 Validation of PrimeFlow RNA in the UK

In the meantime, recruitment of our UK patients has continued. Most recently, a patient with EBV-associated HLH was identified. The patient was thought to have a primary EBV infection which triggered the HLH and was initially treated according to the HLH-2004 protocol (dexamethasone, etoposide, cyclosporine)(193), whereupon the clinical syndrome appeared to resolve. PBMCs from this patient were subjected to this new technique to determine the sensitivity and specificity of PrimeFlow-RNA in the patient setting.

Healthy donor PBMCs were initially subjected to several controls critical for setting up a multicolour cell surface staining panel for the LSR-II flow cytometer. The cells were first stained using isotype controls to set the negative populations, shown in figure 5-15. Isotype controls for CD3 (AF700), CD4 (PE-Texas red), CD8 (AF488), CD19 (PeCy7) and CD56 (PE) were used.

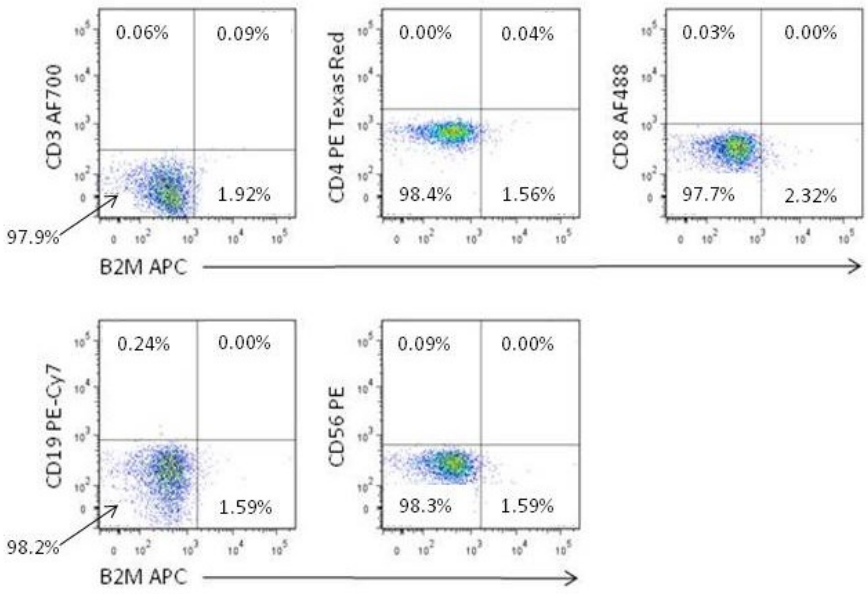

Figure 5-15 - PrimeFlow-RNA assay isotype controls. The PBMC were subjected to the PrimeFlow-RNA protocol using specific appropriate isotype controls for the cell-surface staining and without RNA ISH probes to ensure adequate gating for the negative control cells.

The cells were then stained using the individual lymphoid markers (CD3, CD4, CD8, CD19, CD56) to ensure that following the RNA-ISH technique the fluorescent markers were still fluorescent and showed sufficient separation between the positive and negative populations. The cells were also stained using a dead cell marker, vital dye conjugated to pacific blue, and a marker for monocytes, CD14-pacific blue. All cells staining for either of these parameters were excluded from the analysis.

Finally, the cells were stained using the appropriate isotype controls together with the positive RNA-ISH control, B2M to ensure the B2M probe worked in the presence of antibodies on $1x10^6$ cells (figure 5-16).

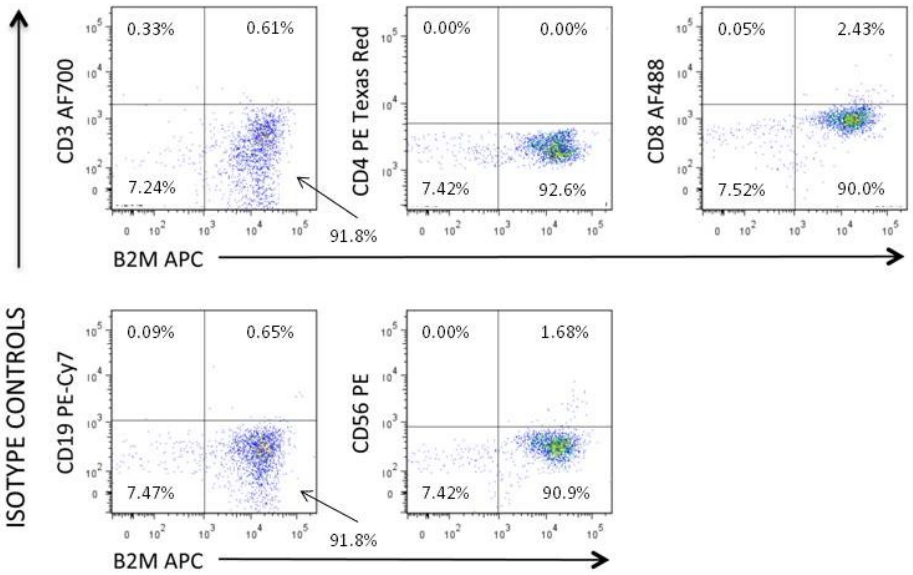

Figure 5-16 -PrimeFlow-RNA assay for B2M positive control. All lymphocyte subsets were stained with isotype controls together with the positive control for the mRNA ISH, B2M.

Having established an appropriate set of cell surface fluorophores on healthy donor PBMCs, and given the healthy donor PBMCs showed a very small EBV load (<500 EBV copies per million B-cells), it was inappropriate to test the EBER probe set directly on donor PBMCs. We therefore went ahead and performed the cell surface staining and the EBER-ISH on the patient's PBMCs. Figure 5-17 shows the results of the combined analysis of EBER expression by ISH with cell surface staining. The top panel shows lymphocyte gating by forward and side scatter. As with

all HLH cases we have previously observed, the percentage of monocytes in the peripheral blood had increased significantly. The bottom panel shows the results of the dual staining, and demonstrates that the EBV-positive population in this case is the $CD4^+$ T-cells, and that there is no significant EBER expression in any of the other lymphocyte subsets, including $CD19^+$ B-cells. Importantly, the EBER-positive population and the EBER negative populations are separated by approximately one log of fluorescence, eradicating the worry about assay sensitivity and subjective interpretation of results. One small issue remains to be resolved. There are minor compensation issues with the CD3-AF700 and EBER-APC as seen in figure 5-18, bottom right-hand panel. When taking this assay forward, it will be preferable to substitute the AF-700 for an alternative, more suitable fluorophore.

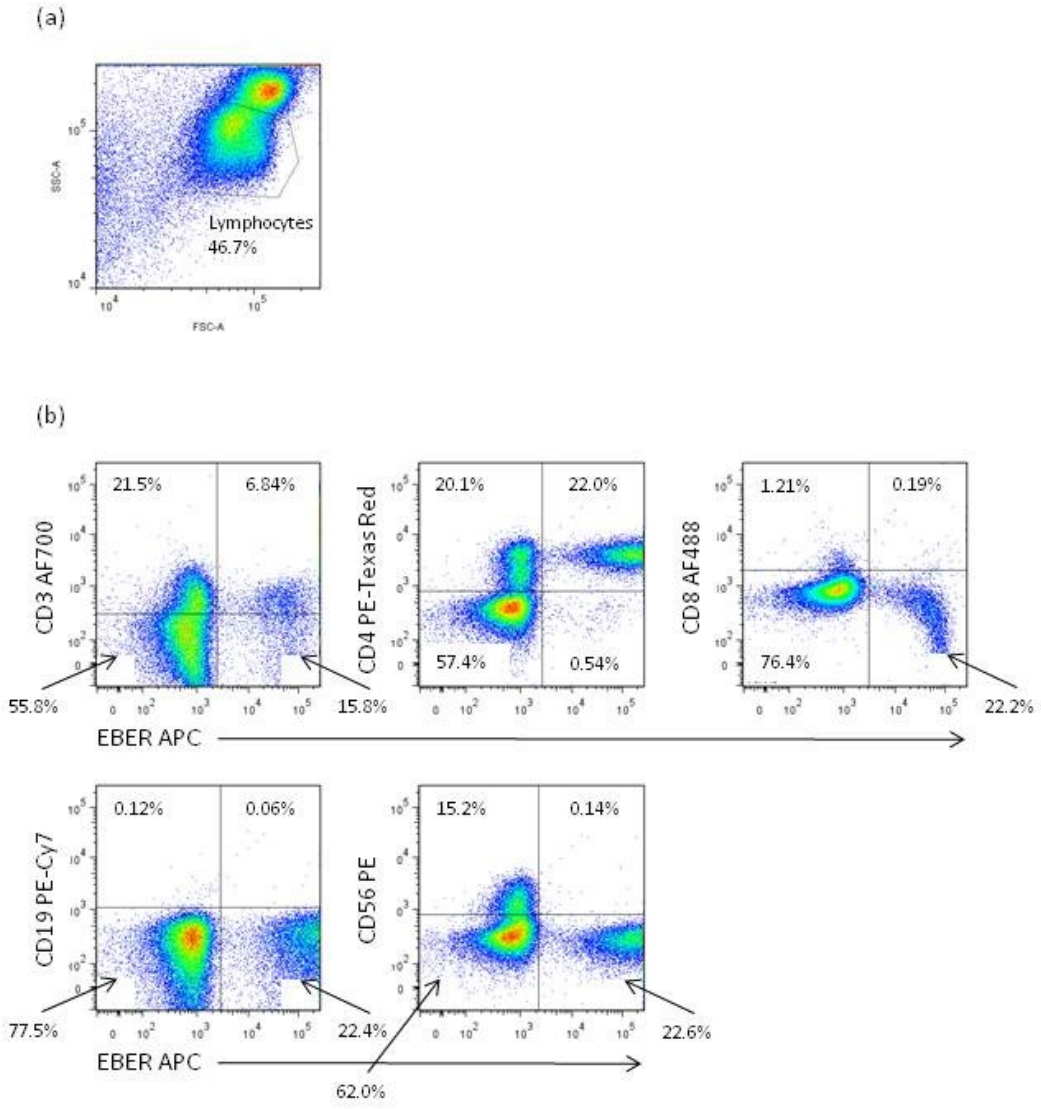

Figure 5-17 - PrimeFlow-RNA assay on PBMC from an EBV-associated HLH patient. (a) PBMC were analysed by FSC and SSC to identify the lymphocyte subsets and to provide the appropriate gating strategy. (b) The lymphocyte subsets were stained for specific subset markers and subjected to the PrimeFlow-RNA protocol to detect the presence of EBERs. The lymphocyte subset infected with EBV was the $CD4^+$ cells.

Finally, figure 5-18 shows the results of ISH for B2M and cell surface staining. All cell subtypes are positive for B2M, as expected.

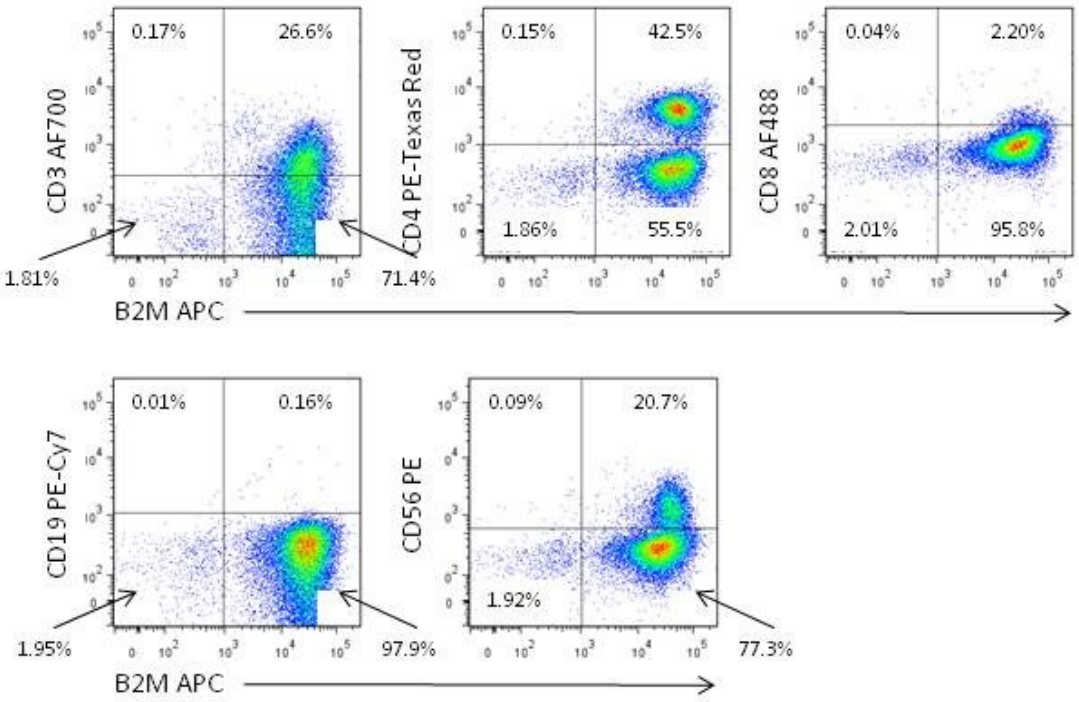

Figure 5-18 - PrimeFlow-RNA assay on PBMC from an EBV-associated HLH patient. The lymphocyte subsets were stained for specific subset markers and subjected to the PrimeFlow protocol to detect the presence of the positive control mRNA B2M. As shown, all the subsets were positive for B2M.

Interestingly we were able to follow the progress of this patient after HLH-2004 treatment. Figure 5-19 shows the results of the PrimeFlow RNA performed on PBMCs from the same patient 2 months following HLH-2004 treatment. This shows that although the patient remained symptom-free, EBV-positive $CD4^+$-T cells remained in the blood of the patient and furthermore, the number of EBV-positive cells appeared to be expanding from 52% of $CD4^+$ cells

2 weeks following treatment, to 72% at 2 months following treatment. The patient had, in the meantime, received a diagnosis of CAEBV, which can be presumed to be the trigger for the HLH.

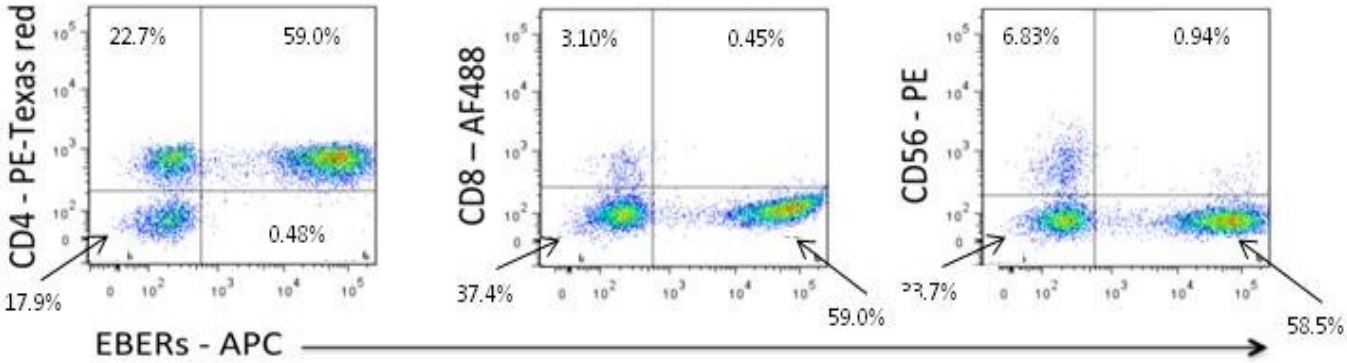

Figure 5-19 - PrimeFlow-RNA assay on PBMC from an EBV-associated HLH patient 2 months following HLH-2004 treatment. PBMC from the HLH patient were subjected to PrimeFlow-RNA to determine the % of EBER-positive $CD4^+$-T cells following HLH-2004 treatment.

We re-analysed the patient PBMC sampled prior to treatment using an antibody panel employing a PE-Cy5-conjugated CD4 antibody that unfortunately did not work. However, we were able to ascertain from the CD3 and CD8 staining that the percentage of EBER-positive $CD4^+$-T cells was 12%. Table 5-2 gives a breakdown of the expansion of the EBV-positive $CD4^+$-T cells and indicated an expansion of the $CD4^+$ cells as a percentage of total lymphocytes. Unexpectedly, we observed that instead of reducing the number of EBV-positive CD4 T cells in the PBMC, treatment with the HLH-2004 protocol was associated with an expansion of the EBV-infected $CD4^+$ T cells.

	PRE-HLH 2004	2 WEEKS POST HLH 2004	2 MONTHS POST HLH 2004
% EBER positive CD4	12% CD4	52% CD4	72% CD4
% CD4 total	30%	50%	82%

Table 5-2 – Expansion of the $CD4^+$, EBV-positive T-cell population in the patient after HLH-2004 treatment. The percentage of $CD4^+$ cells infected with EBV rose from 12% to 72% over this period, and $CD4^+$ cells represented 82% of the total PBMCs by 2 months after treatment.

We have previously demonstrated that EBV-infected T cells or NK cells present in the PBMC of HLH patients only express the viral EBERs. However, now that we have developed an assay to identify the EBV-infected subset directly from patient PBMC, we were able to purify the EBV-positive cells and examine the viral gene expression. We therefore isolated RNA from the $CD4^+$ T-cells from the pre-treatment, the 2 weeks post treatment and the 2 months post treatment samples. We performed Q-RT-PCR for the viral mRNA transcripts EBNA-1 from the Q-promoter (Qp), LMP1, LMP2A, LMP2-TR, EBNA-2 and BZLF1. Figure 5-20 shows the results of these analyses. Similarly to that previously demonstrated, we did not detect EBV transcripts in the pre-treatment cells other than the EBERs. However, in both post-treatment samples we were able to detect reliable levels of EBNA-1 from the Q-promoter (Qp), LMP1, LMP2A and the novel LMP2B-TR transcript. These levels are small, and by comparison with published work (38) this suggests that they may be expressed in only a subset of the EBER-positive cells. Not surprisingly, we were unable to detect EBNA-2 transcripts, given they are B cell-specific. Additionally, we were only able to detect vanishingly small levels of BZLF2 transcripts, indicating the infected cells are not entering lytic replication. This is important in the context of the expansion of the infected cells following treatment.

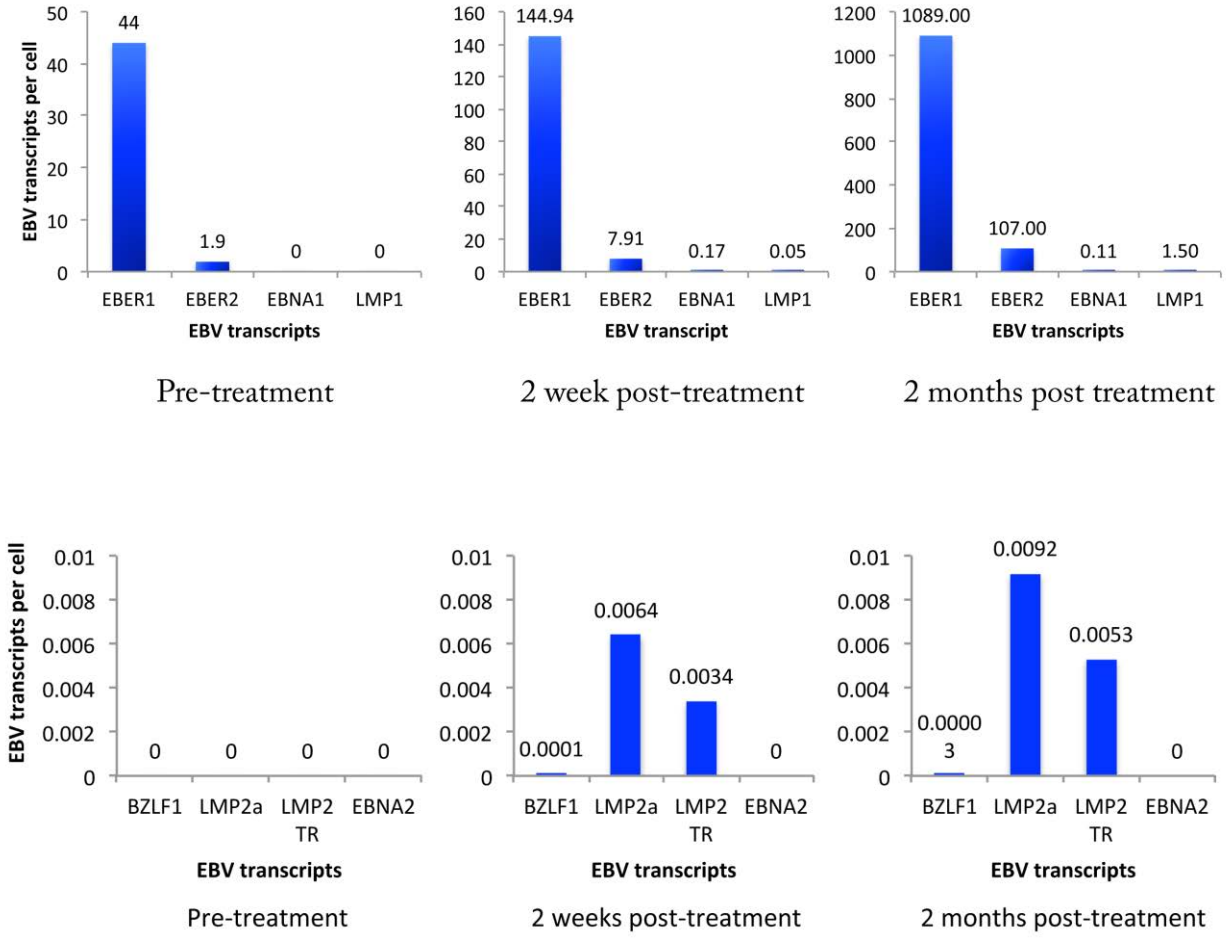

Figure 5-20 - Analysis of EBV transcripts in the HLH case before, 2 weeks post and 2 months post treatment. Viral transcripts were measured by Q-RT-PCR and are represented as absolute viral transcripts per cell. Given there was only one sample for each time point, the assays were performed in triplicate resulting in no standard deviation.

When the $CD4^+$ T-cell receptors were analysed by the clinical team, there was a significant population with identical rearrangements, indicating that the disease represents a clonal

expansion of a single EBV-infected cell. This reinforces the hypothesis that EBV infection in non-B-cell disorders is an early event.

5.7 Discussion

The total number of patient PBMCs used in this final experiment was only $2x10^6$, compared to $20x10^6$ for conventional cell sorting and QPCR. This technique has the potential to revolutionise the way in which EBV-associated disorders are diagnosed. As discussed earlier, the clinical criteria for EBV-associated HLH are ill-defined, and the analysis of which lymphocyte subset is infected is vital for the correct diagnosis as well as management; anti-B-cell antibodies, as used in PTLD, will not be effective if the offending population is CD20 negative. We propose a strategy by which we are able to offer quick and reliable testing on small numbers of cells, foreseeing a future in which it is used routinely in a clinical setting.

The combination of ISH and cell surface staining can also be exploited for further therapeutic purposes. The presence or absence of druggable targets on the infected cell population can be quickly determined, allowing the rapid deduction of an appropriate personalised regimen. For example, CCR4, a chemokine receptor, has been detected on the surface of ENKTL cells(424); a monoclonal antibody to it, Mogamulizumab, has shown promising results when used to treat cutaneous T-cell lymphoma (425) and is a potentially useful agent. Another example is the Programmed Death Ligand (PD1) pathway (reviewed in (426)). Ligation of PD-1, a molecule found on the surface of effector T-cells (as well as other immune cells), results in suppression of their action and contributes to a “tumour-permissive” environment (427); PD1 ligand 1 (PD1-L1)

is upregulated by LMP1 (428) and is expressed on NKTL (429). This pathway is the subject of intense scrutiny and it is likely that it will become a major target for pharmaceutical intervention; by analysing the expression of the relevant proteins on the EBV-infected cell, the suitability of this could be determined for each patient.

In summary, I have described a new technique for quickly and reliably performing simultaneous ISH and cell surface staining for analysis by flow cytometry. Unlike previous techniques, this is accurate using only $1x10^6$ PBMCs, making it appropriate for use in the paediatric population. Not only does this permit the rapid deduction of which lymphocyte subset is infected with EBV, it also allows further analysis of the characteristics of the infected cells and could contribute significantly to the speedy selection of appropriate treatment regimens.

CHAPTER 6 - CONCLUSIONS AND FURTHER WORK

Despite the wealth of information about EBV in B-cell conditions, its role in T- and NK-cell disorders remains remarkably enigmatic. This can be attributed to several factors – the relative rarity of these diseases, their geographic distribution outside the West, and, perhaps most of all, the difficulty in reproducing them *in vitro*. I have demonstrated three approaches to studying these conditions – at a molecular level, by using cell lines, and by systematically recruiting and effectively investigating the clinical cases that are encountered.

LMP1 is the most obvious candidate for a pathogenic protein in ENKTL. It has well-described oncogenic functions (6, 42, 73) and is expressed (although to variable degrees) in ENKTL specimens (51, 52, 57). When microarray analysis of the effects of its expression in primary NK cells was undertaken, 109 genes were significantly upregulated and 146 downregulated. Further analysis of these genes revealed that pathways involved in response to cellular stress and cell cycle were significantly enriched, which is in keeping with the known effects of LMP1 on epithelial and B-cells.

However, when the specific genes altered were compared with published data, there was no significant overlap between the gene expression profile induced by LMP1 in NK cells, B-cells and epithelial cells. This is not altogether surprising as the cell backgrounds are very different, and on further analysis of the published data we have shown that the gene expression profiles engendered by LMP1 are not similar when B-cells and epithelial cells are compared, suggesting a very specific, cell-type dependent, role for the protein in these malignancies.

Most interestingly, there is a significant overlap in genes differentially regulated by LMP1 in primary NK cells and those expressed in ENKTL samples compared to uninfected NK cells. This is encouraging evidence that LMP1 is important in NK lymphomagenesis and/or maintenance of the established tumour phenotype. The evidence may be even more convincing if we are able to ascertain which of the ENKTL samples were expressing LMP1; information that we have as yet been unable to extract from the authors of the original ENKTL study.

LMP1 can also be seen to be important when cell lines are examined. It is expressed, at varying levels, in most of the currently available ENKTL and CAEBV cell lines. Endogenous LMP1 expression correlates with survival upon IL-2 withdrawal – when cell lines were considered by LMP1 expression, intermediate levels of the protein were associated with a significant protection, despite the fact that LMP1 itself falls in the absence of the cytokine. Cells expressing high levels of endogenous LMP1 were also less susceptible to apoptosis in response to etoposide, ionomycin and camptothecin. Overexpression of LMP1 in one of the cell lines again resulted in protection from apoptosis as a result of IL-2 withdrawal. This suggests an overlapping survival and proliferation pathway between the cytokine and the protein, which is in keeping with what is known about LMP1 function in B-cells. However, overexpression of LMP1 was also associated with increased sensitivity to ionomycin and camptothecin, although interestingly not etoposide, in the cell lines examined.

LMP2B is much less well-understood, even in the B- and epithelial cell contexts. It is expressed in ENKTL tumours and cell lines (306) and, we can speculate, is likely to be important in lymphomagenesis. However, upon microarray analysis, although the expression of 238 genes

was significantly altered by LMP2B expression in primary NK cells, this did not show significant overlap with the gene expression profile of ENKTL. Overexpression in SNK10 and SNT16 increased susceptibility to apoptosis in response to etoposide (although not significantly in SNK10), ionomycin and camptothecin; yet it provided some protection to both cell lines from apoptosis in response to cytokine withdrawal.

Exploitation of the intrinsic pathway to induce apoptosis in malignant cells is an exciting field of pharmacological research. This intricate web of interconnecting processes is disrupted in cancers, and by identifying the key proteins for a particular cell's immortality, specific therapeutic regimens can be devised. I have demonstrated the variability between expression of the BH3 protein family, even within the same diagnosis, giving further weight to the argument for BH3 profiling on clinical cases in order to be able to deliver targeted, appropriate and effective chemotherapy.

Clinical cases of EBV-associated non-B-cell disorders are rare in the UK, and as a result it is difficult to systematically study their features. We have an ongoing network of UK centres and have recruited several interesting patients as a result. We have also set up a collaboration with the largest children's hospital in Ho Chi Minh City to consider HLH in a cohort of patients with similar backgrounds and comorbidities. In order to effectively use what can be very small samples, we have developed a technique of simultaneous in-situ hybridisation to the EBER transcript and cell surface staining; suitable for use on as few as $1x10^6$ PBMCs. This technique is capable of revolutionising the way in which these conditions are studied and treated.

The work in this field is ongoing. Immediate challenges are to subject further patient samples to the PrimeFlow RNA technique and validate it with more conventional methods. Other cell surface markers must be worked up in order to investigate the targeting of novel molecules and pathways in these conditions. Further investment in the Vietnamese laboratories should enable this study to be restarted, and this collaboration is a promising one for both sides of the agreement. The PrimeFlow technique will be particularly appropriate for these tiny samples. Furthermore, we have applied to extend our UK study to include paediatric cases, which will allow direct comparison with the Vietnamese samples.

The study of non-B-cell EBV infections is fascinating, offering as it does a unique opportunity to study the virus outside of its natural habitat. It has the potential to answer many questions about the role of the viral proteins and how, and why, these cells get infected in the first place. The conditions discussed here are rare but devastating, and the clinical impact of work in this field is potentially life-saving.

REFERENCES

1. Burkitt D. A "tumour safari" in East and Central Africa. Br J Cancer. 1962;16:379-86.
2. MARA/ARMA Project Home Page 2014 [Available from: http://www.webcitation.org/getfile?fileid=e519a9d56b2fc9dbcb07c2d0cadf3d5e29009176.
3. Epstein MA, Achong BG, Barr YM. Virus Particles in Cultured Lymphoblasts from Burkitt's Lymphoma. Lancet. 1964;1(7335):702-3.
4. Henle W, Diehl V, Kohn G, Zur Hausen H, Henle G. Herpes-type virus and chromosome marker in normal leukocytes after growth with irradiated Burkitt cells. Science. 1967;157(792):1064-5.
5. zur Hausen H, Schulte-Holthausen H, Klein G, Henle W, Henle G, Clifford P, et al. EBV DNA in biopsies of Burkitt tumours and anaplastic carcinomas of the nasopharynx. Nature. 1970;228(5276):1056-8.
6. Fields BK, DM, Howley P. Virology. 6th ed: Wolters Kluwer Health/Lippincott Williams & Wilkins, c2013.; 2013.
7. Epstein MA, Henle G, Achong BG, Barr YM. MORPHOLOGICAL AND BIOLOGICAL STUDIES ON A VIRUS IN CULTURED LYMPHOBLASTS FROM BURKITT'S LYMPHOMA. J Exp Med. 1965;121:761-70.
8. Kintner CR, Sugden B. The structure of the termini of the DNA of Epstein-Barr virus. Cell. 1979;17(3):661-71.
9. Given D, Yee D, Griem K, Kieff E. DNA of Epstein-Barr virus. V. Direct repeats of the ends of Epstein-Barr virus DNA. J Virol. 1979;30(3):852-62.
10. Raab-Traub N, Flynn K. The structure of the termini of the Epstein-Barr virus as a marker of clonal cellular proliferation. Cell. 1986;47(6):883-9.
11. Given D, Kieff E. DNA of Epstein-Barr virus. IV. Linkage map of restriction enzyme fragments of the B95-8 and W91 strains of Epstein-Barr Virus. J Virol. 1978;28(2):524-42.
12. Baer R, Bankier AT, Biggin MD, Deininger PL, Farrell PJ, Gibson TJ, et al. DNA sequence and expression of the B95-8 Epstein-Barr virus genome. Nature. 1984;310(5974):207-11.
13. Zimber U, Adldinger HK, Lenoir GM, Vuillaume M, Knebel-Doeberitz MV, Laux G, et al. Geographical prevalence of two types of Epstein-Barr virus. Virology. 1986;154(1):56-66.
14. Rickinson AB, Young LS, Rowe M. Influence of the Epstein-Barr virus nuclear antigen EBNA 2 on the growth phenotype of virus-transformed B cells. J Virol. 1987;61(5):1310-7.
15. Abdel-Hamid M, Chen JJ, Constantine N, Massoud M, Raab-Traub N. EBV strain variation: geographical distribution and relation to disease state. Virology. 1992;190(1):168-75.
16. Khanim F, Yao QY, Niedobitek G, Sihota S, Rickinson AB, Young LS. Analysis of Epstein-Barr virus gene polymorphisms in normal donors and in virus-associated tumors from different geographic locations. Blood. 1996;88(9):3491-501.
17. Habeshaw G, Yao QY, Bell AI, Morton D, Rickinson AB. Epstein-barr virus nuclear antigen 1 sequences in endemic and sporadic Burkitt's lymphoma reflect virus strains prevalent in different geographic areas. J Virol. 1999;73(2):965-75.
18. Bornkamm GW, Delius H, Zimber U, Hudewentz J, Epstein MA. Comparison of Epstein-Barr virus strains of different origin by analysis of the viral DNAs. J Virol. 1980;35(3):603-18.
19. Shannon-Lowe CD, Neuhierl B, Baldwin G, Rickinson AB, Delecluse HJ. Resting B cells as a transfer vehicle for Epstein-Barr virus infection of epithelial cells. Proc Natl Acad Sci U S A. 2006;103(18):7065-70.

20. Chesnokova LS, Hutt-Fletcher LM. Fusion of Epstein-Barr virus with epithelial cells can be triggered by alphavbeta5 in addition to alphavbeta6 and alphavbeta8, and integrin binding triggers a conformational change in glycoproteins gHgL. J Virol. 2011;85(24):13214-23.
21. Isobe Y, Sugimoto K, Yang L, Tamayose K, Egashira M, Kaneko T, et al. Epstein-Barr virus infection of human natural killer cell lines and peripheral blood natural killer cells. Cancer Res. 2004;64(6):2167-74.
22. Coleman CB, Wohlford EM, Smith NA, King CA, Ritchie JA, Baresel PC, et al. Epstein-Barr virus type 2 latently infects T cells, inducing an atypical activation characterized by expression of lymphotactic cytokines. J Virol. 2015;89(4):2301-12.
23. Kasahara Y, Yachie A, Takei K, Kanegane C, Okada K, Ohta K, et al. Differential cellular targets of Epstein-Barr virus (EBV) infection between acute EBV-associated hemophagocytic lymphohistiocytosis and chronic active EBV infection. Blood. 2001;98(6):1882-8.
24. Anagnostopoulos I, Hummel M, Kreschel C, Stein H. Morphology, immunophenotype, and distribution of latently and/or productively Epstein-Barr virus-infected cells in acute infectious mononucleosis: implications for the interindividual infection route of Epstein-Barr virus. Blood. 1995;85(3):744-50.
25. Hudnall SD, Ge Y, Wei L, Yang NP, Wang HQ, Chen T. Distribution and phenotype of Epstein-Barr virus-infected cells in human pharyngeal tonsils. Mod Pathol. 2005;18(4):519-27.
26. Trempat P, Tabiasco J, Andre P, Faumont N, Meggetto F, Delsol G, et al. Evidence for Early Infection of Nonneoplastic Natural Killer Cells by Epstein-Barr Virus. J Virol. 2002;76(21):11139-42.
27. Thomas R, Macsween KF, McAulay K, Clutterbuck D, Anderson R, Reid S, et al. Evidence of shared Epstein-Barr viral isolates between sexual partners, and low level EBV in genital secretions. J Med Virol. 2006;78(9):1204-9.
28. Karajannis MA, Hummel M, Anagnostopoulos I, Stein H. Strict lymphotropism of Epstein-Barr virus during acute infectious mononucleosis in nonimmunocompromised individuals. Blood. 1997;89(8):2856-62.
29. Lemon SM, Hutt LM, Shaw JE, Li JL, Pagano JS. Replication of EBV in epithelial cells during infectious mononucleosis. Nature. 1977;268(5617):268-70.
30. Thorley-Lawson DA, Hawkins JB, Tracy SI, Shapiro M. The pathogenesis of Epstein-Barr virus persistent infection. Curr Opin Virol. 2013;3(3):227-32.
31. Chaganti S, Bell AI, Pastor NB, Milner AE, Drayson M, Gordon J, et al. Epstein-Barr virus infection in vitro can rescue germinal center B cells with inactivated immunoglobulin genes. Blood. 2005;106(13):4249-52.
32. Hochberg D, Middeldorp JM, Catalina M, Sullivan JL, Luzuriaga K, Thorley-Lawson DA. Demonstration of the Burkitt's lymphoma Epstein-Barr virus phenotype in dividing latently infected memory cells in vivo. Proc Natl Acad Sci U S A. 2004;101(1):239-44.
33. Chaganti S, Heath EM, Bergler W, Kuo M, Buettner M, Niedobitek G, et al. Epstein-Barr virus colonization of tonsillar and peripheral blood B-cell subsets in primary infection and persistence. Blood. 2009;113(25):6372-81.
34. Chaganti S, Ma CS, Bell AI, Croom-Carter D, Hislop AD, Tangye SG, et al. Epstein-Barr virus persistence in the absence of conventional memory B cells: IgM+IgD+CD27+ B cells harbor the virus in X-linked lymphoproliferative disease patients. Blood. 2008;112(3):672-9.
35. Laichalk LL, Thorley-Lawson DA. Terminal differentiation into plasma cells initiates the replicative cycle of Epstein-Barr virus in vivo. J Virol. 2005;79(2):1296-307.

36. Frangou P, Buettner M, Niedobitek G. Epstein-Barr virus (EBV) infection in epithelial cells in vivo: rare detection of EBV replication in tongue mucosa but not in salivary glands. J Infect Dis. 2005;191(2):238-42.
37. Alfieri C, Birkenbach M, Kieff E. Early events in Epstein-Barr virus infection of human B lymphocytes. Virology. 1991;181(2):595-608.
38. Tierney RJ, Shannon-Lowe CD, Fitzsimmons L, Bell AI, Rowe M. Unexpected patterns of Epstein-Barr virus transcription revealed by a high throughput PCR array for absolute quantification of viral mRNA. Virology. 2015;474:117-30.
39. Abbot SD, Rowe M, Cadwallader K, Ricksten A, Gordon J, Wang F, et al. Epstein-Barr virus nuclear antigen 2 induces expression of the virus-encoded latent membrane protein. J Virol. 1990;64(5):2126-34.
40. Zimber-Strobl U, Suentzenich KO, Laux G, Eick D, Cordier M, Calender A, et al. Epstein-Barr virus nuclear antigen 2 activates transcription of the terminal protein gene. J Virol. 1991;65(1):415-23.
41. Rowe M, Lear AL, Croom-Carter D, Davies AH, Rickinson AB. Three pathways of Epstein-Barr virus gene activation from EBNA1-positive latency in B lymphocytes. J Virol. 1992;66(1):122-31.
42. Kaye KM, Izumi KM, Kieff E. Epstein-Barr virus latent membrane protein 1 is essential for B-lymphocyte growth transformation. Proc Natl Acad Sci U S A. 1993;90(19):9150-4.
43. Walls EV, Doyle MG, Patel KK, Allday MJ, Catovsky D, Crawford DH. Activation and immortalization of leukaemic B cells by Epstein-Barr virus. Int J Cancer. 1989;44(5):846-53.
44. Cohen JI, Wang F, Mannick J, Kieff E. Epstein-Barr virus nuclear protein 2 is a key determinant of lymphocyte transformation. Proc Natl Acad Sci U S A. 1989;86(23):9558-62.
45. Tomkinson B, Robertson E, Kieff E. Epstein-Barr virus nuclear proteins EBNA-3A and EBNA-3C are essential for B-lymphocyte growth transformation. J Virol. 1993;67(4):2014-25.
46. Tierney RJ, Nagra J, Rowe M, Bell AI, Rickinson AB. The Epstein-Barr virus BamHI C promoter is not essential for B cell immortalization in vitro, but it greatly enhances B cell growth transformation. J Virol. 2015;89(5):2483-93.
47. Tierney R, Nagra J, Hutchings I, Shannon-Lowe C, Altmann M, Hammerschmidt W, et al. Epstein-Barr virus exploits BSAP/Pax5 to achieve the B-cell specificity of its growth-transforming program. J Virol. 2007;81(18):10092-100.
48. Nonkwelo C, Skinner J, Bell A, Rickinson A, Sample J. Transcription start sites downstream of the Epstein-Barr virus (EBV) Fp promoter in early-passage Burkitt lymphoma cells define a fourth promoter for expression of the EBV EBNA-1 protein. J Virol. 1996;70(1):623-7.
49. Schaefer BC, Woisetschlaeger M, Strominger JL, Speck SH. Exclusive expression of Epstein-Barr virus nuclear antigen 1 in Burkitt lymphoma arises from a third promoter, distinct from the promoters used in latently infected lymphocytes. Proc Natl Acad Sci U S A. 1991;88(15):6550-4.
50. Bell AI, Groves K, Kelly GL, Croom-Carter D, Hui E, Chan AT, et al. Analysis of Epstein-Barr virus latent gene expression in endemic Burkitt's lymphoma and nasopharyngeal carcinoma tumour cells by using quantitative real-time PCR assays. J Gen Virol. 2006;87(Pt 10):2885-90.
51. Kanemitsu N, Isobe Y, Masuda A, Momose S, Higashi M, Tamaru J, et al. Expression of Epstein-Barr virus-encoded proteins in extranodal NK/T-cell Lymphoma, nasal type (ENKL): differences in biologic and clinical behaviors of LMP1-positive and -negative ENKL. Clin Cancer Res. 2012;18(8):2164-72.
52. Chiang AK, Tao Q, Srivastava G, Ho FC. Nasal NK- and T-cell lymphomas share the same type of Epstein-Barr virus latency as nasopharyngeal carcinoma and Hodgkin's disease. Int J Cancer. 1996;68(3):285-90.
53. Miyashita EM, Yang B, Lam KM, Crawford DH, Thorley-Lawson DA. A novel form of Epstein-Barr virus latency in normal B cells in vivo. Cell. 1995;80(4):593-601.

54. Young L, Alfieri C, Hennessy K, Evans H, O'Hara C, Anderson KC, et al. Expression of Epstein-Barr virus transformation-associated genes in tissues of patients with EBV lymphoproliferative disease. N Engl J Med. 1989;321(16):1080-5.
55. Kurth J, Spieker T, Wustrow J, Strickler GJ, Hansmann LM, Rajewsky K, et al. EBV-infected B cells in infectious mononucleosis: viral strategies for spreading in the B cell compartment and establishing latency. Immunity. 2000;13(4):485-95.
56. Parker A, Bowles K, Bradley JA, Emery V, Featherstone C, Gupte G, et al. Management of post-transplant lymphoproliferative disorder in adult solid organ transplant recipients - BCSH and BTS Guidelines. Br J Haematol. 2010;149(5):693-705.
57. Harabuchi Y, Imai S, Wakashima J, Hirao M, Kataura A, Osato T, et al. Nasal T-cell lymphoma causally associated with Epstein-Barr virus: clinicopathologic, phenotypic, and genotypic studies. Cancer. 1996;77(10):2137-49.
58. Noguchi T, Ikeda K, Yamamoto K, Yoshida I, Ashiba A, Tsuchiyama J, et al. Antisense oligodeoxynucleotides to latent membrane protein 1 induce growth inhibition, apoptosis and Bcl-2 suppression in Epstein-Barr virus (EBV)-transformed B-lymphoblastoid cells, but not in EBV-positive natural killer cell lymphoma cells. British Journal of Haematology. 2001;114(1):84-92.
59. Leight ER, Sugden B. EBNA-1: a protein pivotal to latent infection by Epstein-Barr virus. Reviews in medical virology. 2000;10(2):83-100.
60. Levitskaya J, Sharipo A, Leonchiks A, Ciechanover A, Masucci MG. Inhibition of ubiquitin/proteasome-dependent protein degradation by the Gly-Ala repeat domain of the Epstein-Barr virus nuclear antigen 1. Proc Natl Acad Sci U S A. 1997;94(23):12616-21.
61. Levitskaya J, Coram M, Levitsky V, Imreh S, Steigerwald-Mullen PM, Klein G, et al. Inhibition of antigen processing by the internal repeat region of the Epstein-Barr virus nuclear antigen-1. Nature. 1995;375(6533):685-8.
62. Kennedy G, Komano J, Sugden B. Epstein-Barr virus provides a survival factor to Burkitt's lymphomas. Proc Natl Acad Sci U S A. 2003;100(24):14269-74.
63. Gruhne B, Sompallae R, Marescotti D, Kamranvar SA, Gastaldello S, Masucci MG. The Epstein–Barr virus nuclear antigen-1 promotes genomic instability via induction of reactive oxygen species. Proceedings of the National Academy of Sciences. 2009;106(7):2313-8.
64. Zimber-Strobl U, Kremmer E, Grasser F, Marschall G, Laux G, Bornkamm GW. The Epstein-Barr virus nuclear antigen 2 interacts with an EBNA2 responsive cis-element of the terminal protein 1 gene promoter. EMBO J. 1993;12(1):167-75.
65. Schlager S, Speck SH, Woisetschlager M. Transcription of the Epstein-Barr virus nuclear antigen 1 (EBNA1) gene occurs before induction of the BCR2 (Cp) EBNA gene promoter during the initial stages of infection in B cells. J Virol. 1996;70(6):3561-70.
66. Gordon J, Walker L, Guy G, Brown G, Rowe M, Rickinson A. Control of human B-lymphocyte replication. II. Transforming Epstein-Barr virus exploits three distinct viral signals to undermine three separate control points in B-cell growth. Immunology. 1986;58(4):591-5.
67. Wang F, Gregory CD, Rowe M, Rickinson AB, Wang D, Birkenbach M, et al. Epstein-Barr virus nuclear antigen 2 specifically induces expression of the B-cell activation antigen CD23. Proc Natl Acad Sci U S A. 1987;84(10):3452-6.
68. Harada S, Kieff E. Epstein-Barr virus nuclear protein LP stimulates EBNA-2 acidic domain-mediated transcriptional activation. J Virol. 1997;71(9):6611-8.
69. Murray RJ, Kurilla MG, Brooks JM, Thomas WA, Rowe M, Kieff E, et al. Identification of target antigens for the human cytotoxic T cell response to Epstein-Barr virus (EBV): implications for the immune control of EBV-positive malignancies. J Exp Med. 1992;176(1):157-68.

70. Tamaki H, Beaulieu BL, Somasundaran M, Sullivan JL. Major histocompatibility complex class I-restricted cytotoxic T lymphocyte responses to Epstein-Barr virus in children. J Infect Dis. 1995;172(3):739-46.
71. White RE, Groves IJ, Turro E, Yee J, Kremmer E, Allday MJ. Extensive co-operation between the Epstein-Barr virus EBNA3 proteins in the manipulation of host gene expression and epigenetic chromatin modification. PLoS One. 2010;5(11):e13979.
72. White RE, Ramer PC, Naresh KN, Meixlsperger S, Pinaud L, Rooney C, et al. EBNA3B-deficient EBV promotes B cell lymphomagenesis in humanized mice and is found in human tumors. J Clin Invest. 2012;122(4):1487-502.
73. Wang D, Liebowitz D, Kieff E. An EBV membrane protein expressed in immortalized lymphocytes transforms established rodent cells. Cell. 1985;43(3 Pt 2):831-40.
74. Kulwichit W, Edwards RH, Davenport EM, Baskar JF, Godfrey V, Raab-Traub N. Expression of the Epstein-Barr virus latent membrane protein 1 induces B cell lymphoma in transgenic mice. Proc Natl Acad Sci U S A. 1998;95(20):11963-8.
75. Dawson CW, Rickinson AB, Young LS. Epstein-Barr virus latent membrane protein inhibits human epithelial cell differentiation. Nature. 1990;344(6268):777-80.
76. Wang F, Gregory C, Sample C, Rowe M, Liebowitz D, Murray R, et al. Epstein-Barr virus latent membrane protein (LMP1) and nuclear proteins 2 and 3C are effectors of phenotypic changes in B lymphocytes: EBNA-2 and LMP1 cooperatively induce CD23. J Virol. 1990;64(5):2309-18.
77. Wang D, Liebowitz D, Wang F, Gregory C, Rickinson A, Larson R, et al. Epstein-Barr virus latent infection membrane protein alters the human B-lymphocyte phenotype: deletion of the amino terminus abolishes activity. J Virol. 1988;62(11):4173-84.
78. Peng M, Lundgren E. Transient expression of the Epstein-Barr virus LMP1 gene in human primary B cells induces cellular activation and DNA synthesis. Oncogene. 1992;7(9):1775-82.
79. Huen DS, Henderson SA, Croom-Carter D, Rowe M. The Epstein-Barr virus latent membrane protein-1 (LMP1) mediates activation of NF-kappa B and cell surface phenotype via two effector regions in its carboxy-terminal cytoplasmic domain. Oncogene. 1995;10(3):549-60.
80. Eliopoulos AG, Young LS. Activation of the cJun N-terminal kinase (JNK) pathway by the Epstein-Barr virus-encoded latent membrane protein 1 (LMP1). Oncogene. 1998;16(13):1731-42.
81. Henderson S, Rowe M, Gregory C, Wang F, Kieff E, Rickinson A. Induction of *bcl-2* expression by Epstein-Barr virus Latent Membrane Protein-1 protects infected B cells from programmed cell death. Cell. 1991;65:1107-15.
82. Fukuda M, Longnecker R. Latent membrane protein 2A inhibits transforming growth factor-beta 1-induced apoptosis through the phosphatidylinositol 3-kinase/Akt pathway. Journal of Virology. 2004;78(4):1697-705.
83. Fennewald S, van Santen V, Kieff E. Nucleotide sequence of an mRNA transcribed in latent growth-transforming virus infection indicates that it may encode a membrane protein. J Virol. 1984;51(2):411-9.
84. Eliopoulos AG, Rickinson AB. Epstein-Barr virus: LMP1 masquerades as an active receptor. Curr Biol. 1998;8(6):R196-8.
85. Hennessy K, Fennewald S, Hummel M, Cole T, Kieff E. A membrane protein encoded by Epstein-Barr virus in latent growth-transforming infection. Proc Natl Acad Sci U S A. 1984;81(22):7207-11.
86. Izumi KM, Kaye KM, Kieff ED. Epstein-Barr virus recombinant molecular genetic analysis of the LMP1 amino-terminal cytoplasmic domain reveals a probable structural role, with no component essential for primary B-lymphocyte growth transformation. J Virol. 1994;68(7):4369-76.

87. Kaye KM, Izumi KM, Mosialos G, Kieff E. The Epstein-Barr virus LMP1 cytoplasmic carboxy terminus is essential for B-lymphocyte transformation; fibroblast cocultivation complements a critical function within the terminal 155 residues. J Virol. 1995;69(2):675-83.
88. Eliopoulos AG, Young LS. LMP1 structure and signal transduction. Seminars in Cancer Biology. 2001;11(6):435-44.
89. Cahir-McFarland ED, Davidson DM, Schauer SL, Duong J, Kieff E. NF-kappa B inhibition causes spontaneous apoptosis in Epstein-Barr virus-transformed lymphoblastoid cells. Proc Natl Acad Sci U S A. 2000;97(11):6055-60.
90. Edwards RH, Marquitz AR, Raab-Traub N. Changes in Expression Induced by Epstein-Barr Virus LMP1-CTAR1: Potential Role of bcl3. MBio. 2015;6(2).
91. Eliopoulos AG, Gallagher NJ, Blake SM, Dawson CW, Young LS. Activation of the p38 mitogen-activated protein kinase pathway by Epstein-Barr virus-encoded latent membrane protein 1 coregulates interleukin-6 and interleukin-8 production. J Biol Chem. 1999;274(23):16085-96.
92. Seavey MM, Dobrzanski P. The many faces of Janus kinase. Biochem Pharmacol. 2012;83(9):1136-45.
93. Higuchi M, Kieff E, Izumi KM. The Epstein-Barr virus latent membrane protein 1 putative Janus kinase 3 (JAK3) binding domain does not mediate JAK3 association or activation in B-lymphoma or lymphoblastoid cell lines. J Virol. 2002;76(1):455-9.
94. Au WC, Moore PA, LaFleur DW, Tombal B, Pitha PM. Characterization of the interferon regulatory factor-7 and its potential role in the transcription activation of interferon A genes. J Biol Chem. 1998;273(44):29210-7.
95. Ning S, Hahn AM, Huye LE, Pagano JS. Interferon regulatory factor 7 regulates expression of Epstein-Barr virus latent membrane protein 1: a regulatory circuit. J Virol. 2003;77(17):9359-68.
96. Zhang L, Zhang J, Lambert Q, Der CJ, Del Valle L, Miklossy J, et al. Interferon regulatory factor 7 is associated with Epstein-Barr virus-transformed central nervous system lymphoma and has oncogenic properties. J Virol. 2004;78(23):12987-95.
97. Kutz H, Reisbach G, Schultheiss U, Kieser A. The c-Jun N-terminal kinase pathway is critical for cell transformation by the latent membrane protein 1 of Epstein-Barr virus. Virology. 2008;371(2):246-56.
98. Sample J, Liebowitz D, Kieff E. Two related Epstein-Barr virus membrane proteins are encoded by separate genes. J Virol. 1989;63(2):933-7.
99. Laux G, Perricaudet M, Farrell PJ. A spliced Epstein-Barr virus gene expressed in immortalized lymphocytes is created by circularization of the linear viral genome. Embo j. 1988;7(3):769-74.
100. Brielmeier M, Mautner J, Laux G, Hammerschmidt W. The latent membrane protein 2 gene of Epstein-Barr virus is important for efficient B cell immortalization. J Gen Virol. 1996;77 (Pt 11):2807-18.
101. Caldwell RG, Wilson JB, Anderson SJ, Longnecker R. Epstein-Barr virus LMP2A drives B cell development and survival in the absence of normal B cell receptor signals. Immunity. 1998;9(3):405-11.
102. Portis T, Longnecker R. Epstein-Barr virus (EBV) LMP2A mediates B-lymphocyte survival through constitutive activation of the Ras/PI3K/Akt pathway. Oncogene. 2004;23(53):8619-28.
103. Mancao C, Hammerschmidt W. Epstein-Barr virus latent membrane protein 2A is a B-cell receptor mimic and essential for B-cell survival. Blood. 2007;110(10):3715-21.
104. Wasil LR, Tomaszewski MJ, Hoji A, Rowe DT. The effect of Epstein-Barr virus Latent Membrane Protein 2 expression on the kinetics of early B cell infection. PLoS One. 2013;8(1):e54010.
105. Scholle F, Bendt KM, Raab-Traub N. Epstein-Barr virus LMP2A transforms epithelial cells, inhibits cell differentiation, and activates Akt. J Virol. 2000;74(22):10681-9.
106. Pang MF, Lin KW, Peh SC. The signaling pathways of Epstein-Barr virus-encoded latent membrane protein 2A (LMP2A) in latency and cancer. Cell Mol Biol Lett. 2009;14(2):222-47.

107. Miller CL, Longnecker R, Kieff E. Epstein-Barr virus latent membrane protein 2A blocks calcium mobilization in B lymphocytes. J Virol. 1993;67(6):3087-94.
108. Rechsteiner MP, Berger C, Zauner L, Sigrist JA, Weber M, Longnecker R, et al. Latent membrane protein 2B regulates susceptibility to induction of lytic Epstein-Barr virus infection. J Virol. 2008;82(4):1739-47.
109. Rovedo M, Longnecker R. Epstein-barr virus latent membrane protein 2B (LMP2B) modulates LMP2A activity. J Virol. 2007;81(1):84-94.
110. Allen MD, Young LS, Dawson CW. The Epstein-Barr virus-encoded LMP2A and LMP2B proteins promote epithelial cell spreading and motility. J Virol. 2005;79(3):1789-802.
111. Pegtel DM, Subramanian A, Sheen TS, Tsai CH, Golub TR, Thorley-Lawson DA. Epstein-Barr-virus-encoded LMP2A induces primary epithelial cell migration and invasion: possible role in nasopharyngeal carcinoma metastasis. J Virol. 2005;79(24):15430-42.
112. Shah KM, Stewart SE, Wei W, Woodman CB, O'Neil JD, Dawson CW, et al. The EBV-encoded latent membrane proteins, LMP2A and LMP2B, limit the actions of interferon by targeting interferon receptors for degradation. Oncogene. 2009;28(44):3903-14.
113. Rosa MD, Gottlieb E, Lerner MR, Steitz JA. Striking similarities are exhibited by two small Epstein-Barr virus-encoded ribonucleic acids and the adenovirus-associated ribonucleic acids VAI and VAII. Mol Cell Biol. 1981;1(9):785-96.
114. Nanbo A, Inoue K, Adachi-Takasawa K, Takada K. Epstein-Barr virus RNA confers resistance to interferon-alpha-induced apoptosis in Burkitt's lymphoma. EMBO J. 2002;21(5):954-65.
115. Wu Y, Maruo S, Yajima M, Kanda T, Takada K. Epstein-Barr virus (EBV)-encoded RNA 2 (EBER2) but not EBER1 plays a critical role in EBV-induced B-cell growth transformation. J Virol. 2007;81(20):11236-45.
116. Iwakiri D, Zhou L, Samanta M, Matsumoto M, Ebihara T, Seya T, et al. Epstein-Barr virus (EBV)-encoded small RNA is released from EBV-infected cells and activates signaling from Toll-like receptor 3. J Exp Med. 2009;206(10):2091-9.
117. Kapsogeorgou EK, Abu-Helu RF, Moutsopoulos HM, Manoussakis MN. Salivary gland epithelial cell exosomes: A source of autoantigenic ribonucleoproteins. Arthritis Rheum. 2005;52(5):1517-21.
118. Clarke PA, Sharp NA, Clemens MJ. Expression of genes for the Epstein-Barr virus small RNAs EBER-1 and EBER-2 in Daudi Burkitt's lymphoma cells: effects of interferon treatment. J Gen Virol. 1992;73 (Pt 12):3169-75.
119. Di Leva G, Croce CM. Roles of small RNAs in tumor formation. Trends in Molecular Medicine. 2010;16(6):257-67.
120. Kozomara A, Griffiths-Jones S. miRBase: integrating microRNA annotation and deep-sequencing data. Nucleic Acids Res. 2011;39(Database issue):D152-7.
121. Riley KJ, Rabinowitz GS, Yario TA, Luna JM, Darnell RB, Steitz JA. EBV and human microRNAs co-target oncogenic and apoptotic viral and human genes during latency. EMBO J. 2012;31(9):2207-21.
122. Seto E, Moosmann A, Gromminger S, Walz N, Grundhoff A, Hammerschmidt W. Micro RNAs of Epstein-Barr virus promote cell cycle progression and prevent apoptosis of primary human B cells. PLoS Pathog. 2010;6(8):e1001063.
123. Yang IV, Wade CM, Kang HM, Alper S, Rutledge H, Lackford B, et al. Identification of novel genes that mediate innate immunity using inbred mice. Genetics. 2009;183(4):1535-44.
124. Lo AK, To KF, Lo KW, Lung RW, Hui JW, Liao G, et al. Modulation of LMP1 protein expression by EBV-encoded microRNAs. Proc Natl Acad Sci U S A. 2007;104(41):16164-9.
125. Lung RW, Tong JH, Sung YM, Leung PS, Ng DC, Chau SL, et al. Modulation of LMP2A expression by a newly identified Epstein-Barr virus-encoded microRNA miR-BART22. Neoplasia. 2009;11(11):1174-84.

126. Iizasa H, Wulff BE, Alla NR, Maragkakis M, Megraw M, Hatzigeorgiou A, et al. Editing of Epstein-Barr virus-encoded BART6 microRNAs controls their dicer targeting and consequently affects viral latency. J Biol Chem. 2010;285(43):33358-70.
127. Lo AKF, Dawson CW, Jin D-Y, Lo K-W. The pathological roles of BART miRNAs in nasopharyngeal carcinoma. The Journal of Pathology. 2012:n/a-n/a.
128. Henderson S, Huen D, Rowe M, Dawson C, Johnson G, Rickinson A. Epstein-Barr virus-coded BHRF1 protein, a viral homologue of Bcl-2, protects human B cells from programmed cell death. Proc Natl Acad Sci U S A. 1993;90(18):8479-83.
129. Marshall WL, Yim C, Gustafson E, Graf T, Sage DR, Hanify K, et al. Epstein-Barr virus encodes a novel homolog of the bcl-2 oncogene that inhibits apoptosis and associates with Bax and Bak. J Virol. 1999;73(6):5181-5.
130. Bellows DS, Howell M, Pearson C, Hazlewood SA, Hardwick JM. Epstein-Barr virus BALF1 is a BCL-2-like antagonist of the herpesvirus antiapoptotic BCL-2 proteins. J Virol. 2002;76(5):2469-79.
131. Altmann M, Hammerschmidt W. Epstein-Barr virus provides a new paradigm: a requirement for the immediate inhibition of apoptosis. PLoS Biol. 2005;3(12):e404.
132. Kelly GL, Long HM, Stylianou J, Thomas WA, Leese A, Bell AI, et al. An Epstein-Barr virus anti-apoptotic protein constitutively expressed in transformed cells and implicated in burkitt lymphomagenesis: the Wp/BHRF1 link. PLoS Pathog. 2009;5(3):e1000341.
133. McAulay KA, Higgins CD, Macsween KF, Lake A, Jarrett RF, Robertson FL, et al. HLA class I polymorphisms are associated with development of infectious mononucleosis upon primary EBV infection. J Clin Invest. 2007;117(10):3042-8.
134. Crawford DH, Macsween KF, Higgins CD, Thomas R, McAulay K, Williams H, et al. A cohort study among university students: identification of risk factors for Epstein-Barr virus seroconversion and infectious mononucleosis. Clin Infect Dis. 2006;43(3):276-82.
135. Crawford DH, Swerdlow AJ, Higgins C, McAulay K, Harrison N, Williams H, et al. Sexual history and Epstein-Barr virus infection. J Infect Dis. 2002;186(6):731-6.
136. Infectious mononucleosis and its relationship to EB virus antibody. A joint investigation by university health physicians and P.H.L.S. laboratories. Br Med J. 1971;4(5788):643-6.
137. Henle G, Henle W, Diehl V. Relation of Burkitt's tumor-associated herpes-type virus to infectious mononucleosis. Proc Natl Acad Sci U S A. 1968;59(1):94-101.
138. Hallee TJ, Evans AS, Niederman JC, Brooks CM, Voegtly j H. Infectious mononucleosis at the United States Military Academy. A prospective study of a single class over four years. Yale J Biol Med. 1974;47(3):182-95.
139. Hjalgrim H, Askling J, Rostgaard K, Hamilton-Dutoit S, Frisch M, Zhang JS, et al. Characteristics of Hodgkin's lymphoma after infectious mononucleosis. N Engl J Med. 2003;349(14):1324-32.
140. Gustavsen MW, Page CM, Moen SM, Bjolgerud A, Berg-Hansen P, Nygaard GO, et al. Environmental exposures and the risk of multiple sclerosis investigated in a Norwegian case-control study. BMC Neurol. 2014;14:196.
141. Hjalgrim H, Rostgaard K, Johnson PC, Lake A, Shield L, Little AM, et al. HLA-A alleles and infectious mononucleosis suggest a critical role for cytotoxic T-cell response in EBV-related Hodgkin lymphoma. Proc Natl Acad Sci U S A. 2010;107(14):6400-5.
142. Niens M, van den Berg A, Diepstra A, Nolte IM, van der Steege G, Gallagher A, et al. The human leukocyte antigen class I region is associated with EBV-positive Hodgkin's lymphoma: HLA-A and HLA complex group 9 are putative candidate genes. Cancer Epidemiol Biomarkers Prev. 2006;15(11):2280-4.
143. Filipovich AH, Zhang K, Snow AL, Marsh RA. X-linked lymphoproliferative syndromes: brothers or distant cousins? Blood. 2010;116(18):3398-408.

144. Booth K, Burkitt DP, Bassett DJ, Cooke RA, Biddulph J. Burkitt lymphoma in Papua, New Guinea. Br J Cancer. 1967;21(4):657-64.
145. Stewart A. Burkitt lymphoma and malaria. Lancet. 1970;2(7667):300-1.
146. Dalldorf G, Linsell CA, Barnhart FE, Martyn R. AN EPIDEMIOLOGIC APPROACH TO THE LYMPHOMAS OF AFRICAN CHILDREN AND BURKITT'S SACROMA OF THE JAWS. Perspect Biol Med. 1964;7:435-49.
147. Kafuko GW, Burkitt DP. Burkitt's lymphoma and malaria. Int J Cancer. 1970;6(1):1-9.
148. Rainey JJ, Mwanda WO, Wairiumu P, Moormann AM, Wilson ML, Rochford R. Spatial distribution of Burkitt's lymphoma in Kenya and association with malaria risk. Trop Med Int Health. 2007;12(8):936-43.
149. Geser A, Brubaker G, Draper CC. Effect of a malaria suppression program on the incidence of African Burkitt's lymphoma. Am J Epidemiol. 1989;129(4):740-52.
150. Philip T, Lenoir GM, Bryon PA, Gerard-Marchant R, Souillet G, Philippe N, et al. Burkitt-type lymphoma in France among non-Hodgkin malignant lymphomas in Caucasian children. Br J Cancer. 1982;45(5):670-8.
151. Levine PH, Kamaraju LS, Connelly RR, Berard CW, Dorfman RF, Magrath I, et al. The American Burkitt's Lymphoma Registry: eight years' experience. Cancer. 1982;49(5):1016-22.
152. Rickinson AB. Co-infections, inflammation and oncogenesis: future directions for EBV research. Semin Cancer Biol. 2014;26:99-115.
153. Bornkamm GW. Epstein-Barr virus and the pathogenesis of Burkitt's lymphoma: more questions than answers. Int J Cancer. 2009;124(8):1745-55.
154. Polack A, Hortnagel K, Pajic A, Christoph B, Baier B, Falk M, et al. c-myc activation renders proliferation of Epstein-Barr virus (EBV)-transformed cells independent of EBV nuclear antigen 2 and latent membrane protein 1. Proc Natl Acad Sci U S A. 1996;93(19):10411-6.
155. Staege MS, Lee SP, Frisan T, Mautner J, Scholz S, Pajic A, et al. MYC overexpression imposes a nonimmunogenic phenotype on Epstein-Barr virus-infected B cells. Proc Natl Acad Sci U S A. 2002;99(7):4550-5.
156. Kelly G, Bell A, Rickinson A. Epstein-Barr virus-associated Burkitt lymphomagenesis selects for downregulation of the nuclear antigen EBNA2. Nat Med. 2002;8(10):1098-104.
157. Kelly GL, Milner AE, Baldwin GS, Bell AI, Rickinson AB. Three restricted forms of Epstein-Barr virus latency counteracting apoptosis in c-myc-expressing Burkitt lymphoma cells. Proc Natl Acad Sci U S A. 2006;103(40):14935-40.
158. Shimizu N, Tanabe-Tochikura A, Kuroiwa Y, Takada K. Isolation of Epstein-Barr virus (EBV)-negative cell clones from the EBV-positive Burkitt's lymphoma (BL) line Akata: malignant phenotypes of BL cells are dependent on EBV. J Virol. 1994;68(9):6069-73.
159. Komano J, Sugiura M, Takada K. Epstein-Barr virus contributes to the malignant phenotype and to apoptosis resistance in Burkitt's lymphoma cell line Akata. J Virol. 1998;72(11):9150-6.
160. Kuppers R, Rajewsky K, Zhao M, Simons G, Laumann R, Fischer R, et al. Hodgkin disease: Hodgkin and Reed-Sternberg cells picked from histological sections show clonal immunoglobulin gene rearrangements and appear to be derived from B cells at various stages of development. Proc Natl Acad Sci U S A. 1994;91(23):10962-6.
161. Grufferman S, Delzell E. Epidemiology of Hodgkin's disease. Epidemiol Rev. 1984;6:76-106.
162. Harris NL, Jaffe ES, Diebold J, Flandrin G, Muller-Hermelink HK, Vardiman J, et al. World Health Organization classification of neoplastic diseases of the hematopoietic and lymphoid tissues: report of the Clinical Advisory Committee meeting-Airlie House, Virginia, November 1997. J Clin Oncol. 1999;17(12):3835-49.

163. Advani R, Hoppe R. How I treat nodular lymphocyte predominant Hodgkin lymphoma. 2013.
164. Huppmann AR, Nicolae A, Slack GW, Pittaluga S, Davies-Hill T, Ferry JA, et al. EBV may be expressed in the LP cells of nodular lymphocyte-predominant Hodgkin lymphoma (NLPHL) in both children and adults. Am J Surg Pathol. 2014;38(3):316-24.
165. Weiss LM, Strickler JG, Warnke RA, Purtilo DT, Sklar J. Epstein-Barr viral DNA in tissues of Hodgkin's disease. Am J Pathol. 1987;129(1):86-91.
166. Glaser SL, Lin RJ, Stewart SL, Ambinder RF, Jarrett RF, Brousset P, et al. Epstein-Barr virus-associated Hodgkin's disease: epidemiologic characteristics in international data. Int J Cancer. 1997;70(4):375-82.
167. Alexander FE, Lawrence DJ, Freeland J, Krajewski AS, Angus B, Taylor GM, et al. An epidemiologic study of index and family infectious mononucleosis and adult Hodgkin's disease (HD): evidence for a specific association with EBV+ve HD in young adults. Int J Cancer. 2003;107(2):298-302.
168. Jarrett RF. Viruses and Hodgkin's lymphoma. Annals of Oncology. 2002;13 (supplement 1):23-9.
169. Brauninger A, Schmitz R, Bechtel D, Renne C, Hansmann ML, Kuppers R. Molecular biology of Hodgkin's and Reed/Sternberg cells in Hodgkin's lymphoma. Int J Cancer. 2006;118(8):1853-61.
170. Penn I, Hammond W, Brettschneider L, Starzl TE. Malignant lymphomas in transplantation patients. Transplant Proc. 1969;1(1):106-12.
171. Gottschalk S, Rooney CM, Heslop HE. Post-transplant lymphoproliferative disorders. Annu Rev Med. 2005;56:29-44.
172. Fox CP, Burns D, Parker AN, Peggs KS, Harvey CM, Natarajan S, et al. EBV-associated post-transplant lymphoproliferative disorder following in vivo T-cell-depleted allogeneic transplantation: clinical features, viral load correlates and prognostic factors in the rituximab era. Bone Marrow Transplant. 2014;49(2):280-6.
173. Curtis RE, Travis LB, Rowlings PA, Socie G, Kingma DW, Banks PM, et al. Risk of lymphoproliferative disorders after bone marrow transplantation: a multi-institutional study. Blood. 1999;94(7):2208-16.
174. Swerdlow S. H. CE, Harris N. L., Jaffe E. S., Pileri S.A., Stein H., Thiele J., Vardiman J. W. WHO Classification of Tumours of Haematopoietic and Lymphoid Tissues. Lyon: IARC; 2008.
175. Rasche L, Kapp M, Einsele H, Mielke S. EBV-induced post transplant lymphoproliferative disorders: a persisting challenge in allogeneic hematopoetic SCT. Bone Marrow Transplant. 2014;49(2):163-7.
176. Heslop HE. How I treat EBV lymphoproliferation. 2009.
177. Kroll J, Li S, Levi M, Weinberg A. Lytic and latent EBV gene expression in transplant recipients with and without post-transplant lymphoproliferative disorder. J Clin Virol. 2011;52(3):231-5.
178. Timms JM, Bell A, Flavell JR, Murray PG, Rickinson AB, Traverse-Glehen A, et al. Target cells of Epstein-Barr-virus (EBV)-positive post-transplant lymphoproliferative disease: similarities to EBV-positive Hodgkin's lymphoma. Lancet. 2003;361(9353):217-23.
179. Haque T, Wilkie GM, Jones MM, Higgins CD, Urquhart G, Wingate P, et al. Allogeneic cytotoxic T-cell therapy for EBV-positive posttransplantation lymphoproliferative disease: results of a phase 2 multicenter clinical trial. Blood. 2007;110(4):1123-31.
180. Kimura H. Pathogenesis of chronic active Epstein-Barr virus infection: is this an infectious disease, lymphoproliferative disorder, or immunodeficiency? Rev Med Virol. 2006;16(4):251-61.
181. Virelizier JL, Lenoir G, Griscelli C. Persistent Epstein-Barr virus infection in a child with hypergammaglobulinaemia and immunoblastic proliferation associated with a selective defect in immune interferon secretion. Lancet. 1978;2(8083):231-4.

182. Rickinson AB. Chronic, symptomatic Epstein-Barr virus infections. Immunol Today. 1986;7(1):13-4.
183. Jones JF, Shurin S, Abramowsky C, Tubbs RR, Sciotto CG, Wahl R, et al. T-cell lymphomas containing Epstein-Barr viral DNA in patients with chronic Epstein-Barr virus infections. N Engl J Med. 1988;318(12):733-41.
184. Kikuta H, Taguchi Y, Tomizawa K, Kojima K, Kawamura N, Ishizaka A, et al. Epstein-Barr virus genome-positive T lymphocytes in a boy with chronic active EBV infection associated with Kawasaki-like disease. Nature. 1988;333(6172):455-7.
185. Kawa-Ha K, Ishihara S, Ninomiya T, Yumura-Yagi K, Hara J, Murayama F, et al. CD3-negative lymphoproliferative disease of granular lymphocytes containing Epstein-Barr viral DNA. J Clin Invest. 1989;84(1):51-5.
186. Cohen JI, Jaffe ES, Dale JK, Pittaluga S, Heslop HE, Rooney CM, et al. Characterization and treatment of chronic active Epstein-Barr virus disease: a 28-year experience in the United States. Blood. 2011;117(22):5835-49.
187. Kimura H, Morishima T, Kanegane H, Ohga S, Hoshino Y, Maeda A, et al. Prognostic factors for chronic active Epstein-Barr virus infection. J Infect Dis. 2003;187(4):527-33.
188. Kimura H, Hoshino Y, Kanegane H, Tsuge I, Okamura T, Kawa K, et al. Clinical and virologic characteristics of chronic active Epstein-Barr virus infection. Blood. 2001;98(2):280-6.
189. Kimura H, Hoshino Y, Hara S, Sugaya N, Kawada J-i, Shibata Y, et al. Differences between T Cell-Type and Natural Killer Cell-Type Chronic Active Epstein-Barr Virus Infection. Journal of Infectious Diseases. 2005;191(4):531-9.
190. Scott RB, Robb-Smith AHT. Histiocytic medullary reticulosis. LANCET. 1939;234(6047):194-8.
191. Henter JI, Elinder G, Ost A. Diagnostic guidelines for hemophagocytic lymphohistiocytosis. The FHL Study Group of the Histiocyte Society. Semin Oncol. 1991;18(1):29-33.
192. Janka GE, Schneider EM. Modern management of children with haemophagocytic lymphohistiocytosis. Br J Haematol. 2004;124(1):4-14.
193. Henter JI, Horne A, Arico M, Egeler RM, Filipovich AH, Imashuku S, et al. HLH-2004: Diagnostic and therapeutic guidelines for hemophagocytic lymphohistiocytosis. Pediatr Blood Cancer. 2007;48(2):124-31.
194. Janka GE, Lehmberg K. Hemophagocytic lymphohistiocytosis: pathogenesis and treatment. Hematology Am Soc Hematol Educ Program. 2013;2013:605-11.
195. Stepp SE, Dufourcq-Lagelouse R, Le Deist F, Bhawan S, Certain S, Mathew PA, et al. Perforin gene defects in familial hemophagocytic lymphohistiocytosis. Science. 1999;286(5446):1957-9.
196. Feldmann J, Callebaut I, Raposo G, Certain S, Bacq D, Dumont C, et al. Munc13-4 is essential for cytolytic granules fusion and is mutated in a form of familial hemophagocytic lymphohistiocytosis (FHL3). Cell. 2003;115(4):461-73.
197. zur Stadt U, Schmidt S, Kasper B, Beutel K, Diler AS, Henter JI, et al. Linkage of familial hemophagocytic lymphohistiocytosis (FHL) type-4 to chromosome 6q24 and identification of mutations in syntaxin 11. Hum Mol Genet. 2005;14(6):827-34.
198. zur Stadt U, Rohr J, Seifert W, Koch F, Grieve S, Pagel J, et al. Familial hemophagocytic lymphohistiocytosis type 5 (FHL-5) is caused by mutations in Munc18-2 and impaired binding to syntaxin 11. Am J Hum Genet. 2009;85(4):482-92.
199. Ohadi M, Lalloz MR, Sham P, Zhao J, Dearlove AM, Shiach C, et al. Localization of a gene for familial hemophagocytic lymphohistiocytosis at chromosome 9q21.3-22 by homozygosity mapping. Am J Hum Genet. 1999;64(1):165-71.

200. Barbosa MD, Nguyen QA, Tchernev VT, Ashley JA, Detter JC, Blaydes SM, et al. Identification of the homologous beige and Chediak-Higashi syndrome genes. Nature. 1996;382(6588):262-5.
201. Nagle DL, Karim MA, Woolf EA, Holmgren L, Bork P, Misumi DJ, et al. Identification and mutation analysis of the complete gene for Chediak-Higashi syndrome. Nat Genet. 1996;14(3):307-11.
202. Menasche G, Pastural E, Feldmann J, Certain S, Ersoy F, Dupuis S, et al. Mutations in RAB27A cause Griscelli syndrome associated with haemophagocytic syndrome. Nat Genet. 2000;25(2):173-6.
203. Trottestam H, Horne A, Arico M, Egeler RM, Filipovich AH, Gadner H, et al. Chemoimmunotherapy for hemophagocytic lymphohistiocytosis: long-term results of the HLH-94 treatment protocol. Blood. 2011;118(17):4577-84.
204. My LT, Lien le B, Hsieh WC, Imamura T, Anh TN, Anh PN, et al. Comprehensive analyses and characterization of haemophagocytic lymphohistiocytosis in Vietnamese children. Br J Haematol. 2010;148(2):301-10.
205. Jordan MB, Allen CE, Weitzman S, Filipovich AH, McClain KL. How I treat hemophagocytic lymphohistiocytosis. Blood. 2011;118(15):4041-52.
206. Ay Y, Yildiz B, Unver H, Karapinar DY, Vardar F. Hemophagocytic lymphohistiocytosis associated with H1N1 virus infection and visceral leishmaniasis in a 4.5-month-old infant. Revista da Sociedade Brasileira de Medicina Tropical. 2012;45(3):407-9.
207. Yilmaz S, Oren H, Demircioglu F, Firinci F, Korkmaz A, Irken G. Parvovirus B19: a cause for aplastic crisis and hemophagocytic lymphohistiocytosis. Pediatr Blood Cancer. 2006;47(6):861.
208. Bay A, Bosnak V, Leblebisatan G, Yavuz S, Yilmaz F, Hizli S. Hemophagocytic lymphohistiocytosis in 2 pediatric patients secondary to hepatitis A virus infection. Pediatr Hematol Oncol. 2012;29(3):211-4.
209. Risdall RJ, McKenna RW, Nesbit ME, Krivit W, Balfour HH, Jr., Simmons RL, et al. Virus-associated hemophagocytic syndrome: a benign histiocytic proliferation distinct from malignant histiocytosis. Cancer. 1979;44(3):993-1002.
210. Imashuku S. Treatment of Epstein-Barr virus-related hemophagocytic lymphohistiocytosis (EBV-HLH); update 2010. Journal of pediatric hematology/oncology. 2011;33(1):35-9.
211. Kawaguchi H, Miyashita T, Herbst H, Niedobitek G, Asada M, Tsuchida M, et al. Epstein-Barr virus-infected T lymphocytes in Epstein-Barr virus-associated hemophagocytic syndrome. J Clin Invest. 1993;92(3):1444-50.
212. Kasahara Y, Yachie A. Cell type specific infection of Epstein-Barr virus (EBV) in EBV-associated hemophagocytic lymphohistiocytosis and chronic active EBV infection. Crit Rev Oncol Hematol. 2002;44(3):283-94.
213. Dolezal MV, Kamel OW, van de Rijn M, Cleary ML, Sibley RK, Warnke RA. Virus-associated hemophagocytic syndrome characterized by clonal Epstein-Barr virus genome. Am J Clin Pathol. 1995;103(2):189-94.
214. Fox CP, Shannon-Lowe C, Gothard P, Kishore B, Neilson J, O'Connor N, et al. Epstein-Barr virus-associated hemophagocytic lymphohistiocytosis in adults characterized by high viral genome load within circulating natural killer cells. Clin Infect Dis.51(1):66-9.
215. Lay JD, Tsao CJ, Chen JY, Kadin ME, Su IJ. Upregulation of tumor necrosis factor-alpha gene by Epstein-Barr virus and activation of macrophages in Epstein-Barr virus-infected T cells in the pathogenesis of hemophagocytic syndrome. J Clin Invest. 1997;100(8):1969-79.
216. Lay JD, Chuang SE, Rowe M, Su IJ. Epstein-barr virus latent membrane protein-1 mediates upregulation of tumor necrosis factor-alpha in EBV-infected T cells: implications for the pathogenesis of hemophagocytic syndrome. J Biomed Sci. 2003;10(1):146-55.
217. Chuang HC, Lay JD, Chuang SE, Hsieh WC, Chang Y, Su IJ. Epstein-Barr virus (EBV) latent membrane protein-1 down-regulates tumor necrosis factor-alpha (TNF-alpha) receptor-1 and confers

resistance to TNF-alpha-induced apoptosis in T cells: implication for the progression to T-cell lymphoma in EBV-associated hemophagocytic syndrome. Am J Pathol. 2007;170(5):1607-17.
218. Fox CP, Shannon-Lowe C, Gothard P, Kishore B, Neilson J, O'Connor N, et al. Epstein-Barr virus-associated hemophagocytic lymphohistiocytosis in adults characterized by high viral genome load within circulating natural killer cells. Clin Infect Dis. 2010;51(1):66-9.
219. Kelesidis T, Humphries R, Terashita D, Eshaghian S, Territo MC, Said J, et al. Epstein-Barr virus-associated hemophagocytic lymphohistiocytosis in Los Angeles County. J Med Virol. 2012;84(5):777-85.
220. Sato K, Misawa N, Nie C, Satou Y, Iwakiri D, Matsuoka M, et al. A novel animal model of Epstein-Barr virus-associated hemophagocytic lymphohistiocytosis in humanized mice. Blood. 2011;117(21):5663-73.
221. Yang X, Wada T, Imadome K, Nishida N, Mukai T, Fujiwara M, et al. Characterization of Epstein-Barr virus (EBV)-infected cells in EBV-associated hemophagocytic lymphohistiocytosis in two patients with X-linked lymphoproliferative syndrome type 1 and type 2. Herpesviridae. 2012;3(1):1.
222. McBride P. Photographs of a case of rapid destruction of the nose and face. . Journal of Laryngology and Otology. 1897;12:64-6.
223. Woods R. Observations on malignant granuloma of the nose. British Medical Journal. 1921;2:65.
224. Stewart JP. Progressive lethal granulomatous ulceration of the nose. . Journal of Laryngology. 1933;48:657-701.
225. Harris NL, Jaffe ES, Stein H, Banks PM, Chan JK, Cleary ML, et al. A revised European-American classification of lymphoid neoplasms: a proposal from the International Lymphoma Study Group. Blood. 1994;84(5):1361-92.
226. Ishii Y, Yamanaka N, Ogawa K, Yoshida Y, Takami T, Matsuura A, et al. Nasal T-cell lymphoma as a type of so-called "lethal midline granuloma". Cancer. 1982;50(11):2336-44.
227. Kanavaros P, Lescs MC, Briere J, Divine M, Galateau F, Joab I, et al. Nasal T-cell lymphoma: a clinicopathologic entity associated with peculiar phenotype and with Epstein-Barr virus. Blood. 1993;81(10):2688-95.
228. Suzumiya J, Takeshita M, Kimura N, Kikuchi M, Uchida T, Hisano S, et al. Expression of adult and fetal natural killer cell markers in sinonasal lymphomas. Blood. 1994;83(8):2255-60.
229. Wong KF, Chan JK, Ng CS, Lee KC, Tsang WY, Cheung MM. CD56 (NKH1)-positive hematolymphoid malignancies: an aggressive neoplasm featuring frequent cutaneous/mucosal involvement, cytoplasmic azurophilic granules, and angiocentricity. Hum Pathol. 1992;23(7):798-804.
230. Chan JK, Tsang WY, Ng CS. Clarification of CD3 immunoreactivity in nasal T/natural killer cell lymphomas: the neoplastic cells are often CD3 epsilon+. Blood. 1996;87(2):839-41.
231. Ho FC, Srivastava G, Loke SL, Fu KH, Leung BP, Liang R, et al. Presence of Epstein-Barr virus DNA in nasal lymphomas of B and 'T' cell type. Hematol Oncol. 1990;8(5):271-81.
232. Au WY, Weisenburger DD, Intragumtornchai T, Nakamura S, Kim WS, Sng I, et al. Clinical differences between nasal and extranasal natural killer/T-cell lymphoma: a study of 136 cases from the International Peripheral T-Cell Lymphoma Project. Blood. 2009;113(17):3931-7.
233. Au WY, Weisenburger DD, Intragumtornchai T, Nakamura S, Kim WS, Sng I, et al. Clinical differences between nasal and extranasal NK/T-cell lymphoma: a study of 136 cases from the International Peripheral T-cell Lymphoma Project. Blood. 2008.
234. Arber DA, Weiss LM, Albujar PF, Chen YY, Jaffe ES. Nasal lymphomas in Peru. High incidence of T-cell immunophenotype and Epstein-Barr virus infection. Am J Surg Pathol. 1993;17(4):392-9.
235. Yoon SO, Suh C, Lee DH, Chi HS, Park CJ, Jang SS, et al. Distribution of lymphoid neoplasms in the Republic of Korea: analysis of 5318 cases according to the World Health Organization classification. Am J Hematol. 2010;85(10):760-4.

236. Au WY, Ma SY, Chim CS, Choy C, Loong F, Lie AK, et al. Clinicopathologic features and treatment outcome of mature T-cell and natural killer-cell lymphomas diagnosed according to the World Health Organization classification scheme: a single center experience of 10 years. Ann Oncol. 2005;16(2):206-14.
237. Canioni D, Arnulf B, Asso-Bonnet M, Raphael M, Brousse N. Nasal natural killer lymphoma associated with Epstein-Barr virus in a patient infected with human immunodeficiency virus. Arch Pathol Lab Med. 2001;125(5):660-2.
238. Cobo F, Talavera P, Busquier H, Concha A. CNK/T-cell brain lymphoma associated with Epstein-Barr virus in a patient with AIDS. Neuropathology. 2007;27(4):396-402.
239. Mukai HY, Kojima H, Suzukawa K, Hori M, Komeno T, Hasegawa Y, et al. Nasal natural killer cell lymphoma in a post-renal transplant patient. Transplantation. 2000;69(7):1501-3.
240. Liang R. Advances in the management and monitoring of extranodal NK/T-cell lymphoma, nasal type. Br J Haematol. 2009.
241. Mizoguchi Y, Nakamura K, Miyagawa S, Nishimura S, Arihiro K, Kobayashi M. A case of adolescent primary adrenal natural killer cell lymphoma. Int J Hematol. 2005;81(4):330-4.
242. Mehes G, Hegyi K, Csonka T, Fazakas F, Kocsis Z, Radvanyi G, et al. Primary uterine NK-cell lymphoma, nasal-type: a unique malignancy of a prominent cell type of the endometrium. Pathol Oncol Res. 2012;18(2):519-22.
243. Liao JB, Hsieh PP, Hwang YC, Lin SL, Wu CS. Cutaneous intravascular natural killer-cell lymphoma: a rare case and review of the literature. Acta Derm Venereol. 2011;91(4):472-3.
244. Chow KF, Ritchie E, Husain S, Alobeid B, Bhagat G. Lethal T- and NK-cell lymphomas mimicking granulomatous panniculitidies: a clinicopathologic study of three cases. J Cutan Pathol. 2011;38(6):483-91.
245. Lepeak LM, Yang DT, Chang JE. Extranodal NK/T-cell lymphoma presenting with primary cardiac involvement. Hematol Rep. 2011;3(2):e9.
246. Guan H, Huang Y, Wen W, Xu M, Zan Q, Zhang Z. Primary central nervous system extranodal NK/T-cell lymphoma, nasal type: case report and review of the literature. J Neurooncol. 2011;103(2):387-91.
247. Hasserjian RP, Harris NL. NK-cell lymphomas and leukemias: a spectrum of tumors with variable manifestations and immunophenotype. Am J Clin Pathol. 127. United States2007. p. 860-8.
248. Huang W, Chang K, Huang G, Hsiao J, Chen H, Chuang S, et al. Bone marrow that is positive for Epstein-Barr virus encoded RNA-1 by in situ hybridization is related with a poor prognosis in patients with extranodal natural killer/T-cell lymphoma, nasal type. Haematologica. 2005;90(8):1063-9.
249. Kim GE, Cho JH, Yang WI, Chung EJ, Suh CO, Park KR, et al. Angiocentric lymphoma of the head and neck: patterns of systemic failure after radiation treatment. J Clin Oncol. 2000;18(1):54-63.
250. Yamaguchi M, Kita K, Miwa H, Nishii K, Oka K, Ohno T, et al. Frequent expression of P-glycoprotein/MDR1 by nasal T-cell lymphoma cells. Cancer. 1995;76(11):2351-6.
251. Egashira M, Kawamata N, Sugimoto K, Kaneko T, Oshimi K. P-glycoprotein expression on normal and abnormally expanded natural killer cells and inhibition of P-glycoprotein function by cyclosporin A and its analogue, PSC833. Blood. 1999;93(2):599-606.
252. Gottesman MM. How cancer cells evade chemotherapy: sixteenth Richard and Hinda Rosenthal Foundation Award Lecture. Cancer Res. 1993;53(4):747-54.
253. Kim WS, Song SY, Ahn YC, Ko YH, Baek CH, Kim DY, et al. CHOP followed by involved field radiation: is it optimal for localized nasal natural killer/T-cell lymphoma? Ann Oncol. 2001;12(3):349-52.
254. Trambas C, Wang Z, Cianfriglia M, Woods G. Evidence that natural killer cells express mini P-glycoproteins but not classic 170 kDa P-glycoprotein. Br J Haematol. 2001;114(1):177-84.

255. Kim SJ, Kim K, Kim BS, Kim CY, Suh C, Huh J, et al. Phase II trial of concurrent radiation and weekly cisplatin followed by VIPD chemotherapy in newly diagnosed, stage IE to IIE, nasal, extranodal NK/T-Cell Lymphoma: Consortium for Improving Survival of Lymphoma study. J Clin Oncol. 2009;27(35):6027-32.
256. Jaccard A, Gachard N, Marin B, Rogez S, Audrain M, Suarez F, et al. Efficacy of L-asparaginase with methotrexate and dexamethasone (AspaMetDex regimen) in patients with refractory or relapsing extranodal NK/T-cell lymphoma, a phase 2 study. Blood. 2011;117(6):1834-9.
257. Yamaguchi M, Suzuki R, Kwong YL, Kim WS, Hasegawa Y, Izutsu K, et al. Phase I study of dexamethasone, methotrexate, ifosfamide, L-asparaginase, and etoposide (SMILE) chemotherapy for advanced-stage, relapsed or refractory extranodal natural killer (NK)/T-cell lymphoma and leukemia. Cancer Sci. 2008;99(5):1016-20.
258. Yamaguchi M, Tobinai K, Oguchi M, Ishizuka N, Kobayashi Y, Isobe Y, et al. Phase I/II study of concurrent chemoradiotherapy for localized nasal natural killer/T-cell lymphoma: Japan Clinical Oncology Group Study JCOG0211. J Clin Oncol. 2009;27(33):5594-600.
259. Li ZM, Zhu YJ, Sun J, Xia Y, Huang JJ, Zou BY, et al. Serum beta2-microglobin is a predictor of prognosis in patients with upper aerodigestive tract NK/T-cell lymphoma. Ann Hematol. 2012;91(8):1265-70.
260. Lee J, Suh C, Huh J, Jun HJ, Kim K, Jung C, et al. Effect of positive bone marrow EBV in situ hybridization in staging and survival of localized extranodal natural killer/T-cell lymphoma, nasal-type. Clin Cancer Res. 2007;13(11):3250-4.
261. Huang JJ, Jiang WQ, Lin TY, Huang Y, Xu RH, Huang HQ, et al. Absolute lymphocyte count is a novel prognostic indicator in extranodal natural killer/T-cell lymphoma, nasal type. Ann Oncol. 2011;22(1):149-55.
262. Kim SJ, Kim BS, Choi CW, Choi J, Kim I, Lee YH, et al. Ki-67 expression is predictive of prognosis in patients with stage I/II extranodal NK/T-cell lymphoma, nasal type. Ann Oncol. 2007;18(8):1382-7.
263. Takahara M, Kishibe K, Bandoh N, Nonaka S, Harabuchi Y. P53, N- and K-Ras, and beta-catenin gene mutations and prognostic factors in nasal NK/T-cell lymphoma from Hokkaido, Japan. Hum Pathol. 2004;35(1):86-95.
264. Suzuki R, Suzumiya J, Yamaguchi M, Nakamura S, Kameoka J, Kojima H, et al. Prognostic factors for mature natural killer (NK) cell neoplasms: aggressive NK cell leukemia and extranodal NK cell lymphoma, nasal type. Ann Oncol. 2010;21(5):1032-40.
265. Lee J, Suh C, Park YH, Ko YH, Bang SM, Lee JH, et al. Extranodal natural killer T-cell lymphoma, nasal-type: a prognostic model from a retrospective multicenter study. J Clin Oncol. 2006;24(4):612-8.
266. Kwong YL, Pang AW, Leung AY, Chim CS, Tse E. Quantification of circulating Epstein-Barr virus DNA in NK/T-cell lymphoma treated with the SMILE protocol: diagnostic and prognostic significance. Leukemia. 2014;28(4):865-70.
267. Wu X, Li P, Zhao J, Yang X, Wang F, Yang YQ, et al. A clinical study of 115 patients with extranodal natural killer/T-cell lymphoma, nasal type. Clin Oncol (R Coll Radiol). 2008;20(8):619-25.
268. Siu LL, Chan V, Chan JK, Wong KF, Liang R, Kwong YL. Consistent patterns of allelic loss in natural killer cell lymphoma. Am J Pathol. 2000;157(6):1803-9.
269. Siu LL, Wong KF, Chan JK, Kwong YL. Comparative genomic hybridization analysis of natural killer cell lymphoma/leukemia. Recognition of consistent patterns of genetic alterations. Am J Pathol. 1999;155(5):1419-25.
270. Ko YH, Choi KE, Han JH, Kim JM, Ree HJ. Comparative genomic hybridization study of nasal-type NK/T-cell lymphoma. Cytometry. 2001;46(2):85-91.

271. Wong KF, Chan JK, Kwong YL. Identification of del(6)(q21q25) as a recurring chromosomal abnormality in putative NK cell lymphoma/leukaemia. Br J Haematol. 1997;98(4):922-6.
272. Huang Y, de Reynies A, de Leval L, Ghazi B, Martin-Garcia N, Travert M, et al. Gene expression profiling identifies emerging oncogenic pathways operating in extranodal NK/T-cell lymphoma, nasal type. Blood. 2010;115(6):1226-37.
273. Iqbal J, Kucuk C, Deleeuw RJ, Srivastava G, Tam W, Geng H, et al. Genomic analyses reveal global functional alterations that promote tumor growth and novel tumor suppressor genes in natural killer-cell malignancies. Leukemia. 2009;23(6):1139-51.
274. Bouchekioua A, Scourzic L, de Wever O, Zhang Y, Cervera P, Aline-Fardin A, et al. JAK3 deregulation by activating mutations confers invasive growth advantage in extranodal nasal-type natural killer cell lymphoma. Leukemia. 2014;28(2):338-48.
275. Quoc Trung L, Espinoza JL, Takami A, Nakao S. Resveratrol induces cell cycle arrest and apoptosis in malignant NK cells via JAK2/STAT3 pathway inhibition. PLoS One. 2013;8(1):e55183.
276. Coppo P, Gouilleux-Gruart V, Huang Y, Bouhlal H, Bouamar H, Bouchet S, et al. STAT3 transcription factor is constitutively activated and is oncogenic in nasal-type NK/T-cell lymphoma. Leukemia. 2009;23(9):1667-78.
277. Manso R, Rodriguez-Pinilla SM, Lombardia L, Ruiz de Garibay G, Del Mar Lopez M, Requena L, et al. An A91V SNP in the perforin gene is frequently found in NK/T-cell lymphomas. PLoS One. 2014;9(3):e91521.
278. Harabuchi Y, Yamanaka N, Kataura A, Imai S, Kinoshita T, Mizuno F, et al. Epstein-Barr virus in nasal T-cell lymphomas in patients with lethal midline granuloma. Lancet. 1990;335(8682):128-30.
279. Chan JK, Yip TT, Tsang WY, Ng CS, Lau WH, Poon YF, et al. Detection of Epstein-Barr viral RNA in malignant lymphomas of the upper aerodigestive tract. Am J Surg Pathol. 1994;18(9):938-46.
280. Chan JKC, Quintanilla-Martinez L, Ferry JA, Peh SC. Extranodal NK/T-cell lymphoma, nasal type. In: Jaffe ES, Harris NL, Stein H, Vardiman JW, editors. World Health Organization Classfication of Tumours of Haematopoietic and Lymphoid Tissues. 4th ed. Lyon: IARC Press; 2007. p. 285-8.
281. Tao Q, Ho FC, Loke SL, Srivastava G. Epstein-Barr virus is localized in the tumour cells of nasal lymphomas of NK, T or B cell type. Int J Cancer. 1995;60(3):315-20.
282. Minarovits J, Hu LF, Imai S, Harabuchi Y, Kataura A, Minarovits-Kormuta S, et al. Clonality, expression and methylation patterns of the Epstein-Barr virus genomes in lethal midline granulomas classified as peripheral angiocentric T cell lymphomas. J Gen Virol. 1994;75 (Pt 1):77-84.
283. Teo W-L, Tan S-Y. Loss of Epstein-Barr Virus–Encoded RNA Expression in Cutaneous Dissemination of Natural Killer/T-Cell Lymphoma. Journal of Clinical Oncology. 2011;29(12):e342-e3.
284. van Gorp J, Brink A, Oudejans JJ, van den Brule AJ, van den Tweel JG, Jiwa NM, et al. Expression of Epstein-Barr virus encoded latent genes in nasal T cell lymphomas. J Clin Pathol. 1996;49(1):72-6.
285. Young LS, Rickinson AB. Epstein-Barr virus: 40 years on. Nat Rev Cancer. 2004;4(10):757-68.
286. Hsieh PP, Tung CL, Chan AB, Liao JB, Wang JS, Tseng HH, et al. EBV viral load in tumor tissue is an important prognostic indicator for nasal NK/T-cell lymphoma. Am J Clin Pathol. 2007;128(4):579-84.
287. Au W-Y, Pang A, Choy C, Chim C-S, Kwong Y-L. Quantification of circulating Epstein-Barr virus (EBV) DNA in the diagnosis and monitoring of natural killer cell and EBV-positive lymphomas in immunocompetent patients. Blood. 2004;104(1):243-9.
288. Ito Y, Kimura H, Maeda Y, Hashimoto C, Ishida F, Izutsu K, et al. Pretreatment EBV-DNA copy number is predictive of response and toxicities to SMILE chemotherapy for extranodal NK/T-cell lymphoma, nasal type. Clin Cancer Res. 2012.

289. Wang ZY, Liu QF, Wang H, Jin J, Wang WH, Wang SL, et al. Clinical implications of plasma Epstein-Barr virus DNA in early-stage extranodal nasal-type NK/T-cell lymphoma patients receiving primary radiotherapy. Blood. 2012.
290. Kim SJ, Choi JY, Hyun SH, Ki CS, Oh D, Ahn YC, et al. Risk stratification on the basis of Deauville score on PET-CT and the presence of Epstein-Barr virus DNA after completion of primary treatment for extranodal natural killer/T-cell lymphoma, nasal type: a multicentre, retrospective analysis. Lancet Haematol. 2015;2(2):e66-74.
291. Suzushima H, Asou N, Fujimoto T, Nishimura S, Okubo T, Yamasaki H, et al. Lack of the expression of EBNA-2 and LMP-1 in T-cell neoplasms possessing Epstein-Barr virus. Blood. 1995;85(2):480-6.
292. Liu MT, Chen YR, Chen SC, Hu CY, Lin CS, Chang YT, et al. Epstein-Barr virus latent membrane protein 1 induces micronucleus formation, represses DNA repair and enhances sensitivity to DNA-damaging agents in human epithelial cells. Oncogene. 2004;23(14):2531-9.
293. Rowe M, Khanna R, Jacob CA, Argaet V, Kelly A, Powis S, et al. Restoration of endogenous antigen processing in Burkitt's lymphoma cells by Epstein-Barr virus latent membrane protein-1: coordinate up-regulation of peptide transporters and HLA-class I antigen expression. Eur J Immunol. 1995;25(5):1374-84.
294. Lee DY, Sugden B. The LMP1 oncogene of EBV activates PERK and the unfolded protein response to drive its own synthesis. Blood. 2008;111(4):2280-9.
295. Harabuchi Y, Takahara M, Kishibe K, Moriai S, Nagato T, Ishii H. Nasal natural killer (NK)/T-cell lymphoma: clinical, histological, virological, and genetic features. Int J Clin Oncol. 2009;14(3):181-90.
296. Takahara M, Kis LL, Nagy N, Liu A, Harabuchi Y, Klein G, et al. Concomitant increase of LMP1 and CD25 (IL-2-receptor α) expression induced by IL-10 in the EBV-positive NK lines SNK6 and KAI3. International Journal of Cancer. 2006;119(12):2775-83.
297. Dybkaer K, Iqbal J, Zhou G, Geng H, Xiao L, Schmitz A, et al. Genome wide transcriptional analysis of resting and IL2 activated human natural killer cells: gene expression signatures indicative of novel molecular signaling pathways. BMC Genomics. 2007;8:230.
298. Gilligan K, Sato H, Rajadurai P, Busson P, Young L, Rickinson A, et al. Novel transcription from the Epstein-Barr virus terminal EcoRI fragment, DIJhet, in a nasopharyngeal carcinoma. J Virol. 1990;64(10):4948-56.
299. Sadler RH, Raab-Traub N. The Epstein-Barr virus 3.5-kilobase latent membrane protein 1 mRNA initiates from a TATA-Less promoter within the first terminal repeat. J Virol. 1995;69(7):4577-81.
300. Chen H, Lee JM, Zong Y, Borowitz M, Ng MH, Ambinder RF, et al. Linkage between STAT regulation and Epstein-Barr virus gene expression in tumors. J Virol. 2001;75(6):2929-37.
301. D'Souza B, Rowe M, Walls D. The bfl-1 gene is transcriptionally upregulated by the Epstein-Barr virus LMP1, and its expression promotes the survival of a Burkitt's lymphoma cell line. J Virol. 2000;74(14):6652-8.
302. Fries KL, Miller WE, Raab-Traub N. Epstein-Barr virus latent membrane protein 1 blocks p53-mediated apoptosis through the induction of the A20 gene. J Virol. 1996;70(12):8653-9.
303. Wang S, Rowe M, Lundgren E. Expression of the Epstein Barr virus transforming protein LMP1 causes a rapid and transient stimulation of the Bcl-2 homologue Mcl-1 levels in B-cell lines. Cancer Res. 1996;56(20):4610-3.
304. Nakamura H, Ishii C, Suehiro M, Iguchi A, Kuroda K, Shimizu K, et al. The latent membrane protein 1 (LMP1) encoded by Epstein-Barr virus induces expression of the putative oncogene Bcl-3 through activation of the nuclear factor-kappaB. Virus Res. 2008;131(2):170-9.
305. Kawanishi M. Expression of Epstein-Barr virus latent membrane protein 1 protects Jurkat T cells from apoptosis induced by serum deprivation. Virology. 1997;228(2):244-50.

306. Fox CP, Haigh TA, Taylor GS, Long HM, Lee SP, Shannon-Lowe C, et al. A novel latent membrane 2 transcript expressed in Epstein-Barr virus-positive NK- and T-cell lymphoproliferative disease encodes a target for cellular immunotherapy. Blood. 2010;116(19):3695-704.
307. Bollard CM, Gottschalk S, Leen AM, Weiss H, Straathof KC, Carrum G, et al. Complete responses of relapsed lymphoma following genetic modification of tumor-antigen presenting cells and T-lymphocyte transfer. Blood. 2007;110(8):2838-45.
308. Ramakrishnan R, Donahue H, Garcia D, Tan J, Shimizu N, Rice AP, et al. Epstein-Barr Virus BART9 miRNA Modulates LMP1 Levels and Affects Growth Rate of Nasal NK T Cell Lymphomas. PLoS One. 2011;6(11):e27271.
309. Ian MX, Lan SZ, Cheng ZF, Dan H, Qiong LH. Suppression of EBNA1 expression inhibits growth of EBV-positive NK/T cell lymphoma cells. Cancer biology & therapy. 2008;7(10):1602-6.
310. Yang L, Aozasa K, Oshimi K, Takada K. Epstein-Barr virus (EBV)-encoded RNA promotes growth of EBV-infected T cells through interleukin-9 induction. Cancer Res. 2004;64(15):5332-7.
311. Nagato T, Kobayashi H, Kishibe K, Takahara M, Ogino T, Ishii H, et al. Expression of interleukin-9 in nasal natural killer/T-cell lymphoma cell lines and patients. Clin Cancer Res. 2005;11(23):8250-7.
312. Suzuki R, Suzumiya J, Nakamura S, Aoki S, Notoya A, Ozaki S, et al. Aggressive natural killer-cell leukemia revisited: large granular lymphocyte leukemia of cytotoxic NK cells. Leukemia. 2004;18(4):763-70.
313. Ruskova A, Thula R, Chan G. Aggressive Natural Killer-Cell Leukemia: report of five cases and review of the literature. Leuk Lymphoma. 2004;45(12):2427-38.
314. Song SY, Kim WS, Ko YH, Kim K, Lee MH, Park K. Aggressive natural killer cell leukemia: clinical features and treatment outcome. Haematologica. 2002;87(12):1343-5.
315. Ryder J, Wang X, Bao L, Gross SA, Hua F, Irons RD. Aggressive natural killer cell leukemia: report of a Chinese series and review of the literature. Int J Hematol. 2007;85(1):18-25.
316. Ishida F, Ko YH, Kim WS, Suzumiya J, Isobe Y, Oshimi K, et al. Aggressive natural killer cell leukemia: therapeutic potential of L-asparaginase and allogeneic hematopoietic stem cell transplantation. Cancer Sci. 2012;103(6):1079-83.
317. Kerr JFR, Wyllie AH, Currie AR. Apoptosis: A Basic Biological Phenomenon with Wide-ranging Implications in Tissue Kinetics. Br J Cancer. 1972;26(4):239-57.
318. Savill J, Fadok V. Corpse clearance defines the meaning of cell death. Nature. 2000;407(6805):784-8.
319. Taylor RC, Cullen SP, Martin SJ. Apoptosis: controlled demolition at the cellular level. Nat Rev Mol Cell Biol. 2008;9(3):231-41.
320. Timmer JC, Salvesen GS. Caspase substrates. Cell Death Differ. 2007;14(1):66-72.
321. Thiede B, Treumann A, Kretschmer A, Sohlke J, Rudel T. Shotgun proteome analysis of protein cleavage in apoptotic cells. Proteomics. 2005;5(8):2123-30.
322. Rao L, Perez D, White E. Lamin proteolysis facilitates nuclear events during apoptosis. J Cell Biol. 1996;135(6 Pt 1):1441-55.
323. Wyllie AH. Glucocorticoid-induced thymocyte apoptosis is associated with endogenous endonuclease activation. Nature. 1980;284(5756):555-6.
324. Letai A, Bassik MC, Walensky LD, Sorcinelli MD, Weiler S, Korsmeyer SJ. Distinct BH3 domains either sensitize or activate mitochondrial apoptosis, serving as prototype cancer therapeutics. Cancer Cell. 2002;2(3):183-92.
325. Dustin ML, Long EO. Cytotoxic immunological synapses. Immunol Rev. 2010;235(1):24-34.
326. Lopez JA, Jenkins MR, Rudd-Schmidt JA, Brennan AJ, Danne JC, Mannering SI, et al. Rapid and unidirectional perforin pore delivery at the cytotoxic immune synapse. J Immunol. 2013;191(5):2328-34.

327. Sutton VR, Davis JE, Cancilla M, Johnstone RW, Ruefli AA, Sedelies K, et al. Initiation of apoptosis by granzyme B requires direct cleavage of bid, but not direct granzyme B-mediated caspase activation. J Exp Med. 2000;192(10):1403-14.
328. Blink EJ, Trapani JA, Jans DA. Perforin-dependent nuclear targeting of granzymes: A central role in the nuclear events of granule-exocytosis-mediated apoptosis? Immunol Cell Biol. 1999;77(3):206-15.
329. Saelens X, Festjens N, Vande Walle L, van Gurp M, van Loo G, Vandenabeele P. Toxic proteins released from mitochondria in cell death. Oncogene. 2004;23(16):2861-74.
330. Wang X. The expanding role of mitochondria in apoptosis. Genes Dev. 2001;15(22):2922-33.
331. Tsujimoto Y, Gorham J, Cossman J, Jaffe E, Croce CM. The t(14;18) chromosome translocations involved in B-cell neoplasms result from mistakes in VDJ joining. Science. 1985;229(4720):1390-3.
332. Vaux DL, Cory S, Adams JM. Bcl-2 gene promotes haemopoietic cell survival and cooperates with c-myc to immortalize pre-B cells. Nature. 1988;335(6189):440-2.
333. Czabotar PE, Lessene G, Strasser A, Adams JM. Control of apoptosis by the BCL-2 protein family: implications for physiology and therapy. Nature Reviews Molecular Cell Biology. 2013;15:49-63.
334. Kuwana T, Bouchier-Hayes L, Chipuk JE, Bonzon C, Sullivan BA, Green DR, et al. BH3 domains of BH3-only proteins differentially regulate Bax-mediated mitochondrial membrane permeabilization both directly and indirectly. Mol Cell. 2005;17(4):525-35.
335. Chipuk JE, Moldoveanu T, Llambi F, Parsons MJ, Green DR. The BCL-2 family reunion. Mol Cell. 2010;37(3):299-310.
336. Kuwana T, Mackey MR, Perkins G, Ellisman MH, Latterich M, Schneiter R, et al. Bid, Bax, and lipids cooperate to form supramolecular openings in the outer mitochondrial membrane. Cell. 2002;111(3):331-42.
337. Chipuk JE, Fisher JC, Dillon CP, Kriwacki RW, Kuwana T, Green DR. Mechanism of apoptosis induction by inhibition of the anti-apoptotic BCL-2 proteins. Proc Natl Acad Sci U S A. 2008;105(51):20327-32.
338. Kvansakul M, Hinds MG. Structural biology of the Bcl-2 family and its mimicry by viral proteins. Cell Death Dis. 2013;4:e909.
339. Willis SN, Fletcher JI, Kaufmann T, van Delft MF, Chen L, Czabotar PE, et al. Apoptosis initiated when BH3 ligands engage multiple Bcl-2 homologs, not Bax or Bak. Science. 2007;315(5813):856-9.
340. Li H, Zhu H, Xu CJ, Yuan J. Cleavage of BID by caspase 8 mediates the mitochondrial damage in the Fas pathway of apoptosis. Cell. 1998;94(4):491-501.
341. Luo X, Budihardjo I, Zou H, Slaughter C, Wang X. Bid, a Bcl2 interacting protein, mediates cytochrome c release from mitochondria in response to activation of cell surface death receptors. Cell. 1998;94(4):481-90.
342. Zha J, Weiler S, Oh KJ, Wei MC, Korsmeyer SJ. Posttranslational N-myristoylation of BID as a molecular switch for targeting mitochondria and apoptosis. Science. 2000;290(5497):1761-5.
343. Happo L, Cragg MS, Phipson B, Haga JM, Jansen ES, Herold MJ, et al. Maximal killing of lymphoma cells by DNA damage-inducing therapy requires not only the p53 targets Puma and Noxa, but also Bim. Blood. 2010;116(24):5256-67.
344. Erlacher M, Michalak EM, Kelly PN, Labi V, Niederegger H, Coultas L, et al. BH3-only proteins Puma and Bim are rate-limiting for gamma-radiation- and glucocorticoid-induced apoptosis of lymphoid cells in vivo. Blood. 2005;106(13):4131-8.
345. Robertson LE, Plunkett W, McConnell K, Keating MJ, McDonnell TJ. Bcl-2 expression in chronic lymphocytic leukemia and its correlation with the induction of apoptosis and clinical outcome. Leukemia. 1996;10(3):456-9.

346. Pettersson M, Jernberg-Wiklund H, Larsson LG, Sundstrom C, Givol I, Tsujimoto Y, et al. Expression of the bcl-2 gene in human multiple myeloma cell lines and normal plasma cells. Blood. 1992;79(2):495-502.
347. Anderson MA, Huang D, Roberts A. Targeting BCL2 for the treatment of lymphoid malignancies. Semin Hematol. 2014;51(3):219-27.
348. Strasser A, Harris AW, Jacks T, Cory S. DNA damage can induce apoptosis in proliferating lymphoid cells via p53-independent mechanisms inhibitable by Bcl-2. Cell. 1994;79(2):329-39.
349. Oltersdorf T, Elmore SW, Shoemaker AR, Armstrong RC, Augeri DJ, Belli BA, et al. An inhibitor of Bcl-2 family proteins induces regression of solid tumours. Nature. 2005;435(7042):677-81.
350. Rooswinkel RW, Kooij Bvd, Verheij M, Borst J. Bcl-2 is a better ABT-737 target than Bcl-xL or Bcl-w and only Noxa overcomes resistance mediated by Mcl-1, Bfl-1, or Bcl-B. Cell Death & Disease. 2012;3(8).
351. Souers AJ, Leverson JD, Boghaert ER, Ackler SL, Catron ND, Chen J, et al. ABT-199, a potent and selective BCL-2 inhibitor, achieves antitumor activity while sparing platelets. Nat Med. 2013;19(2):202-8.
352. Nguyen M, Marcellus RC, Roulston A, Watson M, Serfass L, Murthy Madiraju SR, et al. Small molecule obatoclax (GX15-070) antagonizes MCL-1 and overcomes MCL-1-mediated resistance to apoptosis. Proc Natl Acad Sci U S A. 2007;104(49):19512-7.
353. Zhang Y, Nagata H, Ikeuchi T, Mukai H, Oyoshi MK, Demachi A, et al. Common cytological and cytogenetic features of Epstein-Barr virus (EBV)-positive natural killer (NK) cells and cell lines derived from patients with nasal T/NK-cell lymphomas, chronic active EBV infection and hydroa vacciniforme-like eruptions. Br J Haematol. 2003;121(5):805-14.
354. Nagata H, Konno A, Kimura N, Zhang Y, Kimura M, Demachi A, et al. Characterization of novel natural killer (NK)-cell and {gamma}{delta} T-cell lines established from primary lesions of nasal T/NK-cell lymphomas associated with the Epstein-Barr virus. Blood. 2001;97(3):708-13.
355. Oyoshi MK, Nagata H, Kimura N, Zhang Y, Demachi A, Hara T, et al. Preferential Expansion of V?9-J?P/V?2-J?3 ?? T Cells in Nasal T-Cell Lymphoma and Chronic Active Epstein-Barr Virus Infection. Am J Pathol. 2003;162(5):1629-38.
356. Herold MJ, van den Brandt J, Seibler J, Reichardt HM. Inducible and reversible gene silencing by stable integration of an shRNA-encoding lentivirus in transgenic rats. Proc Natl Acad Sci U S A. 2008;105(47):18507-12.
357. Rowe M, Evans HS, Young LS, Hennessy K, Kieff E, Rickinson AB. Monoclonal antibodies to the latent membrane protein of Epstein-Barr virus reveal heterogeneity of the protein and inducible expression in virus-transformed cells. J Gen Virol. 1987;68 (Pt 6):1575-86.
358. Huang DW, Sherman BT, Lempicki RA. Systematic and integrative analysis of large gene lists using DAVID bioinformatics resources. Nature Protocols. 2008;4(1):44-57.
359. Huang DW, Sherman BT, Lempicki RA. Bioinformatics enrichment tools: paths toward the comprehensive functional analysis of large gene lists. 2009.
360. DAVID Functional Annotation Bioinformatics Microarray Analysis 2014 [6.7:[Available from: http://david.abcc.ncifcrf.gov/home.jsp.
361. Vockerodt M, Morgan SL, Kuo M, Wei W, Chukwuma MB, Arrand JR, et al. The Epstein-Barr virus oncoprotein, latent membrane protein-1, reprograms germinal centre B cells towards a Hodgkin's Reed-Sternberg-like phenotype. J Pathol. 2008;216(1):83-92.
362. Oliveros JC. VENNY. An interactive tool for comparing lists with Venn Diagrams. http://bioinfogp.cnb.csic.es/tools/venny/index.html. 2007 [

363. Swanson BJ, Jack HM, Lyons GE. Characterization of myocyte enhancer factor 2 (MEF2) expression in B and T cells: MEF2C is a B cell-restricted transcription factor in lymphocytes. Mol Immunol. 1998;35(8):445-58.
364. Zhou W, Feng X, Ren C, Jiang X, Liu W, Huang W, et al. Over-expression of BCAT1, a c-Myc target gene, induces cell proliferation, migration and invasion in nasopharyngeal carcinoma. Mol Cancer. 2013;12:53.
365. Eden A, Benvenisty N. Involvement of branched-chain amino acid aminotransferase (Bcat1/Eca39) in apoptosis. FEBS Lett. 1999;457(2):255-61.
366. SNCA synuclein, alpha (non A4 component of amyloid precursor) [Homo sapiens (human)] - Gene - NCBI: Pubs; 2014 [Available from: http://www.ncbi.nlm.nih.gov/pubmed/.
367. Mason P, Liang B, Li L, Fremgen T, Murphy E, Quinn A, et al. SCD1 Inhibition Causes Cancer Cell Death by Depleting Mono-Unsaturated Fatty Acids. PLoS One. 2012;7(3).
368. Locasale JW, Grassian AR, Melman T, Lyssiotis CA, Mattaini KR, Bass AJ, et al. Phosphoglycerate dehydrogenase diverts glycolytic flux and contributes to oncogenesis. Nat Genet. 2011;43(9):869-74.
369. Khursheed M, Kolla JN, Kotapalli V, Gupta N, Gowrishankar S, Uppin SG, et al. ARID1B, a member of the human SWI/SNF chromatin remodeling complex, exhibits tumour-suppressor activities in pancreatic cancer cell lines. Br J Cancer. 2013;108(10):2056-62.
370. Ashmole I, Duffy SM, Leyland ML, Bradding P. The contribution of Orai(CRACM)1 and Orai(CRACM)2 channels in store-operated Ca2+ entry and mediator release in human lung mast cells. PLoS One. 2013;8(9):e74895.
371. Dhanoa BS, Cogliati T, Satish AG, Bruford EA, Friedman JS. Update on the Kelch-like (KLHL) gene family. Hum Genomics. 2013;7(1):13.
372. Zhang H, Wang D, Sun H, Hall RA, Yun CC. MAGI-3 regulates LPA-induced activation of Erk and RhoA. Cell Signal. 2007;19(2):261-8.
373. Kumar A, Mocklinghoff S, Yumoto F, Jaroszewski L, Farr CL, Grzechnik A, et al. Structure of a novel winged-helix like domain from human NFRKB protein. PLoS One. 2012;7(9):e43761.
374. Hu JK, Wang L, Li Y, Yang K, Zhang P, Chen XZ, et al. The mRNA and protein expression of A-kinase anchor proteins 13 in human colorectal cancer. Clin Exp Med. 2010;10(1):41-9.
375. Grau L, Luque-Garcia JL, Gonzalez-Peramato P, Theodorescu D, Palou J, Fernandez-Gomez JM, et al. A Quantitative Proteomic Analysis Uncovers the Relevance of CUL3 in Bladder Cancer Aggressiveness. PLoS One. 2013;8(1).
376. Tsutsui T, Laboratory of Gene Regulation GSoMaPS, University of Toyama, 2630 Sugitani, Toyama 930-0194, Japan, Fukasawa R, Laboratory of Gene Regulation GSoMaPS, University of Toyama, 2630 Sugitani, Toyama 930-0194, Japan, Tanaka A, Laboratory of Gene Regulation GSoMaPS, University of Toyama, 2630 Sugitani, Toyama 930-0194, Japan, et al. Identification of target genes for the CDK subunits of the Mediator complex. Genes to Cells. 2014;16(12):1208-18.
377. Yajima I, Kumasaka M, Thang ND, Yanagishita T, Ohgami N, Kallenberg D, et al. Zinc finger protein 28 as a novel melanoma-related molecule. J Dermatol Sci. 2009;55(1):68-70.
378. Chen Y, Peng H, Wei H, Sun R, Tian Z. CD49a promotes T-cell-mediated hepatitis by driving T helper 1 cytokine and interleukin-17 production. Immunology. 2014;141(3):388-400.
379. Cao MY, Davidson D, Yu J, Latour S, Veillette A. Clnk, a Novel Slp-76–Related Adaptor Molecule Expressed in Cytokine-Stimulated Hemopoietic Cells. 1999.
380. Guttinger M, Sutti F, Panigada M, Porcellini S, Merati B, Mariani M, et al. Epithelial V-like Antigen (EVA), a Novel Member of the Immunoglobulin Superfamily, Expressed in Embryonic Epithelia with a Potential Role as Homotypic Adhesion Molecule in Thymus Histogenesis. J Cell Biol. 1998;141(4):1061-71.

381. Vladimirova V, Mikeska T, Waha A, Soerensen N, Xu J, Reynolds PC, et al. Aberrant methylation and reduced expression of LHX9 in malignant gliomas of childhood. Neoplasia. 2009;11(7):700-11.
382. Narsinh KH, Sun N, Sanchez-Freire V, Lee AS, Almeida P, Hu S, et al. Single cell transcriptional profiling reveals heterogeneity of human induced pluripotent stem cells. J Clin Invest. 2011;121(3):1217-21.
383. Schneider S, Smith T, Hansen U. SCOREM: statistical consolidation of redundant expression measures. Nucleic Acids Res. 2012;40(6):e46.
384. Okoniewski MJ, Yates T, Dibben S, Miller CJ. An annotation infrastructure for the analysis and interpretation of Affymetrix exon array data. Genome Biol. 2007;8(5):R79.
385. Annmap Genome Browser 2014 [Available from: http://annmap.cruk.manchester.ac.uk/.
386. Dai M, Wang P, Boyd AD, Kostov G, Athey B, Jones EG, et al. Evolving gene/transcript definitions significantly alter the interpretation of GeneChip data. Nucleic Acids Res. 2005;33(20):e175.
387. Li H, Zhu D, Cook M. A statistical framework for consolidating "sibling" probe sets for Affymetrix GeneChip data. BMC Genomics. 2008;9:188.
388. Microarray Lab 2014 [Available from: http://brainarray.mbni.med.umich.edu/Brainarray/Database/CustomCDF/CDF_download.asp.
389. Takimoto T, Furukawa M, Hatano M, Umeda R. Epstein-Barr virus nuclear antigen-positive nasopharyngeal hybrid cells. Ann Otol Rhinol Laryngol. 1984;93(2 Pt 1):166-9.
390. Dawson CW, Eliopoulos AG, Blake SM, Barker R, Young LS. Identification of functional differences between prototype Epstein-Barr virus-encoded LMP1 and a nasopharyngeal carcinoma-derived LMP1 in human epithelial cells. Virology. 2000;272(1):204-17.
391. Iqbal J, Weisenburger DD, Chowdhury A, Tsai MY, Srivastava G, Greiner TC, et al. Natural killer cell lymphoma shares strikingly similar molecular features with a group of non-hepatosplenic gammadelta T-cell lymphoma and is highly sensitive to a novel aurora kinase A inhibitor in vitro. Leukemia. 2011;25(2):348-58.
392. Westermann AJ, Gorski SA, Vogel J. Dual RNA-seq of pathogen and host. Nat Rev Microbiol. 2012;10(9):618-30.
393. Finotello F, Lavezzo E, Bianco L, Barzon L, Mazzon P, Fontana P, et al. Reducing bias in RNA sequencing data: a novel approach to compute counts. BMC Bioinformatics. 2014;15 Suppl 1:S7.
394. Rowe M, Fitzsimmons L, Bell AI. Epstein-Barr virus and Burkitt lymphoma. Chin J Cancer. 2014;33(12):609-19.
395. Kelly GL, Milner AE, Tierney RJ, Croom-Carter DS, Altmann M, Hammerschmidt W, et al. Epstein-Barr virus nuclear antigen 2 (EBNA2) gene deletion is consistently linked with EBNA3A, -3B, and -3C expression in Burkitt's lymphoma cells and with increased resistance to apoptosis. J Virol. 2005;79(16):10709-17.
396. Shannon-Lowe C, Adland E, Bell AI, Delecluse HJ, Rickinson AB, Rowe M. Features distinguishing Epstein-Barr virus infections of epithelial cells and B cells: viral genome expression, genome maintenance, and genome amplification. J Virol. 2009;83(15):7749-60.
397. Kis LL, Takahara M, Nagy N, Klein G, Klein E. IL-10 can induce the expression of EBV-encoded latent membrane protein-1 (LMP-1) in the absence of EBNA-2 in B lymphocytes and in Burkitt lymphoma- and NK lymphoma-derived cell lines. Blood. 2006;107(7):2928-35.
398. Takahara M, Kis LL, Nagy N, Liu A, Harabuchi Y, Klein G, et al. Concomitant increase of LMP1 and CD25 (IL-2-receptor alpha) expression induced by IL-10 in the EBV-positive NK lines SNK6 and KAI3. Int J Cancer. 2006;119(12):2775-83.

399. Ishii H, Takahara M, Nagato T, Kis LL, Nagy N, Kishibe K, et al. Monocytes enhance cell proliferation and LMP1 expression of nasal natural killer/T-cell lymphoma cells by cell contact-dependent interaction through membrane-bound IL-15. Int J Cancer. 2012;130(1):48-58.
400. Schneider U, Schwenk HU, Bornkamm G. Characterization of EBV-genome negative "null" and "T" cell lines derived from children with acute lymphoblastic leukemia and leukemic transformed non-Hodgkin lymphoma. Int J Cancer. 1977;19(5):621-6.
401. Robertson MJ, Cochran KJ, Cameron C, Le JM, Tantravahi R, Ritz J. Characterization of a cell line, NKL, derived from an aggressive human natural killer cell leukemia. Exp Hematol. 1996;24(3):406-15.
402. Gregory CD, Rowe M, Rickinson AB. Different Epstein-Barr virus-B cell interactions in phenotypically distinct clones of a Burkitt's lymphoma cell line. J Gen Virol. 1990;71 (Pt 7):1481-95.
403. O'Connor L, Strasser A, O'Reilly LA, Hausmann G, Adams JM, Cory S, et al. Bim: a novel member of the Bcl-2 family that promotes apoptosis. EMBO J. 1998;17(2):384-95.
404. U M, Miyashita T, Shikama Y, Tadokoro K, Yamada M. Molecular cloning and characterization of six novel isoforms of human Bim, a member of the proapoptotic Bcl-2 family. FEBS Lett. 2001;509(1):135-41.
405. Strasser A. The role of BH3-only proteins in the immune system. Nat Rev Immunol. 2005;5(3):189-200.
406. Hande KR. Etoposide: four decades of development of a topoisomerase II inhibitor. Eur J Cancer. 1998;34(10):1514-21.
407. Rothenberg ML. Topoisomerase I inhibitors: review and update. Ann Oncol. 1997;8(9):837-55.
408. Gil-Parrado S, Fernandez-Montalvan A, Assfalg-Machleidt I, Popp O, Bestvater F, Holloschi A, et al. Ionomycin-activated calpain triggers apoptosis. A probable role for Bcl-2 family members. J Biol Chem. 2002;277(30):27217-26.
409. Minowada J, Onuma T, Moore GE. Rosette-forming human lymphoid cell lines. I. Establishment and evidence for origin of thymus-derived lymphocytes. J Natl Cancer Inst. 1972;49(3):891-5.
410. Del Gaizo Moore V, Letai A. BH3 profiling--measuring integrated function of the mitochondrial apoptotic pathway to predict cell fate decisions. Cancer Lett. 2013;332(2):202-5.
411. Gregory CD, Dive C, Henderson S, Smith CA, Williams GT, Gordon J, et al. Activation of Epstein-Barr virus latent genes protects human B cells from death by apoptosis. Nature. 1991;349(6310):612-4.
412. Rowe M, Peng-Pilon M, Huen DS, Hardy R, Croom-Carter D, Lundgren E, et al. Upregulation of bcl-2 by the Epstein-Barr virus latent membrane protein LMP1: a B-cell-specific response that is delayed relative to NF-kappa B activation and to induction of cell surface markers. J Virol. 1994;68(9):5602-12.
413. Le Clorennec C, Youlyouz-Marfak I, Adriaenssens E, Coll J, Bornkamm GW, Feuillard J. EBV latency III immortalization program sensitizes B cells to induction of CD95-mediated apoptosis via LMP1: role of NF-kappaB, STAT1, and p53. Blood. 2006;107(5):2070-8.
414. Sarosiek KA, Chi X, Bachman JA, Sims JJ, Montero J, Patel L, et al. BID preferentially activates BAK while BIM preferentially activates BAX, affecting chemotherapy response. Mol Cell. 2013;51(6):751-65.
415. Biswas SC, Greene LA. Nerve growth factor (NGF) down-regulates the Bcl-2 homology 3 (BH3) domain-only protein Bim and suppresses its proapoptotic activity by phosphorylation. J Biol Chem. 2002;277(51):49511-6.
416. Werner AB, Tait SW, de Vries E, Eldering E, Borst J. Requirement for aspartate-cleaved bid in apoptosis signaling by DNA-damaging anti-cancer regimens. J Biol Chem. 2004;279(27):28771-80.
417. Zhang Y, Ohyashiki JH, Takaku T, Shimizu N, Ohyashiki K. Transcriptional profiling of Epstein-Barr virus (EBV) genes and host cellular genes in nasal NK/T-cell lymphoma and chronic active EBV infection. Br J Cancer. 2006;94(4):599-608.

418. Billard C. BH3 mimetics: status of the field and new developments. Mol Cancer Ther. 2013;12(9):1691-700.
419. Lawrence JB, Villnave CA, Singer RH. Sensitive, high-resolution chromatin and chromosome mapping in situ: presence and orientation of two closely integrated copies of EBV in a lymphoma line. Cell. 1988;52(1):51-61.
420. Hislop AD, Kuo M, Drake-Lee AB, Akbar AN, Bergler W, Hammerschmitt N, et al. Tonsillar homing of Epstein-Barr virus-specific CD8+ T cells and the virus-host balance. J Clin Invest. 2005;115(9):2546-55.
421. Njie R, Bell AI, Jia H, Croom-Carter D, Chaganti S, Hislop AD, et al. The effects of acute malaria on Epstein-Barr virus (EBV) load and EBV-specific T cell immunity in Gambian children. J Infect Dis. 2009;199(1):31-8.
422. Kimura H, Miyake K, Yamauchi Y, Nishiyama K, Iwata S, Iwatsuki K, et al. Identification of Epstein-Barr virus (EBV)-infected lymphocyte subtypes by flow cytometric in situ hybridization in EBV-associated lymphoproliferative diseases. J Infect Dis. 2009;200(7):1078-87.
423. Kawabe S, Ito Y, Gotoh K, Kojima S, Matsumoto K, Kinoshita T, et al. Application of Flow Cytometric in situ Hybridization Assay to Epstein-Barr Virus (EBV)-associated T/NK Lymphoproliferative Diseases. Cancer Sci. 2012.
424. Kumai T, Nagato T, Kobayashi H, Komabayashi Y, Ueda S, Kishibe K, et al. CCL17 and CCL22/CCR4 signaling is a strong candidate for novel targeted therapy against nasal natural killer/T-cell lymphoma. Cancer Immunol Immunother. 2015;64(6):697-705.
425. Duvic M, Pinter-Brown LC, Foss FM, Sokol L, Jorgensen JL, Challagundla P, et al. Phase 1/2 study of mogamulizumab, a defucosylated anti-CCR4 antibody, in previously treated patients with cutaneous T-cell lymphoma. Blood. 2015;125(12):1883-9.
426. Xia Y, Jeffrey Medeiros L, Young KH. Signaling pathway and dysregulation of PD1 and its ligands in lymphoid malignancies. Biochim Biophys Acta. 2015.
427. Honda T, Egen JG, Lammermann T, Kastenmuller W, Torabi-Parizi P, Germain RN. Tuning of antigen sensitivity by T cell receptor-dependent negative feedback controls T cell effector function in inflamed tissues. Immunity. 2014;40(2):235-47.
428. Green MR, Rodig S, Juszczynski P, Ouyang J, Sinha P, O'Donnell E, et al. Constitutive AP-1 activity and EBV infection induce PD-L1 in Hodgkin lymphomas and posttransplant lymphoproliferative disorders: implications for targeted therapy. Clin Cancer Res. 2012;18(6):1611-8.
429. Chen BJ, Chapuy B, Ouyang J, Sun HH, Roemer MG, Xu ML, et al. PD-L1 expression is characteristic of a subset of aggressive B-cell lymphomas and virus-associated malignancies. Clin Cancer Res. 2013;19(13):3462-73.